

The amyloidogenic properties of the CAP superfamily proteins

**De amyloïdogene eigenschappen van eiwitten uit de CAP
superfamilie**
(met een samenvatting in het Nederlands)

Proefschrift

ter verkrijging van de graad van doctor aan de
Universiteit Utrecht
op gezag van de
rector magnificus, prof.dr. H.R.B.M. Kummeling,
ingevolge het besluit van het college voor promoties
in het openbaar te verdedigen op
maandag 22 juni 2020 des middags te 2.30 uur

door

Jie Sheng

geboren op 10 januari 1989
te Shaanxi, China

Promotor:

Prof. dr. J.B. Helms

Copromotoren:

Dr. B.M. Gadella

Dr. D.V. Kaloyanova

Contents

Chapter 1	General introduction	1
Chapter 2	Zinc binding regulates amyloid-like aggregation of GAPR-1	31
Chapter 3	Metal ions and redox balance regulate distinct amyloid-like aggregation pathways of GAPR-1	53
Chapter 4	The less conserved metal-binding site in human CRISP1 remains sensitive to zinc ions and permits Zn ²⁺ -dependent protein oligomerization	79
Chapter 5	Summarizing discussion	103
	Nederlandse samenvatting	
Addendum	Acknowledgement	133
	About the author	
	List of publications	

ISBN: 978-94-6375-928-1

Layout and Cover design: Yuanyuan Zeng & Jie Sheng

Printed by: Ridderprint BV, www.ridderprint.nl

Copyright © 2020 by Jie Sheng

No part of this thesis could be reproduced, stored in a retrieval system, or transmitted in any form without permission of the author. For the copy rights of articles that have been accepted for publication, please refer to the policy of the respective journals.

Chapter 1

General introduction

1 Protein folding

Proteins can be considered as the workhorses of the cell, controlling functions in essentially all biological processes that enable life. Due to their complex three-dimensional structures, proteins can execute their functions in a highly specific manner. A polypeptide chain synthesized on a ribosome is, however, intrinsically unfolded and acquires a three-dimensional conformation during and after synthesis. This process is referred to as protein folding, which involves a stochastic search of many conformations accessible to a polypeptide chain rather than a series of mandatory steps between specific partially folded states (Dobson, 2003). Thus, diverse intermediates exist during the protein folding process, including unfolded and partially folded proteins. Also between the time of synthesis and degradation, proteins can adopt a multitude of possible conformations within a living system (Chiti and Dobson, 2006).

Proteins correctly folded into their native state are energetically stable in crowded biological environments and are able to interact with natural partners to fulfill their physiological roles (Chiti and Dobson, 2006; Dobson, 2003). To guarantee correct protein folding, various factors including chaperones and folding catalysts are present to guide folding steps and to prevent unproductive interactions of folding intermediates with other molecules (Christis et al., 2008). Failure of a protein to acquire its native structure enhances the generation of a fully or partially unfolded protein (Chandel et al., 2018). In incompletely folded proteins, regions that are normally buried in the native state may become exposed to the solvent, making them prone to interact inappropriately with other molecules and/or vulnerable to aggregation (Chiti and Dobson, 2006). The nature of protein aggregates can be either disordered, with an amorphous morphology, or ordered, with a highly ordered arrangement, as exemplified by amyloids (Chiti and Dobson, 2017).

2 Amyloids

2.1 Introduction

Amyloids are highly structured protein aggregates found in all kingdoms of life (Tayeb-fligelman et al., 2017). The formation of amyloid fibrils is triggered by (partial) unfolding or misfolding of soluble proteins/peptides, which then self-assemble into insoluble fibers that are largely resistant to degradation (Chiti and Dobson, 2006, 2017). Amyloidosis is the accumulation of pathogenic amyloids and each disease is characterized by aggregation of specific proteins and/or peptides (Chiti and Dobson, 2017). Well-known examples of amyloid

diseases include Alzheimer's disease, Parkinson's disease, Diabetes type 2 and spongiform encephalopathies (*e.g.* Mad cow disease) (Chiti and Dobson, 2006, 2017).

Typically, amyloid fibrils are around 5-15 nm in width and several micrometers in length, containing a cross β -sheet structure (Toyama and Weissman, 2011). Amyloid-forming proteins or peptides can initially be intrinsically disordered (*e.g.* islet amyloid polypeptide (IAPP), tau, α -synuclein), partially folded or natively folded (*e.g.* β 2-microglobulin, transthyretin) (Chiti and Dobson, 2017). Oligomers formed during initial aggregation are relatively small and unstable clusters that can dissociate due to relatively weak intermolecular interactions. With aggregation proceeding, these oligomers undergo internal structural rearrangements, yielding stable structures that are larger in size and enriched in β -sheet structures (Chiti and Dobson, 2017). Further growth through the addition of monomers is accompanied by additional, sometimes dramatic structural reorganizations, eventually leading to the formation of highly ordered fibrils (Figure 1) (Chiti and Dobson, 2017). Amyloid fibrils are defined by a cross- β sheet architecture, in which β -strands are oriented perpendicularly to the fibril axis (Figure 1) (Toyama and Weissman, 2011). Amyloid-specific dyes, such as Thioflavin T (ThT) and Congo Red, are commonly used to identify the presence of amyloid fibrils (Groenning, 2010; Yakupova et al., 2019). The combined presence of these features (specific tinctorial properties, fibrillar morphology, cross- β structure) are required for protein aggregates to be classified as amyloid fibrils (Chiti and Dobson, 2017). Disordered or (partially) native-like aggregates can also grow without major structural conversion into large amorphous or native-like aggregates (Figure 1) (Chiti and Dobson, 2006). A single protein can even form fibrils with different morphologies depending on the environmental conditions (Anderson et al., 2006; Petkova et al., 2005). Recently, fibrils were discovered in bacteria with a cross- α architecture that shares morphological and tinctorial characteristics with canonical cross- β amyloids (Tayeb-fligelman et al., 2017).

The assembly of proteins or peptides into highly ordered amyloid fibrils is a complex and dynamic process. Amyloid formation generally proceeds via a nucleated growth mechanism (Figure 2A), typically consisting of a lag phase, an elongation phase and a plateau phase (Alam et al., 2017; Chiti and Dobson, 2006). During the lag phase, the oligomeric nucleus, or seed, is formed, which is usually thermodynamically unfavorable (Chatani and Yamamoto, 2018) and thus determines the rate of amyloid formation. Once the nucleus is formed, fibril growth proceeds rapidly by further association of monomers to the nucleus. This elongation phase is thermodynamically highly favorable (Alam et al., 2017; Chiti and Dobson, 2006).

Secondary nucleation is an additional mechanism of fibril growth that requires the presence of pre-existing fibrils formed through the primary nucleated growth pathway (Figure 2B) (Cohen et al., 2013; Gaspar et al., 2017). Pre-existing fibrils can *e.g.* catalyse nucleation of monomers on their surface or form new nuclei by fragmentation (Gaspar et al., 2017).

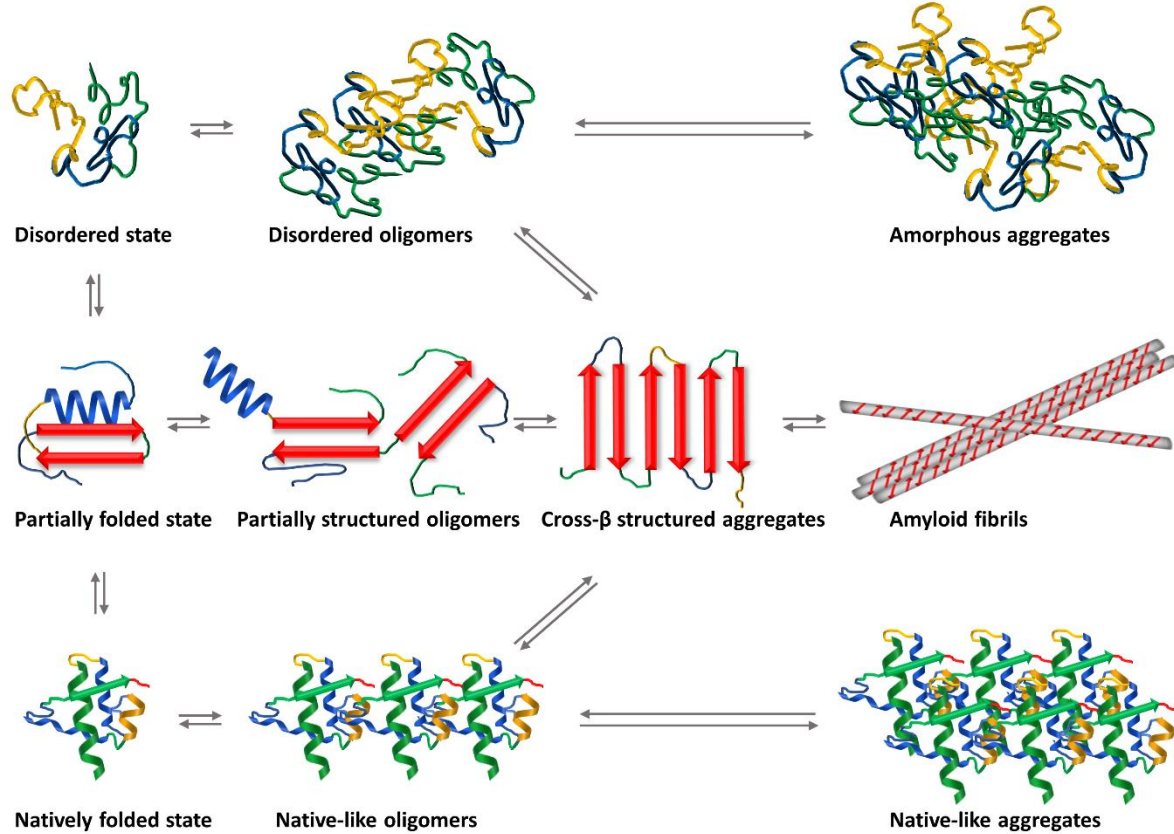


Figure 1. Schematic illustration of protein aggregation. Intrinsically disordered, partially folded or natively folded protein initially generate disordered, partially structured or native-like oligomers, respectively. With aggregation proceeding, these oligomers undergo internal structural rearrangement yielding stable structures with an increased β -sheet content. Further growth results in the formation of highly ordered amyloid fibrils. Disordered or native-like oligomers can grow without major structural conversion into large amorphous or native-like aggregates. Modified from Chiti and Dobson, 2017.

In the case of amyloid formation by globular proteins, partial unfolding is required for exposure of aggregation-prone regions that are hidden within the native structure (Grignaschi et al., 2018; Saad et al., 2017; Saldaño et al., 2017; Zhao et al., 2013). However, it is now evident that very small local fluctuations within the native structure of globular proteins can already be sufficient to trigger native-like aggregation, which can convert into amyloid-like oligomers and fibrils (Chattopadhyay et al., 2015; Grignaschi et al., 2018) (Figure 2C).

Domain swapping is another mechanism for the formation of native-like aggregates that can convert into amyloid fibrils (Jaskólski, 2001; Jurczak et al., 2016). It involves a structural element of a monomeric protein that is replaced by the same element from another monomer of the same protein. In this process, partial unfolding of closed monomers is followed by

adhesion and reconstruction of the original fold with elements from different monomers (Jaskólski, 2001) (Figure 2D).

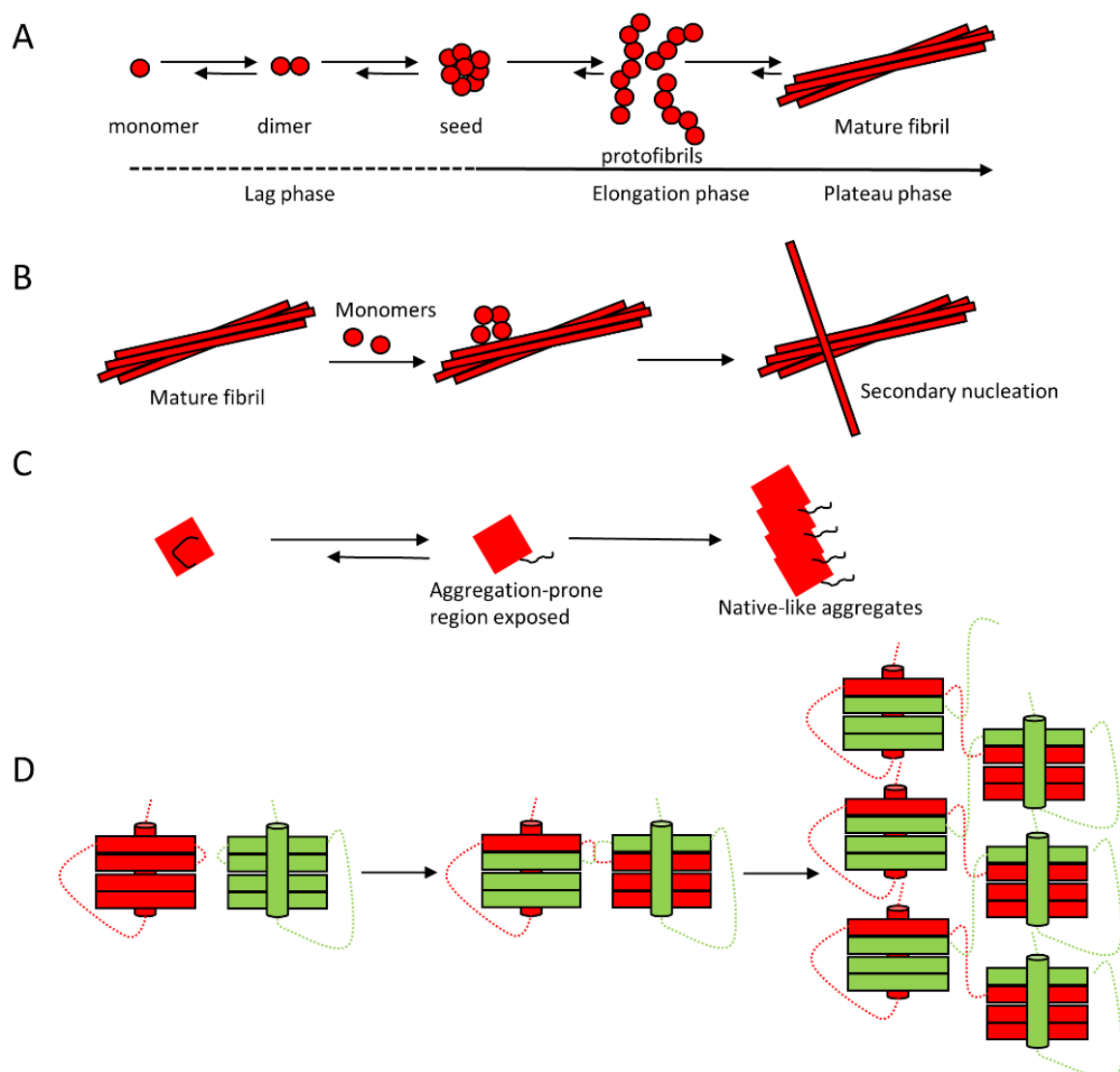


Figure 2. Mechanisms of protein amyloid formation. Different mechanisms have been described for the formation of amyloid fibrils including (A) "Nucleated growth" pathway; (B) Secondary nucleation pathway; (C) Conformational transition pathway; (D) 3D domain swapping pathway. Modified from Kumar et al., 2011, Verma et al., 2015, Grignaschi et al., 2018, and Janowski et al., 2001.

2.2 Pathological and functional amyloids

Amyloids are strongly associated with physiological disorders. To date, about 50 amyloid-forming peptides or proteins have been identified that give rise to an even greater number of diseases including Alzheimer's Disease (AD) (Murphy and III, 2010), Parkinson's Disease (PD) (Irwin et al., 2013), Huntington's Disease (McGowan et al., 2000), Prion Disease (Ghetti et al., 1996), Amyotrophic Lateral Sclerosis (ALS) (Kerman et al., 2010), and Diabetes type II (Marzban et al., 2003). These diseases are characterized by the formation of extracellular deposition of amyloid fibrils (plaques) or intracellular inclusions with amyloid-like properties,

and in each case the disease-specific protein(s) are the predominant components of the deposits (Chiti and Dobson, 2006).

There is still a lack of detailed understanding of the cause(s) of amyloid formation in many of these diseases. Numerous genetic and environmental factors can facilitate aberrant protein aggregation (Alam et al., 2017). Familial forms of amyloid-related diseases are often linked to specific mutations which increase the propensity of a protein to aggregate (Alam et al., 2017; Blokhuis et al., 2013; Saldaño et al., 2017). Environmental factors, such as temperature, pH, and oxidative stress, can damage protein stability and lead to aggregation (Alam et al., 2017; Cheignon et al., 2018; Milto et al., 2014; Skoulakis and Goodfellow, 2003). To guarantee proper functioning of proteins in the cell, several strategies are involved in protecting against protein aggregation (Alam et al., 2017). Chaperones (*e.g.* Hsp70, Hsp100 and Hsp104) are involved in refolding and reactivating of aggregated proteins (Haslberger et al., 2008; Tessarz et al., 2008; Ungelenk et al., 2016; Zietkiewicz et al., 2004). Hsp70 can disaggregate α -synuclein fibrils *in vitro* within minutes (Gao et al., 2015). In higher eukaryotes, only limited refolding activity exists and therefore, degradation of misfolded proteins by proteases is important to prevent protein aggregation (Alam et al., 2017; Goldberg, 2003). Autophagy is another alternative route to clear up aggregated proteins, such as those formed by TDP-43, α -synuclein, tau and A β (Barmada et al., 2014; Cho et al., 2014; Falcon et al., 2018; Webb et al., 2003). During aging, these protein quality-control systems become exhausted, causing cells to lose the ability to degrade and reactivate misfolded and aggregated proteins. This may explain the close association of amyloid pathology with age-related neurodegenerative diseases (Alam et al., 2017; Cohen and Dillin, 2009; Morley et al., 2002).

Amyloid fibrils are commonly deposited in the extracellular space of tissues and organs. The accumulation of amyloid fibrils in various organs or tissues can cause cell degeneration and loss of functions (Chiti and Dobson, 2017; Verma et al., 2015). However, there is an increased understanding that pathogenicity in neurodegenerative amyloid-related diseases arises from oligomeric intermediates generated during the aggregation process (Chiti and Dobson, 2017; Verma et al., 2015). Oligomeric intermediates generated during amyloid fibril formation are structurally heterogeneous and have a transient nature (Chiti and Dobson, 2006, 2017). The high toxicity of these oligomers compared to mature fibrils is thought to be due to the exposure of hydrophobic patches on the surface of oligomers (Chiti and Dobson, 2017). In oligomers, these patches are more abundantly present than in fibrils, enhancing the chance of interaction with cellular molecules (Lasagna-Reeves et al., 2012; Lee et al., 2018; Verma et al., 2015).

Moreover, the small size of oligomers makes it relatively easy to diffuse through cells and tissues (Lambert et al., 1998; Verma et al., 2015). They can also target cellular membranes, resulting in membrane permeabilization, enhanced Ca^{2+} influx, oxidative stress, and cell death (Demuro et al., 2005; Kaye et al., 2004). Finally, toxic species can be transmitted between cells and amplified via prion-like mechanisms that is commonly found in many neurodegenerative diseases (Frost and Diamond, 2010). In these mechanisms, known as templated conformation change, the non-pathogenic form of prion protein (PrP^{C}) is induced to misfold when it comes into contact with a pathogenic conformation of prion protein (PrP^{Sc}) (Frost and Diamond, 2010).

In recent years, increasing evidence emerged that the presence of amyloid is not strictly related to pathogenesis, but is also involved in physiological processes. The amyloid structures enable their use as scaffolds for biochemical activities, and the compact nature of amyloid makes it ideal as a means for protein storage (Jackson and Hewitt, 2017). Functional amyloids have been discovered in a variety of processes, such as the storage of peptide hormones (Jacob et al., 2016; Maji et al., 2009), fertilization (Egge et al., 2015; Hewitson et al., 2017; Roan et al., 2017), pigmentation (Bissig et al., 2016), necroptosis (Liu et al., 2017), antimicrobial responses (Jang et al., 2011), adaptation to stress (Audas et al., 2016; Saad et al., 2017), cellular dormancy (Woodruff et al., 2018), protection of bacteria from stress (Van Gerven et al., 2015), regulation of fungal-host and fungal-fungal interactions (Lipke et al., 2012), modulation of epigenetic heritable phenotypes in yeast (Alberti et al., 2009), and persistence of long-term memory in *Drosophila* (Majumdar et al., 2012). Recent studies describe the presence of reversible non-membrane-bound organelles in the cell, which are biomolecular condensates with characteristics of functional amyloids (Banani et al., 2017; Woodruff et al., 2018). For example, Balbiani bodies are amyloid-like cages sequestering RNA, proteins and membranous organelles. They exist in dormant oocytes and disappear when oocytes start their maturation process (Boke et al., 2016; Pepling et al., 2007). Amyloid bodies are a second example of solid phase biomolecular condensates consisting of physiological, reversible amyloids that promote cellular dormancy under stress (Audas et al., 2016; Woodruff et al., 2018).

In contrast to pathogenic amyloidogenesis, the intermediates produced during functional amyloid formation have not been observed to cause toxicity to cells (Jackson and Hewitt, 2017). However, functional amyloids are not intrinsically non-toxic (Bissig et al., 2016; Jackson and Hewitt, 2017; Kerje et al., 2004; Maji et al., 2009; Watt et al., 2011). Increasing evidence indicates that the assembly of functional amyloids is highly regulated to avoid the toxicity of

prefibrillar oligomers to cells. Several protective mechanisms have been proposed, including regulation of the expression of amyloidogenic proteins, minimizing the generation of prefibrillar oligomers, rapid disassembly of amyloid fibrils to monomers and sequestering the amyloid aggregation within membrane bound compartments (Jackson and Hewitt, 2017).

The differences between functional and pathological amyloids are not clear-cut. Firstly, there are many structural similarities between the two types of amyloids. For example, functional amyloids formed by yeast pyruvate kinase Cdc19 share several structural features with dysfunctional amyloids formed by human insulin or A β 42, including a β -sheet structure, thermodynamic stability, and the ability to be stained by the thioflavin T dye (Grignaschi et al., 2018). One hypothesis is that physiologically relevant protein aggregation might be a precursor of pathological events, but the exact relationship between physiological and pathological aggregates is unclear (Cereghetti et al., 2018). Secondly, there are now clear indications for the presence of so-called “Amyloid-disaggregase machineries” that can inhibit or safely reverse misfolded oligomers and amyloids. These findings suggest that also disease-associated amyloids, like functional amyloids, do not necessarily represent terminal, irreversible protein aggregates (Chuang et al., 2018; Mack and Shorter, 2016). Several intracellular strategies (*e.g.* autophagy, the ubiquitin-proteasome system (UPS), molecular chaperones and protein disaggregases) are utilized to degrade toxic oligomers and amyloids (Chuang et al., 2018; Gautam et al., 2017).

2.3 Factors involved in modulating protein amyloid formation

The ability to form amyloid fibrils is now regarded as a generic property of most, if not all polypeptides. This idea was first postulated when proteins that were not associated with any amyloid disease, formed amyloid fibrils under a variety of non-physiological conditions (Chiti et al., 1999; Guijarro et al., 1998). It was reinforced by the generation of mixed fibrils comprising of two unrelated peptides (Macphee and Dobson, 2000). The generic nature of proteins to form amyloid fibrils can be attributed to the fundamental physicochemical properties of the polypeptide chain which is capable of forming strong hydrogen bonds (Macphee and Dobson, 2000). Natively folded globular proteins have little tendency to aggregate because the peptide backbone is involved in a series of stabilizing interactions and aggregation-prone segments such as clusters of hydrophobic amino acids are inaccessible for intermolecular interactions (Chiti et al., 2000; Macphee and Dobson, 2000). Destabilizing factors such as amino acid mutations, low pH, shear forces and high temperature, can cause the exposure of

aggregation-prone regions in partially unfolded proteins (Chiti et al., 2000; Grignaschi et al., 2018; Saad et al., 2017; Saldaño et al., 2017; Zhao et al., 2013).

Interactions with other biomolecules can play also a crucial role in promoting protein amyloid formation (Bekard and Dunstan, 2009; Cheignon et al., 2018; Milto et al., 2014; Saldaño et al., 2017; Skoulakis and Goodfellow, 2003; Yoshimura et al., 2012). Consequently, amyloids are often part of heterogeneous composites *in vivo*, containing *e.g.* lipids/membranes, glycosaminoglycans (GAGs), nucleic acids and/or metal ions, as will be discussed below.

2.3.1 Lipids/Membranes

The interaction of amyloidogenic proteins with membranes has been investigated for two main reasons: Membranes favor the formation of amyloid and, in turn, this process can damage membranes, which is considered to be a main mechanism of amyloid toxicity (Relini et al., 2014). The membrane surface provides a platform for proteins that reduces their three-dimensional distribution in solution to a two-dimensional surface upon binding, causing the bound proteins to reach much higher local concentrations (Kinnunen, 2009). Upon binding, the amphipathic nature of lipids allows electrostatic as well as hydrophobic interactions with proteins, which favors conformational changes leading to oligomerization and eventually fibril formation (Kinnunen, 2009; Relini et al., 2014). Different factors, such as the lipid composition and the presence of membrane microdomains, enriched in cholesterol and sphingolipids, provide the membrane with the physicochemical properties that govern the structural state of proteins (Kinnunen, 2009).

The interaction of oligomers and amyloid fibrils with membranes changes the membrane organization and dynamics (Relini et al., 2014). Prefibrillar aggregates, rather than mature fibrils, are detrimental to membrane integrity (Andreasen et al., 2015; Relini et al., 2014). Amyloid aggregates can form pores or well-organized channels in the bilayer of membranes, resulting in membrane depolarization and Ca^{2+} leakage (Relini et al., 2014). Amyloid-induced membrane permeabilization can also be due to the disassembly of lipid bilayer organization, causing membrane defects and/or thinning (Relini et al., 2014).

2.3.2 GAGs

Glycosaminoglycans (GAGs) are long, unbranched polysaccharides containing repeating disaccharide units with a high negative-charge density. GAGs are abundant on the surface of cells or in the extracellular matrix (ECM) of multicellular organisms (Bishop et al., 2007). They

are divided into non-sulfated and sulfated GAGs. Hyaluronic acid (HA) belongs to non-sulfated GAGs, whereas chondroitin sulfate (CS), dermatan sulfate (DS), keratan sulfate (KS), heparin and heparan sulfate (HS) belong to sulfated GAGs. GAGs play essential roles in cellular and tissue homeostasis, pathogenesis and regeneration (Almond, 2018; Kamhi et al., 2013; Yamada et al., 2011). GAGs, especially HS and its highly sulfated derivative heparin can induce amyloid formation of a variety of proteins/peptides, including A β , tau, α -synuclein, gelsolin, β 2-microglobulin and IAPP (Ariga et al., 2010; Cohlberg et al., 2002; Iannuzzi et al., 2015; Potter et al., 2015; So et al., 2017; Solomon et al., 2011). Heparin has been shown to accelerate the formation of fibrils, to enhance their stability and to decrease amyloid toxicity by favoring benign aggregation pathways (Vilasi et al., 2011). Heparin can also induce amyloid formation in polypeptides with low intrinsic propensity to aggregate (Madine et al., 2013). Electrostatic interactions are important in heparin-protein interactions (Iannuzzi et al., 2015). Moreover, heparin can act as a scaffold increasing local protein concentrations and changing their orientation. Together, these effects can promote protein oligomerization and fibril formation (Motamedi-Shad et al., 2009).

2.3.3 Metal ions

Metals play diverse roles in biological processes. A variety of metal ions such as manganese, magnesium, iron, copper and zinc, can be incorporated into proteins, serving a structural or functional purpose (Barnham and Bush, 2014). Metal ions can also play a physiological role in the regulation of protein oligomerization and are intimately associated with both pathological and functional amyloid formation (Jacob et al., 2016; Joppe et al., 2019; Kawahara et al., 2017; Kim et al., 2018; Liu et al., 2016; Sirangelo and Iannuzzi, 2017). Metal ions can facilitate protein oligomerization and/or aggregation in several ways. Metal binding can stabilize a conformation within an intrinsically disordered protein or induce a conformational rearrangement within a natively folded protein, yielding specific aggregation-prone conformers (Leal et al., 2012). Furthermore, metal ions can neutralize specific charged residues or bridge protein units, favoring the formation of aggregates (Leal et al., 2012). Iron, zinc and copper are the three most abundant trace metals in organisms, with 3-5 g, 2-4 g and 75-100 mg total amounts in the human body, respectively (Milto et al., 2016; Osredkar and Sustar, 2011). Dyshomeostasis of these biometals is related to several neurodegenerative diseases (Joppe et al., 2019; Kawahara et al., 2017; Kim et al., 2018; Sirangelo and Iannuzzi, 2017; Stelmashook et al., 2014). The balance between zinc and copper, rather than their absolute concentrations, seems critical for proper functioning of many proteins (Osredkar and Sustar, 2011). For

instance, a disbalance of zinc and copper homeostasis leads to structural alterations in amyloid precursor protein (APP), causing aberrant processing by secretases (Gerber et al., 2017). This results in the elevated production of cytotoxic A β peptides involved in Alzheimer's disease (Budimir, 2011; Gerber et al., 2017; Lee et al., 2014; Stelmashook et al., 2014). Superoxide dismutase 1 (SOD1), which plays a major role in ALS, requires the binding of both Zn²⁺ and Cu²⁺ as cofactors for structural stability and proper functioning (Sirangelo and Iannuzzi, 2017). Furthermore, dyshomeostasis of redox-active metals such as iron and copper also generates reactive oxygen species (ROS), which can trigger protein aggregation and cellular toxicity (Joppe et al., 2019).

3 CAP superfamily

3.1 Introduction

The CAP superfamily of proteins consists of three subfamilies: cysteine-rich secretory (CRISP) proteins, antigen 5 (Ag5), and pathogenesis-related 1 (PR-1) proteins (Gibbs et al., 2008) (Figure 3A). CAP superfamily members are present in a wide variety of species, including animals, plants and microorganisms (Gibbs et al., 2008). CRISP proteins are enriched in the mammalian male reproductive tract and in the venom of vertebrate like snakes and lizards (Koppers et al., 2011; Yamazaki and Morita, 2004). Ag5 proteins exist in venom that is produced in the secretory ducts of numerous stinging insects and can elicit a strong allergenic response in humans (Calvo et al., 2007; Charlab et al., 1999; Hoffman, 1985a; King and Spangfort, 2000; Mans et al., 2008; Valenzuela et al., 2002). PR-1 proteins are dramatically up-regulated in response to the pathogen infection in plants (Breen et al., 2017).

CAP superfamily members are characterized by the presence of a common CAP domain, also known as sperm coating protein (SCP) domain (Gibbs et al., 2008). Most CAP proteins are synthesized with an N-terminal signal peptide for secretion into the extracellular space, exhibiting endo- or paracrine functions (Gibbs et al., 2008). The majority of CAP superfamily proteins also contain C-terminal extensions (Figure 3B). These include a variety of domains (*e.g.* the cysteine-rich domain (CRD), C-type lectin (CTL) domain, transmembrane domains, limulus factor C, Coch-5b2, and Lgl1 (LCCL) domains), all of which contribute to the functional diversity of CAP superfamily proteins, allowing a role in diverse processes ranging from reproduction, cancer to immune defense (Breen et al., 2017; Gibbs et al., 2008).

3.2 CAP subfamilies

3.2.1 CRISP proteins

CRISP proteins are found in the mammalian reproductive system and in a variety of snake venoms (Koppers et al., 2011; Ros et al., 2015; Shikamoto et al., 2005; Suzuki et al., 2008; Wang et al., 2005, 2010). In addition to the structurally conserved CAP domain, CRISP proteins contain an N-terminal signal peptide and a CRD (Gibbs et al., 2008; Koppers et al., 2011; Ros et al., 2015). CRISP proteins are characterized by 16 cysteine residues, 6 of which are in the CAP domain and 10 in the CRD (Koppers et al., 2011; Ros et al., 2015; Shikamoto et al., 2005; Suzuki et al., 2008; Wang et al., 2005, 2010). All the cysteines participate in intradomain disulfide bonds (Guo et al., 2005; Koppers et al., 2011; Shikamoto et al., 2005; Wang et al., 2005). Within the CRD, there is an ion channel regulatory region (ICR) that is connected to the CAP domain via a hinge (Gibbs et al., 2008) (Figure 3B). A relatively high rotational freedom exists between the hinge and the ICR (Gibbs et al., 2006).

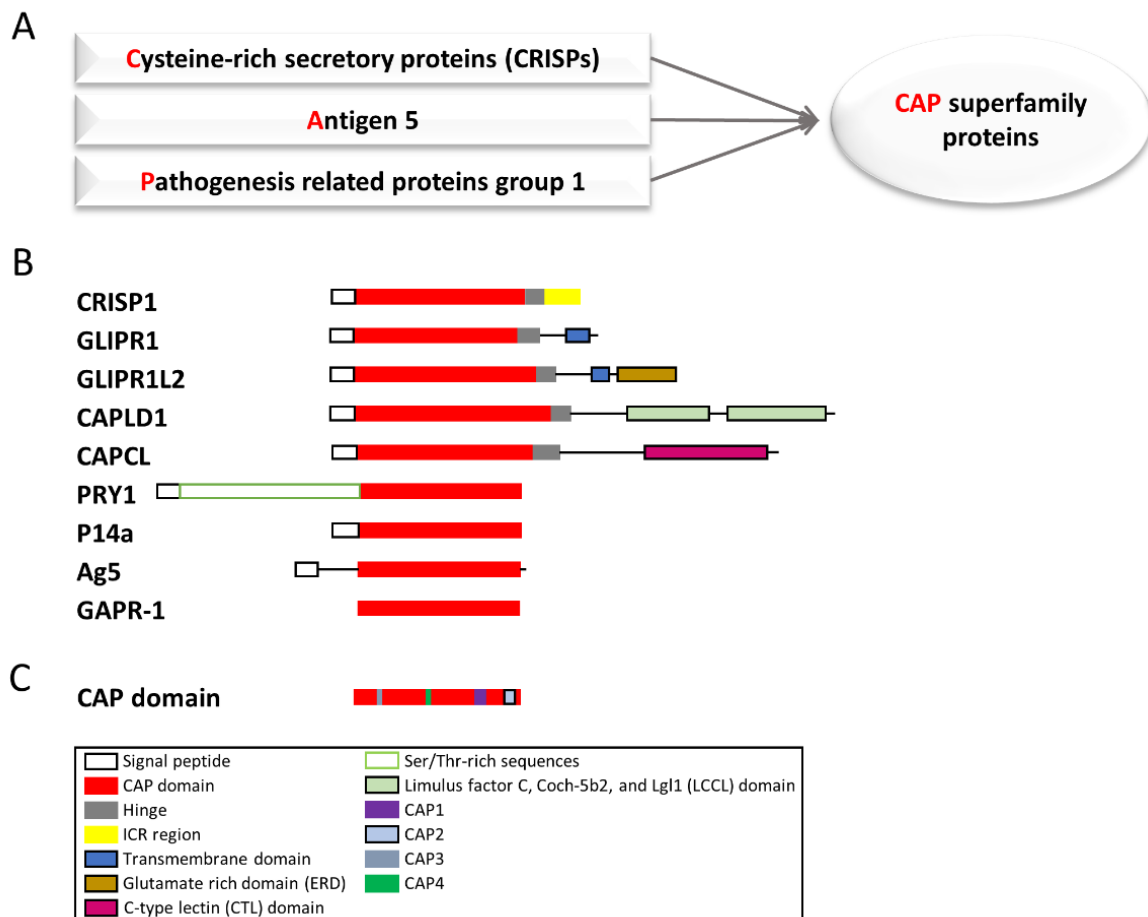


Figure 3. The CAP superfamily of proteins. (A) CAP superfamily proteins are composed of Cysteine-rich secretory proteins, Antigen 5, and Pathogenesis related proteins group 1; (B) Most CAP superfamily proteins consist of a conserved CAP domain, an N-terminal signal peptide and a C-terminal extension. GAPR-1 is the only CAP member consisting exclusively of a CAP domain; (C) Conserved CAP motifs in the CAP domain. Modified from Gibbs et al., 2008, and Darwiche et al., 2018.

In mammals, there are four CRISPs present, named CRISP1, CRISP2, CRISP3 and CRISP4 (Gibbs et al., 2008; Koppers et al., 2011; Ros et al., 2015). Whereas CRISP4 has only been reported in rodents such as rat (Nolan et al., 2006) and mouse (Jalkanen et al., 2005), the other three CRISP proteins are more generally expressed and have been found in *e.g.* humans (Busso et al., 2005; Hayashi et al., 1996; Kjeldsen et al., 1996), horses (Giese et al., 2002a, 2002b; Schambony et al., 1998), guinea pigs (Hardy et al., 1988), mice (Evans et al., 2015; Kasahara et al., 1989; Rankin et al., 1992) and rats (Maeda et al., 1998; Roberts et al., 2008). CRISP1 is expressed by the epithelia of epididymis and secreted to the lumen where it binds to the sperm surface during spermatozoa maturation (Ros et al., 2015). CRISP2 is specifically expressed in the testis and localizes to the acrosome, the connecting piece, and outer fibers of the sperm tail (Koppers et al., 2011). CRISP3 is broadly expressed and except the reproductive tract, CRISP3 is also present in lacrimal gland, salivary gland, pancreas, spleen, thymus, neutrophils and submandibular gland (Gibbs et al., 2008). CRISP3 expressed by cells in the prostate is present in seminal vesicles and seminal plasma (Koppers et al., 2011), and associates to sperm surface during ejaculation (Koppers et al., 2011; Ros et al., 2015). CRISP3 expression is significantly deregulated in- and a (potential) biomarker for- several forms of cancer, such as prostate cancer, oral squamous cell carcinoma and multiple myeloma (Gibbs et al., 2008). CRISP4 is found in epididymis and its function is believed to be quite similar to CRISP1 (Jalkanen et al., 2005; Nolan et al., 2006). CRISP proteins play diverse roles in mammalian fertilization, including cell-cell fusion, protection of the ejaculated sperm cells against premature activation, involvement in interactions with the oviduct and cumulus oocyte complex, sperm motility regulation, chemo-attractant of sperm, *etc* (Bjartell et al., 2007; Burnett et al., 2011; Cohen et al., 2011; Gibbs et al., 2011; Jalkanen et al., 2005; Maeda et al., 1998; Novak et al., 2010; Turunen et al., 2012). However, the molecular mechanism of action of CRISP proteins in these processes remain to be established.

3.2.2 Ag5 proteins

Ag5 proteins are found in numerous venomous insects where they play a key role in modulating the host immune response (Ameri et al., 2008; Calvo et al., 2007; Charlab et al., 1999; Hoffman, 1985b; King and Spangfort, 2000; Kovalick et al., 1998; Mans et al., 2008; Valenzuela et al., 2002). Ag5 proteins are one of the most ubiquitous classes of salivary proteins in hematophagous animals (Assumpção et al., 2013). The biological function of this subfamily members remains largely unknown. Recent studies revealed that members of this subfamily are metal-binding proteins with pro- or antioxidant activities (Assumpção et al., 2013).

3.2.3 PR-1 proteins

PR-1 proteins are ubiquitously expressed across plant species and are among the most abundant proteins produced in response to pathogen infection (Breen et al., 2017). Moreover, PR-1 proteins are involved in abiotic stress responses, such as drought, cold temperature and salt stress (Liu et al., 2013; Seo et al., 2008, 2010). PR-1 proteins are also suggested to play a role in plant growth and development (Lotan et al., 1989; Memelink et al., 1990). Sterol binding, antimicrobial function, defense signal amplification and pathogen effector recognition are suggested functions of these proteins (Breen et al., 2017).

3.3 CAP domain

The CAP domain contains four conserved CAP motifs, termed CAP1-4 (Gibbs et al., 2008) (Figure 3C). The presence of these CAP motifs and the resultant CAP domain are characteristic for (and define) this protein superfamily (Gibbs et al., 2008).

The CAP motifs contribute to a conserved tertiary core structure with a unique α - β - α sandwich, in which α -helices flank a central antiparallel β -sheet (Gibbs et al., 2008). This α - β - α fold is stabilized by a buried hydrogen bond network and, in some cases, also by several disulfide bonds (Gibbs et al., 2008). The CAP domain contains approximately 150 amino acids, and alignment of the amino acids shows that ~30 are conserved or homologous (Finn et al., 2006). These conserved amino acids are mainly localized in the four CAP motifs (Gibbs et al., 2008). Except these four conserved motifs, there is little sequence homology within the CAP domain of superfamily members (Gibbs et al., 2008). The CAP domain contains a conserved central cavity (Gibbs et al., 2008) (Figure 4). This central cavity contains two histidine residues and two acidic amino acids which are usually glutamic acid (Gibbs et al., 2008). Several CAP superfamily members are shown to interact with different metal ions via the conserved central cavity (Assumpção et al., 2013; Darwiche et al., 2016; Maldera et al., 2011; Shikamoto et al., 2005; Suzuki et al., 2008). Altogether, the structural properties of CAP domain suggest a structure-related molecular mechanism of the CAP domain in regulating the function of CAP superfamily members.

Several functions have been suggested for the CAP domain: protease activity in the venom duct of a cone snail (Milne et al., 2003), lipid binding and export activity of yeast CAP proteins and PR-1 proteins (Breen et al., 2017; Choudhary and Schneider, 2012; Darwiche et al., 2018), inhibitor of integrin function and anti-inflammatory scavenger of eicosanoids in the saliva of blood-feeding insects (Xu et al., 2012), negative regulation of autophagy (Olrichs et al., 2014), and inhibitor of collagen-induced platelet aggregation in the salivary gland of bloodsucking insects (Assumpção et al., 2013). However, the exact role of CAP domain present in the wide range of superfamily members has largely remained elusive.

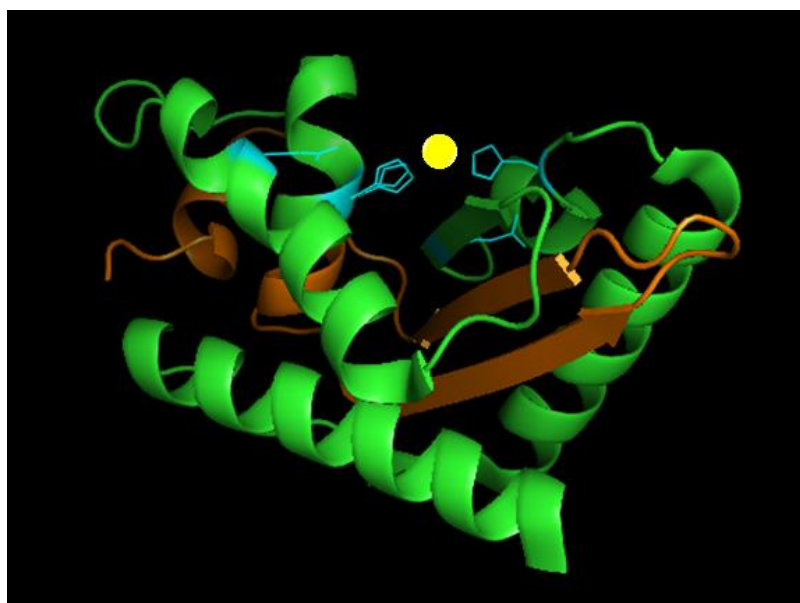


Figure 4. The crystal structure of GPR-1. CAP1 and CAP2 motifs are present in the C-terminal part of GPR-1 and are highlighted in orange. The two conserved histidines and two conserved glutamic acids within the central cavity are shown in blue. Yellow represents the predicted position of a putative metal ion (not present in the crystal structure). The three-dimensional structure of GPR-1 was generated using **1SMB (PDB file)** (Serrano et al., 2004) and PyMOL for molecular graphics visualization.

3.4 GPR-1

Golgi-Associated plant Pathogenesis Related protein 1 (GPR-1), also known as GLIPR2 or C9orf19, is a mammalian CAP protein of 17 kDa that has an unusually high pI of 9.4 (Eberle et al., 2002). According to phylogenetic analysis, the GPR-1 subfamily is suggested to be the most ancient family member in vertebrates and the earliest family member to diverge from bacterial family members during evolution (Abraham and Chandler, 2017). The first mammalian CAP proteins most likely belonged to this GPR-1 subfamily (Abraham and Chandler, 2017; Gibbs et al., 2008; Olrichs and Helms, 2016). Structurally, GPR-1 can be considered a functional CAP unit: among CAP superfamily proteins, GPR-1 is the only member which consists almost exclusively of a CAP domain without an N-terminal (signal)

peptide or C-terminal extension (Eberle et al., 2002) (Figure 3B). Therefore, GAPR-1 is a suitable model to study the structure-function relationship of the CAP domain (Olrichs and Helms, 2016).

GAPR-1 is associated with lipid-enriched microdomains at the cytosolic leaflet of Golgi membranes (Eberle et al., 2002). GAPR-1 is highly expressed in immune-related tissues and cells, such as the lung, monocytes, uterus, spleen and embryonic tissue (Eberle et al., 2002). These observations could suggest that GAPR-1 at the Golgi complex fulfills a role in immunity that is comparable to the role of PR-1 proteins in plants. In fibrotic kidney, GAPR-1 expression is significantly increased and it was shown to promote epithelial to mesenchymal transition *in vitro* in a renal epithelial cell line (Baxter et al., 2007). More recently, GAPR-1 was discovered to regulate type I interferon signaling pathway in response to Toll-like receptor 4 activation (Zhou et al., 2016). GAPR-1 also acts as a negative regulator of autophagy (Shoji-Kawata et al., 2013). Autophagy is an intracellular bulk degradation system that also plays an important role in the immune system (Kuballa et al., 2012). GAPR-1 negatively regulates autophagy by interacting with Beclin 1, an autophagy inducer (Shoji-Kawata et al., 2013). In this process, GAPR-1 is suggested to tether Beclin 1 to the Golgi apparatus and as a result, prevent Beclin 1 to function in autophagy (Shoji-Kawata et al., 2013). The exact molecular mechanism of how GAPR-1 participates in these biological functions remains, however, largely unclear.

GAPR-1 interacts in various ways with biological membranes. GAPR-1 interacts with negatively charged phospholipids, due to its highly positive charge. It has a special preference for phosphatidylinositol (PI) with remarkable binding characteristics (Van Galen et al., 2010). GAPR-1 can also directly interact with caveolin-1 on Golgi membranes (Eberle et al., 2002). Together with its N-terminal myristylation, GAPR-1 is strongly associated to raft-like lipid microdomains in the Golgi membrane (Van Galen et al., 2010).

Another notable property of GAPR-1 is its strong tendency to form homodimers. GAPR-1 forms homodimers on Golgi membranes (Serrano et al., 2004) and recombinant GAPR-1 crystallizes as a dimer (Groves et al., 2004). GAPR-1 also dimerizes in the presence of inositol hexakisphosphate (IP6) (Van Galen et al., 2012). Compared to the crystal structure of GAPR-1 in the absence of IP6, there are no major conformational changes within GAPR-1 monomeric units in the presence of IP6. However, in the crystallographic dimer, one of the monomeric subunits is rotated by 28.5 degrees. Mutants representing the alternative dimeric structures differ in membrane-tethering properties, indicating a regulatory mechanism of GAPR-1

interaction with lipid bilayers via homodimerization (Van Galen et al., 2012). In this respect, it is interesting to note that the dimeric/oligomeric state of GAPR-1 could also be related to its interaction with Beclin 1. Beclin 1 is suggested to bind to the equatorial groove of GAPR-1 which consists of five conserved residues (Li et al., 2017). However, in the GAPR-1 pentad mutant, the equatorial groove of one monomer is partially occluded by the other, which could abrogate its interaction with Beclin 1 (Li et al., 2017).

GAPR-1 has the propensity to form amyloid-like fibrils by prolonged incubation with negatively charged liposomes (Olricks et al., 2014) (Figure 5). Additionally, GAPR-1 was shown to bind the anti-oligomer antibody A11, suggesting that its native conformation contains a fold that is also present in certain amyloid oligomeric intermediates (Olricks et al., 2014). In this respect it is interesting to note that the crystal structure of GAPR-1 dimer displays a continuous β -sheet extending beyond the monomeric subunits (Groves et al., 2004). GAPR-1 is not only able to form amyloids, but also possesses anti- β -amyloid aggregation activity (Olricks et al., 2014). GAPR-1 effectively inhibits A β fibril formation by binding to oligomeric A β structures *in vitro* (Olricks et al., 2014). There are indications that GAPR-1 is associated with amyloid-related diseases. GAPR-1 gene expression is associated with the development of diabetic neuropathy (Zhang et al., 2015). GAPR-1 is also detected in neonatally induced neurodegeneration in the rat hippocampus (Karlsson et al., 2015). However, it is not clear whether GAPR-1 amyloid formation or its anti-amyloid aggregation activity are directly involved in these diseases or whether these properties play a role in other function(s).

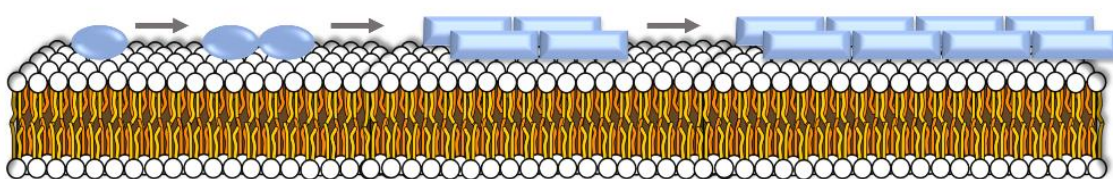


Figure 5. Scheme of GAPR-1 di/oligomerization on membranes. Upon binding of GAPR-1 monomers to membranes (blue ovals, left), GAPR-1 dimers, tetramers and higher molecular weight structures can be formed. Somewhere during the initiation process, subtle structural changes occur as are indicated by the transition to rectangular structures. Modified from Olricks and Helms, 2016.

3.5 Amyloidogenic properties of the CAP domain?

Analysis of structural determinants for the amyloidogenic propensity of GAPR-1 predicted amyloid-prone segments in the CAP1 and CAP2 motifs (Olricks et al., 2014). Due to the high conservation, CAP proteins from all taxa contain these potentially amyloidogenic segments within these signature motifs. This opens the possibility that a common function of the CAP

domain lies within this structural property (Olrichs and Helms, 2016). Several clues in literature provide support for this hypothesis.

Allurin, a truncated CRISP protein from the female tract of *Xenopus*, functions as a sperm chemoattractant (Burnett et al., 2008). Allurin was shown to be present in egg jelly (“egg water”) as stable, SDS- and 2-mercaptoethanol-resistant multimers (Sugiyama et al., 2009). Moreover, oligomerization of rat CRISP1 was regulated by Zn^{2+} binding and crucial for its association to spermatozoa during epididymal maturation (Maldera et al., 2011). Similar to GAPR-1, human CRISP2 forms ThT-positive structures via interaction with PI-containing liposomes (Olrichs et al., 2014). Natrin, a CRISP protein from snake venom, modulates inflammation via inducing expression of vascular endothelial cell adhesion proteins (Wang et al., 2010). This is proposed to involve heparan sulfate- and Zn^{2+} -dependent dimerization and/or oligomerization of natrin (Wang et al., 2010).

Less direct indications for the amyloidogenic propensity of CAP family members come from observations that a number of CAP family members were shown to dimerize. PR-1-type pathogenesis-related protein (PR-1-5) identified in wheat exists primarily as homodimers *in vitro* and is resistant to proteases. Interestingly, a PR-1-5 monomeric mutant revealed a diminished protease resistance (Lu et al., 2013). The dimeric PR-1-5 is able to interact with ToxA and is involved in ToxA-induced necrosis in sensitive wheat (Lu et al., 2014). Other CAP family members that were shown to form dimers include Fpr1 from *Fusarium oxysporum* (Prados-Rosales et al., 2012), and an *Ancylostoma*-secreted protein secreted by infective larvae of the human hookworm *Necator americanus* (Na-ASP-2) (Asojo et al., 2005). Several other CAP family members were shown to crystalize as stable dimers (*e.g.* an *Ancylostoma*-secreted protein from *Ostertagia ostertagi* (Oo-ASP-1) (Borloo et al., 2013), Na-ASP-1 (Asojo, 2011), and hookworm platelet inhibitor (HPI) (Ma et al., 2015)). These structural properties and possible structure-function relationships of the CAP domain merits investigations in view of the recent discoveries on functional amyloid-like aggregates and their importance in regulating biological functions.

4 Outline of the thesis

GAPR-1 is a member of the CAP superfamily of proteins that are characterized by the presence of a structurally conserved CAP domain. The role of this domain and its conserved structure in relation to the diverse functions of CAP proteins is still poorly understood. GAPR-1 consists almost exclusively of a CAP domain and serves as a good model to study the structural

properties of the CAP domain. The aim of the research described in this thesis was to characterize the molecular mechanisms regulating the oligomerization and amyloidogenic properties of GAPR-1.

The ability of GAPR-1 to bind Zn^{2+} and its relationship with oligomerization and formation of amyloid-like structures in the presence of GAGs are addressed in **Chapter 2**. An alternative GAPR-1 amyloid-like aggregation pathway is described in **Chapter 3**. Here, we show that Cu^{2+} induces this alternative aggregation pathway independently of the conserved metal binding site of the CAP domain. In addition, the effect of modulating the redox balance on GAPR-1 aggregation is investigated. The molecular mechanisms of the distinct aggregation pathways are elucidated, which reveals the involvement of reversible cysteine protection in Zn^{2+} -dependent aggregation. In **Chapter 4**, we expand our findings on the structural properties of GAPR-1 to human CRISP1. We show that the nature of Zn^{2+} -induced oligomerization of the CAP domain is a conserved property that exists in another CAP family member as well. In **Chapter 5**, the physiological relevance of the results described in Chapter 2-4 is discussed in the light of recent discoveries on reversible protein aggregation as a novel concept for regulation of biological processes.

Reference

- Abraham, A., and Chandler, D.E. (2017). Tracing the evolutionary history of the CAP superfamily of proteins using amino acid sequence homology and conservation of splice sites. *J. Mol. Evol.* *85*, 137–157.
- Alam, P., Siddiqi, K., Chturvedi, S.K., and Khan, R.H. (2017). Protein aggregation: From background to inhibition strategies. *Int. J. Biol. Macromol.* *103*, 208–219.
- Alberti, S., Halfmann, R., King, O., Kapila, A., and Lindquist, S. (2009). A systematic survey identifies prions and illuminates sequence features of prionogenic proteins. *Cell*. *137*, 146–158.
- Almond, A. (2018). Multiscale modeling of glycosaminoglycan structure and dynamics : current methods and challenges. *Curr. Opin. Struct. Biol.* *50*, 58–64.
- Ameri, M., Wang, X., Wilkerson, M.J., Kanost, M.R., and Broce, A.B. (2008). An immunoglobulin binding protein (antigen 5) of the stable fly (Diptera: Muscidae) salivary gland stimulates bovine immune responses. *J Med Entomol.* *45*, 94–101.
- Anderson, M., Bocharova, O. V., Makarava, N., Breydo, L., Salnikov, V. V., and Baskakov, I. V. (2006). Polymorphism and ultrastructural organization of prion protein amyloid fibrils: An insight from high resolution atomic force microscopy. *J. Mol. Biol.* *358*, 580–596.
- Andreasen, M., Lorenzen, N., and Otzen, D. (2015). Interactions between misfolded protein oligomers and membranes: A central topic in neurodegenerative diseases? *Biochim. Biophys. Acta* *1848*, 1897–1907.
- Ariga, T., Miyatake, T., and Yu, R.K. (2010). Role of proteoglycans and glycosaminoglycans in the pathogenesis of Alzheimer's disease and related disorders: Amyloidogenesis and therapeutic strategies-a review. *J. Neurosci. Res.* *88*, 2303–2315.
- Asojo, O.A. (2011). Structure of a two-CAP-domain protein from the human hookworm parasite *Necator americanus*. *Acta Crystallogr. Sect. D Biol. Crystallogr.* *67*, 455–462.
- Asojo, O.A., Goud, G., Dhar, K., Loukas, A., Zhan, B., Deumic, V., Liu, S., Borgstahl, G.E.O., and Hotez, P.J. (2005). X-ray structure of Na-ASP-2, a pathogenesis-related-1 protein from the nematode parasite, *Necator americanus*, and a vaccine antigen for human hookworm infection. *J. Mol. Biol.* *346*, 801–814.
- Assumpção, T.C.F., Ma, D., Schwarz, A., Reiter, K., Santana, J.M., Andersen, J.F., Ribeiro, J.M.C., Nardone, G., Yu, L.L., and Francischetti, I.M.B. (2013). Salivary antigen-5/CAP family members are Cu²⁺-dependent antioxidant enzymes that scavenge O₂⁻ and inhibit collagen-induced platelet aggregation and neutrophil oxidative burst. *J Biol Chem.* *288*, 14341–14361.
- Audas, T.E., Audas, D.E., Jacob, M.D., Ho, J.J.D., Khacho, M., Wang, M., Perera, J.K., Gardiner, C., Bennett, C.A., Head, T., et al. (2016). Adaptation to stressors by systemic protein amyloidogenesis. *Dev. Cell.* *39*, 155–168.
- Banani, S.F., Lee, H.O., Hyman, A.A., and Rosen, M.K. (2017). Biomolecular condensates: Organizers of cellular biochemistry. *Nat. Rev. Mol. Cell Biol.* *18*, 285–298.
- Barmada, S.J., Serio, A., Arjun, A., Bilican, B., Daub, A., Ando, D.M., Tsvetkov, A., Pleiss, M., Li, X., Peisach, D., et al. (2014). Autophagy induction enhances TDP43 turnover and survival in neuronal ALS models. *Nat Chem Biol* *10*, 677–685.
- Barnham, K.J., and Bush, A.I. (2014). Biological metals and metal-targeting compounds in major neurodegenerative diseases. *Chem Soc Rev* *43*, 6727–6749.
- Baxter, R.M., Crowell, T.P., George, J.A., Getman, M.E., and Gardner, H. (2007). The plant pathogenesis related protein GLIPR-2 is highly expressed in fibrotic kidney and promotes epithelial to mesenchymal transition in vitro. *Matrix Biol.* *26*, 20–29.
- Bekard, I.B., and Dunstan, D.E. (2009). Shear-induced deformation of bovine insulin in couette flow. *J. Phys. Chem. B* *113*, 8453–8457.
- Bishop, J.R., Schuksz, M., and Esko, J.D. (2007). Heparan sulphate proteoglycans fine-tune mammalian physiology. *Nature* *446*, 1030–1037.
- Bissig, C., Rochin, L., and Niel, G. van (2016). PMEL amyloid fibril formation: The bright steps of pigmentation. *Int. J. Mol. Sci.* *17*, 1438.
- Bjartell, A.S., Al-Ahmadie, H., Serio, A.M., Eastham, J.A., Eggener, S.E., Fine, S.W., Udby, L., Gerald, W.L., Vickers, A.J., Lilja, H., et al. (2007). Association of cysteine-rich secretory protein 3 and β -microseminoprotein with outcome after radical prostatectomy. *Clin. Cancer Res.* *13*, 4130–

- 4138.
- Blokhuis, A.M., Groen, E.J.N., Koppers, M., Berg, L.H. Van Den, and Pasterkamp, R.J. (2013). Protein aggregation in amyotrophic lateral sclerosis. *Acta Neuropathol* 125, 777–794.
- Boke, E., Ruer, M., Wühr, M., Coughlin, M., Lemaitre, R., Gygi, S.P., Alberti, S., Drechsel, D., Hyman, A.A., and Mitchison, T.J. (2016). Amyloid-like self-assembly of a cellular compartment. *Cell* 166, 637–650.
- Borloo, J., Geldhof, P., Peelaers, I., Van Meulder, F., Ameloot, P., Callewaert, N., Vercruysse, J., Claerebout, E., Strelkov, S. V., Weeks, S.D., et al. (2013). Structure of Ostertagia ostertagi ASP-1: Insights into disulfide-mediated cyclization and dimerization. *Acta Crystallogr. Sect. D Biol. Crystallogr.* 69, 493–503.
- Breen, S., Williams, S.J., Outram, M., Kobe, B., and Solomon, P.S. (2017). Emerging insights into the functions of pathogenesis-related protein 1. *Trends Plant Sci.* 22, 871–879.
- Budimir, A. (2011). Metal ions, Alzheimer's disease and chelation therapy. *Acta Pharm.* 61, 1–14.
- Burnett, L.A., Xiang, X., Bieber, A.L., and Chandler, D.E. (2008). Crisp proteins and sperm chemotaxis: Discovery in amphibians and explorations in mammals. *Int. J. Dev. Biol.* 52, 489–501.
- Burnett, L.A., Anderson, D.M., Rawls, A., Bieber, A.L., and Chandler, D.E. (2011). Mouse sperm exhibit chemotaxis to allurin, a truncated member of the cysteine-rich secretory protein family. *Dev. Biol.* 360, 318–328.
- Busso, D., Cohen, D.J., Hayashi, M., Kasahara, M., and Cuasnicú, P.S. (2005). Human testicular protein TPX1/CRISP-2: Localization in spermatozoa, fate after capacitation and relevance for gamete interaction. *Mol. Hum. Reprod.* 11, 299–305.
- Calvo, E., Dao, A., Pham, V.M., and Ribeiro, J.M.C. (2007). An insight into the sialome of Anopheles funestus reveals an emerging pattern in anopheline salivary protein families. *Insect Biochem Mol Biol.* 37, 164–175.
- Cereghetti, G., Saad, S., Dechant, R., and Peter, M. (2018). Reversible, functional amyloids: Towards an understanding of their regulation in yeast and humans. *Cell Cycle.* 17, 1545–1558.
- Chandel, T.I., Zaman, M., Khan, M.V., Ali, M., Rabbani, G., Ishtikhar, M., and Khan, R.H. (2018). A mechanistic insight into protein-ligand interaction, folding, misfolding, aggregation and inhibition of protein aggregates: An overview. *Int. J. Biol. Macromol.* 106, 1115–1129.
- Charlab, R., Valenzuela, J.G., Rowton, E.D., and Ribeiro, J.M. (1999). Toward an understanding of the biochemical and pharmacological complexity of the saliva of a hematophagous sand fly Lutzomyia longipalpis. *Proc. Natl. Acad. Sci. USA* 96, 15155–15160.
- Chatani, E., and Yamamoto, N. (2018). Recent progress on understanding the mechanisms of amyloid nucleation. *Biophys. Rev.* 10, 527–534.
- Chattopadhyay, M., Nwadibia, E., Strong, C.D., Gralla, E.B., Valentine, J.S., and Whitelegge, J.P. (2015). The disulfide bond, but not zinc or dimerization, controls initiation and seeded growth in amyotrophic lateral sclerosis-linked Cu, Zn superoxide dismutase (SOD1) fibrillation. *J. Biol. Chem.* 290, 30624–30636.
- Cheignon, C., Tomas, M., Bonnefont-Rousselot, D., Faller, P., Hureau, C., and Collin, F. (2018). Oxidative stress and the amyloid beta peptide in Alzheimer's disease. *Redox Biol.* 14, 450–464.
- Chiti, F., and Dobson, C.M. (2006). Protein misfolding, functional amyloid, and human disease. *Annu. Rev. Biochem.* 75, 333–366.
- Chiti, F., and Dobson, C.M. (2017). Protein misfolding, amyloid formation, and human disease: A summary of progress over the last decade. *Annu. Rev. Biochem.* 86, 27–68.
- Chiti, F., Webster, P., Taddei, U., Clark, A., Stefani, M., Ramponi, G., and Dobson, C.M. (1999). Designing conditions for in vitro formation of amyloid protofilaments and fibrils. *Proc. Natl. Acad. Sci. USA* 96, 3590–3594.
- Chiti, F., Bucciantini, M., White, P., Ramponi, G., and Dobson, C.M. (2000). Mutational analysis of the propensity for amyloid formation by a globular protein. *EMBO Journal* 19, 1441–1449.
- Cho, M.-H., Cho, K., Kang, H.-J., Jeon, E.-Y., Kim, H.-S., Kwon, H.-J., Kim, H.-M., Kim, D.-H., and Yoon, S.-Y. (2014). Autophagy in microglia degrades extracellular β -amyloid fibrils and regulates the NLRP3 inflammasome. *Autophagy* 10, 1761–1775.
- Choudhary, V., and Schneider, R. (2012). Pathogen-Related Yeast (PRY) proteins and members of the CAP superfamily are secreted sterol-binding proteins. *Proc. Natl. Acad. Sci. USA* 109, 16882–16887.

- Christis, C., Lubsen, N.H., and Braakman, I. (2008). Protein folding includes oligomerization-examples from the endoplasmic reticulum and cytosol. *FEBS J.* 275, 4700–4727.
- Chuang, E., Hori, A.M., Hesketh, C.D., and Shorter, J. (2018). Amyloid assembly and disassembly. *J. Cell Sci.* 131, 1–18.
- Cohen, E., and Dillin, A. (2009). The insulin paradox: aging, proteotoxicity and neurodegeneration. *Nat Rev Neurosci.* 9, 759–767.
- Cohen, D.J., Maldera, J.A., Vasen, G., Ernesto, J.I., Munoz, M.W., Battistone, M.A., and Cuasnicu, P.S. (2011). Epididymal protein CRISP1 plays different roles during the fertilization process. *J. Androl.* 32, 672–678.
- Cohen, S.I.A., Linse, S., Luheshi, L.M., Hellstrand, E., White, D.A., Rajah, L., Otzen, D.E., Vendruscolo, M., Dobson, C.M., and Knowles, T.P.J. (2013). Proliferation of amyloid- β 42 aggregates occurs through a secondary nucleation mechanism. *Proc Natl Acad Sci USA.* 110, 9758–9763.
- Cohlberg, J.A., Li, J., Uversky, V.N., and Fink, A.L. (2002). Heparin and other glycosaminoglycans stimulate the formation of amyloid fibrils from α -synuclein in vitro. *Biochemistry* 41, 1502–1511.
- Darwiche, R., Kelleher, A., Hudspeth, E.M., Schneider, R., and Asojo, O.A. (2016). Structural and functional characterization of the CAP domain of pathogen-related yeast 1 (Pry1) protein. *Sci. Rep.* 6, 28838.
- Darwiche, R., Atab, O. El, Cottier, S., and Schneider, R. (2018). The function of yeast CAP family proteins in lipid export, mating, and pathogen defense. *FEBS Lett.* 592, 1304–1311.
- Demuro, A., Mina, E., Kaye, R., Milton, S.C., Parker, I., and Glabe, C.G. (2005). Calcium dysregulation and membrane disruption as a ubiquitous neurotoxic mechanism of soluble amyloid oligomers. *J. Biol. Chem.* 280, 17294–17300.
- Dobson, C.M. (2003). Protein folding and misfolding. *Nature* 426, 884–890.
- Eberle, H.B., Serrano, R.L., Füllekrug, J., Schlosser, A., Lehmann, W.D., Lottspeich, F., Kaloyanova, D., Wieland, F.T., and Helms, J.B. (2002). Identification and characterization of a novel human plant pathogenesis-related protein that localizes to lipid-enriched microdomains in the Golgi complex. *J. Cell Sci.* 115, 827–838.
- Egge, N., Muthusubramanian, A., and Cornwall, G.A. (2015). Amyloid properties of the mouse egg zona pellucida. *PLoS ONE.* 10, 1–19.
- Evans, J., D'Sylva, R., Volpert, M., Jamsai, D., Merriner, D.J., Nie, G., Salamonsen, L.A., and O'Bryan, M.K. (2015). Endometrial CRISP3 is regulated throughout the mouse estrous and human menstrual cycle and facilitates adhesion and proliferation of endometrial epithelial cells. *Biol. Reprod.* 92, 1–10.
- Falcon, B., Noad, J., McMahon, H., Randow, F., and Goedert, M. (2018). Galectin-8-mediated autophagy and seeded tau aggregation protects against seeded tau aggregation. *J. Biol. Chem.* 293, 2438–2451.
- Finn, R.D., Mistry, J., Schuster-Bockler, B., Griffiths-Jones, S., Hollich, V., Lassmann, T., Moxon, S., Marshall, M., Khanna, A., Durbin, R., et al. (2006). Pfam: clans, web tools and services. *Nucleic Acids Res.* 34, D247–D251.
- Frost, B., and Diamond, M.I. (2010). Prion-like mechanisms in neurodegenerative diseases. *Nat. Rev. Neurosci.* 11, 155–159.
- Van Galen, J., Van Balkom, B.W.M., Serrano, R.L., Kaloyanova, D., Eerland, R., Stüven, E., and Helms, J.B. (2010). Binding of GAPR-1 to negatively charged phospholipid membranes: unusual binding characteristics to phosphatidylinositol. *Mol. Membr. Biol.* 27, 81–91.
- Van Galen, J., Olrichs, N.K., Schouten, A., Serrano, R.L., Nolte-'t Hoen, E.N.M., Eerland, R., Kaloyanova, D., Gros, P., and Helms, J.B. (2012). Interaction of GAPR-1 with lipid bilayers is regulated by alternative homodimerization. *Biochim. Biophys. Acta.* 1818, 2175–2183.
- Gao, X., Carroni, M., Nussbaum-Krammer, C., Mogk, A., Nillegoda, N.B., Szlachet, A., Guibrid, D.L., Saibil, H.R., Mayer, M.P., and Bukau, B. (2015). Human Hsp70 disaggregase reverses Parkinson's-linked α -synuclein amyloid fibrils. *Mol. Cell* 59, 781–793.
- Gaspar, R., Meisl, G., Buell, A.K., Young, L., Kaminski, C.F., Knowles, T.P.J., Sparr, E., and Linse, S. (2017). Secondary nucleation of monomers on fibril surface dominates α -synuclein aggregation and provides autocatalytic amyloid amplification. *Q Rev Biophys.* 50, e6.

- Gautam, S., Karmakar, S., Batra, R., Sharma, P., Pradhan, P., Singh, J., Kundu, B., and Chowhury, P.K. (2017). Polyphenols in combination with β -cyclodextrin can inhibit and disaggregate α -synuclein amyloids under cell mimicking conditions: A promising therapeutic alternative. *Biochim. Biophys. Acta* 1865, 589–603.
- Gerber, H., Wu, F., Dimitrov, M., Osuna, G.M.G., and Fraering, P.C. (2017). Zinc and copper differentially modulate amyloid precursor protein processing by γ -secretase and amyloid- β peptide production. *J. Biol. Chem.* 292, 3751–3767.
- Van Gerven, N., Klein, R.D., Hultgren, S.J., and Remaut, H. (2015). Bacterial amyloid formation: Structural insights into curli biogenesis. *Trends Microbiol.* 23, 693–706.
- Ghetti, B., Piccardo, P., Frangione, B., Bugiani, O., Giaccone, G., Young, K., Prelli, F., Farlow, M.R., Dlouhy, S.R., and Tagliavini, F. (1996). Prion protein amyloidosis. *Brain Pathol.* 6, 127–145.
- Gibbs, G.M., Scanlon, M.J., Swarbrick, J., Curtis, S., Gallant, E., Dulhunty, A.F., and O'Bryan, M.K. (2006). The cysteine-rich secretory protein domain of Tpx-1 is related to ion channel toxins and regulates ryanodine receptor Ca^{2+} signaling. *J. Biol. Chem.* 281, 4156–4163.
- Gibbs, G.M., Roelants, K., and O'Bryan, M.K. (2008). The CAP superfamily: cysteine-rich secretory proteins, antigen 5, and pathogenesis-related 1 proteins-roles in reproduction, cancer, and immune defense. *Endocr. Rev.* 29, 865–897.
- Gibbs, G.M., Orta, G., Reddy, T., Koppers, A.J., Martínez-López, P., de la Vega-Beltrán, J.L., Lo, J.C.Y., Veldhuis, N., Jamsai, D., McIntyre, P., et al. (2011). Cysteine-rich secretory protein 4 is an inhibitor of transient receptor potential M8 with a role in establishing sperm function. *Proc. Natl. Acad. Sci. USA* 108, 7034–7039.
- Giese, A., Jude, R., Kuiper, H., Piumi, F., Schambony, A., Guérin, G., Distl, O., Töpfer-Petersen, E., and Leeb, T. (2002a). Molecular characterization of the equine AEG1 locus. *Gene* 292, 65–72.
- Giese, A., Jude, R., Kuiper, H., Raudsepp, T., Piumi, F., Schambony, A., Guérin, G., Chowdhary, B.P., Distl, O., Töpfer-Petersen, E., et al. (2002b). Molecular characterization of the equine testis-specific protein 1 (TPX1) and acidic epididymal glycoprotein 2 (AEG2) genes encoding members of the cysteine-rich secretory protein (CRISP) family. *Gene* 299, 101–109.
- Goldberg, A.L. (2003). Protein degradation and protection against misfolded or damaged proteins. *Nature* 426, 895–899.
- Grignaschi, E., Cereghetti, G., Grigolato, F., Kopp, M.R.G., Caimi, S., Faltova, L., Saad, S., Peter, M., and Arosio, P. (2018). A hydrophobic low-complexity region regulates aggregation of the yeast pyruvate kinase Cdc19 into amyloid-like aggregates in vitro. *J. Biol. Chem.* 293, 11424–11432.
- Groenning, M. (2010). Binding mode of Thioflavin T and other molecular probes in the context of amyloid fibrils-current status. *J. Chem. Biol.* 3, 1–18.
- Groves, M.R., Kuhn, A., Hendricks, A., Radke, S., Serrano, R.L., Helms, J.B., and Sinning, I. (2004). Crystallization of a Golgi-associated PR-1-related protein (GAPR-1) that localizes to lipid-enriched microdomains. *Acta Crystallogr D Biol Crystallogr.* 60, 730–732.
- Guijarro, J.I., Sunde, M., Jones, J.A., Campbell, I.D., and Dobson, C.M. (1998). Amyloid fibril formation by an SH3 domain. *Proc Natl Acad Sci USA.* 95, 4224–4228.
- Guo, M., Teng, M., Niu, L., Liu, Q., Huang, Q., and Hao, Q. (2005). Crystal structure of the cysteine-rich secretory protein stecrisp reveals that the cysteine-rich domain has a K^{+} channel inhibitor-like fold. *J. Biol. Chem.* 280, 12405–12412.
- Hardy, D.M., Huang, T.T.F., Driscoll, W.J., Tung, K.K., and Wild, G.C. (1988). Purification and characterization of the primary acrosomal autoantigen of guinea pig epididymal spermatozoa. *Biol Reprod* 38, 423–437.
- Haslberger, T., Zdanowicz, A., Brand, I., Kirstein, J., Turgay, K., Mogk, A., and Bukau, B. (2008). Protein disaggregation by the AAA+ chaperone ClpB involves partial threading of looped polypeptide segments. *Nat. Struct. Mol. Biol.* 15, 641–650.
- Hayashi, M., Fujimoto, S., Takano, H., Ushiki, T., Abe, K., Ishikura, H., Yoshida, M.C., Kirchhoff, C., Ishibashi, T., and Kasahara, M. (1996). Characterization of a human glycoprotein with a potential role in sperm-egg fusion: cDNA cloning, immunohistochemical localization, and chromosomal assignment of the gene (AEG1). *Genomics* 32, 367–374.
- Hewetson, A., Do, H.Q., Myers, C., Muthusubramanian, A., Sutton, R.B., Wylie, B.J., and Cornwall, G.A. (2017). Functional amyloids in reproduction. *Biomolecules.* 7, 1–15.
- Hoffman, D.R. (1985a). Allergens in Hymenoptera venom XV: The immunologic basis of vespid

- venom. *J Allergy Clin Immunol.* 75, 611–613.
- Hoffman, D.R. (1985b). Allergens in Hymenoptera venom XIV: IgE binding activities of venom proteins from three species of vespids. *J Allergy Clin Immunol* 75, 606–610.
- Iannuzzi, C., Irace, G., and Sirangelo, I. (2015). The effect of glycosaminoglycans (GAGs) on amyloid aggregation and toxicity. *Molecules* 20, 2510–2528.
- Irwin, D.J., Lee, V.M.-Y., and Trojanowski, J.Q. (2013). Parkinson's disease dementia: convergence of α -synuclein, tau and amyloid- β pathologies. *Nat. Rev. Neurosci.* 14, 626–636.
- Jackson, M.P., and Hewitt, E.W. (2017). Why are functional amyloids non-toxic in humans? *Biomolecules* 7, 1–13.
- Jacob, R.S., Das, S., Ghosh, S., Anoop, A., Jha, N.N., Khan, T., Singru, P., Kumar, A., and Maji, S.K. (2016). Amyloid formation of growth hormone in presence of zinc: Relevance to its storage in secretory granules. *Sci. Rep.* 6, 23370.
- Jalkanen, J., Huhtaniemi, I., and Poutanen, M. (2005). Mouse cysteine-rich secretory protein 4 (CRISP4): A member of the crisp family exclusively expressed in the epididymis in an androgen-dependent manner. *Biol. Reprod.* 72, 1268–1274.
- Jang, H., Arce, F.T., Mustata, M., Ramachandran, S., Capone, R., Nussinov, R., and Lal, R. (2011). Antimicrobial protegrin-1 forms amyloid-like fibrils with rapid kinetics suggesting a functional link. *Biophys. J.* 100, 1775–1783.
- Janowski, R., Kozak, M., Jankowska, E., Grzonka, Z., Grubb, A., Abrahamson, M., and Jaskolski, M. (2001). Human cystatin C, an amyloidogenic protein, dimerizes through three-dimensional domain swapping. *Nat. Struct. Biol.* 8, 316–320.
- Jaskólski, M. (2001). 3D Domain swapping, protein oligomerization, and amyloid formation. *Acta Biochim. Pol.* 48, 807–827.
- Joppe, K., Roser, A., Maass, F., and Lingor, P. (2019). The contribution of iron to protein aggregation disorders in the central nervous system. *Front. Neurosci.* 13, 1–11.
- Jurczak, P., Groves, P., Szymanska, A., and Rodziewicz-Motowidlo, S. (2016). Human cystatin C monomer, dimer, oligomer, and amyloid structures are related to health and disease. *FEBS Lett.* 590, 4192–4201.
- Kamhi, E., Joo, E.J., Dordick, J.S., and Linhardt, R.J. (2013). Glycosaminoglycans in infectious disease. *Biol. Rev* 88, 928–943.
- Karlsson, O., Berg, A.L., Hanrieder, J., Arnerup, G., Lindström, A.-K., and Brittebo, E.B. (2015). Intracellular fibril formation, calcification, and enrichment of chaperones, cytoskeletal, and intermediate filament proteins in the adult hippocampus CA1 following neonatal exposure to the nonprotein amino acid BMAA. *Arch. Toxicol.* 89, 423–436.
- Kasahara, M., Gutknecht, J., Brew, K., Spurr, N., and Goodfellow, P.N. (1989). Cloning and mapping of a testis-specific gene with sequence similarity to a sperm-coating glycoprotein gene. *Genomics* 5, 527–534.
- Kawahara, M., Kato-Negishi, M., and Tanaka, K. (2017). Cross talk between neurometals and amyloidogenic proteins at the synapse and the pathogenesis of neurodegenerative diseases. *Metallomics.* 9, 619–633.
- Kayed, R., Sokolov, Y., Edmonds, B., McIntire, T.M., Milton, S.C., Hall, J.E., and Glabe, C.G. (2004). Permeabilization of lipid bilayers is a common conformation-dependent activity of soluble amyloid oligomers in protein misfolding diseases. *J. Biol. Chem.* 279, 46363–46366.
- Kerje, S., Sharma, P., Gunnarsson, U., Kim, H., Bagchi, S., Fredriksson, R., Schütz, K., Jensen, P., Heijne, G. von, Okimoto, R., et al. (2004). The dominant white, dun and smoky color variants in chicken are associated with insertion/deletion polymorphisms in the PMEL17 gene. *Genetics* 168, 1507–1518.
- Kerman, A., Liu, H.-N., Croul, S., Bilbao, J., Rogaeva, E., Zinman, L., Robertson, J., and Chakrabarty, A. (2010). Amyotrophic lateral sclerosis is a non-amyloid disease in which extensive misfolding of SOD1 is unique to the familial form. *Acta Neuropathol* 119, 335–344.
- Kim, A.C., Lim, S., and Kim, Y.K. (2018). Metal ion effects on A β and tau aggregation. *Int. J. Mol. Sci.* 19, 1–15.
- King, T.P., and Spangfort, M.D. (2000). Structure and biology of stinging insect venom allergens. *Int Arch Allergy Immunol* 123, 99–106.
- Kinnunen, P.K.J. (2009). Amyloid formation on lipid membrane surfaces. *Open Biol. J.* 2, 163–175.

- Kjeldsen, L., Cowland, J.B., Johnsen, A.H., and Borregaard, N. (1996). SGP28, a novel matrix glycoprotein in specific granules of human neutrophils with similarity to a human testis-specific gene product and to a rodent sperm-coating glycoprotein. *FEBS Lett.* 380, 246–250.
- Koppers, A.J., Reddy, T., and O'Bryan, M.K. (2011). The role of cysteine-rich secretory proteins in male fertility. *Asian J. Androl.* 13, 111–117.
- Kovalick, G.E., Schreiber, M.C., Dickason, A.K., and Cunningham, R.A. (1998). Structure and expression of the Antigen 5-related gene of *Drosophila melanogaster*. *Insect Biochem. Mol. Biol.* 28, 491–500.
- Kuballa, P., Nolte, W.M., Castoreno, A.B., and Xavier, R.J. (2012). Autophagy and the immune system. *Annu. Rev. Immunol.* 30, 611–646.
- Kumar, S., Rezaei-Ghaleh, N., Terwel, D., Thal, D.R., Richard, M., Hoch, M., Donald, J.M.M., Wüllner, U., Glebov, K., Heneka, M.T., et al. (2011). Extracellular phosphorylation of the amyloid beta-peptide promotes formation of toxic aggregates during the pathogenesis of Alzheimer's disease. *EMBO Jounral* 30, 2255–2265.
- Lambert, M.P., Barlow, A.K., Chromy, B.A., Edwards, C., Freed, R., Liosatos, M., Morgan, T.E., Rozovsky, I., Trommer, B., Viola, K.L., et al. (1998). Diffusible, nonfibrillar ligands derived from A β 1-42 are potent central nervous system neurotoxins. *Proc Natl Acad Sci USA.* 95, 6448–6453.
- Lasagna-Reeves, C.A., Castillo-Carranza, D.L., Sengupta, U., Guerrero-Munoz, M.J., Kiritoshi, T., Neugebauer, V., Jackson, G.R., and Kaye, R. (2012). Alzheimer brain-derived tau oligomers propagate pathology from endogenous tau. *Sci. Rep.* 2, 700.
- Leal, S.S., Botelho, H.M., and Gomes, C.M. (2012). Metal ions as modulators of protein conformation and misfolding in neurodegeneration. *Coord. Chem. Rev.* 256, 2253–2270.
- Lee, H.J., Korshavn, K.J., Kochi, A., Derrick, J.S., and Lim, M.H. (2014). Cholesterol and metal ions in Alzheimer's disease. *Chem. Soc. Rev.* 43, 6672–6682.
- Lee, J.-E., Sang, J.C., Rodrigues, M., Carr, A.R., Horrocks, M.H., De, S., Bongiovanni, M.N., Flagmeier, P., Dobson, C.M., Wales, D.J., et al. (2018). Mapping surface hydrophobicity of α -Synuclein oligomers at the nanoscale. *Nano Lett.* 18, 7494–7501.
- Li, Y., Zhao, Y., Su, M., Glover, K., Chakravarthy, S., Colbert, C.L., Levine, B., and Sinha, S.C. (2017). Structural insights into the interaction of the conserved mammalian proteins GAPR-1 and Beclin 1, a key autophagy protein. *Acta Crystallogr D Struct Biol.* 73, 775–792.
- Lipke, P.N., Garcia, M.C., Alsteens, D., Ramsook, C.B., Klotz, S.A., and Dufrêne, Y.F. (2012). Strengthening relationships: amyloids create adhesion nanodomains in yeasts. *Trends Microbiol.* 20, 59–65.
- Liu, S., Liu, H., Johnston, A., Hanna-Addams, S., Reynoso, E., Xiang, Y., and Wang, Z. (2017). MLKL forms disulfide bond-dependent amyloid-like polymers to induce necroptosis. *Proc Natl Acad Sci USA.* 114, E7450–E7459.
- Liu, W., Zhang, F., Zhang, W., Song, L., Wu, W., and Chen, Y. (2013). Arabidopsis Di19 functions as a transcription factor and modulates PR1, PR2, and PR5 expression in response to drought stress. *Mol. Plant* 6, 1487–1502.
- Liu, Z., Song, F., Ma, Z.L., Xiong, Q., Wang, J., Guo, D., and Sun, G. (2016). Bivalent copper ions promote fibrillar aggregation of KCTD1 and induce cytotoxicity. *Sci. Rep.* 6, 32658.
- Lotan, T., Ori, N., and Fluhr, R. (1989). Pathogenesis-related proteins are developmentally regulated in tobacco flowers. *Plant Cell* 1, 881–887.
- Lu, S., Faris, J.D., Sherwood, R., and Edwards, M.C. (2013). Dimerization and protease resistance: New insight into the function of PR-1. *J. Plant Physiol.* 170, 105–110.
- Lu, S., Faris, J.D., Sherwood, R., Friesen, T.L., and Edwards, M.C. (2014). A dimeric PR-1-type pathogenesis-related protein interacts with ToxA and potentially mediates ToxA-induced necrosis in sensitive wheat. *Mol. Plant Pathol.* 15, 650–663.
- Ma, D., Francischetti, I.M.B., Ribeiro, J.M.C., and Andersen, J.F. (2015). The structure of hookworm platelet inhibitor (HPI), a CAP superfamily member from *Ancylostoma caninum*. *Acta Crystallogr F Struct Biol Commun* 71, 643–649.
- Mack, K.L., and Shorter, J. (2016). Engineering and evolution of molecular chaperones and protein disaggregases with enhanced activity. *Front. Mol. Biosci.* 3, 8.
- Macphree, C.E., and Dobson, C.M. (2000). Formation of mixed fibrils demonstrates the generic nature

- and potential utility of amyloid nanostructures. *J. Am. Chem. Soc.* 122, 12707–12713.
- Madine, J., Davies, H.A., Hughes, E., and Middleton, D.A. (2013). Heparin promotes the rapid fibrillization of a peptide with low intrinsic amyloidogenicity. *Biochemistry* 52, 8984–8992.
- Maeda, T., Sakashita, M., Ohba, Y., and Nakanishi, Y. (1998). Molecular cloning of the rat Tpx-1 responsible for the interaction between spermatogenic and Sertoli cells. *Biochem. Biophys. Res. Commun.* 248, 140–146.
- Maji, S.K., Perrin, M.H., Sawaya, M.R., Jessberger, S., Vadodaria, K., Rissman, R.A., Singru, P.S., Nilsson, K.P.R., Simon, R., Schubert, D., et al. (2009). Functional amyloids as natural storage of peptide hormones in pituitary secretory granules. *Science*. 325, 328–332.
- Majumdar, A., Cesario, W.C., White-Grindley, E., Jiang, H., Ren, F., Khan, M.R., Li, L., Choi, E.M.-L., Kannan, K., Guo, F., et al. (2012). Critical role of amyloid-like oligomers of *Drosophila* Orb2 in the persistence of memory. *Cell* 148, 515–529.
- Maldera, J.A., Vasen, G., Ernesto, J.I., Weigel-Muñoz, M., Cohen, D.J., and Cuasnicu, P.S. (2011). Evidence for the involvement of zinc in the association of CRISP1 with rat sperm during epididymal maturation. *Biol. Reprod.* 85, 503–510.
- Mans, B.J., Andersen, J.F., Francischetti, I.M.B., Valenzuela, J.G., Schwan, T.G., Pham, V.M., Garfield, M.K., Hammer, C.H., and Ribeiro, J.M.C. (2008). Comparative sialomics between hard and soft ticks: Implications for the evolution of blood-feeding behavior. *Insect Biochem Mol Biol.* 38, 42–58.
- Marzban, L., Park, K., and Verchere, C.B. (2003). Islet amyloid polypeptide and type 2 diabetes. *Exp. Gerontol.* 38, 347–351.
- McGowan, D.P., Van Roon-Mom, W., Holloway, H., Bates, G.P., Mangiarini, L., Cooper, G.J.S., Faull, R.L.M., and Snell, R.G. (2000). Amyloid-like inclusions in Huntington’s disease. *Neuroscience* 100, 677–680.
- Memelink, J., Linthorst, H.J.M., Schilperoort, R.A., and Hoge, J.H.C. (1990). Tobacco genes encoding acidic and basic isoforms of pathogenesis-related proteins display different expression patterns. *Plant Mol. Biol.* 14, 119–126.
- Milne, T.J., Abbenante, G., Tyndall, J.D.A., Halliday, J., and Lewis, R.J. (2003). Isolation and characterization of a cone snail protease with homology to CRISP proteins of the pathogenesis-related protein superfamily. *J. Biol. Chem.* 278, 31105–31110.
- Milto, I. V., Suhodolo, I. V., Prokopieva, V.D., and Klimenteva, T.K. (2016). Molecular and cellular bases of iron metabolism in humans. *Biochem.* 81, 549–564.
- Milto, K., Michailova, K., and Smirnovas, V. (2014). Elongation of mouse prion protein amyloid-like fibrils: Effect of temperature and denaturant concentration. *PLoS One* 9, 1–5.
- Morley, J.F., Brignull, H.R., Weyers, J.J., and Morimoto, R.I. (2002). The threshold for polyglutamine-expansion protein aggregation and cellular toxicity is dynamic and influenced by aging in *Caenorhabditis elegans*. *Proc Natl Acad Sci USA* 99, 10417–10422.
- Motamedi-Shad, N., Monsellier, E., and Chiti, F. (2009). Amyloid formation by the model protein muscle acylphosphatase is accelerated by heparin and heparan sulphate through a scaffolding-based mechanism. *J. Biochem.* 146, 805–814.
- Murphy, M.P., and III, H.L. (2010). Alzheimer’s disease and the β -amyloid peptide. *J. Alzheimer’s Dis.* 19, 311.
- Nolan, M. a, Wu, L., Bang, H.J., Jelinsky, S. a, Roberts, K.P., Turner, T.T., Kopf, G.S., and Johnston, D.S. (2006). Identification of rat cysteine-rich secretory protein 4 (Crisp4) as the ortholog to human CRISP1 and mouse Crisp4. *Biol. Reprod.* 74, 984–991.
- Novak, S., Smith, T.A., Paradis, F., Burwash, L., Dyck, M.K., Foxcroft, G.R., and Dixon, W.T. (2010). Biomarkers of in vivo fertility in sperm and seminal plasma of fertile stallions. *Theriogenology* 74, 956–967.
- Olrichs, N.K., and Helms, J.B. (2016). Novel insights into the function of the conserved domain of the CAP superfamily of proteins. *AIMS Biophys.* 3, 232–246.
- Olrichs, N.K., Mahalka, A.K., Kaloyanova, D., Kinnunen, P.K., and Helms, J.B. (2014). Golgi-Associated plant Pathogenesis Related protein 1 (GAPR-1) forms amyloid-like fibrils by interaction with acidic phospholipids and inhibits A β aggregation. *Amyloid* 21, 88–96.
- Osredkar, J., and Sustar, N. (2011). Copper and zinc, biological role and significance of copper/zinc imbalance. *J. Clin. Toxicol.* s, 3.

- Pepling, M.E., Wilhelm, J.E., Hara, A.L.O., Gephardt, G.W., and Spradling, A.C. (2007). Mouse oocytes within germ cell cysts and primordial follicles contain a Balbiani body. *Proc Natl Acad Sci USA* 104, 187–192.
- Petkova, A.T., Leapman, R.D., Guo, Z., Yau, W.-M., Mattson, M.P., and Tycko, R. (2005). Self-Propagating, Molecular-Level Polymorphism in Alzheimer's beta-Amyloid Fibrils. *Science*. 307, 262–265.
- Potter, K.J., Werner, I., Denroche, H.C., Montane, J., Plesner, A., Chen, Y., Lei, D., Soukhatcheva, G., Warnock, G.L., Oberholzer, J., et al. (2015). Amyloid formation in human islets is enhanced by heparin and inhibited by heparinase. *Am. J. Transplant.* 15, 1519–1530.
- Prados-Rosales, R.C., Roldán-Rodríguez, R., Serena, C., López-Berges, M.S., Guarro, J., Martínez-del-Pozo, Á., and Di Pietro, A. (2012). A PR-1-like protein of *Fusarium oxysporum* functions in virulence on mammalian hosts. *J. Biol. Chem.* 287, 21970–21979.
- Rankin, T.L., Tsuruta, K.J., Holland, M.K., Griswold, M.D., and Orgebin-Crist, M.-C. (1992). Isolation, immunolocalization, and sperm-association of three proteins of 18, 25, and 29 kilodaltons secreted by the mouse epididymis. *Biol. Reprod.* 46, 747–766.
- Relini, A., Marano, N., and Gliozzi, A. (2014). Probing the interplay between amyloidogenic proteins and membranes using lipid monolayers and bilayers. *Adv. Colloid Interface Sci.* 207, 81–92.
- Roan, N.R., Sandi-Monroy, N., Kohgadai, N., Usmani, S.M., Hamil, K.G., Neidleman, J., Montano, M., Ständker, L., Röcker, A., Cavois, M., et al. (2017). Semen amyloids participate in spermatozoa selection and clearance. *ELife*. 6, e24888.
- Roberts, K.P., Ensrud-Bowlin, K.M., Piehl, L.B., Parent, K.R., Bernhardt, M.L., and Hamilton, D.W. (2008). Association of the protein D and protein E forms of rat CRISP1 with epididymal sperm. *Biol. Reprod.* 79, 1046–1053.
- Ros, V.G. Da, Muñoz, M.W., Battistone, M.A., Brukman, N., Carvajal, G., Curci, L., Gomez-Elias, M.D., Cohen, D.J., and Cuasnicú, P.S. (2015). From the epididymis to the egg: Participation of CRISP proteins in mammalian fertilization. *Asian J. Androl.* 17, 711–715.
- Saad, S., Cereghetti, G., Feng, Y., Picotti, P., Peter, M., and Dechant, R. (2017). Reversible protein aggregation is a protective mechanism to ensure cell cycle restart after stress. *Nat. Cell Biol.* 19, 1202–1213.
- Saldaño, T.E., Zanotti, G., Parisi, G., and Fernandez-Alberti, S. (2017). Evaluating the effect of mutations and ligand binding on transthyretin homotetramer dynamics. *PLoS ONE*. 12, 1–20.
- Schambony, A., Gentzel, M., Wolfes, H., Raida, M., Neumann, U., and Töpfer-Petersen, E. (1998). Equine CRISP-3: primary structure and expression in the male genital tract. *Biochim Biophys Acta* 1387, 206–216.
- Seo, P.J., Lee, A., Xiang, F., and Park, C. (2008). Molecular and functional profiling of arabidopsis pathogenesis-related genes: insights into their roles in salt response of seed germination. *Plant Cell Physiol* 49, 334–344.
- Seo, P.J., Kim, M.J., Park, J., Kim, S., Jeon, J., Lee, Y., Kim, J., and Park, C. (2010). Cold activation of a plasma membrane-tethered NAC transcription factor induces a pathogen resistance response in Arabidopsis. *Plant J.* 61, 661–671.
- Serrano, R.L., Kuhn, A., Hendricks, A., Helms, J.B., Sinning, I., and Groves, M.R. (2004). Structural analysis of the human Golgi-associated plant pathogenesis related protein GAPR-1 implicates dimerization as a regulatory mechanism. *J. Mol. Biol.* 339, 173–183.
- Shikamoto, Y., Suto, K., Yamazaki, Y., Morita, T., and Mizuno, H. (2005). Crystal structure of a CRISP family Ca²⁺-channel blocker derived from snake venom. *J. Mol. Biol.* 350, 735–743.
- Shoji-Kawata, S., Sumpter, R., Leveno, M., Campbell, G.R., Zou, Z., Kinch, L., Wilkins, A.D., Sun, Q., Pallauf, K., MacDuff, D., et al. (2013). Identification of a candidate therapeutic autophagy-inducing peptide. *Nature* 494, 201–206.
- Sirangelo, I., and Iannuzzi, C. (2017). The role of metal binding in the amyotrophic lateral sclerosis-related aggregation of copper-zinc superoxide dismutase. *Molecules*. 22, 1–13.
- Skoulakis, S., and Goodfellow, J.M. (2003). The pH-dependent stability of wild-type and mutant transthyretin oligomers. *Biophys. J.* 84, 2795–2804.
- So, M., Hata, Y., Naiki, H., and Goto, Y. (2017). Heparin-induced amyloid fibrillation of β 2-microglobulin explained by solubility and a supersaturation-dependent conformational phase diagram. *Protein Sci.* 26, 1024–1036.

- Solomon, J.P., Bourgault, S., Powers, E.T., and Kelly, J.W. (2011). Heparin binds 8 kDa gelsolin cross- β -sheet oligomers and accelerates amyloidogenesis by hastening fibril extension. *Biochemistry* 50, 2486–2498.
- Stelmashook, E. V., Isaev, N.K., Genrikhs, E.E., Amelkina, G.A., Khaspekoy, L.G., Skrebitsky, V.G., and Illarioshkin, S.N. (2014). Role of zinc and copper ions in the pathogenetic mechanisms of Alzheimer's and Parkinson's diseases. *Biochemistry* 79, 391–396.
- Sugiyama, H., Burnett, L., Xiang, X., Olson, J., Willis, S., Miao, A.M.Y., Akema, T., Bieber, A.L., and Chandler, D.E. (2009). Purification and multimer formation of allurin, a sperm chemoattractant from *Xenopus laevis* egg jelly. *Mol. Reprod. Dev.* 76, 527–536.
- Suzuki, N., Yamazaki, Y., Brown, R.L., Fujimoto, Z., Morita, T., and Mizuno, H. (2008). Structures of pseudodechetoxin and pseudodecin, two snake-venom cysteine-rich secretory proteins that target cyclic nucleotide-gated ion channels: implications for movement of the C-terminal cysteine-rich domain. *Acta Crystallogr D Biol Crystallogr* 64, 1034–1042.
- Tayeb-fligelman, E., Tabachnikov, O., Moshe, A., Goldshmidt-tran, O., Sawaya, M.R., Coquelle, N., Colletier, J., and Landau, M. (2017). The cytotoxic *Staphylococcus aureus* PSMA3 reveals a cross- α amyloid-like fibril. *Science* 355, 21–24.
- Tessarz, P., Mogk, A., and Bukau, B. (2008). Substrate threading through the central pore of the Hsp104 chaperone as a common mechanism for protein disaggregation and prion propagation. *Mol. Microbiol.* 68, 87–97.
- Toyama, B.H., and Weissman, J.S. (2011). Amyloid structure: Conformational diversity and consequences. *Annu. Rev. Biochem.* 80, 557–585.
- Turunen, H.T., Sipilä, P., Krutskikh, A., Toivanen, J., Mankonen, H., Hämäläinen, V., Björkgren, I., Huhtaniemi, I., and Poutanen, M. (2012). Loss of cysteine-rich secretory protein 4 (Crisp4) leads to deficiency in sperm-zona pellucida interaction in mice. *Biol. Reprod.* 86, 1–8.
- Ungelenk, S., Moayed, F., Ho, C., Grousl, T., Scharf, A., Mashaghi, A., Tans, S., Mayer, M.P., Mogk, A., and Bukau, B. (2016). Small heat shock proteins sequester misfolding proteins in near-native conformation for cellular protection and efficient refolding. *Nat. Commun.* 7, 13673.
- Valenzuela, J.G., Pham, V.M., Garfield, M.K., Francischetti, I.M.B., and Ribeiro, J.M.C. (2002). Toward a description of the sialome of the adult female mosquito *Aedes aegypti*. *Insect Biochem. Mol. Biol.* 32, 1101–1122.
- Verma, M., Vats, A., and Taneja, V. (2015). Toxic species in amyloid disorders: Oligomers or mature fibrils. *Ann. Indian Acad. Neurol.* 18, 138–145.
- Vilasi, S., Sarcina, R., Maritato, R., de Simone, A., Irace, G., and Sirangelo, I. (2011). Heparin induces harmless fibril formation in amyloidogenic W7FW14F apomyoglobin and amyloid aggregation in wild-type protein *In vitro*. *PLoS One* 6, e22076.
- Wang, J., Shen, B., Guo, M., Lou, X., Duan, Y., Cheng, X.P., Teng, M., Niu, L., Liu, Q., Huang, Q., et al. (2005). Blocking effect and crystal structure of natrin toxin, a cysteine-rich secretory protein from *Naja atra* venom that targets the BKCa channel. *Biochemistry* 44, 10145–10152.
- Wang, Y.-L., Kuo, J.-H., Lee, S.-C., Liu, J.-S., Hsieh, Y.-C., Shih, Y.-T., Chen, C.-J., Chiu, J.-J., and Wu, W.-G. (2010). Cobra CRISP functions as an inflammatory modulator via a novel Zn²⁺- and heparan sulfate-dependent transcriptional regulation of endothelial cell adhesion molecules. *J. Biol. Chem.* 285, 37872–37883.
- Watt, B., Tenza, D., Lemmon, M.A., Kerje, S., Raposo, G., Andersson, L., and Marks, M.S. (2011). Mutations in or near the transmembrane domain alter PMEL amyloid formation from functional to pathogenic. *PLoS Genet.* 7, e1002286.
- Webb, J.L., Ravikumar, B., Atkins, J., Skepper, J.N., and Rubinstein, D.C. (2003). Alpha-synuclein is degraded by both autophagy and the proteasome. *J. Biol. Chem.* 278, 25009–25013.
- Woodruff, J.B., Hyman, A.A., and Boke, E. (2018). Organization and function of non-dynamic biomolecular condensates. *Trends Biochem. Sci.* 43, 81–94.
- Xu, X., Francischetti, I.M.B., Lai, R., Ribeiro, J.M.C., and Andersen, J.F. (2012). Structure of protein having inhibitory disintegrin and leukotriene scavenging functions contained in single domain. *J. Biol. Chem.* 287, 10967–10976.
- Yakupova, E.I., Bobyleva, L.G., Vikhlyantsev, I.M., and Bobylev, A.G. (2019). Congo red and amyloids: History and relationship. *Biosci. Rep.* 39, BSR20181415.
- Yamada, S., Sugahara, K., and Özbek, S. (2011). Evolution of glycosaminoglycans comparative

- biochemical study. *Commun. Integr. Biol.* 4, 150–158.
- Yamazaki, Y., and Morita, T. (2004). Structure and function of snake venom cysteine-rich secretory proteins. *Toxicon* 44, 227–231.
- Yoshimura, Y., Lin, Y., Yagi, H., Lee, Y.-H., Kitayama, H., Sakurai, K., So, M., Ogi, H., Naiki, H., and Goto, Y. (2012). Distinguishing crystal-like amyloid fibrils and glass-like amorphous aggregates from their kinetics of formation. *Proc Natl Acad Sci USA* 109, 14446–14451.
- Zhang, L., Qu, S., Liang, A., Jiang, H., and Wang, H. (2015). Gene expression microarray analysis of the sciatic nerve of mice with diabetic neuropathy. *Int. J. Mol. Med.* 35, 333–339.
- Zhao, L., Buxbaum, J.N., and Reixach, N. (2013). Age-related oxidative modifications of transthyretin modulate its amyloidogenicity. *Biochemistry* 52, 1913–1926.
- Zhou, Q., Hao, L., Huang, W., and Cai, Z. (2016). The Golgi-Associated Plant Pathogenesis-Related Protein GAPR-1 enhances type I interferon signaling pathway in response to Toll-Like receptor 4. *Inflammation* 39, 706–717.
- Zietkiewicz, S., Krzewska, J., and Liberek, K. (2004). Successive and synergistic action of the Hsp70 and Hsp100 chaperones in protein disaggregation. *J. Biol. Chem.* 279, 44376–44383.

Zinc binding regulates amyloid-like aggregation of GAPR-1

Jie Sheng[§], Nick K. Olrichs[§], Willie J. Geerts[#], Xueyi Li[‡], Ashfaq Ur Rehman[&], Barend M. Gadella[§], Dora V. Kaloyanova[§], J. Bernd Helms[§]

[§] Department of Biochemistry and Cell Biology, Faculty of Veterinary Medicine, Utrecht University, Utrecht, the Netherlands

[#] Biomolecular Imaging, Bijvoet Center, Utrecht University, Utrecht, the Netherlands.

[‡] School of Pharmacy, Shanghai Jiao Tong University, Shanghai, China

Department of Neurology, Massachusetts General Hospital and Harvard Medical School, Charlestown, USA

[&] Department of Bioinformatics and Biostatistics, Shanghai Jiao Tong University, Shanghai, China

Published as

Sheng, J., Olrichs, N. K., Geerts, W. J., Li, X., Rehman, A. U., Gadella, B. M., Kaloyanova, D. V. and Helms, J. B. (2019). Zinc binding regulates amyloid-like aggregation of GAPR-1. Biosci. Rep. 39, BSR20182345.

Abstract

Members of the CAP superfamily (Cysteine-rich secretory proteins, Antigen 5, and Pathogenesis-related 1 proteins) are characterized by the presence of a CAP domain that is defined by four sequence motifs and a highly conserved tertiary structure. A common structure-function relationship for this domain is hitherto unknown. A characteristic of several CAP proteins is their formation of amyloid-like structures in the presence of lipids. Here we investigate the structural modulation of Golgi-Associated plant Pathogenesis Related protein 1 (GAPR-1) by known interactors of the CAP domain, preceding amyloid-like aggregation. Using isothermal titration calorimetry, we demonstrate that GAPR-1 binds zinc ions. Zn^{2+} binding causes a slight but significant conformational change as revealed by CD, tryptophan fluorescence and trypsin digestion. The Zn^{2+} -induced conformational change was required for the formation of GAPR-1 oligomers and amyloid-like assemblies in the presence of heparin, as shown by ThT fluorescence and TEM. Molecular dynamic simulations show binding of Zn^{2+} to His54 and His103. Mutation of these two highly conserved residues resulted in strongly diminished amyloid-like aggregation. Finally, we show that proteins from the cysteine-rich secretory protein (CRISP) subfamily are also able to form ThT-positive structures *in vitro* in a heparin- and Zn^{2+} -dependent manner, suggesting that oligomerization regulated by metal ions could be a common structural property of the CAP domain.

Introduction

Golgi-Associated plant Pathogenesis Related protein 1 (GAPR-1), also known as GLIPR-2, is a mammalian protein that mainly localizes to lipid-enriched microdomains at the cytosolic leaflet of Golgi membranes (Eberle et al., 2002). GAPR-1 acts as a negative regulator of autophagy via the interaction with the essential autophagy effector Beclin 1. GAPR-1 retains Beclin 1 at the Golgi apparatus, thereby interfering with autophagy initiation (Shoji-Kawata et al., 2013). GAPR-1 was also found to regulate type I interferon signaling activation in response to Toll-like receptor 4 (Zhou et al., 2016).

GAPR-1 has a high affinity for membranes containing negatively charged lipids. We previously showed that membrane-bound GAPR-1 has a tendency to form homodimers, both on liposomes and on Golgi membranes (Van Galen et al., 2012; Serrano et al., 2004). Moreover, prolonged incubation with negatively charged liposomes resulted in the formation of amyloid-like fibrils (Olricks et al., 2014). GAPR-1 has been associated with amyloid-related diseases. GAPR-1 was found to be enriched in sites of induced neurodegeneration in rat hippocampus as well as in the insoluble proteome of multiple sclerosis (MS) patients (Karlsson et al., 2015; Ofengeim et al., 2015) and was proposed to regulate the development of diabetic neuropathy (Zhang et al., 2015). Whether these pathologies are related to the amyloidogenic properties of GAPR-1, however, remains to be investigated.

The structural determinants for the amyloidogenic propensity of GAPR-1 are still unknown. Natively folded GAPR-1 binds the amyloid oligomer-specific antibody A11 and its presence was shown to inhibit amyloid β (A β) aggregation into amyloid fibrils, indicating an intrinsic amyloid-related structure (Olricks et al., 2014). In this respect, it is interesting to note that the crystal structure of GAPR-1 displays a dimeric arrangement with a near continuous β -sheet that extends beyond the monomeric subunits (Serrano et al., 2004). This suggests that subtle structural changes might be sufficient to induce amyloid formation. Indeed, upon membrane binding, oligomerization and fibrillation of GAPR-1 are rapidly initiated and enhanced by several factors including cholesterol (Olricks et al., 2014).

GAPR-1 belongs to the CAP (Cysteine-rich secretory proteins, Antigen 5, and Pathogenesis-related 1) superfamily of proteins, members of which are found in a widespread variety of biological species with a remarkable diversity in functions (Gibbs et al., 2008). Characteristic for CAP superfamily members is the presence of a CAP domain (or Sperm Coating Protein (SCP) domain) with four signature sequence motifs and a highly conserved tertiary structure

with a unique α - β - α sandwich fold. Family members have an extension or an additional domain predominantly at the C-terminus of the CAP domain.

The role of the CAP domain in relation to the high diversity of functions of CAP proteins is still poorly understood. General functions that have been proposed include: i) protease activity involving highly conserved catalytic amino acids at the dimer interface (Serrano et al., 2004), ii) lipid binding to a central cavity (Choudhary and Schneider, 2012; Darwiche et al., 2017), and iii) structural domain, regulating protein oligomerization (Olricks and Helms, 2016; Olricks et al., 2014). Each of these functions requires structural flexibility of the CAP domain but so far, this has not been described. Here we focused on the structural consequences of known interactors with the CAP domain. For several CAP proteins, it has been shown that metal binding is critical for specific functions (Assumpção et al., 2013; Darwiche et al., 2016; Maldera et al., 2011; Wang et al., 2010) and that two highly conserved histidines of the CAP tetrad coordinate Zn^{2+} or other divalent metal ions. GAPR-1 consists almost exclusively of a CAP domain and the GAPR-1 subfamily was recently described to be the earliest evolutionary ancestor within the CAP superfamily (Abraham and Chandler, 2017). GAPR-1 is therefore a suitable model protein to study the CAP domain structure-function relationship. In the present study, we show that GAPR-1 specifically binds zinc ions and that the formation of GAPR-1 oligomers and amyloid-like structures in the presence of heparin is regulated by zinc binding. We also provide evidence that metal-regulated oligomerization could be a common property of the CAP domain within the superfamily.

Materials and methods

Reagents

Heparin was purchased from Santa Cruz Biotechnology (Heidelberg, Germany); Mouse CRISP2, human CRISP3 and mouse CRISP4 from R&D Systems (Minneapolis, USA); Trypsin from Thermo Fisher SCIENTIFIC (Eindhoven, the Netherlands); Thioflavin T, ZnCl_2 , ZnSO_4 and ethylenediaminetetraacetic acid (EDTA) from Sigma-Aldrich (St. Louis, USA).

Plasmids

pQE60-GAPR-1 WT plasmid was described before (Groves et al., 2004; Serrano et al., 2004). pQE60-GAPR-1 H54A and pQE60-GAPR-1 H103A mutants were generated by site-directed mutagenesis using the following mutagenic primers. Altered sequences are shown in bold in

Table 1. Mutations in GAPR-1 were verified by DNA sequencing (Baseclear, Leiden, the Netherlands).

Table 1. Primers used for site-directed mutagenesis

GAPR-1		
mutation	Forward	Reverse
H54A	5'-gaggatcctcaaggccagcccgaggtcc-3'	5'-ggactccgggctggccttgaggatcctc-3'
H103A	5-cggggactggagccttcacgccatg-3'	5'-catggccgtcaaggtccagtcctccg-3'

Protein expression and purification

Both wild type and mutant GAPR-1 expression and purification were described before (Groves et al., 2004; Serrano et al., 2004). Briefly, the protein was over-expressed in *E.coli* XL-1 Blue host cells and induced by 1 mM isopropyl β -D-1-thiogalactopyranoside (IPTG) overnight at 18 °C. After cell pelleting and homogenization with a high pressure homogenizer (Avestin, Mannheim, Germany), soluble proteins were collected by two step centrifugation for 30 min at 14,000 g followed by 30 min at 100,000 g. GAPR-1 was purified by cation exchange chromatography using SP Sepharose FF (GE Healthcare, USA) eluted with a linear gradient of 0-400 mM NaCl in 25 mM Tris, pH 8.0. The purity of the isolated proteins was confirmed by SDS-PAGE and Coomassie blue staining.

Isothermal Titration Calorimetry

Isothermal titration calorimetric (ITC) analysis was carried out with a Low Volume NanoITC (TA Instruments-Waters LLC, New Castle, DE). The 50 μ l syringe contained 1.5 mM ZnSO₄ prepared in buffer containing 25 mM Tris, 50 mM NaCl, pH 7.4 (NT-50), and the 200 μ l cell contained 60 μ M GAPR-1 in NT-50 buffer. All solutions were degassed under vacuum for 10 min before use. Titrations were incremental with 2 μ l injections at 300 s intervals. Experiments were performed at 20 °C. The instrumental default setting plots exothermic events in the upward direction. Data were analyzed using Nano Analyze software (TA Instruments-Waters LLC, New Castle, DE).

Circular Dichroism

Measurements of 15 μ M GAPR-1 in the presence of 0-100 μ M Zn²⁺ in NT-50 buffer were performed on a JASCO J-810 spectropolarimeter (Jasco Co. Ltd., Tokyo, Japan), using a 1 mm path length quartz cuvette, 1 nm bandwidth, 0.2 nm resolution, 1 s response time, and a scan

speed of 20 nm/min. Temperature was controlled with a Peltier device at 37 °C. Measurements were repeated four times.

Tryptophan fluorescence assay

Tryptophan fluorescence was measured on a CLARIOstar microplate reader (BMG Labtech, Germany) using a 280 nm excitation filter and the maximum emission was measured at 336 nm. Fluorescence intensities of GAPR-1 (30 µM) in the presence of increasing concentrations of Zn²⁺ (0-500 µM) were normalized to the initial fluorescence intensity of GAPR-1 in the absence of Zn²⁺.

Trypsin digestion

A total of 30 µM GAPR-1 was incubated with increasing Zn²⁺ concentrations (0-500 µM) in a total volume of 20 µl NT-50 buffer at 37 °C for 30 min, after which trypsin was added in a molar ratio of 1:50 (trypsin: GAPR-1) and incubated at 37 °C for 30 min. The reaction was terminated by addition of sample buffer. Protein samples were analyzed by SDS-PAGE and Western blot using five different peptide GAPR-1 antibodies as listed in Table 2.

Table 2. List of GAPR-1 antibodies used in Western blot analysis

	peptide	origin	produced
Ab1 (N-term.)	³ KSASKQFHNE ¹²	Mouse mAb	Abmart (Shanghai, China)
Ab2	⁴⁰ QQYSEALAST ⁴⁹	Mouse mAb	Abmart (Shanghai, China)
Ab3	⁵³ KHSPSSRGQ ⁶²	Mouse mAb	Abmart (Shanghai, China)
Ab4	⁸¹ YNFQQPGFTS ⁹⁰	Mouse mAb	Abmart (Shanghai, China)
Ab5 (C-term.)	¹⁴³ GFFEENVLPKK ¹⁵⁴	Rabbit pAb	Described before (Eberle et al., 2002)

Thioflavin T fluorescence assay

Kinetics of zinc induced GAPR-1 amyloid-like aggregation in presence of heparin was monitored by Thioflavin T (ThT) fluorescence. Reaction mixtures contained 15 µM GAPR-1, 37.5 µM heparin and 50 µM ThT with or without 100 µM Zn²⁺ in NT-50 buffer and were incubated in sealed 96-well plates (Flat Clear Bottom Black Polystyrene, Corning, USA) at 37 °C for 24 h. Fluorescence was measured in a CLARIOstar microplate reader (BMG Labtech, Germany). ThT fluorescence emission was recorded at 488 nm after excitation at 449 nm with agitation before every measurement. The results represent the means (+/- S.D.) of three independent experiments.

Western blot analysis of GAPR-1 oligomerization

The formation of higher order structures by GAPR-1 was analyzed by Western blot. GAPR-1 was incubated with 37.5 μM heparin in the presence and absence of 100 μM Zn^{2+} in NT-50 buffer at 37 °C. Aliquots were taken after 0, 2, 7 and 20 h, respectively, mixed with non-reducing Laemmli sample buffer, boiled for 5 min and separated by SDS-PAGE. Proteins were transferred to 0.45 μm Nitrocellulose membranes (Amersham Protran GE Healthcare) by Western blotting at 90 V for 1 h and visualized using rabbit polyclonal anti-GAPR-1 antibody (see Table 2) and HRP-labeled goat anti-rabbit secondary antibodies with ECL detection.

Transmission electron microscopy

A total of 15 μM GAPR-1 was incubated with 37.5 μM heparin in the presence or absence of 100 μM Zn^{2+} at 37 °C for 6 h, 18 h and 3 days. 10 μl of each prepared sample was placed on a 100 mesh glow discharged gold grid (Quantifoil Micro Tools GmbH, Jena, Germany). After 30 sec, excess fluid was removed, and the grid was washed twice with ddH₂O for 30 sec each time. Afterwards, the grid was negatively stained with 2% uranyl acetate in ddH₂O twice for, 15 sec and 30 sec, respectively. After the excess fluid was removed from the grid, it was dried on air. Samples were viewed in Tecnai 20 LaB6 transmission electron microscope (FEI, Eindhoven, the Netherlands) at 200 kV. Images were recorded using a 4K square pixel Eagle CCD camera (FEI, Eindhoven, the Netherlands).

Prediction of the Zn^{2+} binding sites

Prediction studies were performed in two ways: 1) a protein-protein interaction network was built to predict the homologous structure for GAPR-1 via the online database STRING v10.5 (<http://string.embl.de/>). Three clusters of homologous proteins were retrieved, with or without crystallographic structures deposited in the PDB database (www.rcsb.org). In order to find the Zn^{2+} binding site, a total of three protein crystals were extracted from the clusters, one from each cluster. Protein superimposition was done via PyMol v1.7 (www.pymol.org), which led to PDB code 3qr1 crystalized with Zn^{2+} ; 2) the Zn^{2+} binding site was determined using the online ZincBinder program (Srivastava and Kumar, 2018) (<http://proteininformatics.org/mkumar/znbinder/index.html>). The threshold was set to default in support vector machine (SVM), which classifies the zinc and non-zinc binding sites in protein sequences. ZincBinder accuracy of results commonly measured by the quantity of True Positives (TP), True Negatives (TN), False Positives (FP) and False Negatives (FN). In the prediction system the total prediction accuracy, Matthew's correlation co-efficient (MCC), sensitivity and specificity was calculated by following equations.

$$\begin{aligned}\text{Sensitivity} &= (\text{TP} / (\text{TP} + \text{FN})) * 100 \\ \text{Specificity} &= (\text{TN} / (\text{TN} + \text{FP})) * 100 \\ \text{Accuracy} &= (\text{TP} + \text{TN} / (\text{TP} + \text{FP} + \text{TN} + \text{FN})) * 100 \\ \text{MCC} &= ((\text{TP} * \text{TN}) - (\text{FP} * \text{FN})) / \sqrt{(\text{TP} + \text{FN}) * (\text{TP} + \text{FP}) * (\text{TN} + \text{FP}) * (\text{TN} + \text{FN})}\end{aligned}$$

TP and TN are correctly predicted zinc metal binding sites and non-zinc metal binding sites, respectively. FP and FN are wrongly predicted zinc metal binding sites and non-zinc metal binding sites, respectively. The sites predicted by the ZincBinder program were cross validated with the K_{DEEP} program for physiochemical properties, i.e. dissociation constant, the binding energy of Zn²⁺ and the binding efficiency in the protein.

Results

Zn²⁺ binding properties of GAPR-1

Zinc ions have been shown to bind the CAP domain and therefore we investigated zinc binding to GAPR-1 using isothermal titration calorimetry (ITC). To this end, Zn²⁺ was repeatedly titrated into a GAPR-1 solution and the released heat was monitored by ITC (Figure 1A). A representative titration curve shows the repetitive release of energy, confirming the binding of Zn²⁺ to GAPR-1. Binding was specific for Zn²⁺ as energy release was not observed in the absence of metal ions (data not shown) nor in the presence of other metal ions, such as Ca²⁺ (Figure 1B). The thermodynamic parameters of GAPR-1–Zn²⁺ interaction were determined from the binding isotherm. The apparent dissociation constant is in the micromolar range (K_d= 76 +/- 12 μM) with n=1.6 +/- 0.3 (Figure 1A, bottom panel).

Next, we examined the effect of zinc binding on possible structural rearrangement(s) of GAPR-1 by CD spectroscopy. In the absence of zinc ions, a typical far-UV CD spectrum of GAPR-1 was observed with two minima at 207 and 222 nm, consistent with the predominant presence of α-helical elements (Figure 1C). When 15 μM GAPR-1 was incubated with up to 100 μM Zn²⁺ at 37 °C, no significant changes in the far-UV CD spectrum were observed, indicating that zinc binding does not cause any major changes in GAPR-1 secondary structural elements. To confirm this finding, we also monitored the intrinsic tryptophan fluorescence of GAPR-1 upon the addition of zinc. Intrinsic tryptophan fluorescence has been used extensively to monitor small conformational changes within a protein (Ghisaidoobe and Chung, 2014). GAPR-1 contains three tryptophan residues and recombinant GAPR-1 in solution emits light at 336 nm upon exposure to UV light. No shift in tryptophan emission maximum was observed upon addition of 100 μM Zn²⁺ (not shown). Increasing the ZnCl₂ concentration did, however, cause a slight reduction in the emission intensity (Figure 1D). The changes were reversed upon

addition of excess EDTA (Figure 1D), confirming that these effects were zinc-induced and reversible. In line with previous structural studies on other metal-bound CAP superfamily proteins, the moderate quenching of GAPR-1 intrinsic fluorescence combined with the CD data suggest no major structural rearrangements upon zinc binding.

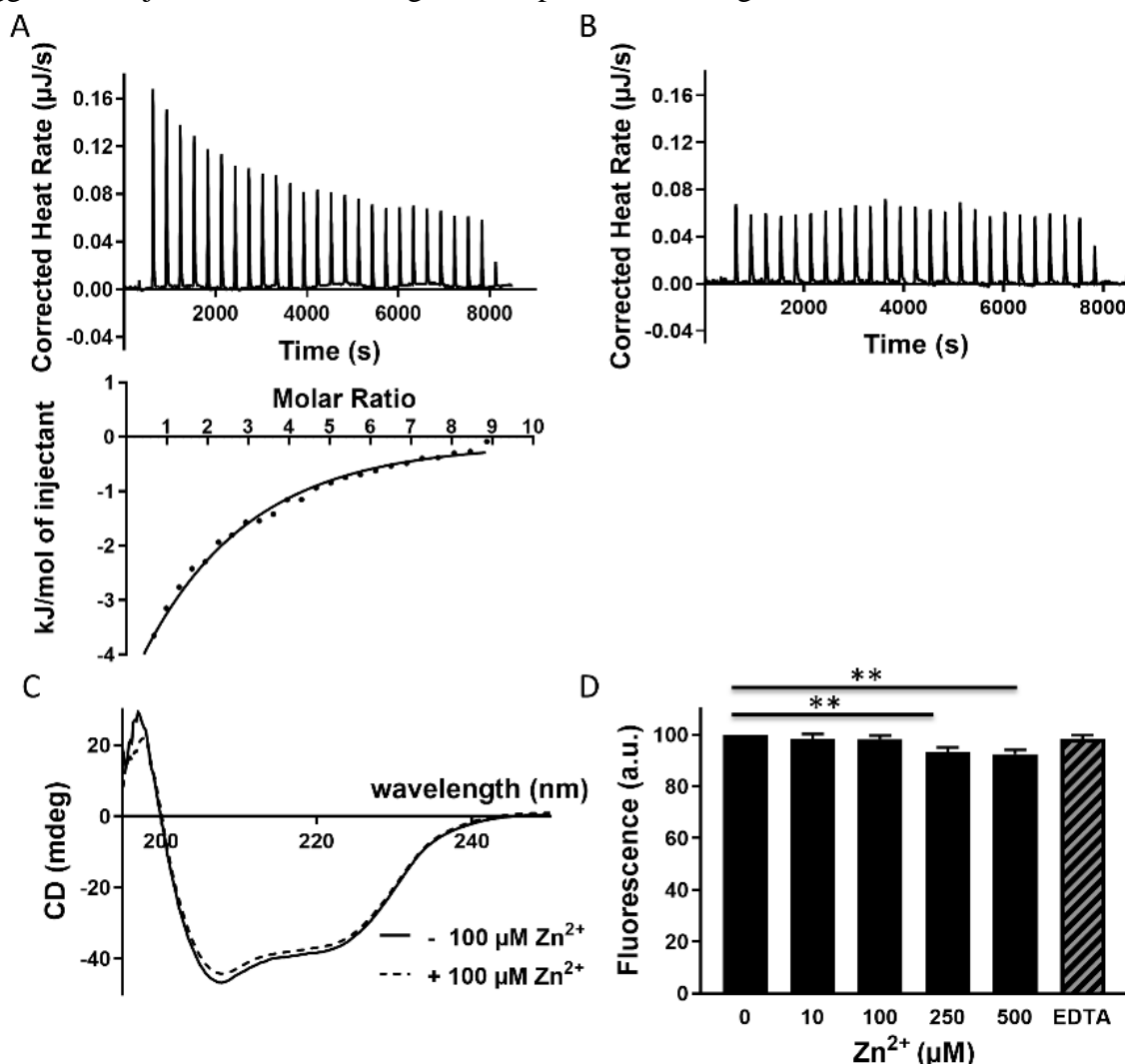


Figure 1. Zn^{2+} binding to GAPR-1. (A) ITC thermogram of Zn^{2+} titration into 60 μM GAPR-1. The upper panel represents the corrected heat rate. The lower panel shows the released heat compared with molar ratio of Zn^{2+} to GAPR-1. (B) ITC thermogram of Ca^{2+} titration into GAPR-1. (C) Far-UV CD spectra of 15 μM GAPR-1, recorded in the absence (solid line) and presence (dashed line) of 100 μM Zn^{2+} . (D) Intrinsic tryptophan fluorescence of GAPR-1 in the absence or presence of Zn^{2+} (0-500 μM , as indicated). EDTA (1 mM) was subsequently added to the sample containing 500 μM Zn^{2+} . Fluorescence intensities were normalized to the initial fluorescence intensity of GAPR-1 in the absence of Zn^{2+} . The results represent the means (\pm S.D.) of three independent experiments. Stars indicate the statistical significance using t-test (two-sample assuming equal variances): ** $P < 0.01$.

Zn^{2+} binding enhances susceptibility of GAPR-1 to trypsin digestion

To further examine the effect of zinc binding on the GAPR-1 structure, we used limited trypsin proteolysis in combination with Western blot analysis. GAPR-1 was incubated with trypsin for 30 min at 37 $^{\circ}\text{C}$ in the presence or absence of zinc. Despite the presence of many lysines and

arginines, GAPR-1 in its apo-form is completely resistant to digestion under the conditions employed (Figure 2A). However, trypsin treatment after titration of GAPR-1 with Zn^{2+} resulted in the appearance of a digestion product of ~12 kDa (Figure 2A). This suggests that a trypsin cleavage site buried within the protein structure becomes exposed upon zinc binding. To obtain information on the position of the cleavage site, different GAPR-1 antibodies were used (see Materials and Methods, Table 2). All of the tested antibodies except the C-terminal antibody (Ab5) recognized the 12 kDa band (Figure 2B), suggesting that the most probable site of cleavage is in a cluster of three lysines (Lys110, 113 and 114). Inspection of the GAPR-1 crystal structure (PDB: 1SMB) revealed that these three lysine residues are located in a loop preceding the C-terminal β -hairpin (Supplementary Figure 1).

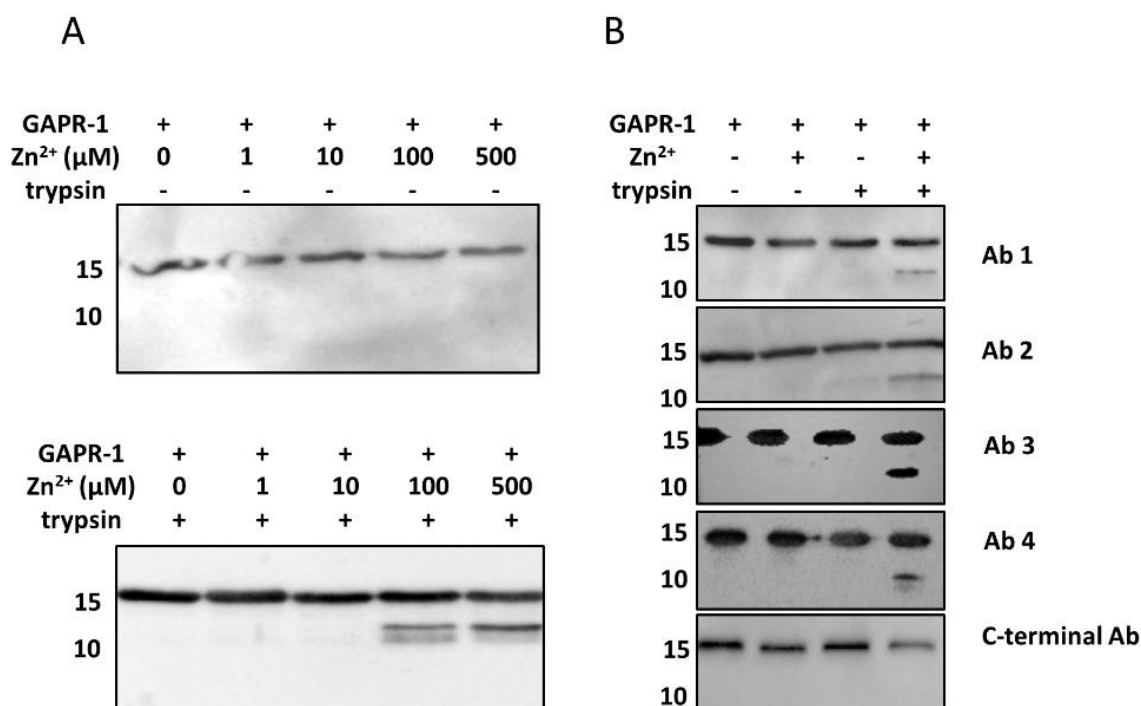


Figure 2. Zn^{2+} binding induces a conformational change in GAPR-1. (A) Western blot analysis of limited trypsin digestion of GAPR-1 using N-terminal GAPR-1 antibody. GAPR-1 (30 μM) was incubated in the presence of Zn^{2+} (0-500 μM) at 37 °C for 30 min, followed by incubation without (upper panel) or with (lower panel) trypsin in the molar ratio of 1:50 (trypsin: GAPR-1) for 30 min at 37 °C. (B) Western blot analysis of limited trypsin digestion of GAPR-1 incubated with 100 μM Zn^{2+} using five different GAPR-1 antibodies (see Table 2, Materials and Methods).

Zn^{2+} mediates amyloid-like aggregation of GAPR-1 in the presence of heparin

Given the subtle structural changes in the tertiary structure of GAPR-1 upon Zn^{2+} binding, we investigated whether Zn^{2+} binding affects the oligomerization/amyloid-like properties of GAPR-1. To this end, we used negatively charged polysaccharide heparin, which is commonly used to study aggregation induction and kinetics *in vitro* of amyloidogenic proteins (Cohlberg et al., 2002; Ramachandran and Udgaonkar, 2011). Heparin serves as a platform to catalyze the seeding process as the first step in amyloid formation by increasing local protein concentrations. GAPR-1 was incubated with heparin in the presence or absence of zinc and ThT fluorescence was monitored over time (Figure 3A). When GAPR-1 was incubated both with heparin and with zinc ions, an immediate and rapid increase in ThT fluorescence intensity was observed. The fluorescence increase continued gradually over time reaching a plateau after approximately 12-15 h (Figure 3A). The immediate ThT increase indicates that oligomeric seeds are instantly formed upon binding of GAPR-1 to heparin in the presence of zinc ions. Furthermore, in the absence of Zn^{2+} the increase in ThT fluorescence after 20 h was negligible. In the absence of heparin or when Zn^{2+} was added in the presence of a molar excess of EDTA, ThT fluorescence did not increase significantly (Figure 3A). ThT fluorescence increased in a zinc concentration-dependent manner in the range of 0-1,000 μM Zn^{2+} (Figure 3B). Taken together, these results indicate that zinc binding triggers amyloid-like aggregation of GAPR-1 in the presence of heparin.

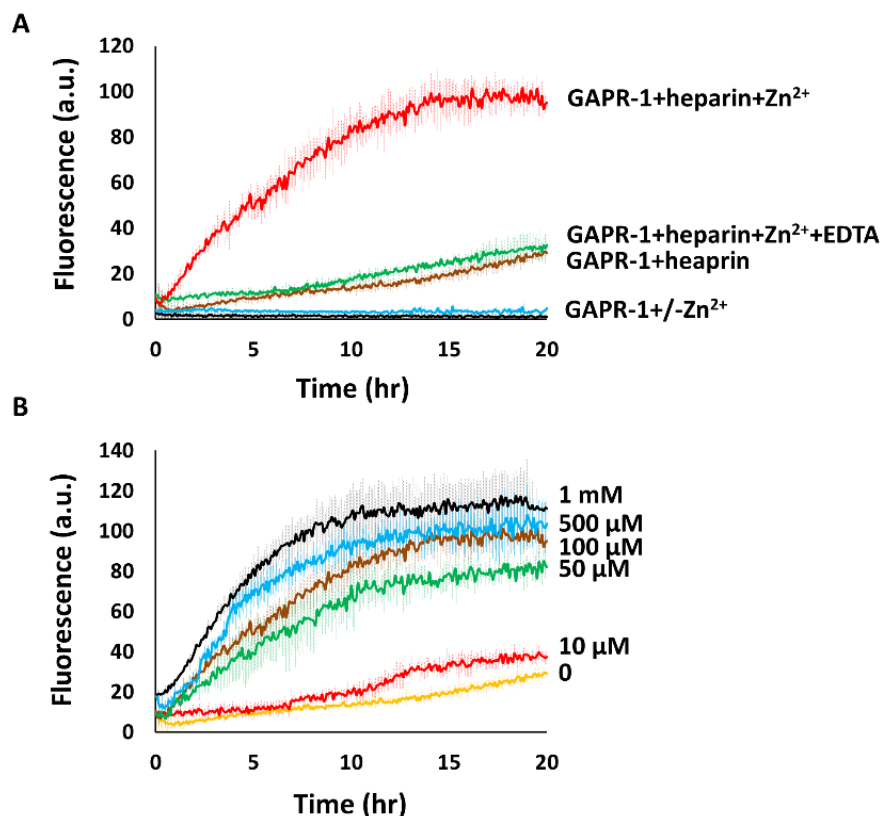


Figure 3. Zn^{2+} induces heparin-mediated GAPR-1 amyloid-like aggregation. (A) Kinetics of ThT fluorescence enhancement of 15 μM GAPR-1 incubated with 37.5 μM heparin and 100 μM Zn^{2+} at 37

°C. The results represent the means (line in bold +/- S.D.) of three independent experiments. GAPR-1 incubated in the absence of heparin and/or Zn^{2+} and in the presence of 1 mM EDTA are shown as controls. (B) ThT fluorescence enhancement of 15 μM GAPR-1 incubated with 37.5 μM heparin in the presence of increasing concentrations of Zn^{2+} (0-1,000 μM) at 37 °C. The results represent the means (line in bold +/- S.D.) of three independent experiments.

The formation of higher order structures by GAPR-1 was confirmed by Western blot analysis. GAPR-1 was incubated at 37 °C with heparin in the presence and absence of 100 μM Zn^{2+} and aliquots were taken after 0, 2, 7 and 20 h, respectively. Only in samples containing both heparin and Zn^{2+} , an increasing amount of high molecular weight products became visible over time (Figure 4A). In the absence of heparin and/or zinc, only monomers and dimers were detected before and after 20 h incubation (Figure 4A).

GAPR-1 oligomeric/amyloid-like structures induced by Zn^{2+} and heparin were visualized by transmission electron microscopy (TEM). After 6 h of incubation, mainly small and spherical oligomers of approximately 5-10 nm in diameter were observed (Figure 4B, panel a). Prolonged incubation of 18 or 72 h resulted in the formation of large amyloid-like aggregates of approximately 0.5 μm up to several μm (Figure 4B, panel b and c, respectively). GAPR-1 incubated with heparin in the absence of zinc showed small irregular clusters with diameters of approximately 50-100 nm (Figure 4B, panel d). Aggregates were absent from TEM images of GAPR-1 and heparin controls, respectively (not shown).

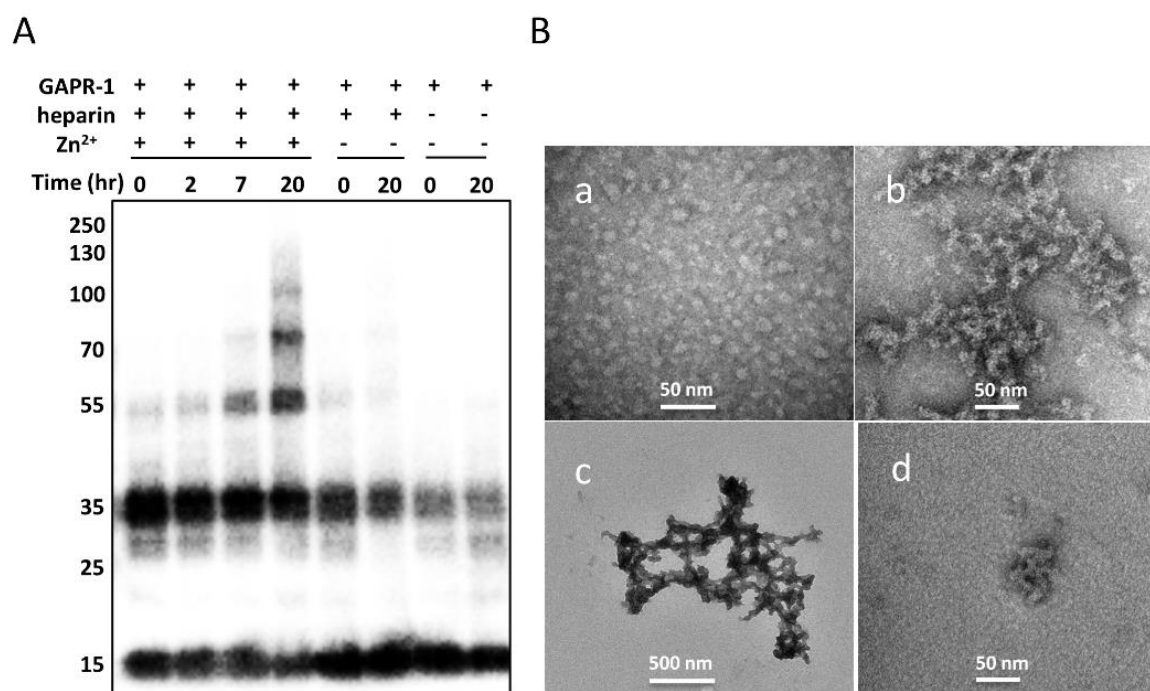


Figure 4. GAPR-1 forms oligomeric and amyloid-like structures in a zinc- and heparin-dependent manner. (A) Western blot analysis of GAPR-1 (15 μM) after incubation in the absence or presence of 37.5 μM heparin and/or 100 μM Zn^{2+} at 37 °C for 0, 2, 7 and 20 h, respectively. (B) Transmission electron micrographs of 15 μM GAPR-1 following incubation with 37.5 μM heparin and 100 μM Zn^{2+}

at 37 °C for 6 h (a), 18 h (b) and 72 h (c). GAPR-1 incubated with heparin in the absence of Zn^{2+} for 18 h (d). Scale bars represent 50 nm in panel a, b and d, and 500 nm in panel c.

Putative metal ion binding site of GAPR-1

Zn^{2+} ions are coordinated by two highly conserved histidine residues in the CAP domain of snake venom CRISPs and GLIPR-1 (Asojo et al., 2011; Suzuki et al., 2008; Wang et al., 2010). Using Bioinformatic tools calculating the minimal energy for metal ion binding, His54 and His103 were identified as the most likely amino acids involved in the coordination of Zn^{2+} at the GAPR-1 protein surface (Figure 5A). This identification is based on: 1) His54 and His103 were in close proximity, whereas all other predicted residues were distant from each other or buried (inaccessible for zinc binding) (His17 and His24 are indicated in Supplementary Figure 1); and 2) His54 and His103 face each other in an opposite direction and possess enough binding affinity for Zn^{2+} . The 3D structure of GAPR-1 docked with Zn^{2+} to the predicted site was compared with the crystal structure of Zn^{2+} -bound GLIPR1 (Asojo et al., 2011) (Figure 5B). The root-mean square deviation (RMSD) between the crystals of Zn^{2+} -bound GLIPR1 and GAPR-1 was less than 1.937 Å, indicative of a high similarity. Zn^{2+} binding to GLIPR1 and GAPR-1 showed a tetrahedral geometry with two histidines and two water molecules (Figure 5C). The predicted Zn^{2+} binding residues in GAPR-1 (His54 and His103) were found to be in the same overall conformation as His79 and His137 in GLIPR1, except for a slight rotation of the corresponding histidine residues (Figure 5C, right panel). As a result, the distance between the two histidine residues in GLIPR1 (His79 and His137) and in GAPR-1 (His54 and His103) was 5.1 Å and 5.4 Å, respectively. The physiochemical properties, including dissociation constant (pKd), the binding energy (ΔG) and the binding efficiency (LE), was similar in zinc binding between GLIPR1 and GAPR-1 as shown in Figure 5D.

To confirm the bioinformatic predictions on the involvement of H54A and H103A in Zn^{2+} binding and amyloid-like aggregation, we constructed two GAPR-1 point-mutants in which either one of these conserved histidines was mutated to alanine (H54A and H103A). ThT fluorescence assay in the presence of heparin was performed to assess whether mutations in the putative metal binding pocket compromised zinc-induced amyloid-like aggregation. Figure 6A shows that for both H54A and H103A ThT fluorescence increase was severely diminished when incubated with heparin in the presence of Zn^{2+} . Moreover, no trypsin cleavage was observed in the presence of Zn^{2+} for these mutants (Figure 6B). These results confirm the involvement of

the two conserved histidines in zinc binding. At this stage, however, we cannot exclude the possibility that other residues are also involved in zinc binding.

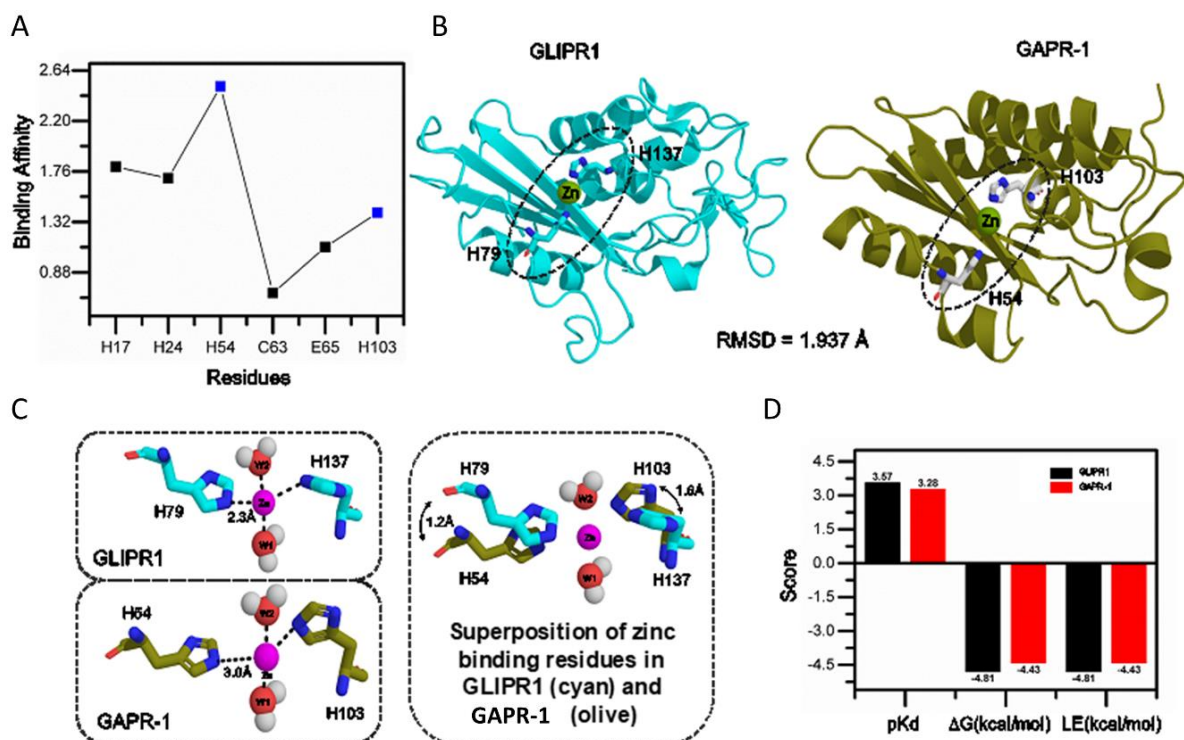


Figure 5. Co-ordination of zinc to GPR-1 by His54 and His103. (A) Zn^{2+} binding site was predicted via ZincBinder. Zn^{2+} binding favors a tetrahedral geometry hierarchy and each residue in the potential binding site was analyzed for binding affinity. (B) Comparison of the 3D structure of GPR-1 with the predicted Zn^{2+} -binding site to the structure of Zn^{2+} -bound GLIPR1. The root-mean square deviation (RMSD) between the crystals of Zn^{2+} -bound GLIPR1 and GPR-1 was less than 1.937 Å, indicative of a high similarity. (C) Comparison of the distance between the two histidine residues and Zn^{2+} in GLIPR1 and in GPR-1. Left panel represents the tetrahedral geometry of Zn^{2+} binding in GLIPR1 and GPR-1; right panel illustrates the superposition of the two Zn^{2+} binding residues in GLIPR1 and GPR-1 and shows a rotation by 1.2 Å for His54 and 1.6 Å for His103 in GPR-1 relative to His79 and His137 in GLIPR1, respectively. Each residue was labelled according to the crystallographic numbering. W represents a water molecule. (D) Physiochemical properties of zinc binding between GLIPR1 and GPR-1 were compared. K_{DEEP} was utilized for analyzing the dissociation constant (pKd), the binding energy ($\Delta\Delta G$) and the binding efficiency (LE). The corresponding score for GLIPR1 and GPR-1 was plotted as a bar graph.

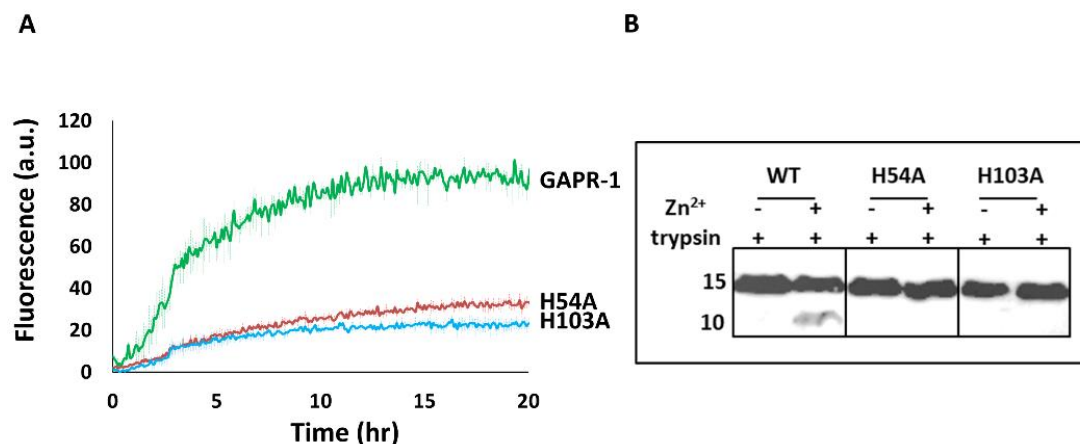


Figure 6. Mutation of the putative GPR-1 metal-binding pocket affects amyloid formation. (A) Kinetics of ThT fluorescence enhancement of 15 μ M GPR-1 WT, H54A or H103A, respectively,

incubated with 5 μM heparin and 100 μM Zn^{2+} at 37 $^{\circ}\text{C}$. The results represent the means (line in bold +/- S.D.) of three independent experiments. (B) Western blot analysis of limited trypsin digestion of GAPR-1 WT, H54A and H103A incubated with 100 μM Zn^{2+} , using N-terminal GAPR-1 antibody.

In sequence alignments with other family members, H54A and H103A of GAPR-1 align with two highly conserved histidines on either side of the groove of the CAP domain (Gibbs et al., 2008; Relini et al., 2014). Given the highly conserved nature of the histidine binding site for Zn^{2+} binding, our findings suggest that zinc-dependent formation of amyloid-like structures may be a common property of other CAP proteins as well. We tested various proteins from the CRISP subfamily for amyloidogenic properties by monitoring ThT fluorescence. Recombinant mouse CRISP2, mouse CRISP4 and human CRISP3, respectively, were incubated with heparin in the presence or absence of Zn^{2+} and ThT fluorescence was monitored for 20 h. Figure 7 shows that for both mCRISP2 and mCRISP4, a Zn^{2+} -dependent increase in ThT fluorescence occurred over time, whereas for hCRISP3 with or without Zn^{2+} no significant increase was observed.

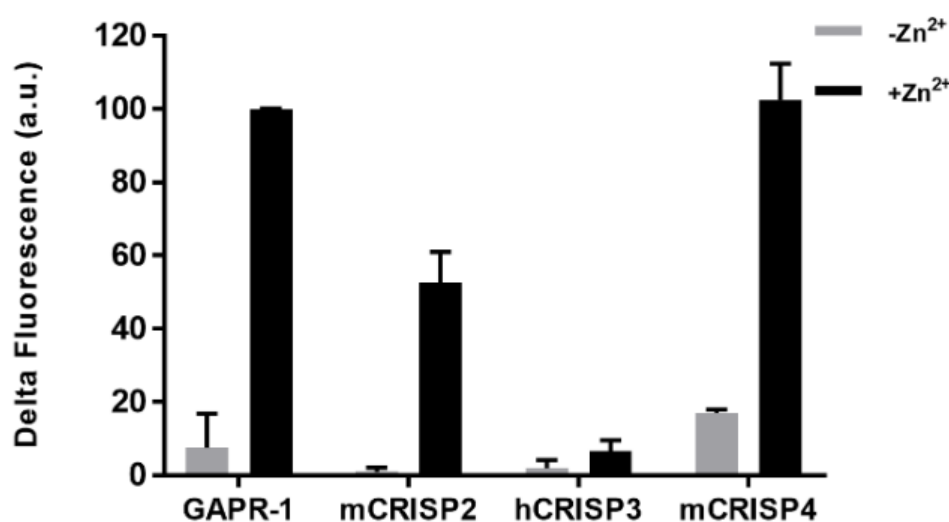


Figure 7. Zn^{2+} induces mouse CRISP2 and mouse CRISP4 amyloid formation. A total of 2.5 μM GAPR-1, mouse CRISP2, human CRISP3 or mouse CRISP4 was incubated with 6.25 μM heparin in absence and presence of 100 μM Zn^{2+} at 37 $^{\circ}\text{C}$ for 20 h. ThT fluorescence assay was performed and the ThT fluorescence was expressed as the difference between the end point and the starting point (delta fluorescence). The results represent the means (+/- S.D.) of three independent experiments.

Discussion

Zinc binding was previously shown to be required for specific functions of CAP protein family members. For example, Natrin, a CAP protein present in snake venom, modulates inflammation through transcriptional regulation of vascular cell adhesion proteins in a Zn^{2+} - and heparan sulfate-dependent manner (Wang et al., 2010). Also, oligomeric complexes of Zn^{2+} -bound

CRISP1 are involved in association to sperm during epididymal maturation (Maldera et al., 2011).

In the present study, we identify GAPR-1 as a zinc binding protein and demonstrate the role of zinc in the regulation of the formation of amyloid-like structures by GAPR-1 in the presence of heparin. Zinc ions play a crucial and complex role in the modulation of amyloidogenic aggregation pathways of many proteins and peptides including tau, A β , islet amyloid polypeptide (IAPP), transthyretin (TTR) and superoxide dismutase 1 (SOD1) (Huang et al., 2014; Nedumpully-Govindan et al., 2015; Oztug Durer et al., 2009; Palmieri et al., 2010). Zinc binding can cause conformational changes or stabilize certain molecular orientations which in turn can either trigger, alter or inhibit the formation of cytotoxic amyloid structures (Lee et al., 2018, 2017; Nedumpully-Govindan et al., 2015; Seetharaman et al., 2010). In recent years also zinc-dependent functional amyloids have been discovered (Garnier et al., 2017; Jacob et al., 2016). Our data presented here provide some clues on the molecular mechanism of how zinc regulates the propensity of GAPR-1 to form amyloid-like assemblies in the presence of heparin. Zinc binding does not result in a major structural rearrangement as determined by CD spectroscopy and tryptophan fluorescence. In agreement with our observations, crystal structures of other CAP superfamily members in complex with Zn²⁺ also did not reveal major conformational changes within the CAP domain (Asojo et al., 2011; Suzuki et al., 2008; Wang et al., 2010). However, the increased susceptibility of GAPR-1 to trypsin digestion clearly demonstrates that zinc binding leads to a (slight) structural change that results in an exposure of a cleavage site in the C-terminal part of the protein. The trypsin cleavage site is not in direct proximity of the zinc binding site. Flexibility in the C-terminal part of the CAP domain is of particular interest as it contains the conserved CAP1 and CAP2 motifs, which were identified by amyloid prediction algorithms as amyloid-prone sequences (Olricks and Helms, 2016). This therefore suggests that the amyloid-related features within the GAPR-1 native structure can be tweaked by external factors such as zinc ions.

Heparin is a glycosaminoglycan (GAG), a family of long unbranched polysaccharides consisting of disaccharide repeating subunits with a large number of sulfate groups. Heparin and other GAGs are intimately involved in modulating amyloid formation of many proteins (Iannuzzi et al., 2015) including α -synuclein (Mehra et al., 2018), tau (Goedert et al., 1996), A β (Mclaurin et al., 1999; Stewart et al., 2017) and transthyretin (Bourgault et al., 2011; Noborn et al., 2011). GAPR-1 has a high isoelectric point of 9.4 which allows interaction with the negatively charged heparin *in vitro*. Heparin binding to other CAP proteins has also been

observed (Assumpção et al., 2013; Wang et al., 2010). Electron microscopy shows the formation of small protein clusters when GAPR-1 is incubated with heparin alone, indicating that heparin could serve as a platform for GAPR-1 aggregation. However, without Zn^{2+} binding this does not result in the formation of ThT-positive amyloid-like structures. These data suggest that the small conformational change is required but not sufficient for subsequent amyloid-like aggregation. Additionally to the conformational change, a protein-concentrating step is required to initiate or catalyze amyloid formation. Previously, we showed that oligomerization and fibrillation of GAPR-1 occurs spontaneously upon interaction with negatively charged liposomes without the necessity of metal ions (Van Galen et al., 2012). The initial binding step based on electrostatic interactions of the positively charged GAPR-1 with both the negatively charged liposomes and heparin are likely to be comparable and reflect a concentration step using two different platforms. We suggest that hydrophobic interactions with the membrane stabilize structural rearrangements in the CAP domain, affecting the structural stability in such a way that amyloid-prone regions become increasingly exposed over time. In the absence of membranes, other mechanisms such as Zn^{2+} binding can also induce structural rearrangements. Our studies identify a two-step mechanism in the amyloid-like aggregation of GAPR-1: i) a concentration step. Different platforms (membranes, heparin) can serve this purpose and allow the formation of amyloid seeds; and ii) a conformational change. Different molecules (lipids, Zn^{2+} ions) can serve this purpose and only a subtle conformational change is required. The exact molecular mechanism will be the subject of further studies.

There is growing evidence that di-/oligomerization of the CAP domain is important for the function of CAP superfamily members (Borloo et al., 2013; Lu et al., 2013; Maldera et al., 2011; Serrano et al., 2004; Sugiyama et al., 2009). This suggests that the CAP domain could serve as a scaffold to localize and enhance the action of other domains in CAP proteins through oligomerization (Olricks and Helms, 2016). We show here that other CAP superfamily members with an additional C-terminal domain, i.e. mouse CRISP2 and CRISP4, also form ThT-positive structures in a zinc- and heparin-dependent manner. This strongly suggests that oligomerization and/or amyloid-like aggregation is a common property of the CAP domain. Although human CRISP3 did not show this characteristic in the presence of heparin and zinc, it does not rule out the possibility that other factors will trigger oligomerization of this particular protein. CAP family members are present in a wide variety of unique environment, each facing an entirely different spectrum of cell surface lipids, GAGs or other potential activating agents.

Zinc binding regulates amyloid-like aggregation of GAPR-1

In addition, the extension of the CAP domain is different for every family member, allowing another level of regulation.

In conclusion, we propose that amyloid-like oligomerization is a common property of the CAP domain in CAP superfamily members and involved in regulating the diverse biological functions of the various family members.

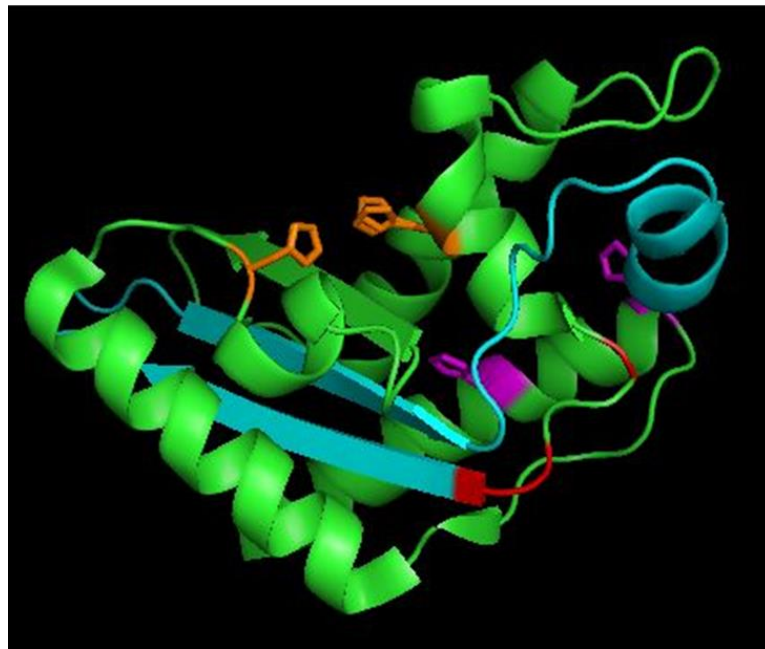
References

- Abraham, A., and Chandler, D.E. (2017). Tracing the evolutionary history of the CAP superfamily of proteins using amino acid sequence homology and conservation of splice sites. *J. Mol. Evol.* 85, 137–157.
- Asojo, O.A., Koski, R.A., and Bonafé, N. (2011). Structural studies of human glioma pathogenesis-related protein 1. *Acta Crystallogr. Sect. D Biol. Crystallogr.* 67, 847–855.
- Assumpção, T.C.F., Ma, D., Schwarz, A., Reiter, K., Santana, J.M., Andersen, J.F., Ribeiro, J.M.C., Nardone, G., Yu, L.L., and Francischetti, I.M.B. (2013). Salivary antigen-5/CAP family members are Cu²⁺-dependent antioxidant enzymes that scavenge O₂^{•-} and inhibit collagen-induced platelet aggregation and neutrophil oxidative burst. *J. Biol. Chem.* 288, 14341–14361.
- Borloo, J., Geldhof, P., Peelaers, I., Van Meulder, F., Ameloot, P., Callewaert, N., Vercruysse, J., Claerebout, E., Strelkov, S. V., and Weeks, S.D. (2013). Structure of Ostertagia ostertagi ASP-1: Insights into disulfide-mediated cyclization and dimerization. *Acta Crystallogr. Sect. D Biol. Crystallogr.* 69, 493–503.
- Bourgault, S., Solomon, J.P., Reixach, N., and Kelly, J.W. (2011). Sulfated glycosaminoglycans accelerate transthyretin amyloidogenesis by quaternary structural conversion. *Biochemistry* 50, 1001–1015.
- Choudhary, V., and Schneider, R. (2012). Pathogen-Related Yeast (PRY) proteins and members of the CAP superfamily are secreted sterol-binding proteins. *Proc. Natl. Acad. Sci. USA* 109, 16882–16887.
- Cohlberg, J.A., Li, J., Uversky, V.N., and Fink, A.L. (2002). Heparin and other glycosaminoglycans stimulate the formation of amyloid fibrils from α -Synuclein in vitro. *Biochemistry* 41, 1502–1511.
- Darwiche, R., Kelleher, A., Hudspeth, E.M., Schneider, R., and Asojo, O.A. (2016). Structural and functional characterization of the CAP domain of pathogen-related yeast 1 (Pry1) protein. *Sci. Rep.* 6, 28838.
- Darwiche, R., Mène-Saffrané, L., Gfeller, D., Asojo, O.A., and Schneider, R. (2017). The pathogen-related yeast protein Pry1, a member of the CAP protein superfamily, is a fatty acid-binding protein. *J. Biol. Chem.* 292, 8304–8314.
- Eberle, H.B., Serrano, R.L., Füllekrug, J., Schlosser, A., Lehmann, W.D., Lottspeich, F., Kaloyanova, D., Wieland, F.T., and Helms, J.B. (2002). Identification and characterization of a novel human plant pathogenesis-related protein that localizes to lipid-enriched microdomains in the Golgi complex. *J. Cell Sci.* 115, 827–838.
- Van Galen, J., Olrichs, N.K., Schouten, A., Serrano, R.L., Nolte-'t Hoen, E.N.M., Eerland, R., Kaloyanova, D., Gros, P., and Helms, J.B. (2012). Interaction of GAPR-1 with lipid bilayers is regulated by alternative homodimerization. *Biochim. Biophys. Acta.* 1818, 2175–2183.
- Garnier, C., Devred, F., Byrne, D., Puppo, R., Roman, A.Y., Malesinski, S., Golovin, A. V., Lebrun, R., Ninkina, N.N., and Tsvetkov, P.O. (2017). Zinc binding to RNA recognition motif of TDP-43 induces the formation of amyloid-like aggregates. *Sci. Rep.* 7, 6812.
- Ghisaidoobe, A.B.T., and Chung, S.J. (2014). Intrinsic tryptophan fluorescence in the detection and analysis of proteins: A focus on förster resonance energy transfer techniques. *Int. J. Mol. Sci.* 15, 22518–22538.
- Gibbs, G.M., Roelants, K., and O'Bryan, M.K. (2008). The CAP superfamily: cysteine-rich secretory proteins, antigen 5, and pathogenesis-related 1 proteins-roles in reproduction, cancer, and immune defense. *Endocr. Rev.* 29, 865–897.
- Goedert, M., Jakes, R., Spillantini, M.G., Hasegawa, M., Smith, M.J., and Crowther, R.A. (1996). Assembly of microtubule-associated protein tau into Alzheimer-like filaments induced by sulphated glycosaminoglycans. *Nature* 383, 550–553.
- Groves, M.R., Kuhn, A., Hendricks, A., Radke, S., Serrano, R.L., Helms, J.B., and Sinning, I. (2004). Crystallization of a Golgi-associated PR-1-related protein (GAPR-1) that localizes to lipid-enriched microdomains. *Acta Crystallogr D Biol Crystallogr* 60, 730–732.
- Huang, Y., Wu, Z., Cao, Y., Lang, M., Lu, B., and Zhou, B. (2014). Zinc binding directly regulates tau toxicity independent of tau hyperphosphorylation. *Cell Rep.* 8, 831–842.
- Iannuzzi, C., Irace, G., and Sirangelo, I. (2015). The effect of glycosaminoglycans (GAGs) on amyloid

- aggregation and toxicity. *Molecules* 20, 2510–2528.
- Jacob, R.S., Das, S., Ghosh, S., Anoop, A., Jha, N.N., Khan, T., Singru, P., Kumar, A., and Maji, S.K. (2016). Amyloid formation of growth hormone in presence of zinc: Relevance to its storage in secretory granules. *Sci. Rep.* 6, 23370.
- Karlsson, O., Berg, A.L., Hanrieder, J., Arnerup, G., Lindström, A.-K., and Brittebo, E.B. (2015). Intracellular fibril formation, calcification, and enrichment of chaperones, cytoskeletal, and intermediate filament proteins in the adult hippocampus CA1 following neonatal exposure to the nonprotein amino acid BMAA. *Arch. Toxicol.* 89, 423–436.
- Lee, M.-C., Yu, W.-C., Shih, Y.-H., Chen, C.-Y., Guo, Z.-H., Huang, S.-J., Chan, J.C.C., and Chen, Y.-R. (2018). Zinc ion rapidly induces toxic, off-pathway amyloid- β oligomers distinct from amyloid- β derived diffusible ligands in Alzheimer's disease. *Sci. Rep.* 8, 1–16.
- Lee, M., Wang, T., Makhlynets, O. V., Wu, Y., Polizzi, N.F., Wu, H., Gosavi, P.M., Stöhr, J., Korendovych, I. V., DeGrado, W.F., et al. (2017). Zinc-binding structure of a catalytic amyloid from solid-state NMR. *Proc Natl Acad Sci USA* 114, 6191–6196.
- Lu, S., Faris, J.D., Sherwood, R., and Edwards, M.C. (2013). Dimerization and protease resistance: New insight into the function of PR-1. *J. Plant Physiol.* 170, 105–110.
- Maldera, J.A., Vasen, G., Ernesto, J.I., Weigel-Muñoz, M., Cohen, D.J., and Cuasnicu, P.S. (2011). Evidence for the involvement of zinc in the association of CRISP1 with rat sperm during epididymal maturation. *Biol. Reprod.* 85, 503–510.
- Mclaurin, J., Franklin, T., Zhang, X., Deng, J., and Fraser, P.E. (1999). Interactions of Alzheimer amyloid-beta peptides with glycosaminoglycans effects on fibril nucleation and growth. *Eur. J. Biochem* 266, 1101–1110.
- Mehra, S., Ghosh, D., Kumar, R., Mondal, M., Gadhe, L.G., Das, S., Anoop, A., Jha, N.N., Jacob, R.S., Chatterjee, D., et al. (2018). Glycosaminoglycans have variable effects on α -synuclein aggregation and differentially affect the activities of the resulting amyloid fibrils. *J. Biol. Chem.* 293, 12975–12991.
- Nedumpully-Govindan, P., Yang, Y., Andorfer, R., Cao, W., and Ding, F. (2015). Promotion or inhibition of islet amyloid polypeptide aggregation by zinc coordination depends on its relative concentration. *Biochemistry* 54, 7335–7344.
- Noborn, F., O'Callaghan, P., Hermansson, E., Zhang, X., Ancsin, J.B., Damas, A.M., Dacklin, I., Presto, J., Johansson, J., Saraiva, M.J., et al. (2011). Heparan sulfate/heparin promotes transthyretin fibrillization through selective binding to a basic motif in the protein. *Proc Natl Acad Sci USA* 108, 5584–5589.
- Ofengeim, D., Ito, Y., Najafov, A., Zhang, Y., Shan, B., DeWitt, J.P., Ye, J., Zhang, X., Chang, A., Vakifahmetoglu-Norberg, H., et al. (2015). Activation of necroptosis in multiple sclerosis. *Cell Rep.* 10, 1836–1849.
- Olrichs, N.K., and Helms, J.B. (2016). Novel insights into the function of the conserved domain of the CAP superfamily of proteins. *AIMS Biophys.* 3, 232–246.
- Olrichs, N.K., Mahalka, A.K., Kaloyanova, D., Kinnunen, P.K., and Helms, J.B. (2014). Golgi-Associated plant Pathogenesis Related protein 1 (GAPR-1) forms amyloid-like fibrils by interaction with acidic phospholipids and inhibits A β aggregation. *Amyloid* 21, 88–96.
- Oztug Durer, Z.A., Cohlberg, J.A., Dinh, P., Padua, S., Ehrenclou, K., Downes, S., Tan, J.K., Nakano, Y., Bowman, C.J., Hoskins, J.L., et al. (2009). Loss of metal ions, disulfide reduction and mutations related to familial ALS promote formation of amyloid-like aggregates from superoxide dismutase. *PLoS One* 4, e5004.
- Palmieri, L. de C., Lima, L.M.T.R., Freire, J.B.B., Bleicher, L., Polikarpov, I., Almeida, F.C.L., and Foguel, D. (2010). Novel Zn²⁺-binding sites in human transthyretin: Implications for amyloidogenesis and retinol-binding protein recognition. *J. Biol. Chem.* 285, 31731–31741.
- Ramachandran, G., and Udgaonkar, J.B. (2011). Understanding the kinetic roles of the inducer heparin and of rod-like protofibrils during amyloid fibril formation by Tau protein. *J. Biol. Chem.* 286, 38948–38959.
- Relini, A., Marano, N., and Gliozzi, A. (2014). Probing the interplay between amyloidogenic proteins and membranes using lipid monolayers and bilayers. *Adv. Colloid Interface Sci.* 207, 81–92.
- Seetharaman, S. V., Winkler, D.D., Taylor, A.B., Cao, X., Whitson, L.J., Doucette, P.A., Valentine, J.S., Schirf, V., Demeler, B., Carroll, M.C., et al. (2010). Disrupted zinc-binding sites in

- structures of pathogenic SOD1 variants D124V and H80R. *Biochemistry* 49, 5714–5725.
- Serrano, R.L., Kuhn, A., Hendricks, A., Helms, J.B., Sinning, I., and Groves, M.R. (2004). Structural analysis of the human Golgi-associated plant pathogenesis related protein GAPR-1 implicates dimerization as a regulatory mechanism. *J. Mol. Biol.* 339, 173–183.
- Shoji-Kawata, S., Sumpter, R., Leveno, M., Campbell, G.R., Zou, Z., Kinch, L., Wilkins, A.D., Sun, Q., Pallauf, K., MacDuff, D., et al. (2013). Identification of a candidate therapeutic autophagy-inducing peptide. *Nature* 494, 201–206.
- Srivastava, A., and Kumar, M. (2018). Prediction of zinc binding sites in proteins using sequence derived information. *J. Biomol. Struct. Dyn.* 1102, 1–11.
- Stewart, K.L., Hughes, E., Yates, E.A., Middleton, D.A., and Radford, S.E. (2017). Molecular origins of the compatibility between glycosaminoglycans and A β 40 amyloid fibrils. *J. Mol. Biol.* 429, 2449–2462.
- Sugiyama, H., Burnett, L., Xiang, X., Olson, J., Willis, S., Miao, A.M.Y., Akema, T., Bieber, A.L., and Chandler, D.E. (2009). Purification and multimer formation of allurin, a sperm chemoattractant from *Xenopus laevis* egg jelly. *Mol. Reprod. Dev.* 76, 527–536.
- Suzuki, N., Yamazaki, Y., Brown, R.L., Fujimoto, Z., Morita, T., and Mizuno, H. (2008). Structures of pseudechotoxin and pseudecin, two snake-venom cysteine-rich secretory proteins that target cyclic nucleotide-gated ion channels: implications for movement of the C-terminal cysteine-rich domain. *Acta Crystallogr D Biol Crystallogr* 64, 1034–1042.
- Wang, Y.-L., Kuo, J.-H., Lee, S.-C., Liu, J.-S., Hsieh, Y.-C., Shih, Y.-T., Chen, C.-J., Chiu, J.-J., and Wu, W.-G. (2010). Cobra CRISP functions as an inflammatory modulator via a novel Zn²⁺- and heparan sulfate-dependent transcriptional regulation of endothelial cell adhesion molecules. *J. Biol. Chem.* 285, 37872–37883.
- Zhang, L., Qu, S., Liang, A., Jiang, H., and Wang, H. (2015). Gene expression microarray analysis of the sciatic nerve of mice with diabetic neuropathy. *Int. J. Mol. Med.* 35, 333–339.
- Zhou, Q., Hao, L., Huang, W., and Cai, Z. (2016). The Golgi-Associated Plant Pathogenesis-Related Protein GAPR-1 enhances type I interferon signaling pathway in response to Toll-Like receptor 4. *Inflammation* 39, 706–717.

Supplementary Figure



Supplementary Figure 1. Position of lysine residues Lys110, Lys113 and Lys114 in the 3D structure of GAPR-1. Structure of GAPR-1 (PDB: 1SMB) with three lysine residues (Lys110, Lys113 and Lys114) of the putative trypsin cleavage site colored in red. The adjacent C-terminal end is colored in cyan. The putative zinc binding histidines (His54 and His103) are colored orange and shown as side chains. His17 and His24 are colored in magenta and shown as side chains.

Metal ions and redox balance regulate distinct amyloid-like aggregation pathways of GAPR-1

Jie Sheng[§], Nick K. Orlachs[§], Willie J. Geerts[#], Dora V. Kaloyanova[§], J. Bernd Helms[§]

[§] Department of Biochemistry and Cell Biology, Faculty of Veterinary Medicine, Utrecht University, Utrecht, the Netherlands

[#] Biomolecular Imaging, Bijvoet Center, Utrecht University, Utrecht, the Netherlands.

Published as

Sheng, J., Orlachs, N. K., Geerts, W. J., Kaloyanova, D. V. and Helms, J. B. (2019). Metal ions and redox balance regulate distinct amyloid-like aggregation pathways of GAPR-1. Sci. Rep. 9, 15048.

Abstract

Members of the CAP superfamily (Cysteine-rich secretory proteins, Antigen 5, and Pathogenesis-Related 1 proteins) are characterized by the presence of a structurally conserved CAP domain. The common structure-function relationship of this domain is still poorly understood. In this study, we unravel specific molecular mechanisms modulating the quaternary structure of the mammalian CAP protein GAPR-1 (Golgi-Associated plant Pathogenesis-Related protein 1). Copper ions are shown to induce a distinct amyloid-like aggregation pathway of GAPR-1 in the presence of heparin. This involves an immediate shift from native multimers to monomers which are prone to form amyloid-like fibrils. The Cu^{2+} -induced aggregation pathway is independent of a conserved metal-binding site and involves the formation of disulfide bonds during the nucleation process. The elongation process occurs independently of the presence of Cu^{2+} ions, and amyloid-like aggregation can proceed under oxidative conditions. In contrast, the Zn^{2+} -dependent aggregation pathway was found to be independent of cysteines and was reversible upon removal of Zn^{2+} ions. Together, our results provide insight into the regulation of the quaternary structure of GAPR-1 by metal ions and redox homeostasis with potential implications for regulatory mechanisms of other CAP proteins.

Introduction

Golgi-Associated plant Pathogenesis-Related protein (GAPR-1) is a mammalian protein which belongs to the CAP (Cysteine-rich secretory proteins, Antigen 5, and Pathogenesis-related 1 proteins) superfamily of proteins (Gibbs et al., 2008). All members of the CAP superfamily contain a structurally conserved CAP domain containing four conserved CAP motifs (CAP1-4). The CAP domain tertiary structure has a unique α - β - α sandwich fold in which α -helices flank a central antiparallel β -sheet (Gibbs et al., 2008). The CAP domain also contains a conserved central cavity formed by two histidine residues and two acidic amino acids, usually glutamic acid (Gibbs et al., 2008). Several CAP superfamily members have been shown to bind different metal ions via this conserved central cavity (Assumpção et al., 2013; Darwiche et al., 2016; Maldera et al., 2011; Shikamoto et al., 2005; Suzuki et al., 2008; Wang et al., 2010). Most CAP proteins have an N-terminal signal peptide for secretion into the extracellular cell environment where they exhibit endo- or paracrine functions (Gibbs et al., 2008). The presence of a variety of additional domains at the C-terminal or sometimes N-terminal end of the CAP domain underlies the high functional diversity within the CAP superfamily (Breen et al., 2017; Gibbs et al., 2008). Certain specific functions have been attributed to the CAP domain, such as protease activity (Milne et al., 2003) as well as lipid and sterol binding and transport (Breen et al., 2017; Choudhary and Schneider, 2012; Darwiche et al., 2018). However, a common functionality for the CAP domain is still unknown.

GAPR-1 is the most ancient CAP subfamily member in vertebrates that evolved from the CAP/PR domain in bacteria (Abraham and Chandler, 2017; Gibbs et al., 2008). These one-domain proteins evolved in invertebrates and mammals into proteins with two domains, connected via a hinge region. GAPR-1 does not contain a hinge region or any other domain. Hence, GAPR-1 consists almost exclusively of a CAP domain, making it a suitable model protein to study the structure-function relationship of this domain (Olrichs and Helms, 2016). GAPR-1 functions as a negative regulator of autophagy in mammalian cells (Shoji-Kawata et al., 2013). It is associated with lipid-enriched microdomains at the cytosolic leaflet of Golgi membranes where it inhibits autophagy by anchoring the autophagy-inducing protein Beclin 1 to the membrane (Eberle et al., 2002; Shoji-Kawata et al., 2013). GAPR-1 is also involved in the type I interferon signaling pathway in response to Toll-like receptor 4 (Zhou et al., 2016). At a structural level, GAPR-1 forms homodimers on Golgi membranes and crystallizes as a dimer (Serrano et al., 2004). Binding of inositol-hexakisphosphate (IP₆) induces an alternative dimer conformation, with one of the monomers rotated by 28.5 degrees (Van Galen et al., 2012).

Recently, a GAPR-1 mutant, which is defective in interacting with Beclin 1, was shown to adopt yet another dimer conformation (Li et al., 2017). Upon interaction with phosphatidylinositol- and cholesterol-containing liposomes, GAPR-1 forms oligomers and amyloid-like structures (Olrichs et al., 2014). This indicates that structural dynamics play an important role in modulating GAPR-1 function. The physiological and molecular mechanisms underlying these structural dynamics are still poorly understood. The presence of potentially amyloidogenic sequences in the CAP1 and CAP2 motifs (Olrichs et al., 2014) led us to propose the CAP domain as a structural domain, regulating protein-protein interactions via its amyloidogenic properties (Olrichs and Helms, 2016).

Metal homeostasis is frequently involved in the regulation of protein conformational dynamics (Kawahara et al., 2017; Kim et al., 2018; Sirangelo and Iannuzzi, 2017). We recently showed that Zn^{2+} binding to GAPR-1 regulates the formation of amyloid-like structures upon interaction with heparin *in vitro* (Sheng et al., 2019). In this study, we demonstrate that Cu^{2+} induces GAPR-1 fibrillation in the presence of heparin through an alternative pathway. Unlike zinc, copper ions exert their effect independently of the conserved putative metal binding site, but through oxidation of the two cysteine residues in the formation of disulfide-linked oligomeric intermediates. This infers a critical role for redox and metal homeostasis in the regulation of specific high-molecular weight assemblies of GAPR-1.

Methods

Reagents

Heparin was purchased from Santa Cruz Biotechnology (Heidelberg, Germany). Trypsin, DpnI, Phusion DNA Polymerases were obtained from Thermo Fisher SCIENTIFIC (Eindhoven, the Netherlands). Thioflavin T, $ZnCl_2$, $CuCl_2$, $MnCl_2$, $MgCl_2 \cdot 6H_2O$, $CaCl_2 \cdot 2H_2O$, $FeCl_3$, ethylenediaminetetraacetic acid (EDTA), tris(2-carboxyethyl)phosphine hydrochloride (TCEP), β -mercaptoethanol (BME), dithiothreitol (DTT), N-Ethylmaleimide (NEM), methoxypolyethylene glycol maleimide (PEG-maleimide, 5 kDa), reduced and oxidized glutathione (GSH and GSSG) were from Sigma-Aldrich (St. Louis, USA).

Plasmids

pQE60-GAPR-1 WT plasmid was described before (Groves et al., 2004; Serrano et al., 2004). pQE60-GAPR-1 H17A, E86A, C32S, C63S and C32S/C63S mutants were generated by site-

directed mutagenesis using the following mutagenic primers. Altered sequences are shown in bold in Table 1.

Mutations in GAPR-1 were verified by DNA sequencing (BaseClear, Leiden, the Netherlands). The protocol used to express and purify GAPR-1 mutants was the same as described for WT GAPR-1 (Groves et al., 2004; Serrano et al., 2004).

Table 1. Primers used for site-directed mutagenesis

GAPR-1		
mutation	Forward	Reverse
H17A	5'-gtcctgaaggcc g ccaatgagtaccg-3'	5'-cggctactcatt g gccggccttcaggac-3'
E86A	5'-ggtacagt g caatcaagaactataacttc-3'	5'-gttcttgatt g cactgtaccatctatcagc-3'
C32S	5'-cactgaagctc t ccaagaacctcaaccg-3'	5'-ggttctt g gagagcttcagtgggggac-3'
C63S	5-cgtggccag t ctgggggagaacctgcatg-3'	5'-gttctcccc a gactggccacggctggac-3'

Thioflavin T fluorescence assay

The kinetics of GAPR-1 amyloid-like aggregation in the presence of heparin and different metal ions were monitored by Thioflavin T (ThT) fluorescence. Reaction mixtures contained 15 μ M GAPR-1, 37.5 μ M heparin and 50 μ M ThT with 0-1,000 μ M Zn^{2+} , Cu^{2+} , Ca^{2+} , Mg^{2+} , Mn^{2+} and Fe^{3+} , respectively, in NT-50 buffer (25 mM Tris, 50 mM NaCl, pH 7.4), and were incubated in sealed 96-well plates (Flat Clear Bottom Black Polystyrene, Corning, USA) at 37°C for 20 h. Fluorescence was measured in a CLARIOstar microplate reader (BMG LABTECH, Germany). ThT fluorescence emission was recorded at 488 nm after excitation at 449 nm with agitation before every measurement. The results represent the means (+/- S.D.) of three independent experiments.

Transmission electron microscopy (TEM)

15 μ M GAPR-1 was incubated with 37.5 μ M heparin and 100 μ M Cu^{2+} at 37 °C for 3 h and 24 h. 10 μ l of each sample was placed on a 100 mesh glow discharged gold grid (Quantifoil Micro Tools GmbH, Jena, Germany). After 30 sec, excess fluid was removed, and the grid was washed twice with ddH₂O for 30 sec each time. The grid was then negatively stained with 2% uranyl acetate in ddH₂O for twice, 15 sec and 30 sec, respectively. After removal of excess fluid, the grid was dried on air. Samples were viewed in Tecnai 20 LaB6 transmission electron

microscope (FEI, Eindhoven, the Netherlands) at 200 kV. Images were recorded using a 4K square pixel Eagle CCD camera (FEI, Eindhoven, the Netherlands).

Circular dichroism (CD) spectroscopy

CD spectra of GAPR-1 was measured on a JASCO J-810 spectropolarimeter (Jasco Co. Ltd., Tokyo, Japan) at 37 °C as described by Sheng et al., 2019. Briefly, CD spectra of 15 µM GAPR-1 in the presence of 0-100 µM Cu²⁺ in NT-50 buffer were acquired using a quartz cuvette (1 mm path length). Measurements were performed on scanning from 260 to 190 nm and repeated four times.

Trypsin digestion

30 µM GAPR-1 was incubated with increasing Cu²⁺ concentrations (0-500 µM) in a total volume of 20 µl NT-50 buffer at 37 °C for 30 min, after which trypsin was added in a molar ratio of 1:50 (trypsin: GAPR-1) and incubated at 37 °C for 30 min. The reaction was terminated by addition of Laemmli sample buffer. Protein samples were analyzed by SDS-PAGE and Western blot using five different peptide antibodies (Ab 1-5) that are directed against different epitopes in GAPR-1. The epitopes and antibodies are described by Sheng et al., 2019.

Blue Native PAGE

Protein samples (2 µg) were mixed with 4x native sample buffer (200 mM Tris, 40% (v/v) glycerol, 0.08% (w/v) Coomassie Blue G-250 (Sigma-Aldrich, St. Louis, USA), pH 6.8) and loaded onto a 4-20% Mini-PROTEAN TGX Precast gel (Bio-Rad, California, USA). Electrophoresis was carried out using anode buffer (25 mM Tris, 192 mM glycine, pH 7.0), and blue cathode buffer (25 mM Tris, 192 mM glycine, 0.02% (w/v) Coomassie G-250, pH 7.0) (Fiala et al., 2011) at 4 °C for 1 h at 100 V.

SDS-PAGE and Western Blot

Formation of high molecular weight (HMW) structures of WT GAPR-1 and cysteine mutants was analyzed by Western blot. 15 µM WT GAPR-1, C32S GAPR-1, C63S GAPR-1 or C32S/C63S GAPR-1 was incubated with 37.5 µM heparin and 20 µM Cu²⁺ in NT-50 buffer at 37 °C. Aliquots taken at different timepoints (0 h, 3 h and 18 h) were treated with Laemmli sample buffer in the presence or absence of β-mercaptoethanol (BME), separated on SDS PAGE gel and analyzed by Western blot using a C-terminal GAPR-1 antibody (Eberle et al., 2002).

N-Ethylmaleimide (NEM) labeling assay

60 μM GAPR-1 was incubated with 10 mM NEM at room temperature for 1 h in the dark. Unreacted NEM was removed by three repetitive steps of dilution in NT-50 buffer and concentration using Amicon 10 kDa MWCO centrifugal filter (Merck, Darmstadt, Germany). Protein concentration was determined using Pierce Coomassie (Bradford) assay kit (Thermo Fisher, Eindhoven, the Netherlands) and the degree of NEM-modification was determined by subsequent PEG-maleimide labelling and SDS-PAGE.

PEG-maleimide labelling assay

15 μM GAPR-1 was incubated with 100 μM Zn^{2+} or 20 μM Cu^{2+} in the absence or presence of 37.5 μM heparin at 37 °C. Aliquots taken at different timepoints (0, 0.5, 4 and 18 h) were incubated with 1 mM PEG-maleimide at room temperature for 1 h and analyzed by SDS-PAGE with Coomassie blue staining.

Sedimentation analysis

15 μM GAPR-1 was incubated with 100 μM Zn^{2+} or 20 μM Cu^{2+} and 37.5 μM heparin at 37 °C. 2 mM EDTA was added after 1, 4, 6 and 18 h, respectively, and incubated for an additional 30 min at room temperature, followed by centrifugation at 14,000 g for 30 min. Protein content in the pellet fraction was analyzed by SDS-PAGE with Coomassie blue staining and quantified using densitometry (Image Lab, Bio-Rad, California, USA). The results represent the mean (\pm S.D.) of three independent experiments.

Results

Copper ions induce alternative GAPR-1 amyloid-like aggregation

GAPR-1 forms amyloid-like structures when incubated with heparin in the presence of zinc ions (Sheng et al., 2019). Several CAP superfamily members have been reported to bind zinc and other metal ions at a highly conserved putative binding site in the CAP domain (Assumpção et al., 2013; Darwiche et al., 2016; Maldera et al., 2011; Shikamoto et al., 2005; Suzuki et al., 2008; Wang et al., 2010). In order to determine whether the modulation of GAPR-1 amyloidogenicity is specific for zinc, GAPR-1 was incubated with various metal ions in the presence of heparin and ThT fluorescence was monitored over time. In the presence of Cu^{2+} , enhancement of ThT fluorescence intensity was observed. Other metal ions, including Ca^{2+} , Mn^{2+} , Mg^{2+} and Fe^{3+} , had no effect, even at concentrations of 1 mM (Figure. 1A). The increase in ThT fluorescence was Cu^{2+} concentration-dependent (Figure 1B). Compared to equimolar

concentrations of Zn^{2+} , the ThT fluorescence increase induced by Cu^{2+} was significantly lower (Figure 1A). Our previous study had shown that mutations in the putative metal-binding site (H54A and H103A) of the CAP domain impaired zinc-dependent aggregation of GAPR-1 (Sheng et al., 2019) (also shown in Figure 1C, right panel). To determine whether this site is also involved in copper-induced amyloid-like aggregation, we analyzed the effect of Cu^{2+} on GAPR-1 H54A and GAPR-1 H103A mutant proteins. Surprisingly, copper-induced ThT fluorescence enhancement was not significantly affected in both histidine mutants as compared to WT GAPR-1 (Figure 1C). These results suggest that copper-dependent initiation of GAPR-1 amyloid formation is mechanistically different from Zn^{2+} -induced aggregation. In support of this, structural analysis of the aggregates formed in the presence of Cu^{2+} by TEM showed spherical particles of irregular size and clustered amyloid-like fibrillar structures after 3 and 24 h, respectively (Figure 1D) that were morphologically markedly different as compared to the Zn^{2+} -induced oligomers and amyloid-like aggregates (Sheng et al., 2019).

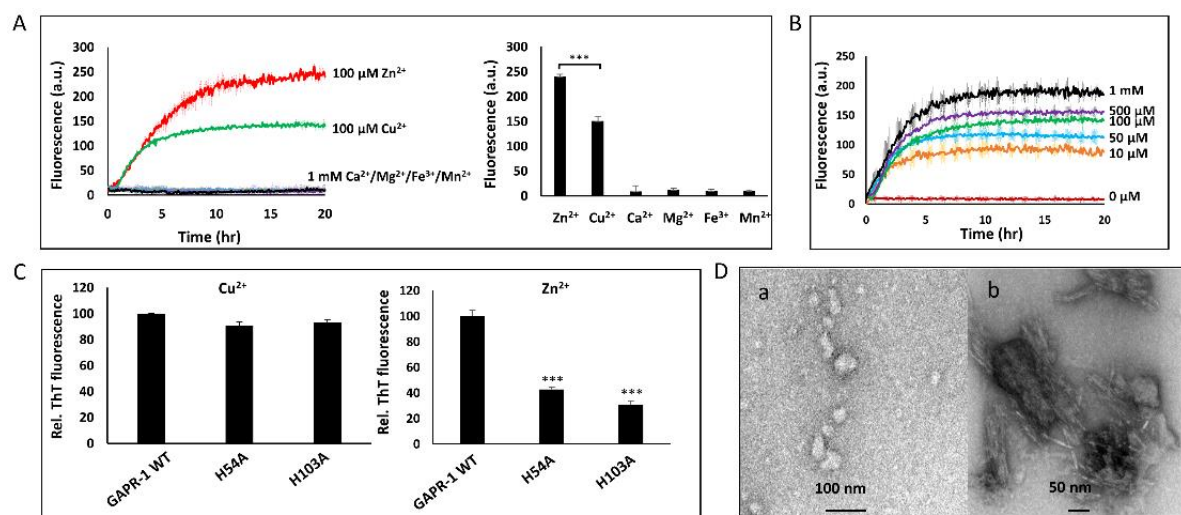


Figure 1. Cu^{2+} induces alternative GAPR-1 amyloid-like aggregation. (A) Kinetics of ThT fluorescence enhancement of 15 μM GAPR-1 incubated with 37.5 μM heparin and 100 μM Zn^{2+} /100 μM Cu^{2+} /1 mM Ca^{2+} /1 mM Mg^{2+} /1 mM Fe^{3+} /1 mM Mn^{2+} at 37 $^{\circ}\text{C}$. The results represent the means (line in bold +/- S.D.) of three independent experiments. ThT fluorescence intensity of each reaction after 20 h incubation is shown in the right panel. Stars indicate the statistical significance using t-test (two-sample assuming equal variances): ***P-value=0.0004 < 0.001. (B) Kinetics of ThT fluorescence enhancement of 15 μM GAPR-1 incubated with 37.5 μM heparin in the presence of increasing concentrations of Cu^{2+} (0-1,000 μM) at 37 $^{\circ}\text{C}$. The results represent the means (line in bold +/- S.D.) of three independent experiments. (C) 15 μM GAPR-1 WT, H54A or H103A was incubated with 5 μM heparin and 100 μM Cu^{2+} (left panel) or Zn^{2+} (right panel) at 37 $^{\circ}\text{C}$. ThT fluorescence intensity after 20 h incubation is shown for the histidine mutants relative to that of WT GAPR-1 for each metal ion, respectively. The results represent the means (+/- S.D.) of three independent experiments. A difference between Cu^{2+} and Zn^{2+} induced amyloid formation is also observed at other heparin concentrations. Stars indicate the statistical significance using t-test (two-sample assuming equal variances): ***P-value < 0.001 (P_{H54A} =0.0002 and P_{H103A} =0.0001). (D) Transmission electron micrographs of 15 μM GAPR-1 following incubation with 37.5 μM heparin and 100 μM Cu^{2+} at 37 $^{\circ}\text{C}$ for 3 h (a) and 24 h (b). Scale bars represent 100 nm in panel a and 50 nm in panel b.

Copper binding induces structural changes in GAPR-1

Zn²⁺-binding to GAPR-1 did not induce a detectable change in the secondary structure of GAPR-1, but exposed a trypsin cleavage site, resulting in the trypsin-dependent release of a ~12 kDa C-terminal fragment (Sheng et al., 2019). Surprisingly, similar results were obtained with Cu²⁺: Copper binding to GAPR-1 did not induce a change in secondary structure as determined by CD spectroscopy (Figure 2A) but did induce a subtle change in the GAPR-1 structure, yielding a trypsin-sensitive proteolytic product of similar molecular weight as in the conditions with zinc (Figure 2B). Using antibodies specific for different regions of GAPR-1, the digestion product was also shown to be cleaved at the C-terminal part of the protein (Figure 2B) suggesting that copper binding causes a similar, if not the same structural change.

Exposure of the trypsin-sensitive cleavage site could be the result of a subtle conformational change and/or a change in the quaternary structure of GAPR-1. Previous studies on plant PR-1 proteins revealed that dimerization was linked directly to protease resistance (Lu et al., 2013). Thus, a shift in the monomer/dimer ratio of GAPR-1 could result in exposure of a trypsin cleavage site that is hidden at the dimer interface. To investigate whether metal binding to GAPR-1 affected its quaternary structure, we employed Blue Native PAGE (BN-PAGE). In the absence of metal ions or in the presence of 100 μ M Zn²⁺, GAPR-1 migrates as a diffuse band at approximately the dimer-tetramer molecular weight range (Figure 2C, upper left panel). Following a 5 min incubation with 100 μ M Cu²⁺, two well-defined bands were visible at molecular weights corresponding to GAPR-1 dimers and monomers (Figure 2C, upper left panel). This suggests that the quaternary structure of GAPR-1 is destabilized by copper binding, resulting in the generation of monomeric species. In marked contrast, Zn²⁺ also induced a shift to monomeric GAPR-1 species, but only at later time points (Figure 2C, upper right panel). The GAPR-1 Histidine mutants H54A and H103A remained sensitive to Cu²⁺ and formed monomers in the presence of this metal ion (Figure 2C), in agreement with the results described in Figure 1C.

To investigate a role for GAPR-1 monomers in the formation of Cu²⁺-induced amyloid-like fibrils, we generated GAPR-1 mutants that are impaired in forming native multimers. A predominantly monomeric protein was observed for mutants E86A and H17A (Figure 2C, lower panel). The highly conserved Glu86 is located along the crystal dimer interface. A previous study on plant PR-1 proteins showed that mutation of the corresponding glutamate impaired its ability to form native dimers (Lu et al., 2013). His17 is another highly conserved

residue that is not located near the dimer interface but part of the CAP3 signature motif. Both mutants were analyzed for their capacity to form amyloid-like aggregates in the presence of heparin. Strikingly, both H17A and E86A mutants showed an increase in ThT fluorescence when incubated with heparin in the absence of metal ions (Figure 2D). In the presence of low concentrations of Zn^{2+} or Cu^{2+} (10 μM), ThT intensity strongly increased. In the absence of heparin no increase in ThT fluorescence was observed under any condition. The monomeric GAPR-1 mutants were analyzed in the limited trypsin digestion assay and both H17A and E86A (Figure 2E) were sensitive to trypsin in the absence of metal ions. The presence of Zn^{2+} or Cu^{2+} enhanced the proteolytic digestion of GAPR-1 H17A and antibody recognition showed that the ~12 kDa digestion product resulted from cleavage of the C-terminal part of the protein (Figure 2E). We therefore consider it likely that exposure of the trypsin-sensitive cleavage site is the result of a subtle conformational change in combination with a change in the quaternary structure of GAPR-1.

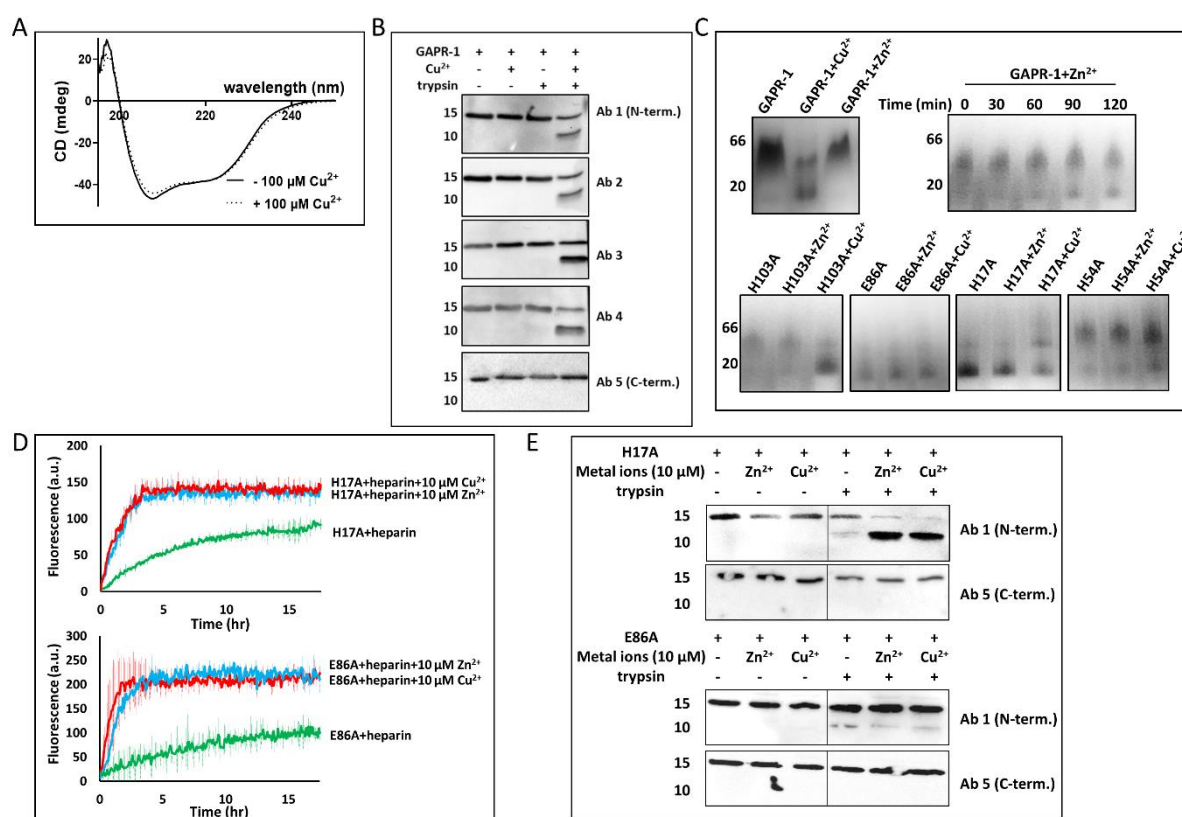


Figure 2. Cu^{2+} binding induces conformational changes in GAPR-1. (A) Far-UV CD spectra of 15 μM GAPR-1, recorded in the absence (solid line) and presence (dotted line) of 100 μM Cu^{2+} . (B) Western blot analysis of limited trypsin digestion of GAPR-1 incubated with Cu^{2+} using five different GAPR-1 antibodies. GAPR-1 was incubated in the absence and presence of 100 μM Cu^{2+} at 37° for 30 min, followed by incubation without or with trypsin in the molar ratio of 1:50 (trypsin: GAPR-1) for 30 min at 37 °C. (C) BN-PAGE analysis of GAPR-1 WT (upper panel) and mutants (lower panel) in the absence and presence of metal ions. 2 μg GAPR-1 WT/mutants were incubated with 100 μM Cu^{2+} or Zn^{2+} at room temperature for 5 min (upper left). 2 μg WT GAPR-1 incubated with 100 μM Zn^{2+} for prolonged times as indicated (upper right). (D) Kinetics of ThT fluorescence enhancement of 15 μM

H17A and E86A, respectively, incubated with 37.5 μM heparin in the absence and presence of 10 μM Zn^{2+} or Cu^{2+} at 37 °C. The results represent the means (line in bold \pm S.D.) of three independent experiments. (E) Trypsin susceptibility of monomeric GAPR-1 mutants in the absence of metal ions. Western blot analysis of limited trypsin digestion of H17A/E86A incubated without or with 10 μM Zn^{2+} or Cu^{2+} using N-terminal and C-terminal GAPR-1 antibodies, respectively.

Copper-induced fibrillation pathway requires disulfide bond formation

Besides histidines, Cu^{2+} is also known to readily interact with cysteines (Rigo et al., 2004). GAPR-1 has two cysteines, which are not involved in disulfide bridge formation within GAPR-1 molecules but could, *e.g.*, be involved in disulfide bridge formation between GAPR-1 molecules during oligomerization. After pre-incubation of GAPR-1 with N-ethylmaleimide (NEM) to modify cysteine residues, no amyloid-like fibers were observed anymore in the ThT fluorescence assay in the presence of heparin and Cu^{2+} (Figure 3A). Western blot analysis confirmed the inability of NEM-modified GAPR-1 to form HMW structures in the presence of Cu^{2+} and heparin (Supplementary Figure 1). To further investigate a role of disulfide bonds in Cu^{2+} -mediated amyloid-like aggregation, WT GAPR-1 was incubated with heparin and 100 μM Cu^{2+} under reducing conditions to prevent disulfide bond formation. Strikingly, with increasing concentrations of DTT, a prolonged delay in the onset of ThT fluorescence increase was observed (Figure 3B). This suggests disulfide bond formation plays a crucial role during the initiation of amyloid formation under reducing conditions. To exclude that fluorescence kinetics were affected by possible interactions between Cu^{2+} and thiol groups of DTT, experiments were repeated using TCEP. A similar delay was observed for 200 μM TCEP, whereas 1 mM TCEP even caused full inhibition over a period of 20 h (Figure 3C). The inhibition of oligomeric and/or amyloid-like structures under reducing conditions was confirmed by Western blot analysis. In the presence of DTT, the amount of oligomers and HMW structures was drastically lower at each timepoint as compared to incubation in the absence of DTT (*i.e.*, Figure 3D, -BME). Both in the absence and presence of DTT, oligomeric and HMW structures were observed after 18 h incubation that were resistant to the routinely applied denaturing conditions of SDS-PAGE (Figure 3D, +BME), consistent with characteristics of amyloid-like fibrils.

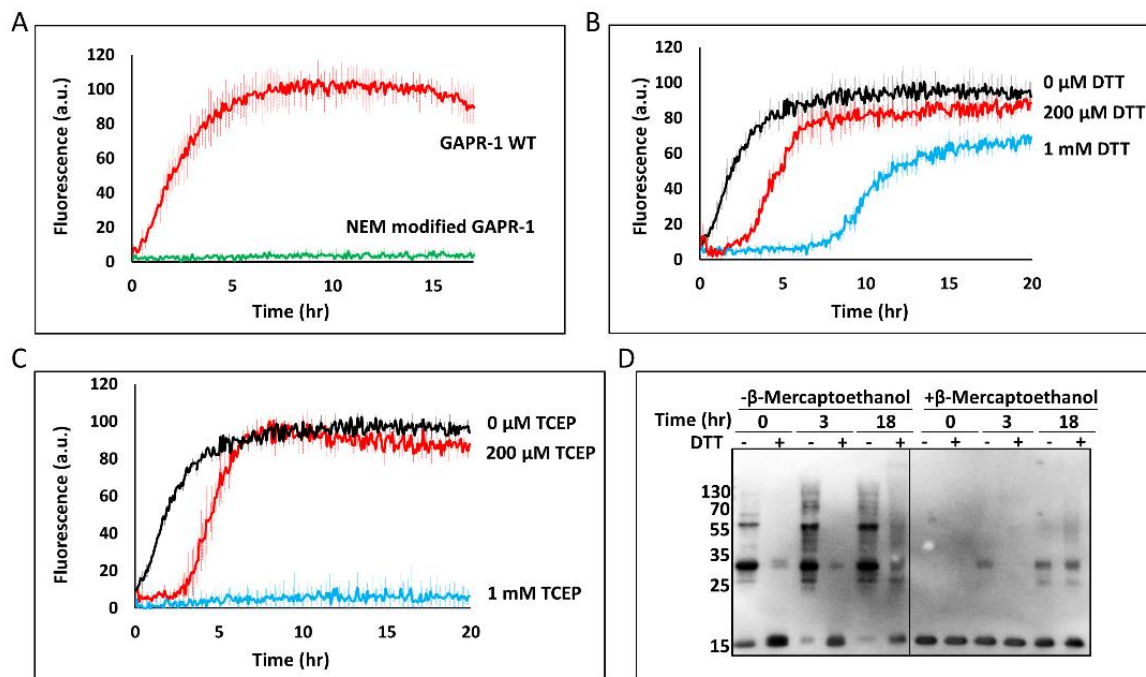


Figure 3. Copper-induced fibrillation pathway requires disulfide bond formation. (A) Kinetics of ThT fluorescence enhancement of 15 μM WT GAPR-1 or NEM-modified GAPR-1 incubated with 37.5 μM heparin and 100 μM Cu²⁺ at 37 °C, (B) in the additional presence of DTT (0-1,000 μM) (C) or TCEP (0-1,000 μM). The results represent the means (line in bold +/- S.D.) of three independent experiments. (D) 15 μM GAPR-1 was incubated with 37.5 μM heparin and 100 μM Cu²⁺ in the absence and presence of 1 mM DTT at 37 °C. Aliquots were taken at 0 h, 3 h and 18 h and Laemmli sample buffer with or without BME was added for SDS-PAGE and Western blot analysis using a C-terminal GAPR-1 antibody.

Cysteine residues of GAPR-1 are involved in Cu²⁺ binding

We assessed the oxidation state of the cysteines in WT GAPR-1 by incubation with PEG-maleimide (~5 kDa), capable of reacting with reduced cysteines. SDS-PAGE analysis shows that for the majority of WT GAPR-1 both cysteines were labeled and that no unlabeled protein was detectable (Figure 4A). To investigate the role of cysteine residues in copper-mediated amyloid-like aggregation in more detail, GAPR-1 mutants were constructed with one (C32S or C63S) or both cysteines (C32S and C63S) mutated to serine. In both GAPR-1 single cysteine mutants, almost complete labeling of the single cysteine with PEG-maleimide was observed, while C32S/C63S remained unlabeled, as expected (Figure 4A). This shows that for all proteins the cysteines are predominantly in the reduced form. Of note: pre-incubation with NEM completely inhibited subsequent labeling with PEG-maleimide (Figure 4A), confirming that inhibition of amyloid-like structures by NEM (Figure 3A) is the result of efficient labeling of both cysteines in GAPR-1 with NEM. All three mutants showed a dramatic inhibition of ThT enhancement. In the presence of 20 μM Cu²⁺, both C32S and C32S/C63S did not show any substantial increase over 20 h, whereas for C63S ThT fluorescence only slightly increased as

compared to WT GAPR-1 (Figure 4B, left panel). The end point of ThT fluorescence (20 h) illustrates the significant differences between WT GAPR-1 and the three cysteine mutants (Figure 4B, right panel). The inability of the cysteine mutants to form HMW structures was confirmed by Western blot analysis under non-reducing conditions. WT GAPR-1, C32S, C63S or C32S/C63S were incubated at 37 °C with heparin and 20 μM Cu^{2+} and aliquots were taken at 0 h, 3 h and 18 h, respectively. For WT GAPR-1 an increasing amount of structures was detected over time (Figure 4C and Supplementary Figure 4). However, only monomers and dimers were observed when one of the two cysteines was mutated. Only monomers were detected in the double cysteine mutant. These results imply that both cysteine residues play a role in the Cu^{2+} -induced amyloid-like aggregation of GAPR-1.

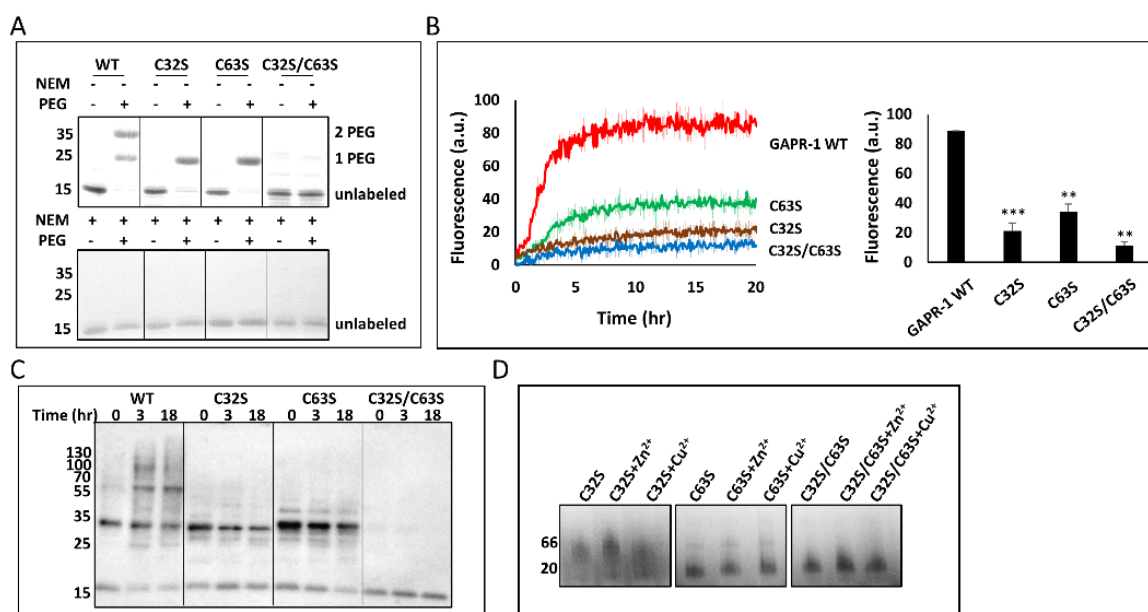


Figure 4. Cysteine residues of GAPR-1 are involved in Cu^{2+} binding. (A) PEG-maleimide labeling of cysteines analyzed by SDS-PAGE. 60 μM GAPR-1 WT, C32S, C63S or C32S/C63S was incubated with 1 mM PEG-maleimide at room temperature for 1 h following a pre-incubation with or without 10 mM NEM at room temperature for 1 h. (B) Kinetics of ThT fluorescence enhancement of 15 μM GAPR-1 WT, C32S, C63S or C32S/C63S incubated with 37.5 μM heparin and 20 μM Cu^{2+} at 37 °C (left panel). ThT fluorescence intensity of the cysteine mutants after 20 h incubation relative to WT GAPR-1 (right panel). The results represent the means (line in bold \pm S.D.) of three independent experiments. Similar results were obtained at 100 μM Cu^{2+} . Stars indicate the statistical significance using t-test (two-sample assuming equal variances): **0.001 < P-value < 0.01; ***P-value < 0.001 ($P_{\text{C32S}}=0.0002$, $P_{\text{C63S}}=0.0017$, $P_{\text{C32S/C63S}}=0.0011$). (C) Western blot analysis of non-reducing SDS-PAGE of 15 μM GAPR-1, C32S, C63S or C32S/C63S incubated with 37.5 μM heparin and 20 μM Cu^{2+} at 37 °C for the indicated time (0, 3 and 18 h). Results were analyzed with C-terminal GAPR-1 antibody. (D) BN-PAGE analysis of GAPR-1 cysteine mutants in the absence and presence of metal ions. 2 μg C32S, C63S or C32S/C63S was incubated with or without 100 μM Zn^{2+} or Cu^{2+} at room temperature for 5 min.

The oligomeric state of each of the cysteine mutants was determined by BN-PAGE. C32S migrated similar to WT GAPR-1, *i.e.* ranging from dimer to tetramer, whereas both C63S and C32S/C63S were predominantly monomeric (Figure 4D). In the presence of Cu^{2+} , the

monomeric content of C32S increased (Figure 4D). Both cysteines in GAPR-1 are not in close proximity of the GAPR-1 dimer interface and therefore it is not clear how these cysteines affect the monomer-oligomeric status of GAPR-1. These results do imply, however, a role of GAPR-1 cysteines both in disulfide bond formation and in affecting the monomeric/oligomeric status of GAPR-1.

Disulfide-bonded oligomers serve as nuclei

Next, we assessed the role of copper in disulfide bond formation during the different stages (initiation and elongation/maturation) of GAPR-1 amyloid-like aggregation. To this end, EDTA was added at different time points during the aggregation process to remove the copper ions. Under non-reducing conditions, GAPR-1 rapidly forms amyloid-like fibers and as expected, addition of EDTA at the onset of the reaction fully inhibited aggregation (Figure 5A, left panel). Surprisingly, addition of EDTA at different time points during aggregation did not halt the process but resulted in an immediate and steep rise in ThT fluorescence, eventually reaching a maximum value nearly twice as high as in the continuous presence of Cu^{2+} (Figure 5A, left panel). These results suggest that Cu^{2+} is not required during the elongation/maturation phase but is required at the onset of the reaction. To investigate this in more detail, we repeated the experiment in the presence of DTT, causing a delay in the initiation phase (see Figure 3B). Under these conditions, addition of EDTA at different time points during the lag-phase strongly inhibited the enhancement of ThT fluorescence during 20 h (Figure 5A, right panel). In contrast, addition of EDTA at 8 h, when ThT fluorescence had commenced to increase, caused again a rapid jump in fluorescence (Figure 5A, right panel). These results confirm that although copper binding is crucial for initiation of GAPR-1 fibrillation, it is not required for its continuation. During the elongation/maturation phase, amyloid-like aggregation is less sensitive to oxidizing/reducing conditions and proceeds more efficiently in the absence of Cu^{2+} ions.

Together, our results indicate a role for Cu^{2+} and redox balance during the initiation phase of GAPR-1 amyloid-like aggregation. To determine whether Cu^{2+} directly affects the redox balance, the assay was repeated using monomeric GAPR-1 mutants E86A and H17A that form amyloid-like aggregates in the absence of Cu^{2+} . These GAPR-1 mutants were incubated with heparin in buffer containing different ratios of reduced and oxidized glutathione (GSH and GSSG, respectively). H17A and E86A in the presence of heparin already caused a modest increase in ThT fluorescence (Figure 5B and 5C, left panel). For both mutants, ThT fluorescence increased dramatically under oxidative condition (0.5 mM GSH/2.5 mM GSSG).

However, under reduced condition (2.5 mM GSH/0.5 mM GSSG), the increase of ThT fluorescence was inhibited (Figure 5B and 5C, left panel). Trypsin digestion assay shows that for both H17A and E86A mutant proteins, proteolysis was also enhanced under oxidative conditions (Figure 5B and 5C), confirming structural changes upon cysteine oxidation.

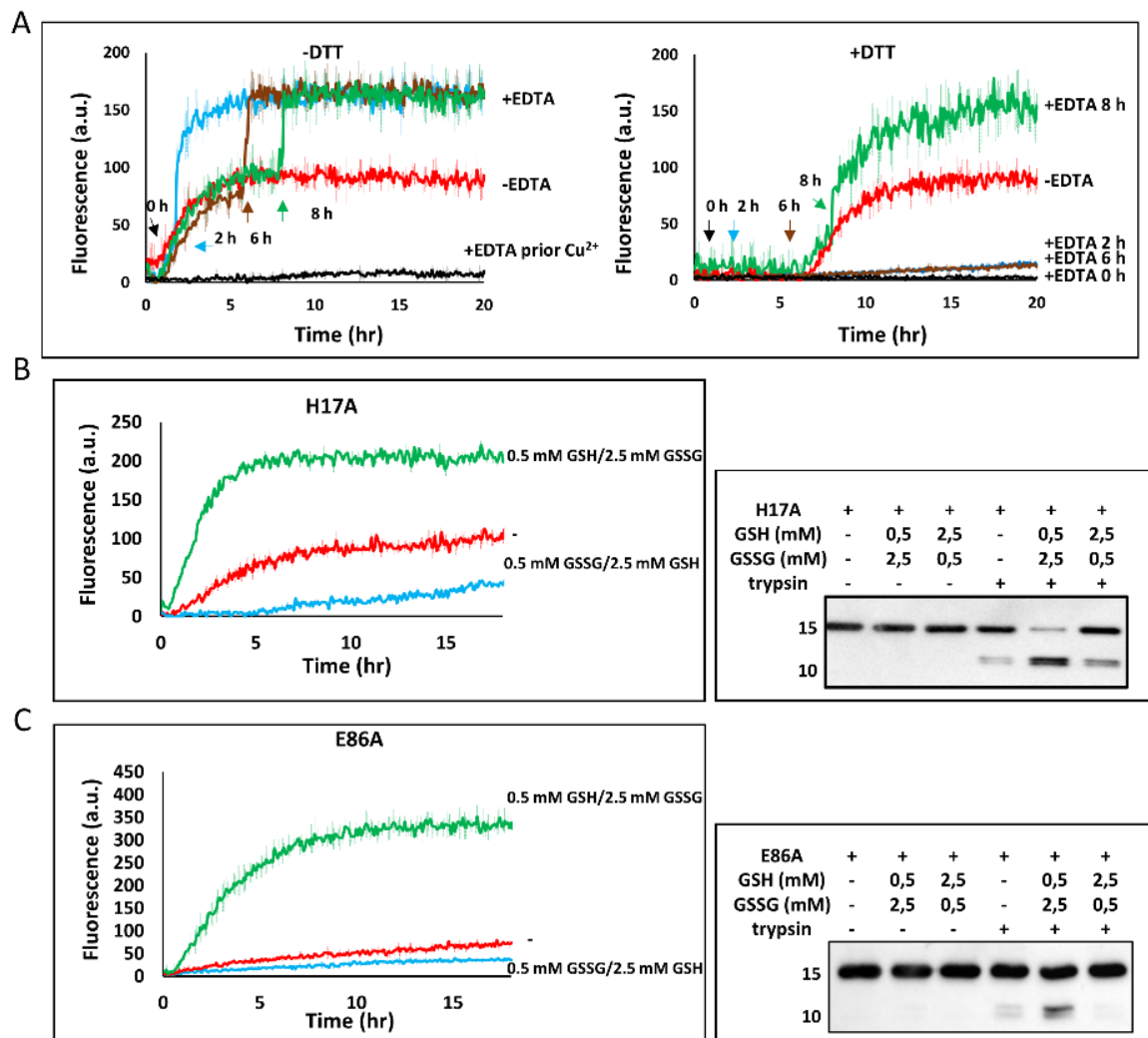


Figure 5. Disulfide-bonded oligomers serve as nuclei. (A) Kinetics of ThT fluorescence enhancement of GPR-1 incubated with heparin and Cu^{2+} under non-reducing (left panel) and reducing (right panel) conditions. 15 μM GPR-1 was incubated with 37.5 μM heparin and 100 μM Cu^{2+} in the absence and presence of 1 mM DTT at 37 $^{\circ}\text{C}$, with addition of 1 mM EDTA at different timepoints (0 h, 2 h, 6 h, and 8 h). (B and C) The left panel shows kinetics of ThT fluorescence enhancement of 15 μM H17A (B) or E86A (C) incubated with 37.5 μM heparin at 37 $^{\circ}\text{C}$ under reducing (0.5 mM GSSG/2.5 mM GSH) and oxidative (0.5 mM GSH/2.5 mM GSSG) conditions, respectively. The right panels represent the Western blot analysis of limited trypsin digestion of H17A/E86A under reducing (0.5 mM GSSG/2.5 mM GSH) and oxidative (0.5 mM GSH/2.5 mM GSSG) conditions using N-terminal GPR-1 antibody. The kinetics are the result of three independent experiments and the results represent the means (line in bold) \pm S.D.

Comparison with zinc-mediated GPR-1 amyloid-like aggregation

The differential effects of Cu^{2+} and Zn^{2+} on amyloid-like aggregation of GPR-1 mutants H54A and H103A suggest that the fibrillation pathway for both metal ions is mechanistically

distinct. Indeed, Zn^{2+} -induced enhancement of ThT fluorescence was not significantly affected for GAPR-1 with NEM-modified cysteines (Figure 6A), indicating that both cysteines do not play a role in this process. In agreement, we found no difference in the zinc-dependent aggregation pathway of GAPR-1 under control and reducing (TCEP) conditions, suggesting that disulfide bond formation does not play a role in the zinc-dependent pathway neither.

The requirement for zinc ions during the distinct stages of fibrillation was also investigated. Addition of EDTA during the fibrillation process (0 h, 1.5 h, 4 h and 18 h, respectively) caused an immediate stop in amyloid-like aggregation in all cases, accompanied by an immediate small reduction in ThT fluorescence (Figure 6B). This suggests that the continuous presence of zinc is required for aggregation to proceed and that upon removal of zinc ions the ThT-positive HMW structures formed partially disintegrate. Sedimentation analysis was used to confirm this. GAPR-1 was incubated with heparin and Zn^{2+} and EDTA was added at different timepoints during fibrillation. Subsequently, HMW structures were sedimented by centrifugation. Figure 6C (left panel) shows that removal of zinc ions at any timepoint notably decreased the amount of sedimented protein. In contrast, removal of Cu^{2+} ions did not decrease the amount of sedimented protein (Figure 6C, right panel).

The results indicate that Zn^{2+} -mediated protein aggregation can at least be partially reversed. To investigate this, we used PEG labeling to monitor the accessibility of GAPR-1 cysteines during Zn^{2+} -induced aggregation. GAPR-1 was incubated under various conditions and after taking aliquots at different times points, the samples were labeled with PEG-maleimide. GAPR-1 incubated with Zn^{2+} and heparin showed progressively fewer accessible cysteines over time (Figure 6D, left panel). We then assessed the reversibility of this process by investigating cysteine accessibility following the removal of zinc ions from HMW structures. To this end, GAPR-1 was first incubated with heparin and Zn^{2+} for 18 h, after which EDTA was added. Following brief incubation, PEG-maleimide was added to label the accessible cysteines. Figure 6D (right panel) shows that the cysteines that were protected from PEG modification in the zinc-aggregates, became highly accessible again after addition of EDTA. This shows that cysteine residues in the zinc-induced GAPR-1 aggregates are shielded from modification in a reversible manner. In marked contrast, the presence of Cu^{2+} , both with or without heparin, inhibited labeling of cysteines as expected through oxidation (Figure 6D, left panel). In addition, cysteine inaccessibility was not reversible in Cu^{2+} -induced GAPR-1 aggregates (Figure 6D, right panel).

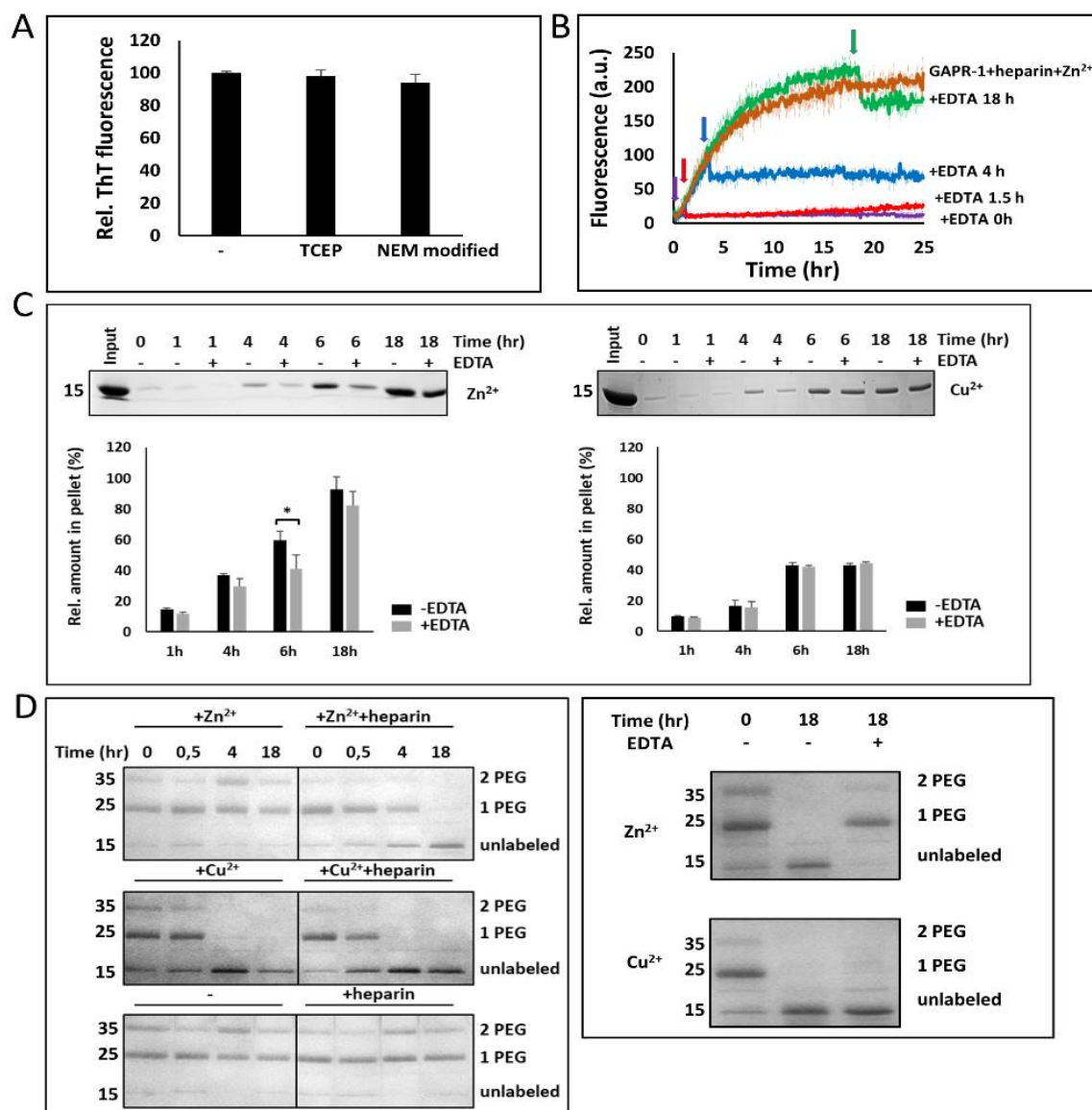


Figure 6. Comparison with zinc-mediated GAPR-1 amyloid-like aggregation. (A) Zinc-dependent ThT fluorescence enhancement of GAPR-1 under reducing conditions or with modified cysteines. 15 μ M GAPR-1, either in the presence of 1 mM TCEP or with NEM-modified cysteines, was incubated with 37.5 μ M heparin and 100 μ M Zn²⁺ for 20 h and ThT fluorescence intensity is shown relative to control conditions (without TCEP and NEM modification). The results represent the means (\pm S.D.) of three independent experiments. (B) Kinetics of ThT fluorescence enhancement of 15 μ M GAPR-1 incubated with 37.5 μ M heparin and 100 μ M Zn²⁺ at 37 $^{\circ}$ C, with addition of 1 mM EDTA at different timepoints (0 h, 1.5 h, 4 h, and 18 h). The results represent the means (line in bold \pm S.D.) of three independent experiments. (C) 15 μ M GAPR-1 was pre-incubated with 100 μ M Zn²⁺ (left panel) or 20 μ M Cu²⁺ (right panel) in the presence of 37.5 μ M heparin at 37 $^{\circ}$ C for 1 h, 4 h, 6 h and 18 h, respectively, followed by incubation with or without 2 mM EDTA at room temperature for 30 min. Following centrifugation at 14,000 g for 30 min, the pellet fraction was analyzed by SDS-PAGE with Coomassie blue staining. The amount of GAPR-1 in the pellet is expressed as a percentage of the total input as determined by densitometry. The results represent the means (\pm S.D.) of three independent experiments. Stars indicate the statistical significance using t-test (two-sample assuming equal variances): *0.01 < P-value=0.0286 < 0.05. (D) 15 μ M GAPR-1 was incubated with or without 100 μ M Zn²⁺ or 20 μ M Cu²⁺ in the absence or presence of 37.5 μ M heparin at 37 $^{\circ}$ C for 0 h, 0.5 h, 4 h and 18 h. This was followed by incubation with 1 mM PEG-maleimide at room temperature for 1 h and analysis by SDS-PAGE with Coomassie blue staining (left panel). 15 μ M GAPR-1 was incubated with 100 μ M

Zn²⁺ or 20 μ M Cu²⁺ and 37.5 μ M heparin at 37 °C for 18 h and subsequently incubated with or without 2 mM EDTA at room temperature for 30 min. PEG labeling was analyzed by SDS-PAGE with Coomassie blue staining (right panel).

Discussion

GAPR-1 exists in various oligomeric forms. It is present as dimers on Golgi membranes and displays amyloidogenic properties *in vitro* that can be regulated by Zn²⁺ binding (Olrachs et al., 2014; Serrano et al., 2004; Sheng et al., 2019). This implies that the mechanisms underlying self-interaction are important for the functionality of GAPR-1 in autophagy and other cellular pathways (Olrachs and Helms, 2016; Olrachs et al., 2014). We have shown here that formation of GAPR-1 amyloid-like structures can occur through distinct molecular pathways dependent on zinc/copper ion binding and redox conditions, providing novel insights into the possible regulatory mechanisms controlling GAPR-1 oligomerization and aggregation.

Using BN-PAGE analysis we show that the native quaternary structure of GAPR-1 is modulated by zinc and copper ions. Recombinant WT GAPR-1 is mainly multimeric (ranging from dimer to tetramer) in solution. Binding of Cu²⁺ causes an immediate dissociation of multimeric into monomeric GAPR-1. In the monomeric state, aggregation-prone regions (APRs) that are hidden in the multimeric state become exposed, resulting in efficient aggregation. This could be due to increased conformational flexibility in the monomer and/or because they were buried in the dimer interface. The exposure of APRs is corroborated by two GAPR-1 mutants, H17A and E86A, that are predominantly monomeric in solution. Incubation of these mutants with heparin caused increased ThT fluorescence without the addition of metal ions. Nonetheless, the presence of either Zn²⁺ or Cu²⁺ additionally enhanced both ThT fluorescence, suggesting that both metal ions stabilize conformations that amplify the amyloidogenic propensity of GAPR-1.

Destabilization of native state multimers is a common mechanism proposed for several other amyloidogenic proteins (Grignaschi et al., 2018; Jurczak et al., 2016; Perlenfein et al., 2017; Saad et al., 2017; Saldaño et al., 2017; Zhao et al., 2013). A well-known example is transthyretin (TTR), which commonly exists as a homotetramer. Various factors such as mutation, oxidation, pH and ligand binding impact the stability of TTR, with dissociation into monomers consequently resulting in pathogenetic fibrillation (Iakovleva et al., 2016; Leach et al., 2018; Saldaño et al., 2017; Skoulakis and Goodfellow, 2003; Zhao et al., 2013). The yeast pyruvate kinase Cdc19 uses similar mechanisms to form functional amyloid (Cereghetti et al.,

2018; Grignaschi et al., 2018; Saad et al., 2017). We now show that metal ions differentially affect the monomeric and oligomeric status of GAPR-1. Whereas Cu^{2+} ions cause an immediate shift from multimeric to monomeric GAPR-1, Zn^{2+} ions cause a similar shift, but only after prolonged incubation. For numerous proteins involved in amyloid-related neurodegenerative diseases, copper and zinc homeostasis plays crucial roles (Gerber et al., 2017; Kawahara et al., 2017; Sirangelo and Iannuzzi, 2017). A well-studied example is superoxide dismutase 1 (SOD1), to which Zn^{2+} and Cu^{2+} binding is required for structural stability and proper function. Either demetallation or aberrant metal binding has been shown to promote protein misfolding and pathogenic aggregation (Banci et al., 2007; Sirangelo and Iannuzzi, 2017; Yiwari et al., 2009). Here we have shown that zinc and copper ions differentially affect the structural regulation of GAPR-1 and speculate that the distinct GAPR-1 oligomeric or amyloid-like structures serve specific physiological purposes. In line with this, many functional amyloids have recently been discovered as a novel physiological mechanism to regulate a variety of cellular activities, including storage of hormone peptides (Jacob et al., 2016; Maji et al., 2009), fertilization (Egge et al., 2015; Hewetson et al., 2017; Roan et al., 2017), necroptosis (Liu et al., 2017), pigmentation (Bissig et al., 2016), antimicrobial responses (Jang et al., 2011) and adaptation to stress conditions (Audas et al., 2016; Saad et al., 2017). Moreover, some functional aggregates are fully reversible in a highly regulated manner (Jacob et al., 2016; Saad et al., 2017; Zhao et al., 2013).

The zinc-induced GAPR-1 amyloid-like aggregation is different from Cu^{2+} -induced aggregation pathway in many ways. Most importantly, Zn^{2+} binds to the putative CAP metal-binding site causes a slow shift to monomeric GAPR-1 species, is independent of the redox conditions and requires the continuous presence of zinc. In addition, the amyloid-like structures formed in the presence of Zn^{2+} have a different structure as shown by TEM and the fact that cysteines in Zn^{2+} -induced GAPR-1 aggregates are protected from modification in a reversible manner illustrates the reversible nature of Zn^{2+} -induced amyloid-like fibrils. Zn^{2+} coordination to cysteines is a known mechanism to protect free thiol groups from oxidation (Lee, 2018; Pace and Weerapana, 2014). However, Zn^{2+} -induced amyloid-like aggregation still occurs in the GAPR-1 mutant without cysteines. We therefore consider it more likely that the two cysteine residues become buried in the amyloid-like structures, making them unavailable for modification. In this respect, it is interesting to note that in the GAPR-1 crystal structure both cysteines are surface-exposed and highly oxidized. In contrast, in the IP6-bound structure of GAPR-1, Cys63 is not oxidized and its side chain is oriented inwards (Van Galen et al., 2012).

Thus, different orientations or exposures of the cysteines in GAPR-1 can have drastic effects on the redox potential of these amino acids. Protection of cysteines could be an essential mechanism for the generation of reversible amyloid aggregates in the presence of Zn^{2+} and to protect these aggregates from becoming irreversible as observed in the Cu^{2+} -induced amyloid fibrils (in which cysteines are accessible for modification).

Cu^{2+} -induced GAPR-1 amyloid-like aggregation does not involve the conserved metal binding site. This was surprising as in the crystal structures of other CAP proteins, several different transition metals, including Cu^{2+} , localize to this binding site (Assumpção et al., 2013; Darwiche et al., 2016; Maldera et al., 2011; Shikamoto et al., 2005; Suzuki et al., 2008; Wang et al., 2010). The copper-induced pathway is modulated by the thiol/disulfide oxidation status of the two cysteines in GAPR-1. This pathway involves formation of copper-catalyzed disulfide-linked oligomeric species that subsequently serve as nuclei for typical amyloid-related fibrils. We show that the redox environment can either inhibit or stimulate the formation of GAPR-1 fibrils. Under reducing conditions, copper ions are required to catalyze formation of oligomeric nuclei, which is the rate limiting step as shown by ThT fluorescence kinetic measurements. A model for the distinct pathways is displayed in Figure 7.

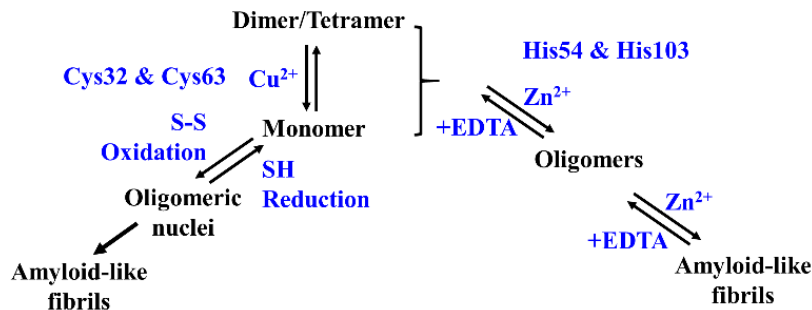


Figure 7. Model of distinct Zn^{2+} - and Cu^{2+} -induced amyloid-like aggregation pathways of GAPR-1 in the presence of heparin. In the Cu^{2+} -induced pathway, GAPR-1 quaternary structure is modulated by Cu^{2+} binding, shifting native multimers to monomers. Redox-dependent disulfide bond formation is crucial during the initiation when oligomeric nuclei are formed. In the Zn^{2+} -dependent pathway, reversible amyloid-like aggregates are formed. Cys32 and Cys63 play essential roles in the Cu^{2+} induced GAPR-1 aggregation pathway, while His54 and His103 are important in the Zn^{2+} induced aggregation pathway.

GAPR-1 is mainly localized at the cytosolic side of Golgi membrane (Eberle et al., 2002), where cysteines tend to remain in the reduced state (Rietsch and Beckwith, 1998). Hence, the cytosolic orientation makes the involvement of disulfide bonds in GAPR-1 oligomerization less likely to occur. However, neighboring positively charged residues, such as the lysine adjacent to Cys32 of GAPR-1, lower the pK_a value of its thiol group (Cumming et al., 2004) favoring the thiolate

form, which is very reactive towards oxidants and thiols (Cai and Yan, 2013). Cu^{2+} is a redox-active metal ion which is able to catalyze formation of disulfides (Cavallini et al., 1969). Disulfide bridges are dynamic in response to the changes of redox environment in the cell (Cai and Yan, 2013) and often play critical roles in amyloid formation (Anoop et al., 2014; Chattopadhyay et al., 2015; Furukawa et al., 2011; Liu et al., 2017).

Are these properties reflected in other members of the CAP superfamily? At the molecular level, one of the cysteine residues of GAPR-1 (Cys63) is semi-conserved within the superfamily while Cys32 is non-conserved. Compared to GAPR-1, other CAP superfamily members generally contain more cysteine residues including in their CAP domain, most of which are involved in disulfide bridges. These are thought to convey structural stability in the extracellular environment, where most CAP family members reside. While the importance of redox buffers (*e.g.* glutathione, cysteine, thioredoxin) for maintaining a reducing intracellular environment is well established, the extracellular space is commonly regarded as an oxidizing redox-inert microenvironment. However, emerging evidence shows that the extracellular redox environment is dynamic, carefully regulated and intimately coupled to intracellular metabolism (Banerjee, 2012; Mcbean et al., 2015). Likewise, extracellular zinc and copper levels are tightly interwoven with the regulation of cellular signalling pathways (Kaplan and Maryon, 2016; Maret, 2017). As many CAP proteins form functional oligomers *e.g.* during fertilization and immune regulation (Lu et al., 2013, 2014; Maldera et al., 2011; Sugiyama et al., 2009; Wang et al., 2010), the metal ion and redox balance may provide important means to regulate their activity.

References

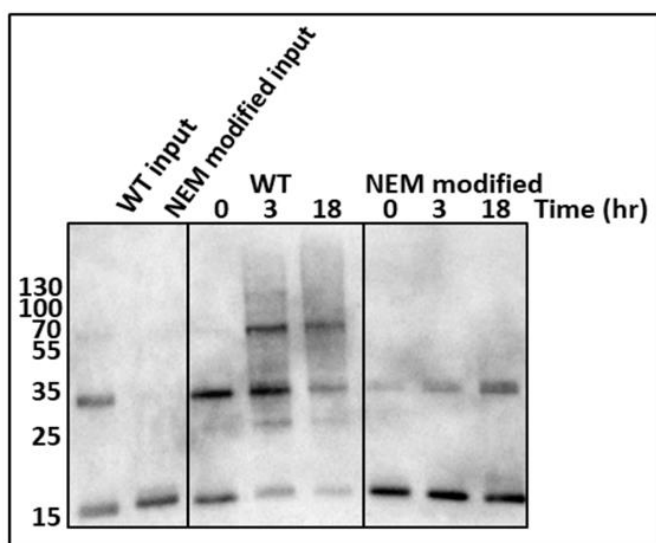
- Abraham, A., and Chandler, D.E. (2017). Tracing the evolutionary history of the CAP superfamily of proteins using amino acid sequence homology and conservation of splice sites. *J. Mol. Evol.* 85, 137–157.
- Anoop, A., Ranganathan, S., Dhaked, B.D., Jha, N.N., Pratihari, S., Ghosh, S., Sahay, S., Kumar, S., Das, S., Kombrabail, M., et al. (2014). Elucidating the role of disulfide bond on amyloid formation and fibril reversibility of somatostatin-14: Relevance to its storage and secretion. *J. Biol. Chem.* 289, 16884–16903.
- Assumpção, T.C.F., Ma, D., Schwarz, A., Reiter, K., Santana, J.M., Andersen, J.F., Ribeiro, J.M.C., Nardone, G., Yu, L.L., and Francischetti, I.M.B. (2013). Salivary antigen-5/CAP family members are Cu²⁺-dependent antioxidant enzymes that scavenge O₂^{•-} and inhibit collagen-induced platelet aggregation and neutrophil oxidative burst. *J. Biol. Chem.* 288, 14341–14361.
- Audas, T.E., Audas, D.E., Jacob, M.D., Ho, J.J.D., Khacho, M., Wang, M., Perera, J.K., Gardiner, C., Bennett, C.A., Head, T., et al. (2016). Adaptation to stressors by systemic protein amyloidogenesis. *Dev. Cell.* 39, 155–168.
- Banci, L., Bertini, I., Durazo, A., Girotto, S., Gralla, E.B., Martinelli, M., Valentine, J.S., Vieru, M., and Whitelegge, J.P. (2007). Metal-free superoxide dismutase forms soluble oligomers under physiological conditions: A possible general mechanism for familial ALS. *Proc Natl Acad Sci USA* 104, 11263–11267.
- Banerjee, R. (2012). Redox outside the box: linking extracellular redox remodeling with intracellular redox metabolism. *J. Biol. Chem.* 287, 4397–4402.
- Bissig, C., Rochin, L., and Niel, G. van (2016). PMEL amyloid fibril formation: The bright steps of pigmentation. *Int. J. Mol. Sci.* 17, 1438.
- Breen, S., Williams, S.J., Outram, M., Kobe, B., and Solomon, P.S. (2017). Emerging insights into the functions of pathogenesis-related protein 1. *Trends Plant Sci.* 22, 871–879.
- Cai, Z., and Yan, L.-J. (2013). Protein oxidative modifications: Beneficial roles in disease and health. *J. Biochem. Pharmacol. Res.* 1, 15–26.
- Cavallini, D., Marco, C. de, Dupre, S., and Rotilio, G. (1969). The copper catalyzed oxidation of cysteine to cystine. *Arch. Biochem. Biophys.* 130, 354–361.
- Cereghetti, G., Saad, S., Dechant, R., and Peter, M. (2018). Reversible, functional amyloids: Towards an understanding of their regulation in yeast and humans. *Cell Cycle.* 17, 1545–1558.
- Chattopadhyay, M., Nwadiibia, E., Strong, C.D., Gralla, E.B., Valentine, J.S., and Whitelegge, J.P. (2015). The disulfide bond, but not zinc or dimerization, controls initiation and seeded growth in amyotrophic lateral sclerosis-linked Cu, Zn superoxide dismutase (SOD1) fibrillation. *J. Biol. Chem.* 290, 30624–30636.
- Choudhary, V., and Schneider, R. (2012). Pathogen-Related Yeast (PRY) proteins and members of the CAP superfamily are secreted sterol-binding proteins. *Proc. Natl. Acad. Sci. USA* 109, 16882–16887.
- Cumming, R.C., Andon, N.L., Haynes, P.A., Park, M., Fischer, W.H., and Schubert, D. (2004). Protein disulfide bond formation in the cytoplasm during oxidative stress. *J. Biol. Chem.* 279, 21749–21758.
- Darwiche, R., Kelleher, A., Hudspeth, E.M., Schneider, R., and Asojo, O.A. (2016). Structural and functional characterization of the CAP domain of pathogen-related yeast 1 (Pry1) protein. *Sci. Rep.* 6, 28838.
- Darwiche, R., Atab, O. El, Cottier, S., and Schneider, R. (2018). The function of yeast CAP family proteins in lipid export, mating, and pathogen defense. *FEBS Lett.* 592, 1304–1311.
- Eberle, H.B., Serrano, R.L., Füllekrug, J., Schlosser, A., Lehmann, W.D., Lottspeich, F., Kaloyanova, D., Wieland, F.T., and Helms, J.B. (2002). Identification and characterization of a novel human plant pathogenesis-related protein that localizes to lipid-enriched microdomains in the Golgi complex. *J. Cell Sci.* 115, 827–838.
- Egge, N., Muthusubramanian, A., and Cornwall, G.A. (2015). Amyloid properties of the mouse egg zona pellucida. *PLoS ONE.* 10, e0129907.
- Fiala, G.J., Schamel, W.W.A., and Blumenthal, B. (2011). Blue native polyacrylamide gel electrophoresis (BN-PAGE) for analysis of multiprotein complexes from cellular lysates. *J Vis*

- Exp. 48, 2164.
- Furukawa, Y., Kaneko, K., and Nukina, N. (2011). Tau protein assembles into isoform- and disulfide-dependent polymorphic fibrils with distinct structural properties. *J. Biol. Chem.* 286, 27236–27246.
- Van Galen, J., Olich, N.K., Schouten, A., Serrano, R.L., Nolte-'t Hoen, E.N.M., Eerland, R., Kaloyanova, D., Gros, P., and Helms, J.B. (2012). Interaction of GAPR-1 with lipid bilayers is regulated by alternative homodimerization. *Biochim. Biophys. Acta.* 1818, 2175–2183.
- Gerber, H., Wu, F., Dimitrov, M., Osuna, G.M.G., and Fraering, P.C. (2017). Zinc and copper differentially modulate amyloid precursor protein processing by γ -secretase and amyloid- β peptide production. *J. Biol. Chem.* 292, 3751–3767.
- Gibbs, G.M., Roelants, K., and O'Bryan, M.K. (2008). The CAP superfamily: cysteine-rich secretory proteins, antigen 5, and pathogenesis-related 1 proteins-roles in reproduction, cancer, and immune defense. *Endocr. Rev.* 29, 865–897.
- Grignaschi, E., Cereghetti, G., Grigolato, F., Kopp, M.R.G., Caimi, S., Faltova, L., Saad, S., Peter, M., and Arosio, P. (2018). A hydrophobic low-complexity region regulates aggregation of the yeast pyruvate kinase Cdc19 into amyloid-like aggregates in vitro. *J. Biol. Chem.* 293, 11424–11432.
- Groves, M.R., Kuhn, A., Hendricks, A., Radke, S., Serrano, R.L., Helms, J.B., and Sinning, I. (2004). Crystallization of a Golgi-associated PR-1-related protein (GAPR-1) that localizes to lipid-enriched microdomains. *Acta Crystallogr D Biol Crystallogr* 60, 730–732.
- Hewetson, A., Do, H.Q., Myers, C., Muthusubramanian, A., Sutton, R.B., Wylie, B.J., and Cornwall, G.A. (2017). Functional amyloids in reproduction. *Biomolecules.* 7, 46.
- Iakovleva, I., Begum, A., Brännström, K., Wijsekera, A., Nilsson, L., Zhang, J., Andersson, P.L., Sauer-Eriksson, A.E., and Olofsson, A. (2016). Tetrabromobisphenol a is an efficient stabilizer of the transthyretin tetramer. *PLoS ONE.* 11, e0153529.
- Jacob, R.S., Das, S., Ghosh, S., Anoop, A., Jha, N.N., Khan, T., Singru, P., Kumar, A., and Maji, S.K. (2016). Amyloid formation of growth hormone in presence of zinc: Relevance to its storage in secretory granules. *Sci. Rep.* 6, 23370.
- Jang, H., Arce, F.T., Mustata, M., Ramachandran, S., Capone, R., Nussinov, R., and Lal, R. (2011). Antimicrobial proteogrin-1 forms amyloid-like fibrils with rapid kinetics suggesting a functional link. *Biophys. J.* 100, 1775–1783.
- Jurczak, P., Groves, P., Szymanska, A., and Rodziewicz-Motowidlo, S. (2016). Human cystatin C monomer, dimer, oligomer, and amyloid structures are related to health and disease. *FEBS Lett.* 590, 4192–4201.
- Kaplan, J.H., and Maryon, E.B. (2016). How mammalian cells acquire copper: An essential but potentially toxic metal. *Biophys. J.* 110, 7–13.
- Kawahara, M., Kato-Negishi, M., and Tanaka, K. (2017). Cross talk between neurometals and amyloidogenic proteins at the synapse and the pathogenesis of neurodegenerative diseases. *Metallomics.* 9, 619–633.
- Kim, A.C., Lim, S., and Kim, Y.K. (2018). Metal ion effects on A β and tau aggregation. *Int. J. Mol. Sci.* 19, 128.
- Leach, B.I., Zhang, X., Kelly, J.W., Dyson, H.J., and Wright, P.E. (2018). NMR measurements reveal the structural basis of transthyretin destabilization by pathogenic mutations. *Biochemistry.* 57, 4421–4430.
- Lee, S.R. (2018). Critical role of zinc as either an antioxidant or a prooxidant in cellular systems. *Oxid. Med. Cell. Longev.* 2018, 9156285.
- Li, Y., Zhao, Y., Su, M., Glover, K., Chakravarthy, S., Colbert, C.L., Levine, B., and Sinha, S.C. (2017). Structural insights into the interaction of the conserved mammalian proteins GAPR-1 and Beclin 1, a key autophagy protein. *Acta Crystallogr D Struct Biol.* 73, 775–792.
- Liu, S., Liu, H., Johnston, A., Hanna-Addams, S., Reynoso, E., Xiang, Y., and Wang, Z. (2017). MLKL forms disulfide bond-dependent amyloid-like polymers to induce necroptosis. *Proc Natl Acad Sci USA.* 114, E7450–E7459.
- Lu, S., Faris, J.D., Sherwood, R., and Edwards, M.C. (2013). Dimerization and protease resistance: New insight into the function of PR-1. *J. Plant Physiol.* 170, 105–110.
- Lu, S., Faris, J.D., Sherwood, R., Friesen, T.L., and Edwards, M.C. (2014). A dimeric PR-1-type pathogenesis-related protein interacts with ToxA and potentially mediates ToxA-induced

- necrosis in sensitive wheat. *Mol. Plant Pathol.* 15, 650–663.
- Maji, S.K., Perrin, M.H., Sawaya, M.R., Jessberger, S., Vadodaria, K., Rissman, R.A., Singru, P.S., Nilsson, K.P.R., Simon, R., Schubert, D., et al. (2009). Functional amyloids as natural storage of peptide hormones in pituitary secretory granules. *Science*. 325, 328–332.
- Maldera, J.A., Vasen, G., Ernesto, J.I., Weigel-Muñoz, M., Cohen, D.J., and Cuasnicu, P.S. (2011). Evidence for the involvement of zinc in the association of CRISP1 with rat sperm during epididymal maturation. *Biol. Reprod.* 85, 503–510.
- Maret, W. (2017). Zinc in cellular regulation: The nature and significance of “Zinc Signals.” *Int. J. Mol. Sci.* 18, E2285.
- Mcbean, G.J., Aslan, M., Griffiths, H.R., and Torrão, R.C. (2015). Thiol redox homeostasis in neurodegenerative disease. *Redox Biol.* 5, 186–194.
- Milne, T.J., Abbenante, G., Tyndall, J.D.A., Halliday, J., and Lewis, R.J. (2003). Isolation and characterization of a cone snail protease with homology to CRISP proteins of the pathogenesis-related protein superfamily. *J. Biol. Chem.* 278, 31105–31110.
- Olrichs, N.K., and Helms, J.B. (2016). Novel insights into the function of the conserved domain of the CAP superfamily of proteins. *AIMS Biophys.* 3, 232–246.
- Olrichs, N.K., Mahalka, A.K., Kaloyanova, D., Kinnunen, P.K., and Helms, J.B. (2014). Golgi-Associated plant Pathogenesis Related protein 1 (GAPR-1) forms amyloid-like fibrils by interaction with acidic phospholipids and inhibits A β aggregation. *Amyloid* 21, 88–96.
- Pace, N.J., and Weerapana, E. (2014). Zinc-binding cysteines: Diverse functions and structural motifs. *Biomolecules*. 4, 419–434.
- Perlenfein, T.J., Mehlhoff, J.D., and Murphy, R.M. (2017). Insights into the mechanism of cystatin C oligomer and amyloid formation and its interaction with β -amyloid. *J. Biol. Chem.* 292, 11485–11498.
- Rietsch, A., and Beckwith, J. (1998). The genetics of disulfide bond metabolism. *Annu. Rev. Genet.* 32, 163–184.
- Rigo, A., Corazza, A., Paolo, M.L. di, Rossetto, M., Ugolini, R., and Scarpa, M. (2004). Interaction of copper with cysteine: Stability of cuprous complexes and catalytic role of cupric ions in anaerobic thiol oxidation. *J. Inorg. Biochem.* 98, 1495–1501.
- Roan, N.R., Sandi-Monroy, N., Kohgadai, N., Usmani, S.M., Hamil, K.G., Neidleman, J., Montano, M., Ständker, L., Röcker, A., Cavois, M., et al. (2017). Semen amyloids participate in spermatozoa selection and clearance. *ELife*. 6, e24888.
- Saad, S., Cereghetti, G., Feng, Y., Picotti, P., Peter, M., and Dechant, R. (2017). Reversible protein aggregation is a protective mechanism to ensure cell cycle restart after stress. *Nat. Cell Biol.* 19, 1202–1213.
- Saldaño, T.E., Zanotti, G., Parisi, G., and Fernandez-Alberti, S. (2017). Evaluating the effect of mutations and ligand binding on transthyretin homotetramer dynamics. *PLoS ONE*. 12, e0181019.
- Serrano, R.L., Kuhn, A., Hendricks, A., Helms, J.B., Sinning, I., and Groves, M.R. (2004). Structural analysis of the human Golgi-associated plant pathogenesis related protein GAPR-1 implicates dimerization as a regulatory mechanism. *J. Mol. Biol.* 339, 173–183.
- Sheng, J., Olrichs, N.K., Geerts, W.J., Li, X., Rehman, A.U., Gadella, B.M., Kaloyanova, D. V, and Helms, J.B. (2019). Zinc binding regulates amyloid-like aggregation of GAPR-1. *Biosci. Rep.* 39, BSR20182345.
- Shikamoto, Y., Suto, K., Yamazaki, Y., Morita, T., and Mizuno, H. (2005). Crystal structure of a CRISP family Ca²⁺-channel blocker derived from snake venom. *J. Mol. Biol.* 350, 735–743.
- Shoji-Kawata, S., Sumpter, R., Leveno, M., Campbell, G.R., Zou, Z., Kinch, L., Wilkins, A.D., Sun, Q., Pallauf, K., MacDuff, D., et al. (2013). Identification of a candidate therapeutic autophagy-inducing peptide. *Nature* 494, 201–206.
- Sirangelo, I., and Iannuzzi, C. (2017). The role of metal binding in the amyotrophic lateral sclerosis-related aggregation of copper-zinc superoxide dismutase. *Molecules*. 22, 1429.
- Skoulakis, S., and Goodfellow, J.M. (2003). The pH-dependent stability of wild-type and mutant transthyretin oligomers. *Biophys. J.* 84, 2795–2804.
- Sugiyama, H., Burnett, L., Xiang, X., Olson, J., Willis, S., Miao, A.M.Y., Akema, T., Bieber, A.L., and Chandler, D.E. (2009). Purification and multimer formation of allurin, a sperm chemoattractant

- from *Xenopus laevis* egg jelly. *Mol. Reprod. Dev.* 76, 527–536.
- Suzuki, N., Yamazaki, Y., Brown, R.L., Fujimoto, Z., Morita, T., and Mizuno, H. (2008). Structures of pseudechetoxin and pseudecin, two snake-venom cysteine-rich secretory proteins that target cyclic nucleotide-gated ion channels: implications for movement of the C-terminal cysteine-rich domain. *Acta Crystallogr D Biol Crystallogr* 64, 1034–1042.
- Wang, Y.-L., Kuo, J.-H., Lee, S.-C., Liu, J.-S., Hsieh, Y.-C., Shih, Y.-T., Chen, C.-J., Chiu, J.-J., and Wu, W.-G. (2010). Cobra CRISP functions as an inflammatory modulator via a novel Zn²⁺- and heparan sulfate-dependent transcriptional regulation of endothelial cell adhesion molecules. *J. Biol. Chem.* 285, 37872–37883.
- Yiwari, A., Liba, A., Sohn, S.H., Seetharaman, S. V., Bilsel, O., Matthews, R.C., Hart, P.J., Valentine, J.S., and Hayward, L.J. (2009). Metal deficiency increases aberrant hydrophobicity of mutant superoxide dismutases that cause amyotrophic lateral sclerosis. *J. Biol. Chem.* 284, 27746–27758.
- Zhao, L., Buxbaum, J.N., and Reixach, N. (2013). Age-related oxidative modifications of transthyretin modulate its amyloidogenicity. *Biochemistry* 52, 1913–1926.
- Zhou, Q., Hao, L., Huang, W., and Cai, Z. (2016). The Golgi-Associated Plant Pathogenesis-Related Protein GAPR-1 enhances type I interferon signaling pathway in response to Toll-Like receptor 4. *Inflammation* 39, 706–717.

Supplementary Figure



Supplementary Figure 1. Cysteines are essential in Cu^{2+} -induced GPR-1 amyloid-like aggregation. 15 μM WT GPR-1 with or without NEM-modified cysteines was incubated with 37.5 μM heparin and 20 μM Cu^{2+} at 37 °C. Aliquots taken from 0 h, 3 h and 18 h were analyzed by non-reducing SDS-PAGE and Western blot using a C-terminal GPR-1 antibody.

The less conserved metal-binding site in human CRISP1 remains sensitive to zinc ions and permits Zn^{2+} -dependent protein oligomerization

Jie Sheng, Nick K. Olrichs[#], Bart M. Gadella[#], Dora V. Kaloyanova, J. Bernd Helms

Department of Biochemistry and Cell Biology, Faculty of Veterinary Medicine, Utrecht University, Utrecht, the Netherlands

[#] Contributed equally

Submitted for publication

Abstract

Cysteine-rich secretory proteins (CRISPs) are a subgroup of the CRISP, antigen 5 and PR-1 (CAP) superfamily that are characterized by the presence of a conserved CAP domain. Two conserved histidines in the CAP domain are proposed to function as a zinc-binding site with unknown function. Human CRISP1 is, however, one of the few family members that lack one of these characteristic histidine residues. We therefore investigated the Zn^{2+} -dependent oligomerization properties of human CRISP1. To this end, we developed an expression and purification method, involving maltose-binding protein (MBP)-tagging in combination with a low expression XL-1 Blue bacterial system. Moderate yields of a soluble recombinant MBP-tagged full-length human CRISP1 and MBP-tagged CAP domain of CRISP1 (CRISP1^{ΔC}) were obtained. The metal ion binding to the conserved CAP domain and its role in oligomerization of CRISP1 were studied. Zinc ions specifically induced oligomerization of both recombinant MBP-CRISP1 and MBP-CRISP1^{ΔC} *in vitro*. We show that the conserved His142 in the CAP domain is essential for this Zn^{2+} dependent oligomerization process, confirming a role of the CAP metal-binding site in the interaction with Zn^{2+} . Furthermore, Zn^{2+} -regulated MBP-CRISP1 and MBP-CRISP1^{ΔC} oligomerization is reversible upon removal of zinc ions. Condensation of proteins is characteristic for maturing sperm in the epididymis and this process was previously found to be Zn^{2+} -dependent. Thus, Zn^{2+} -induced CRISP1 oligomerization may shed novel insights into the formation of functional protein complexes involved in mammalian fertilization.

Introduction

In mammals, before sperm become fully competent to fertilize an egg, spermatozoa must undergo a series of morphological, biochemical and physical changes in male and female tracts, known as epididymal maturation and capacitation, respectively (Yanagimachi, 1994). During epididymal maturation, spermatozoa pass through the epididymis where an extensive remodeling of the sperm plasma membrane takes place, including the acquisition of epididymal proteins (Gadella, 2017; Sullivan and Miesusset, 2016). Some of these proteins contribute to the acquisition of sperm's ability to bind and penetrate through the extracellular structures surrounding the oocyte, while others are involved in preventing the occurrence of premature capacitation, also known as decapacitation factors (Cornwall, 2009; Gadella, 2017).

Cysteine-rich secretory protein 1 (CRISP1) is a member of CRISP subgroup of proteins which belongs to the CRISP, antigen 5 and PR-1 (CAP) superfamily (Gibbs et al., 2008). CRISP1 is expressed by the epithelia of the epididymis and secreted into the lumen of the epididymal duct where it associates with the sperm surface during spermatozoa maturation (Ros et al., 2015). CRISP1 is a multifunctional protein playing diverse roles during fertilization (Cohen et al., 2011). CRISP1 associates with the sperm surface with two different affinities during epididymal maturation (Deborah J. Cohen et al., 2000). Loosely bound CRISP1 is released during capacitation and is suggested to function as a decapacitation factor (Roberts et al., 2003), whereas the tightly bound CRISP remains bound after capacitation and participates in sperm-zona pellucida (ZP) interaction (Busso et al., 2007; Deborah J. Cohen et al., 2000). During the acrosome reaction, CRISP1 relocates to the equatorial segment of the sperm head (*i.e.* the specific surface area of sperm involved in the fusion during fertilization) (Bedford et al., 1979). Using a knockout mouse model system, CRISP1 was shown to affect sperm function without, however, leading to a significant reduction in fertility (Ernesto et al., 2015; Muñoz et al., 2018). Double knockout of CRISP1 and CRISP4 in mice revealed that mutant males exhibit an impaired fertility (Muñoz et al., 2019). CRISP1 is also present in the cumulus cell layer surrounding the ovulated oocyte and capable of modulating sperm motility and orientation before fertilisation (Ernesto et al., 2015).

CRISP proteins are composed of an N-terminal signal peptide, a CAP domain and a C-terminal cysteine-rich domain (CRD) (Gibbs et al., 2008). CRISPs are characterized by 16 cysteine residues, 10 of which are located in the CRD domain (Figure 1A and Supplementary Figure 1). All cysteine residues are involved in intradomain disulfide bond formation (Guo et al., 2005;

Koppers et al., 2011; Shikamoto et al., 2005; Wang et al., 2005). The CRD domain contains an ion channel regulatory (ICR) region and a hinge that connects the ICR region to the CAP domain (Gibbs et al., 2008).

The structurally conserved CAP domain contains four signature motifs (CAP1-4) that define the CAP superfamily (Gibbs et al., 2008). Another characteristic of the CAP superfamily is the presence of two conserved histidines and glutamates on either side of a cleft across the protein surface of the CAP domain (Gibbs et al., 2008). An increasing number of studies show that these two histidines form a zinc-binding site (Asojo et al., 2011; Maldera et al., 2011; Sheng et al., 2019a; Suzuki et al., 2008; Wang et al., 2010). Although the biological function of zinc-binding is not known, we recently showed that Zn^{2+} -binding to an other CAP family member, GAPR-1, can trigger amyloid-like oligomerization (Sheng et al., 2019a). Also several other CRISP proteins were shown to bind Zn^{2+} (*e.g.* natrin (Wang et al., 2010) and pseudocin (Suzuki et al., 2008)), resulting in the formation of high-molecular-weight complexes (*e.g.* rat CRISP1 (Maldera et al., 2011), mouse CRISP2 and mouse CRISP4 (Sheng et al., 2019a)). Furthermore, rat CRISP1 zinc-dependent oligomers were shown to play a functional role in sperm epididymal maturation, suggesting that Zn^{2+} -dependent oligomerization may have functional relevance (Maldera et al., 2011). In this respect it is interesting to note that zinc-dependent oligomerization and amyloid-like fibril formation of GAPR-1 is reversible (Sheng et al., 2019b), providing a potential mechanism for regulation of biological activity of CAP superfamily members via the CAP domain (Olricks and Helms, 2016).

In this study, we investigated the Zn^{2+} -dependent oligomerization properties of human CRISP1. Human CRISP1 is one of the few family members that lack one of the characteristic histidine residues that are involved in Zn^{2+} binding. In the case of human CRISP1, only His142 is conserved, whereas His86 has been replaced with glutamate (Supplementary Figure 1). This substitution provides a negative charge, potentially permitting an alternative means for Zn^{2+} coordination together with the conserved His142. Here, we addressed the question whether human CRISP1 can still bind Zn^{2+} to form oligomers that are believed to function in the reproductive process.

Materials and Methods

Reagents

Restriction enzymes and DNA ligase were purchased from Thermo Fisher Scientific (Eindhoven, the Netherlands). pMAL-c2x vector and XL-1 Blue competent cells were from

Biolab (Barendrecht, the Netherlands). Competent cells Origami™ 2(DE3) pLysS were from Merck (Darmstadt, Germany) and pG-KJE8/BL21 cells were from TaKaRa (Otsu, Japan). All primers were synthesized in Baseclear (Leiden, the Netherlands). ZnCl₂, ethylenediaminetetraacetic acid (EDTA) and Isopropyl β-D-1-thiogalactopyranoside (IPTG) were obtained from Sigma-Aldrich (St. Louis, USA), and bis(sulfosuccinimidyl)suberate (BS₃) was from Pierce Biotechnology (Rockford, IL, USA).

Plasmid construction

The cDNA of human CRISP1 (NM_001131) was obtained from OriGene (Rockville, MD, USA). cDNA of human CRISP1 was used as a template in a PCR reaction. 5'-cggaattcaaaaagaaatcagctagagacc-3' was used as the forward primer, and 5'-gcaagctttcattttatctcagtggtcacaca-3' and 5'-gcaagcttttagcttataaggttcattctttg-3' were used as reverse primers in the cloning of full-length CRISP1 and of the CAP domain of CRISP1 (CRISP^{ΔC}) PCR products into pMAL-c2x vector, respectively. The amplified PCR products were inserted into digested vectors according to the standard protocols. All constructs were verified by DNA sequencing (Baseclear, Leiden, the Netherlands).

Site direct mutagenesis of pMAL-c2x-CRISP1 H142Q and pMAL-c2x-CRISP1^{ΔC} H142Q

pMAL-c2x-CRISP1 and pMAL-c2x-CRISP1^{ΔC} constructs were used as templates. pMAL-c2x-CRISP1 H142Q and pMAL-c2x-CRISP1^{ΔC} H142Q mutants were generated by site-directed mutagenesis using 5'-gatgatgacataactactgaccaatacactcagattgtttgggcc-3' as the forward primer and 5'-ggcccaaacaatctgagtgtattggcagtagttatgtcatc-3' as the reverse primer. Mutations were verified by DNA sequencing (Baseclear, Leiden, the Netherlands).

Expression of MBP-CRISP1/MBP-CRISP1^{ΔC} in XL-1 Blue *E.coli* strain

pMAL-c2x-CRISP1/pMAL-c2x-CRISP1^{ΔC} was transformed into competent XL-1 Blue cells. Transformed bacteria were grown in LB media supplemented with 50 µg/ml ampicillin. The preculture was grown overnight (ON) at 37°C and split 1/100 into fresh LB media with 50 µg/ml ampicillin. After bacteria grew to OD₆₀₀ of 0.5, protein expression was induced with 0.5 mM IPTG and the bacteria were incubated ON at 16 °C. Bacteria were harvested by centrifugation at 4,000 g for 30 min at 4 °C.

The MBP-CRISP1/MBP-CRISP1^{ΔC} bacterial pellets were resuspended in the column buffer (50 mM Tris, 200 mM NaCl, 1 M arginine, pH 7.4, 0.6 µM aprotinin, 1 µM leupeptin-hemisulfate, 1.45 µM pepstatin and 0.5 mM phenylmethylsulfonyl fluoride (PMSF)) at a ratio

of 5 ml buffer per g of bacteria pellet. The bacteria were crushed with a high-pressure homogenizer (Avestin, Mannheim, Germany) and centrifuged at 4,000 g for 30 min at 4 °C. The resultant supernatant was centrifuged again at 100,000 g at 4 °C for 30 min. Expression was analyzed by SDS-PAGE and Coomassie Brilliant blue staining.

Purification and cleavage of MBP-fusion protein

The soluble fraction after 100,000 g centrifugation was mixed with the amylose resin (Biolab, Barendrecht, the Netherlands) and placed in a chromatography column (Biolab, Barendrecht, the Netherlands) at room temperature for 2 h. Non-specifically bound proteins were removed by washing with 10 column volumes (CVs) of washing buffer (50 mM Tris, 200 mM NaCl, pH 7.4) at 4 °C. The protein was eluted with 10 mM maltose in elution buffer (25 mM Tris, 50 mM NaCl, pH 7.4, 0.6 µM aprotinin, 1 µM leupeptin-hemisulfate, 1.45 µM pepstatin and 0.5 mM PMSF) at 4 °C. The eluate was centrifuged at 100,000 g for 30 min at 4 °C to remove aggregated proteins. The purity and solubility of isolated proteins were analyzed by SDS-PAGE and Coomassie blue staining. To remove the MBP tag, the elute was incubated with 1% Factor Xa (Thermo Fisher Scientific, Eindhoven, the Netherlands) at room temperature overnight. The cleaved products were analyzed by SDS-PAGE and Coomassie blue staining and/or Western blot using rabbit polyclonal anti-CRISP1 antibody (Abcam, Cambridge, UK).

Sedimentation analysis

Protein aggregation was analyzed by sedimentation behavior as described previously (Sheng et al., 2019b). In short, 1.5 µM MBP-CRISP1/MBP-CRISP1^{ΔC}/MBP was incubated in the absence or presence of 1 mM metal ions, including Zn²⁺, Cu²⁺, Ca²⁺, Mg²⁺ and Fe³⁺, in 25 mM Tris, 50 mM NaCl, pH 7.4, in a total volume of 100 µl reaction for 10 min at 37 °C, followed by centrifugation at 14,000 g for 1 h at 4 °C. Proteins in the pellet fraction were analyzed by SDS-PAGE and Coomassie blue staining.

Sucrose density gradient centrifugation

Discontinuous sucrose density gradients were prepared by gently layering sucrose densities solutions with decreasing sucrose densities (w/v) on top of one another: 0.5 ml 35%, 0.5 ml 30%, 0.8 ml 25%, 1 ml 20% and 1 ml 15% sucrose (bottom to top) in BeckMan Ultra-Clear tube (Brea, CA, USA).

1.5 µM MBP-CRISP1/MBP-CRISP1^{ΔC} was incubated in the absence or presence of 1 mM Zn²⁺ in 25 mM Tris, 50 mM NaCl, pH 7.4, in a total volume of 1 ml reaction. After incubation at 37

°C for 10 min, the reaction mixture was gently loaded on top of the gradient. The gradient was centrifuged at 210,463 g overnight at 4°C. After centrifugation, fractions of 380 µl were gently collected from top to bottom of the gradient.

Proteins in every fraction were precipitated by chloroform/methanol. Briefly, 1.14 ml chloroform/methanol (1:2) was added to each gradient fraction sample of 380 µl. The sample was then mixed and centrifuged at 13,000 g for 1 h at 4 °C. The supernatant was removed and the protein pellet was air-dried. The samples were resolved in Laemmli sample buffer, loaded on SDS-PAGE gel and analyzed by Western blot using rabbit polyclonal anti-CRISP1 antibody (Abcam, Cambridge, UK).

Protein crosslinking

1.5 µM MBP-CRISP1/MBP-CRISP1^{ΔC}/MBP was incubated in the absence or presence of 1 mM Zn²⁺ at 37 °C in 20 mM Hepes buffer, pH 7.4, in a total volume of 40 µl. After 10 min incubation, each reaction was equally divided into two groups. BS₃ was added in 30-fold molar excess to the protein to one group and incubated for 15 min at room temperature. 0.5 M Tris, pH 7.4 was added to quench the reaction. The other group served as control samples (absence of crosslinker). Proteins and crosslinked products were analyzed by SDS-PAGE and subsequently visualized by Coomassie blue staining or Western blot using rabbit polyclonal anti-CRISP1 antibody (Abcam, Cambridge, UK).

Results

Expression and purification of recombinant human CRISP1 and CRISP1^{ΔC}

The CAP domain is proposed to play an essential role in protein oligomerization of CAP superfamily members (Olrichs and Helms, 2016). To investigate the oligomerization properties of human CRISP1 and the role of the CAP domain in this process, we aimed to overexpress and purify both full-length human CRISP1 and a C-terminal deletion mutant containing only the CAP domain of CRISP1 (CRISP1^{ΔC}) as shown in Figure 1A.

Heterologous overexpression of CRISP proteins has been proven difficult (Gibbs et al., 2006, 2011; Volpert et al., 2014), probably due to the presence of multiple cysteine residues at the C-terminus and the amyloidogenic properties of the CAP domain. We employed different bacterial expression systems, different induction conditions and different tags (His, GST, MBP) to improve the solubility, expression levels and purification of human CRISP1. The constructs that were transformed into different *E. coli* strains are summarized in Figure 1B. The *E. coli*

pG-KJE8/BL21 strain possesses two chaperone systems that enhance the solubility of proteins (Fang et al., 2019; Tian et al., 2016; Yan et al., 2012) and the Origami™ 2(DE3) pLysS strain improves disulfide bond formation in the cytoplasm of *E. coli* (Bessette et al., 1999). Initially, the human CRISP1 coding sequence was optimized according to the codon bias of *E. coli* (Ikemura, 1981) and fused with the N-terminal His-tag. His-CRISP1 was overexpressed in the three different bacterial strains (pG-KJE8/BL21, Origami™ 2(DE3) pLysS and XL-1 Blue) but analysis of expression of the resulting recombinant proteins showed that under these conditions, His-CRISP1 remained mainly insoluble (Supplementary Figure 2).

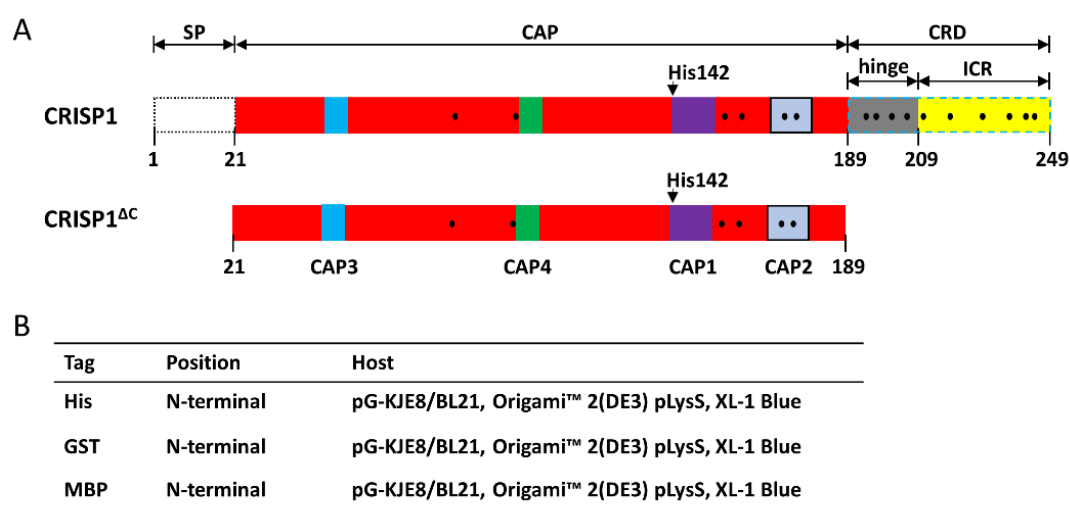


Figure 1. Structural characteristics of human CRISP1 and production strategies. (A) CRISP1 is composed of an N-terminal signal peptide (SP), a CAP domain and a C-terminal cysteine-rich domain (CRD). The CRD domain contains an ion channel regulatory (ICR) region and a hinge connecting CAP domain and ICR region. There are 16 conserved cysteine residues (black dots) in CRISP1, 6 of which are in the CAP domain and 10 are in the CRD domain. Within the CAP domain, there are four conserved CAP signature motifs. His142 is a highly conserved amino acid through CAP superfamily members. (B) Different tags and bacterial strains were used to obtain CRISP1/CRISP1^{ΔC}. His, GST or MBP tag was fused to the N-terminus of CRISP1/CRISP1^{ΔC} (without SP). Protein expression was performed in pG-KJE8/BL21, Origami™ 2(DE3) pLysS and XL-1 Blue strain, respectively.

To improve the solubility of the target proteins, we employed solubility enhancing tags, *i.e.* maltose-binding protein (MBP) and glutathione S-transferase (GST) tags (Kapust and Waugh, 1999). To this end, MBP or GST was fused to the N-terminus of CRISP1. Solubility of the recombinant proteins were tested. MBP-CRISP1 showed better solubility characteristics than GST-CRISP1 expressed in XL-1 Blue cells (Supplementary Figure 3). Expression of MBP-CRISP1 in the specialized bacterial strains Origami™ 2(DE3) or pG-KJE8/BL21 did not benefit the expression for different reasons: MBP-CRISP1 expressed in Origami™ 2(DE3) *E. coli* was recovered mainly in the insoluble fraction; MBP-CRISP1 expressed in pG-KJE8/BL21 *E. coli* could not be purified to homogeneity. Moreover, after MBP-cleavage, CRISP1 became highly sensitive to degradation (Supplementary Figure 4). This indicates that untagged CRISP1

expressed and isolated from pG-KJE8/BL21 *E. coli* strain was unstable.

Overexpression of MBP-CRISP1/CRISP1^{ΔC} in the cloning strain XL-1 Blue is less efficient, but a slow growth rate and a low expression level could be beneficial for protein folding (Siller et al., 2009). The majority of overexpressed MBP-CRISP1 or MBP-CRISP1^{ΔC} remained soluble after expression in XL-1 Blue and remained stable after multiple freeze-thaw cycles. To optimize the expression and recovery of MBP-CRISP1/CRISP1^{ΔC} in XL-1 Blue cells, the experimental conditions were varied, including temperature (16-37 °C), IPTG concentration (0.5–1 mM), duration of protein induction (3–18 h), as well as the presence of various molecules known to improve protein stability (arginine, DTT, glycine). Protein expression was found to be optimal at 16 °C with IPTG (0.5 mM) induction for 18 h and addition of 1 M arginine to the homogenate. Figure 2A shows the expression and solubility characteristics of recombinant MBP-CRISP1 in XL-1 Blue cells. The isolated MBP-CRISP1 was soluble and of high purity (Figure 2B). To obtain tag-free CRISP1 or CRISP1^{ΔC}, the purified constructs were treated with Factor Xa. After cleavage, tag-free CRISP1/CRISP1^{ΔC} remained soluble, but the cleavage efficiency was relatively low (Figure 2C and D). In the case of CRISP1, removal of the tag resulted in the formation of oligomers. For optimal stability and solubility during storage and freeze/thaw cycles, CRISP1 and CRISP1^{ΔC} were stored as MBP-tagged fusion proteins (MBP-CRISP1 and MBP-CRISP1^{ΔC}) at -80 °C. Under these optimized conditions, the yield of MBP-CRISP1 and MBP-CRISP1^{ΔC} after purification was 1.2 mg/l and 1.7 mg/l bacterial culture, respectively.

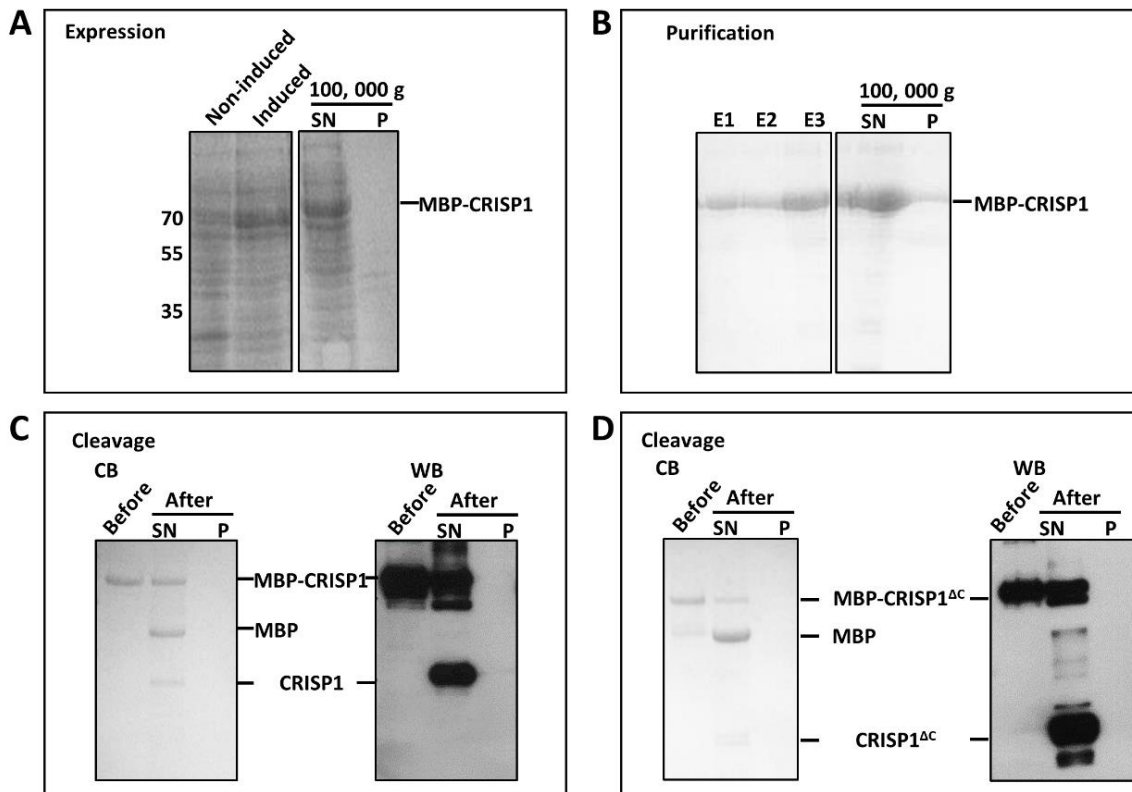


Figure 2. Expression of CRISP1/CRISP1^{ΔC} in XL-1 Blue bacteria and purification. (A) Expression of MBP-CRISP1. Samples before (Non-induced) or after induction (Induced) with IPTG were centrifuged at 100,000 g and the supernatant (SN) and pellet (P) of induced samples were analyzed by SDS-PAGE and Coomassie blue staining. (B) Purification of MBP-CRISP1. MBP-CRISP1 was eluted with maltose (elution fractions (E1-E3)). Elution fraction E3 was centrifuged at 100,000 g and the supernatant (SN) and pellet (P) were analyzed by SDS-PAGE and Coomassie blue staining. (C) Cleavage of MBP-CRISP1. Before and after MBP-CRISP1 cleavage, the fractions were centrifuged at 100,000 g and the supernatant (SN) and pellet (P) were analyzed by SDS-PAGE and Coomassie blue staining or Western blot. (D) Before and after MBP-CRISP1^{ΔC} cleavage, the fractions were centrifuged at 100,000 g and the supernatant (SN) and pellet (P) were analyzed by SDS-PAGE and Coomassie blue staining or Western blot.

Zn²⁺ induces human CRISP1 oligomerization by interaction with the CAP domain

Zn²⁺ interaction with the CAP domain is coordinated by two highly conserved histidine residues (Asojo et al., 2011; Maldera et al., 2011; Sheng et al., 2019a; Suzuki et al., 2008; Wang et al., 2010). In addition, several CAP family members including GAPR-1 (Sheng et al., 2019a) and CRISP subfamily members (rat CRISP1 (Maldera et al., 2011), mouse CRISP2 (Sheng et al., 2019a), mouse CRISP4 (Sheng et al., 2019a) and natrin, a CRISP member present in cobra venom (Wang et al., 2010)) form high molecular weight complexes/oligomers in the presence of Zn²⁺. As human CRISP1 contains only one of the conserved histidines (His142, see also Figure 1A and Supplementary Figure 1), we investigated the Zn²⁺-dependent oligomerization properties of human CRISP1. Sedimentation analysis showed that after incubation with Zn²⁺, both MBP-CRISP1 and MBP-CRISP1^{ΔC} were recovered in the pellet fraction (figure 3A). This

sedimentation behavior was due to an effect of Zn^{2+} on the CRISP1 protein and not due to the MBP-tag as purified MBP did not sediment under these conditions. Other metal ions, including Cu^{2+} , Ca^{2+} , Mg^{2+} and Fe^{3+} did not have an effect on MBP-CRISP1 or MBP-CRISP1 $^{\Delta\text{C}}$ sedimentation (Figure 3A).

To confirm that human CRISP1 oligomerizes in the presence of Zn^{2+} , a sucrose density gradient assay was performed in which monomers of CRISP1 are recovered in the low-density fraction whereas CRISP oligomers appear in the high-density fraction. MBP-CRISP1 or MBP-CRISP1 $^{\Delta\text{C}}$ was incubated in the absence or presence of Zn^{2+} and subsequently loaded on top of the sucrose gradient (see Materials and Methods). After centrifugation, both MBP-CRISP1 and MBP-CRISP1 $^{\Delta\text{C}}$ migrated from the low-density to the high-density sucrose fractions in the presence of Zn^{2+} (Figure 3B), indicating the formation of oligomeric structures. To confirm the Zn^{2+} -dependent formation of oligomeric CRISP1 proteins, a crosslink assay was employed using an amine-to-amine crosslinker (BS_3). Figure 3C shows that in the presence of Zn^{2+} , both MBP-CRISP1 and MBP-CRISP1 $^{\Delta\text{C}}$ formed high molecular weight oligomers, whereas MBP did not oligomerize in the presence of Zn^{2+} . To determine the dose-dependency of Zn^{2+} induced CRISP1 oligomerization, isolated MBP-CRISP1 was incubated with various concentrations (0.001-1 mM) of Zn^{2+} ions. CRISP1 formed high molecular weight oligomers in the presence of 0.3 mM Zn^{2+} or at higher concentrations (Figure 4). EDTA effectively inhibited the formation of oligomers (Figure 4), confirming the role of Zn^{2+} in this process. These combined results show that Zn^{2+} specifically induces human CRISP1 oligomerization, which is triggered by an interaction with the CAP domain of CRISP1. The MBP-tag itself is not involved in this oligomerization process.

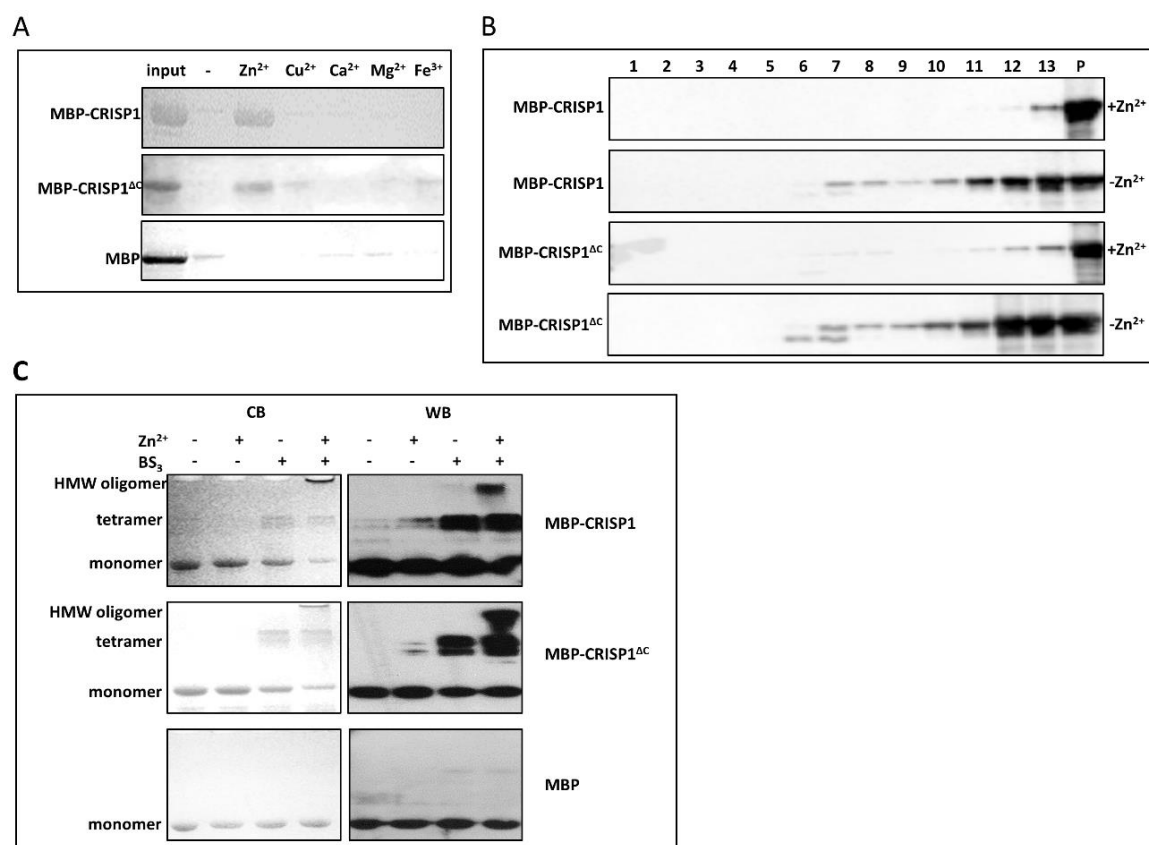


Figure 3. Zn²⁺ induced CRISP1 oligomerization. (A) 1.5 μ M MBP-CRISP1/MBP-CRISP1^{ΔC}/MBP was incubated with 1 mM Zn²⁺/Cu²⁺/Ca²⁺/Mg²⁺/Fe³⁺ at 37 °C for 10 min. Samples were spun down at 14,000 g for 1 h at 4 °C. The pellet fraction was analyzed by SDS-PAGE gel and Coomassie blue staining. (B) 1.5 μ M MBP-CRISP1/MBP-CRISP1^{ΔC} was incubated with or without 1 mM Zn²⁺ at 37 °C for 10 min. The incubations were then loaded on top of the sucrose gradient. After centrifugation at 210,463 g O/N at 4 °C, fractions from the low (1) to high (13) density sucrose gradient were collected, including the pellet (P), and precipitated by chloroform/methanol. Each fraction was analyzed by SDS-PAGE gel and Western blot. (C) 1.5 μ M MBP-CRISP1/MBP-CRISP1^{ΔC}/MBP was incubated with 1 mM Zn²⁺ at 37 °C for 10 min. Cross linker (BS₃) was then added in a 30-fold molar excess to the incubations as indicated. Samples were analyzed by SDS-PAGE and Coomassie blue staining or Western blot.

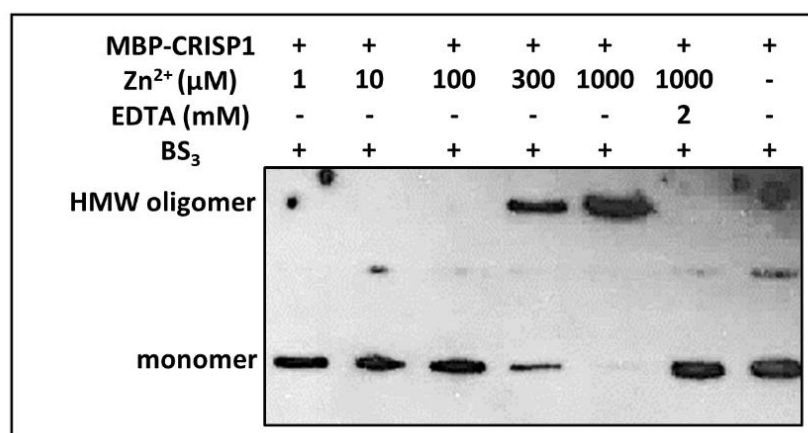


Figure 4. Concentration dependency of Zn²⁺ induced CRISP1 high molecular weight complex formation. 1.5 μ M MBP-CRISP1 was incubated with increasing amount of Zn²⁺ (0-1 mM) as indicated. 2 mM EDTA was added to the incubations containing 1 mM Zn²⁺. After incubation at 37 °C for 10 min,

BS₃ was added in 30-fold molar excess to the proteins. Samples were analyzed by SDS-PAGE gel and Western blot.

Zn²⁺ induced human CRISP1 oligomerization is reversible

Our previous study on GAPR-1 aggregation showed that removal of Zn²⁺ caused a partial disintegration of the Thioflavin T (ThT)-positive structures of GAPR-1 (Sheng et al., 2019b). The potential reversibility of Zn²⁺ mediated human CRISP1 and CRISP1^{ΔC} oligomerization was investigated by a sedimentation assay. Addition of EDTA to both Zn²⁺ induced MBP-CRISP1 and MBP-CRISP1^{ΔC} oligomers resulted in decreased protein recovery in the pellet fraction (Figure 5). This sedimentation behavior indicates that upon release of Zn²⁺, oligomers formed by both full-length and CAP domain of human CRISP1 can be (partially) dissociated again. These results indicate a reversible nature of Zn²⁺-induced human CRISP1 oligomers.

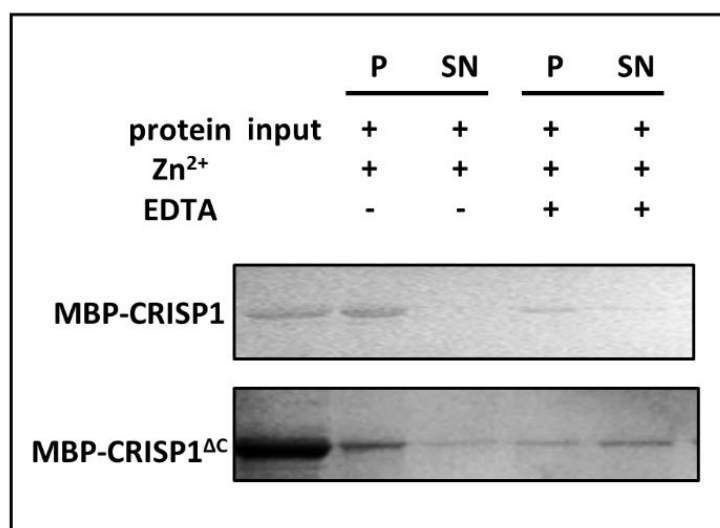


Figure 5. Reversibility of Zn²⁺ induced human CRISP1 oligomerization. 1.5 μM MBP-CRISP1/MBP-CRISP1^{ΔC} was incubated with 1 mM Zn²⁺ at 37 °C for 10 min, followed by addition of 2 mM EDTA (as indicated) and incubated at 37 °C for another 10 min. Samples without treatment by EDTA were controls. All samples were spun down at 14,000 g for 1 h at 4 °C. The pellet fraction (P) and 1/5 of the supernatant (SN) were analyzed by SDS-PAGE gel and Coomassie blue staining.

His142 is essential for Zn²⁺ regulated human CRISP1 oligomerization

The metal-binding site of human CRISP1 has been compromised by replacement of His for Glu at amino acid position 86. To investigate whether the metal binding-site consisting of the conserved His142 and potentially Glu86 is still involved in the Zn²⁺-dependent oligomerization properties of human CRISP1, His142 was mutated to glutamine and subsequently a sedimentation analysis was performed to analyze the effect of Zn²⁺ on the oligomerization properties of MBP-CRISP1 H142Q and MBP-CRISP1^{ΔC} H142Q. Zn²⁺ did not induce enhanced sedimentation of both MBP-CRISP1 H142Q and MBP-CRISP1^{ΔC} H142Q after centrifugation

(Figure 6A). To confirm the absence of high-molecular-weight human CRISP1 oligomers after substitution of His142 with glutamine, MBP-CRISP1 and MBP-CRISP1 H142Q were incubated with Zn^{2+} at 37 °C for different times and subjected to the cross-link assay (Figure 6B). Indeed, Zn^{2+} did not induce high-molecular-weight oligomers of MBP-CRISP1 H142Q, whereas MBP-CRISP1 oligomers were observed. These results confirm an essential role of His142 residue in Zn^{2+} -dependent human CRISP1 oligomerization.

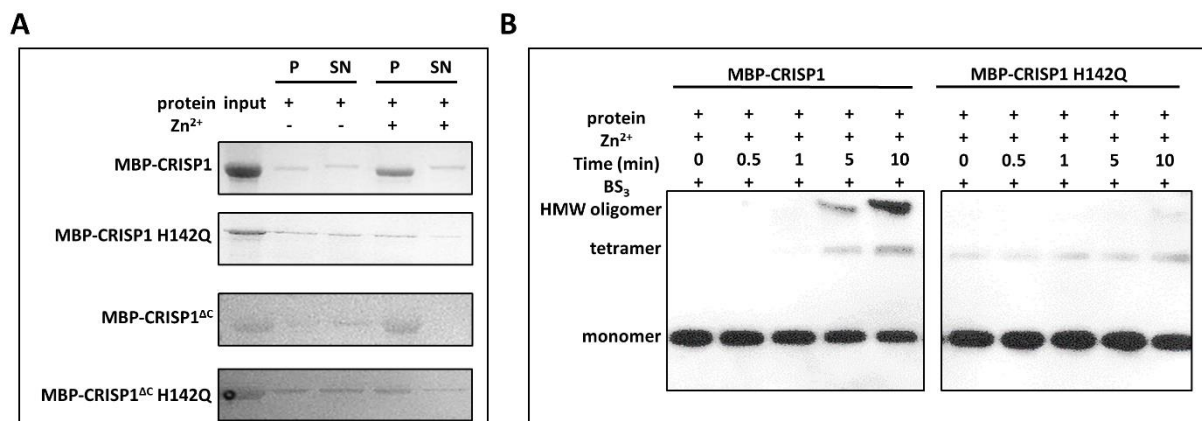


Figure 6. His142 is essential in Zn^{2+} induced human CRISP1 oligomerization. (A) 1.5 μM MBP-CRISP1/MBP-CRISP1 H142Q/MBP-CRISP1 Δ C/MBP-CRISP1 Δ C H142Q was incubated with 1 mM Zn^{2+} at 37 °C for 10 min, respectively. The reactions were spun down at 14,000 g for 1h at 4 °C. The pellet fraction (P) and 1/5 of the supernatant (SN) were analyzed by SDS-PAGE gel and Coomassie blue staining. (B) 1.5 μM MBP-CRISP1/MBP-CRISP1 H142Q was incubated with 1 mM Zn^{2+} at 37 °C for 10 min. BS_3 was added in 30-fold molar excess to CRISP1 and incubated for different time points (0, 0.5, 1, 5 and 10 min). Samples were analyzed by SDS-PAGE gel and Western blot.

Discussion

The structural complexity conferred on CRISP proteins by the high cysteine content has hampered their expression and purification with satisfactory solubility, purity, stability and yield. Attempts to express and purify mouse CRISP4 and mouse Tpx-1 from bacterial cells resulted in the formation of insoluble protein aggregates (Gibbs et al., 2006, 2011). Human and mouse CRISP3 expression in mammalian cells resulted in low expression levels, low yields, and impure protein fractions (Volpert et al., 2014). Expression of His-tagged porcine CRISP1 has also been attempted in porcine endometrial glandular epithelial (PEGE) cells and Chinese hamster ovary cells, but the production was minimal (Vadnais et al., 2008). In this study, we report the expression and purification of CRISP1 and CRISP1 Δ C in *E. coli* in amounts that are sufficient for biochemical studies. MBP-tagging of the CRISP1 protein, in combination with low expression levels, provided optimal conditions for obtaining soluble protein. Low expression levels were achieved with a reduced temperature during induction and by expression in XL-1 Blue bacterial cells. Decreasing the induction temperature is frequently used as one of

the strategies to obtain soluble proteins. At lower temperatures, bacteria grow slowly and have a lower protein expression level, resulting in a lower frequency of protein misfolding and aggregation (Vasina and Baneyx, 1997). This strategy allowed us to obtain sufficient recombinant protein to demonstrate that the metal-ion dependent oligomerization property of CAP family members is conserved in human CRISP1.

The presence of a CAP domain is a characteristic feature of CAP superfamily proteins (Gibbs et al., 2008). It has been proposed that oligomerization and amyloid formation is a common functionality of the CAP domain (Olricks and Helms, 2016). This was recently demonstrated by using GAPR-1 as a model protein of the CAP domain (Sheng et al., 2019a). Zn^{2+} binding to the metal-binding site induces GAPR-1 amyloid-like aggregation in the presence of heparin, suggesting that zinc ion-regulated oligomerization could be a common structural property of the CAP domain with potential relevance for all other CAP proteins (Sheng et al., 2019a). In agreement with this, also rat CRISP1 has been shown to oligomerize in the presence of Zn^{2+} , and similar to GAPR-1, the proposed Zn^{2+} -binding site is formed by the two histidine residues in the CAP domain (Maldera et al., 2011). These two histidines are highly conserved throughout the CAP superfamily of proteins with the exception of only a few family members (See for example Supplementary Figure 1; human CRISP1 and mouse CRISP4). The histidine residue in the CAP1 signature motif is conserved in all family members. The second histidine resides between the CAP3 and CAP4 signature motifs and is not entirely conserved, with replacement of histidine for glutamate (hCRISP1) or aspartate (mouse and rat CRISP4). Glutamate, aspartate and cysteine residues have been identified as protein ligands for zinc atoms (Vallee and Auld, 1990). Therefore, it is likely that Glu86 is involved in Zn^{2+} coordination together with His142 within the conserved metal-binding site in human CRISP1, resulting in Zn^{2+} -dependent oligomerization. Despite this replacement, we previously showed that in the presence of Zn^{2+} and heparin, mouse CRISP4 is triggered to oligomerize and form ThT-positive structures (Sheng et al., 2019a), suggesting metal-binding site is still functional.

For most CAP family members, Zn^{2+} is coordinated by two histidines and mutating one of the two histidines in GAPR-1 for alanine abrogated the Zn^{2+} -dependent fibril formation (Sheng et al., 2019a). Here we show that some variability is permitted for the histidine residue residing between the CAP3 and CAP4 signature motifs. Replacement of this histidine for glutamate (hCRISP1) still permits Zn^{2+} -dependent oligomerization. However, this substitution may result in less efficient Zn^{2+} coordination. In agreement with this, we find that hCRISP1 forms high-molecular-weight oligomers at Zn^{2+} concentrations $\geq 300 \mu\text{M}$, which is much higher than the

half-maximal Zn^{2+} concentration of $\sim 50 \mu\text{M}$ required for the formation of amyloid-like fibrils of GAPR-1 (Sheng et al., 2019a).

A reduced Zn^{2+} sensitivity of hCRISP1 could be an adaptation to the reproductive tract. Zinc is a key element for growth and development and important for the normal functioning of the reproductive system (Fallah et al., 2018; Kerns et al., 2018; Prasad, 2013, 2014). The concentration of Zn^{2+} ions is increasing from proximal to distal regions of the epididymal lumen, with low zinc concentration found in the caput and corpus epididymides and high levels of Zn^{2+} demonstrated in the cauda epididymides (Henkel et al., 2003; Stoltenberg et al., 1996). High Zn^{2+} concentrations have been reported in the epididymis, with concentrations reaching 1 mM in the epididymis of prepubertal rats, and 2 mM in dog and human seminal plasma, respectively (Larminat et al., 1981; Mawson and Fischer, 1953; Saito et al., 1969). The Zn^{2+} concentrations used to induce CRISP1 oligomerization in this study are in the same range (0.3-1 mM) and could therefore be of potential physiological relevance. It has been reported that increasing concentrations of Zn^{2+} in the epididymis play a role in modulating the association of loosely bound rat CRISP1 to sperm surface during epididymal transit and with the presence of rat CRISP1 high-molecular-weight structures in the cauda epididymal fluids (Maldera et al., 2011). Altogether, this indicates that CRISP1 oligomerization could play a functional role in sperm epididymal maturation by increasing concentrations of Zn^{2+} in the fluid of the epididymal lumen.

We previously showed that zinc-mediated GAPR-1 aggregation was (partially) reversed upon addition of EDTA (Sheng et al., 2019b). In addition, the high-molecular-weight structures of rat CRISP1 present in the cauda epididymal fluid partially disintegrated by EDTA-mediated Zn^{2+} chelation (Maldera et al., 2011). Our present study revealed that EDTA also caused the disintegration of oligomers of either full-length CRISP1 or C-terminally truncated human CRISP1 (representing the CAP domain). These results suggest that differential Zn^{2+} concentrations within the reproductive organs may allow spatiotemporal oligomerisation of CRISP proteins by a dynamic and reversible process. Functional protein aggregates play diverse roles in reproduction and fertilization, *e.g.* in hormone peptides storage (Dannies, 2012; Jacob et al., 2016), oocyte dormancy (Pepling et al., 2007; Woodruff et al., 2018), acrosome reaction (Guyonnet et al., 2014), zona pellucida (ZP) formation (Egge et al., 2015), epididymal sperm maturation (Whelly et al., 2012), and in sperm-ZP recognition and fusion (Gadella and Evans, 2011). In contrast to pathological protein aggregation, many functional protein aggregates are reversibly regulated (Audas et al., 2016; Boke et al., 2016; Cereghetti et al., 2018; Dannies,

2012; Guyonnet et al., 2014; Jacob et al., 2016; Wallace et al., 2015). Amyloid aggregates in the acrosomal matrix (AM) are described to be essential for the stability of the AM core which is crucial for sperm-ZP penetration. During acrosome reaction, the disintegration of amyloid aggregates is central for the AM dispersion (Guyonnet et al., 2014). The loosely bound population of CRISP1 is released during sperm capacitation which is concomitant with a decrease in Zn^{2+} levels (Andrews et al., 1994; Debora J. Cohen et al., 2000; Huang et al., 2000). Our combined results provide potential novel insights into the molecular regulation of human CRISP1 function in the reproductive physiology of sperm. Metal ion-regulated oligomerization could be a common structural property of CAP domain-containing proteins (Sheng et al., 2019a). We recently showed that the CAP1 and CAP2 signature motifs contain amyloidogenic propensities, suggesting that amyloid-like aggregation is a common and evolutionary conserved property of this protein family (Olrachs and Helms, 2016; Olrachs et al., 2014). Metal-ion binding could provide a general switch, allowing (reversible) protein oligomerization of CAP family members, permitting execution of their specific biological function. In the case of CRISP1 proteins, we speculate that low Zn^{2+} levels may play a role in the initial steps of capacitation by allowing the disassembly of CRISP1 oligomers from membranes during sperm activation.

References

- Andrews, J.C., Nolan, J.P., Hammerstedt, R.H., and Bavister, B.D. (1994). Role of zinc during hamster sperm capacitation. *Biol. Reprod.* *51*, 1238–1247.
- Asojo, O.A., Koski, R.A., and Bonafé, N. (2011). Structural studies of human glioma pathogenesis-related protein 1. *Acta Crystallogr. Sect. D Biol. Crystallogr.* *67*, 847–855.
- Audas, T.E., Audas, D.E., Jacob, M.D., Ho, J.J.D., Khacho, M., Wang, M., Perera, J.K., Gardiner, C., Bennett, C.A., Head, T., et al. (2016). Adaptation to stressors by systemic protein amyloidogenesis. *Dev. Cell.* *39*, 155–168.
- Bedford, J.M., Moore, H.D.M., and Franklin, L.E. (1979). Significance of the equatorial segment of the acrosome of the spermatozoon in eutherian mammals. *Exp. Cell Res.* *119*, 119–126.
- Bessette, P.H., Åslund, F., Beckwith, J., and Georgiou, G. (1999). Efficient folding of proteins with multiple disulfide bonds in the *Escherichia coli* cytoplasm. *Proc Natl Acad Sci USA* *96*, 13703–13708.
- Boke, E., Ruer, M., Wühr, M., Coughlin, M., Lemaitre, R., Gygi, S.P., Alberti, S., Drechsel, D., Hyman, A.A., and Mitchison, T.J. (2016). Amyloid-like self-assembly of a cellular compartment. *Cell.* *166*, 637–650.
- Busso, D., Cohen, D.J., Maldera, J.A., Dematteis, A., and Cuasnicu, P.S. (2007). A novel function for CRISP1 in rodent fertilization: Involvement in sperm-zona pellucida interaction. *Biol. Reprod.* *77*, 848–854.
- Cereghetti, G., Saad, S., Dechant, R., and Peter, M. (2018). Reversible, functional amyloids: Towards an understanding of their regulation in yeast and humans. *Cell Cycle.* *17*, 1545–1558.
- Cohen, D.J., Maldera, J.A., Vasen, G., Ernesto, J.I., Munoz, M.W., Battistone, M.A., and Cuasnicu, P.S. (2011). Epididymal protein CRISP1 plays different roles during the fertilization process. *J. Androl.* *32*, 672–678.
- Cornwall, G.A. (2009). New insights into epididymal biology and function. *Hum. Reprod. Update* *15*, 213–227.
- Dannies, P.S. (2012). Prolactin and growth hormone aggregates in secretory granules: The need to understand the structure of the aggregate. *Endocr. Rev.* *33*, 254–270.
- Debora J. Cohen, Rochwerger, L., Ellerman, D.A., Morgenfe, M.M., Busso, D., and Cuasnicú, P.S. (2000). Relationship between the association of rat epididymal protein “DE” with spermatozoa and the behavior and function of the protein. *Mol. Reprod. Dev.* *56*, 180–188.
- Egge, N., Muthusubramanian, A., and Cornwall, G.A. (2015). Amyloid properties of the mouse egg zona pellucida. *PLoS ONE.* *10*, e0129907.
- Ernesto, J.I., Muñoz, M.W., Battistone, M.A., Vasen, G., Martínez-López, P., Orta, G., Figueiras-Fierro, D., De la Vega-Beltran, J.L., Moreno, I.A., Guidobaldi, H.A., et al. (2015). CRISP1 as a novel CatSper regulator that modulates sperm motility and orientation during fertilization. *J. Cell Biol.* *210*, 1213–1224.
- Fallah, A., Mohammad-Hasani, A., and Colagar, A.H. (2018). Zinc is an essential element for male fertility: A review of Zn roles in men’s health, germination, sperm quality, and fertilization. *19*, 69–81.
- Fang, Y., Fu, X., Xie, W., Li, L., Liu, Z., Zhu, C., and Mou, H. (2019). Expression, purification and characterisation of chondroitinase AC II with glyceraldehyde-3-phosphate dehydrogenase tag and chaperone (GroEs-GroEL) from *Arthrobacter* sp. CS01. *Int. J. Biol. Macromol.* *129*, 471–476.
- Gadella, B.M. (2017). Reproductive tract modifications of the boar sperm surface. *Mol Reprod Dev* *84*, 822–831.
- Gadella, B.M., and Evans, J.P. (2011). Membrane fusions during mammalian fertilization. In *Adv Exp Med Biol*, pp. 65–80.
- Garbuzynskiy, S.O., Lobanov, M.Y., and Galzitskaya, O. V. (2009). FoldAmyloid: A method of prediction of amyloidogenic regions from protein sequence. *Bioinformatics* *26*, 326–332.
- Gibbs, G.M., Scanlon, M.J., Swarbrick, J., Curtis, S., Gallant, E., Dulhunty, A.F., and O’Bryan, M.K. (2006). The cysteine-rich secretory protein domain of Tpx-1 is related to ion channel toxins and regulates ryanodine receptor Ca²⁺ signaling. *J. Biol. Chem.* *281*, 4156–4163.
- Gibbs, G.M., Roelants, K., and O’Bryan, M.K. (2008). The CAP superfamily: cysteine-rich secretory

- proteins, antigen 5, and pathogenesis-related 1 proteins-roles in reproduction, cancer, and immune defense. *Endocr. Rev.* 29, 865–897.
- Gibbs, G.M., Orta, G., Reddy, T., Koppers, A.J., Martínez-López, P., de la Vega-Beltrán, J.L., Lo, J.C.Y., Veldhuis, N., Jamsai, D., McIntyre, P., et al. (2011). Cysteine-rich secretory protein 4 is an inhibitor of transient receptor potential M8 with a role in establishing sperm function. *Proc. Natl. Acad. Sci. USA* 108, 7034–7039.
- Guo, M., Teng, M., Niu, L., Liu, Q., Huang, Q., and Hao, Q. (2005). Crystal structure of the cysteine-rich secretory protein stecrisp reveals that the cysteine-rich domain has a K⁺ channel inhibitor-like fold. *J. Biol. Chem.* 280, 12405–12412.
- Guyonnet, B., Egge, N., and Cornwall, G.A. (2014). Functional amyloids in the mouse sperm acrosome. *Mol. Cell. Biol.* 34, 2624–2634.
- Henkel, R., Baldauf, C., and Schill, W. (2003). Resorption of the element zinc from spermatozoa by the epididymal epithelium. *Reprod Dom Anim* 38, 97–101.
- Huang, Y., Chu, S., and Chen, Y. (2000). A seminal vesicle autoantigen of mouse is able to suppress sperm capacitation-related events stimulated by serum albumin. *Biol. Reprod.* 63, 1562–1566.
- Ikemura, T. (1981). Correlation between the abundance of *Escherichia coli* transfer RNAs and the occurrence of the respective codons in its protein Genes: A proposal for a synonymous codon choice that is optimal for the *E. coli* translational system. *J. Mol. Biol.* 151, 389–409.
- Jacob, R.S., Das, S., Ghosh, S., Anoop, A., Jha, N.N., Khan, T., Singru, P., Kumar, A., and Maji, S.K. (2016). Amyloid formation of growth hormone in presence of zinc: Relevance to its storage in secretory granules. *Sci. Rep.* 6, 23370.
- Kapust, R.B., and Waugh, D.S. (1999). *Escherichia coli* maltose-binding protein is uncommonly effective at promoting the solubility of polypeptides to which it is fused. *Protein Sci.* 8, 1668–1674.
- Kerns, K., Zigo, M., and Sutovsky, P. (2018). Zinc: A necessary ion for mammalian sperm fertilization competency. *Int. J. Mol. Sci.* 19, 4097.
- Koppers, A.J., Reddy, T., and O'Bryan, M.K. (2011). The role of cysteine-rich secretory proteins in male fertility. *Asian J. Androl.* 13, 111–117.
- Larminat, M.A. de, Cuasnicú, P.S., and Blaquier, J.A. (1981). Changes in trophic and functional parameters of the rat epididymis during sexual maturation. *Biol Reprod* 25, 813–819.
- Maldera, J.A., Vasen, G., Ernesto, J.I., Weigel-Muñoz, M., Cohen, D.J., and Cuasnicu, P.S. (2011). Evidence for the involvement of zinc in the association of CRISP1 with rat sperm during epididymal maturation. *Biol. Reprod.* 85, 503–510.
- Mawson, C.A., and Fischer, M.I. (1953). Zinc and carbonic anhydrase in human semen. *Biochem. J.* 55, 696–700.
- Muñoz, M.W., Battistone, M.A., Carvajal, G., Maldera, J.A., Curci, L., Torres, P., Lombardo, D., Pignataro, O.P., Ros, V.G. Da, and Cuasnicú, P.S. (2018). Influence of the genetic background on reproductive phenotype of mice lacking Cysteine-Rich Secretory Protein 1the (CRISP1). *Biol. Reprod.* 99, 373–383.
- Muñoz, M.W., Carvajal, G., Curci, L., Gonzalez, S.N., and Cuasnicu, P.S. (2019). Relevance of CRISP proteins for epididymal physiology, fertilization, and fertility. *Andrology* 7, 610–617.
- Olrichs, N.K., and Helms, J.B. (2016). Novel insights into the function of the conserved domain of the CAP superfamily of proteins. *AIMS Biophys.* 3, 232–246.
- Olrichs, N.K., Mahalka, A.K., Kaloyanova, D., Kinnunen, P.K., and Helms, J.B. (2014). Golgi-Associated plant Pathogenesis Related protein 1 (GAPR-1) forms amyloid-like fibrils by interaction with acidic phospholipids and inhibits A β aggregation. *Amyloid* 21, 88–96.
- Pepling, M.E., Wilhelm, J.E., Hara, A.L.O., Gephardt, G.W., and Spradling, A.C. (2007). Mouse oocytes within germ cell cysts and primordial follicles contain a Balbiani body. *Proc Natl Acad Sci USA* 104, 187–192.
- Prasad, A.S. (2013). Discovery of human zinc deficiency: Its impact on human health and disease. *Adv Nutr.* 4, 176–190.
- Prasad, A.S. (2014). Zinc is an antioxidant and anti-inflammatory agent: Its role in human health. *Front. Nutr.* 1, 14.
- Roberts, K.P., Wamstad, J.A., Ensrud, K.M., and Hamilton, D.W. (2003). Inhibition of capacitation-associated tyrosine phosphorylation signaling in rat sperm by epididymal protein Crisp-1. *Biol.*

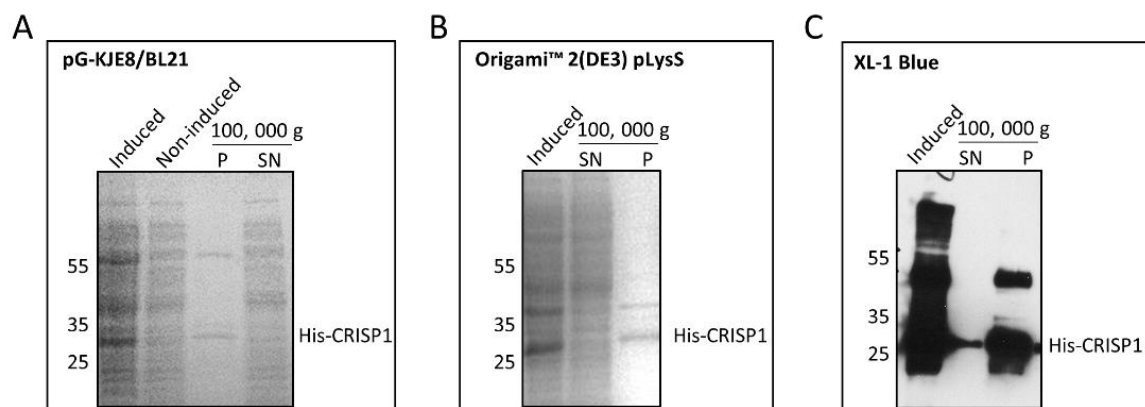
- Reprod. 69, 572–581.
- Ros, V.G. Da, Muñoz, M.W., Battistone, M.A., Brukman, N., Carvajal, G., Curci, L., Gomez-Elias, M.D., Cohen, D.J., and Cuasnicú, P.S. (2015). From the epididymis to the egg: Participation of CRISP proteins in mammalian fertilization. *Asian J. Androl.* 17, 711–715.
- Saito, S., Zeitz, L., Bush, I.M., Lee, R., and Jr, W.F.W. (1969). Zinc uptake in canine or rat spermatozoa. *Am. J. Physiol.* 217, 1039–1043.
- Sheng, J., Olrichs, N.K., Geerts, W.J., Li, X., Rehman, A.U., Gadella, B.M., Kaloyanova, D. V, and Helms, J.B. (2019a). Zinc binding regulates amyloid-like aggregation of GAPR-1. *Biosci. Rep.* 39, BSR20182345.
- Sheng, J., Olrichs, N.K., Geerts, W.J., Kaloyanova, D. V., and Helms, J.B. (2019b). Metal ions and redox balance regulate distinct amyloid-like aggregation pathways of GAPR-1. *Sci. Rep.* 9, 15048.
- Shikamoto, Y., Suto, K., Yamazaki, Y., Morita, T., and Mizuno, H. (2005). Crystal structure of a CRISP family Ca²⁺-channel blocker derived from snake venom. *J. Mol. Biol.* 350, 735–743.
- Siller, E., Dezwaan, D.C., Anderson, J.F., Freeman, B.C., and Barral, J.M. (2009). Slowing bacterial translation speed enhances eukaryotic protein folding efficiency. *J. Mol. Biol.* 396, 1310–1318.
- Stoltenberg, M., Ernst, E., Andreasen, A., and Danscher, G. (1996). Histochemical localization of zinc ions in the epididymis of the rat. *Histochem. J.* 28, 173–185.
- Sullivan, R., and Mieusset, R. (2016). The human epididymis: its function in sperm maturation. *Hum. Reprod. Update* 22, 574–587.
- Suzuki, N., Yamazaki, Y., Brown, R.L., Fujimoto, Z., Morita, T., and Mizuno, H. (2008). Structures of pseudechotoxin and pseudecin, two snake-venom cysteine-rich secretory proteins that target cyclic nucleotide-gated ion channels: implications for movement of the C-terminal cysteine-rich domain. *Acta Crystallogr D Biol Crystallogr* 64, 1034–1042.
- Tian, Y., Chen, J., Yu, H., and Shen, Z. (2016). Overproduction of the Escherichia coli chaperones GroEL-GroES in Rhodococcus ruber improves the activity and stability of cell catalysts harboring a nitrile hydratase. *J. Microbiol. Biotechnol.* 26, 337–346.
- Vadnais, M.L., Foster, D.N., and Roberts, K.P. (2008). Molecular cloning and expression of the CRISP family of proteins in the boar. *Biol. Reprod.* 79, 1129–1134.
- Vallee, B.L., and Auld, D.S. (1990). Active-site zinc ligands and activated H₂O of zinc enzymes. *Proc Natl Acad Sci USA* 87, 220–224.
- Vasina, J.A., and Baneyx, F. (1997). Expression of aggregation-prone recombinant proteins at low temperatures: A comparative study of the Escherichia coli cspA and tac promoter systems. *Protein Expr. Purif.* 9, 211–218.
- Volpert, M., Mangum, J.E., Jamsai, D., D’Sylva, R., O’Bryan, M.K., and McIntyre, P. (2014). Eukaryotic expression, purification and structure/function analysis of native, recombinant CRISP3 from human and mouse. *Sci. Rep.* 4, 4217.
- Wallace, E.W.J., Kear-scott, J.L., Pilipenko, E. V, Schwartz, M.H., Laskowski, P.R., Rojek, A.E., Katanski, C.D., Riback, J.A., Dion, M.F., Franks, A.M., et al. (2015). Reversible, specific, active aggregates of endogenous proteins assemble upon heat stress. *Cell* 162, 1286–1298.
- Wang, J., Shen, B., Guo, M., Lou, X., Duan, Y., Cheng, X.P., Teng, M., Niu, L., Liu, Q., Huang, Q., et al. (2005). Blocking effect and crystal structure of natrin toxin, a cysteine-rich secretory protein from Naja atra venom that targets the BKCa channel. *Biochemistry* 44, 10145–10152.
- Wang, Y.-L., Kuo, J.-H., Lee, S.-C., Liu, J.-S., Hsieh, Y.-C., Shih, Y.-T., Chen, C.-J., Chiu, J.-J., and Wu, W.-G. (2010). Cobra CRISP functions as an inflammatory modulator via a novel Zn²⁺- and heparan sulfate-dependent transcriptional regulation of endothelial cell adhesion molecules. *J. Biol. Chem.* 285, 37872–37883.
- Whelly, S., Johnson, S., Powell, J., Borchardt, C., Hastert, M.C., and Cornwall, G.A. (2012). Nonpathological extracellular amyloid is present during normal epididymal sperm maturation. *PLoS One* 7, e36394.
- Woodruff, J.B., Hyman, A.A., and Boke, E. (2018). Organization and function of non-dynamic biomolecular condensates. *Trends Biochem. Sci.* 43, 81–94.
- Yan, X., Hu, S., Guan, Y., and Yao, S. (2012). Coexpression of chaperonin GroEL/GroES markedly enhanced soluble and functional expression of recombinant human interferon-gamma in Escherichia coli. *Appl Microbiol Biotechnol* 93, 1065–1074.

Yanagimachi, R. (1994). Fertility of mammalian spermatozoa: Its development and relativity. *Zygote* 2, 371–372.

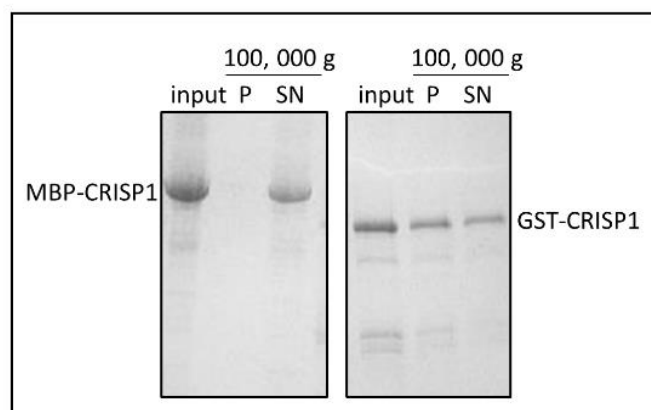
Supplementary Figures



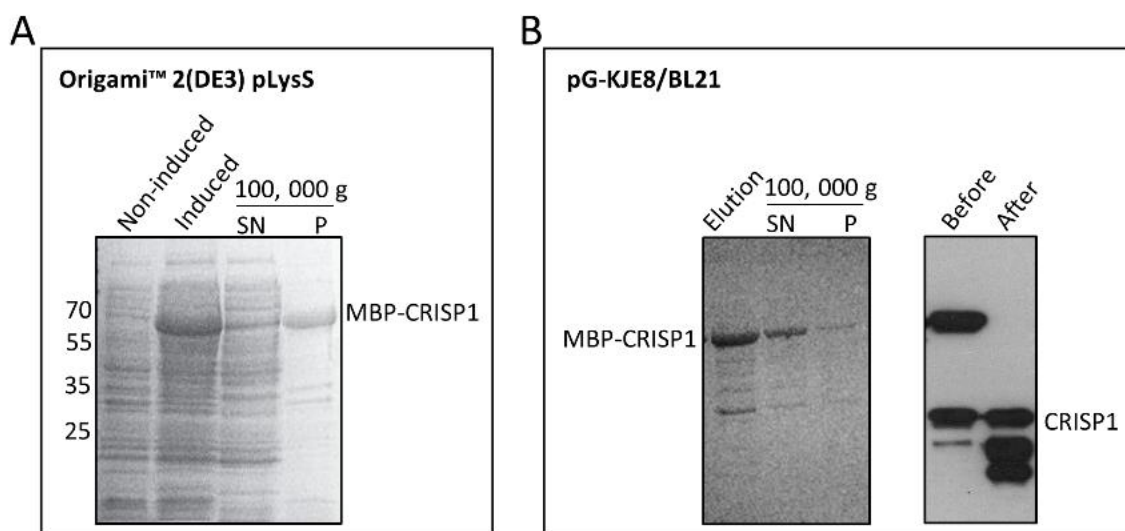
Supplementary Figure 1. Sequence alignment of GAPER-1 and CRISP proteins from mammals and snake venom. The predicted amyloidogenic regions, obtained from amyloid prediction tool FoldAmyloid are highlighted in green (Garbuzynskiy et al., 2009). CAP signature motifs and 16 conserved cysteine residues (*) in CRISP proteins are indicated below the sequences. Two conserved histidine residues and two conserved glutamates involved in the metal binding site of CAP superfamily proteins are highlighted with red boxes. The semi-conserved cysteine in GAPER-1 (Cys63) is indicated with red arrow.



Supplementary Figure 2. Expression of His-CRISP1 in pG-KJEB/BL21, Origami™ 2 (DE3) pLysS, and XL-1 Blue. (A) Expression of His-CRISP1 in pG-KJEB/BL21. Samples before (Non-induced) or after induction (Induced) with IPTG were centrifuged at 100,000 g and the supernatant (SN) and pellet (P) of induced samples were analyzed by SDS-PAGE and Coomassie blue staining. (B) Expression of His-CRISP1 in Origami™ 2 (DE3) pLysS. After induction (Induced) with IPTG, the samples were centrifuged at 100,000 g and the supernatant (SN) and pellet (P) were analyzed by SDS-PAGE and Coomassie blue staining. (C) Expression of His-CRISP1 in XL-1 Blue. After induction (Induced) with IPTG, the samples were centrifuged at 100,000 g and the supernatant (SN) and pellet (P) were analyzed by SDS-PAGE and Western blot.



Supplementary Figure 3. Solubility of MBP-CRISP1 and GST-CRISP1 expressed in XL-1 Blue. Purified MBP-CRISP1 and GST-CRISP1 were centrifuged at 100,000 *g* after incubation at room temperature for 90 min. Supernatant (SN) and pellet (P) were analyzed by SDS-PAGE and Coomassie blue staining.



Supplementary Figure 4. Expression characteristics of MBP-CRISP1 in specialized bacterial strains and MBP cleavage from CRISP1. (A) Expression of MBP-CRISP1 in Origami™ 2 (DE3) pLysS. Samples before (Non-induced) or after induction (Induced) with IPTG were centrifuged at 100,000 *g* and the supernatant (SN) and pellet (P) of induced samples were analyzed by SDS-PAGE and Coomassie blue staining. (B) Purification and solubility (left panel), and cleavage (right panel) of MBP-CRISP1 expressed in pG-KJEB/BL21. Purified MBP-CRISP1 (Elution) was centrifuged at 100,000 *g* and the supernatant (SN) and pellet (P) were analyzed by SDS-PAGE and Coomassie blue staining (left panel). Samples before and after MBP-CRISP1 cleavage (see Materials and Methods for details) were analyzed by SDS-PAGE and Western blot (right panel).

Summarizing discussion

Jie Sheng, Nick K. Orlachs, Bart M. Gadella, Dora V. Kaloyanova, J. Bernd Helms

Department of Biochemistry and Cell Biology, Faculty of Veterinary Medicine, Utrecht University,
Utrecht, the Netherlands

Submitted for publication:

Sheng, J., Orlachs, N. K., Gadella, B. M., Kaloyanova, D. V. and Helms, J. B. Regulation of functional protein aggregation by multiple factors: Implications for the amyloidogenic behavior of the CAP superfamily.

1 Introduction to protein aggregates: two sides of a coin

Protein aggregation is a biochemical process in which proteins accumulate or clump together to form aggregates and/or membrane-less inclusions, either intracellularly or extracellularly (Aguzzi and O’Coonor, 2010; Cereghetti et al., 2018; Iadanza et al., 2018; Stefani and Dobson, 2003). For a long time, protein aggregation was viewed exclusively as a pathological process due to its intimate relation with a number of devastating diseases. Amyloid formation is a distinct type of protein aggregation in which soluble proteins assemble into highly ordered, biochemically stable fibrils with the canonical cross- β structure (Cereghetti et al., 2018; Chiti and Dobson, 2017; Sawaya et al., 2007). To date, approximately 50 amyloid-forming peptides and proteins have been identified as the pathological hallmark of many human disorders (Iadanza et al., 2018). However, the notion that protein aggregation is inherently detrimental to cells has recently been challenged by the identification of protein aggregates that play functional roles in physiology. The structure of amyloids enables their use as scaffolds for biochemical activities and the compact nature of aggregates makes them highly suitable as sites for protein storage. Functional protein aggregates appeared crucial for a variety of biological activities, including the storage of peptide hormones (Jacob et al., 2016; Maji et al., 2009), reproduction (Egge et al., 2015; Hewetson et al., 2017; Roan et al., 2017), pigmentation (Bissig et al., 2016), necroptosis (Liu et al., 2017), antimicrobial responses (Jang et al., 2011), adaptation to stress (Audas et al., 2016; Saad et al., 2017), cellular dormancy (Boke et al., 2016; Pepling et al., 2007; Woodruff et al., 2018), regulating fungal-host and fungal-fungal interactions (Lipke et al., 2012), modulating epigenetic heritable phenotypes in yeast (Alberti et al., 2009) and persistence of long-term memory in *Drosophila* (Majumdar et al., 2012).

The double-sided nature of amyloids as pathological or physiological assemblies, together with several shared structural similarities (*e.g.* β -sheet structure, thermodynamic stability and specific tinctorial properties (Grignaschi et al., 2018)), makes it ambiguous to clearly distinguish between the “bad” and “good” amyloid aggregates. To address this, a better characterization of the nature of protein aggregates will be required by consideration of additional properties, including function, reversibility, infectivity, localization, composition and structure (Cereghetti et al., 2018). Factors affecting the amyloidogenic properties of proteins are summarized in Figure 1 and will be discussed hereafter.

2 Properties of functional aggregates regulation

In contrast to pathological aggregates, functional aggregates are assembled under physiological

conditions without deleterious effects on cells, suggesting that the formation of these two types of aggregates are regulated by different mechanisms. Soluble oligomeric intermediates formed during aberrant amyloid aggregation are detrimental to cells (Sengupta et al., 2016; Stefani, 2010). The presence of these oligomers in cells can result in membrane permeabilization, elevated Ca^{2+} concentrations, oxidative stress and cell death (Demuro et al., 2005; Kaye et al., 2004; Sengupta et al., 2016; Stefani, 2010). Although functional aggregates are not lethal to cells, potentially toxic intermediates do exist during their assembly (Jackson and Hewitt, 2017). For example, aggregation of yeast Sup35 plays an essential role in encoding heritable information. During amyloid assembly of the prion-determining region of yeast Sup35, a variety of oligomers are formed with differences in size and stability. At early stages of aggregation, less compact oligomers are formed which are hydrophobic and highly toxic to neuronal cells. The more mature oligomers are compact and nontoxic for cells (Krishnan et al., 2012). A similar phenomenon is observed for other functional amyloid forming proteins, such as pigment cell-specific pre-melanosomal protein (PMEL) and Orb2, a key protein for long-term memory formation in *Drosophila*. In both cases, the intermediate oligomers are toxic whereas the mature amyloid state is functional (Bissig et al., 2016; Rubén Hervás et al., 2016; Watt et al., 2011). In order to avoid toxicity, functional aggregation must therefore be tightly regulated (Jackson and Hewitt, 2017).

2.1 Kinetics

Different from pathological aggregates, functional aggregation processes often occur with relatively fast kinetics. Rapid growth rates of amyloid fibrils have been proposed as one of the protective mechanisms to minimize the existence of intermediate oligomers (Jackson and Hewitt, 2017; Rubén Hervás et al., 2016). For instance, recombinant PMEL exhibits rapid fibrilization *in vitro*, with a fast transition from the monomeric state to mature amyloids. Unlike pathological amyloids, which typically need several days to be formed *in vitro*, the PMEL fibrillogenic domain requires only several minutes to form fibrils (Bissig et al., 2016; Fowler et al., 2006; Watt et al., 2009). A similar rapid fibrillation is observed for other functional amyloids, such as the antimicrobial peptide protegrin-1 (PG-1), cystatin-related epididymal spermatogenic (CRES) proteins, Orb2, and the bacterial curli protein CsgA (Hewetson et al., 2017; Jang et al., 2011; Rubén Hervás et al., 2016; Sleutel et al., 2017). CsgA monomers form nascent fibrils very fast under native conditions, directly folding and oligomerizing into minimal fibers and bypassing a transition through an intermediate, non-amyloid oligomeric state (Sleutel et al., 2017). When the prion-like domain (PLD) of Orb2 is swapped with the

amyloidogenic polyglutamine tract of exon 1 of the human huntingtin protein, the chimeric Orb2 protein assembled much slower and with a longer existence of highly toxic oligomeric states. This suggests that, in principle, Orb2 can form a toxic conformation. Vice versa, when the amyloidogenic polyglutamine tract of exon 1 of the human huntingtin protein is replaced with the PLD of Orb2, the chimeric huntingtin construct formed nontoxic, short-lived species. Altogether, rapid growth rate seems to be one of the features which can distinguish functional from pathological aggregates (Roberts, 2016).

2.2 Reversibility

As indicated above, protein aggregation has been widely used to control multiple physiological processes in cells. Functional protein aggregation is often characterized by the reversible nature of the aggregation process. Firstly, upon exposure to stress (*e.g.* heat shock, acidosis, nutrient starvation, *etc.*), cells can assemble different types of condensates, such as nuclear amyloid bodies (A-bodies) (Audas et al., 2016), Balbiani bodies (Boke et al., 2016), processing bodies (P-bodies) (Narayanaswamy et al., 2009), heat-shock granules (HSGs) (Wallace et al., 2015) and cytoplasmic foci that contain heterogeneous protein:RNA complexes with amyloid-like biophysical properties (Munder et al., 2016; Saad et al., 2017). A well-studied example is the reversible formation of functional amyloid-like aggregates by yeast pyruvate kinase Cdc19, a central regulator of cellular metabolism and cell growth. Cdc19 forms aggregates under prolonged glucose starvation, which is reversed upon glucose supplementation (Saad et al., 2017). This process protects Cdc19 from stress-induced degradation, thereby ensuring restart of the cell cycle after stress (Saad et al., 2017). Secondly, reversible aggregates are commonly associated with protein storage (Dannies, 2012; Guyonnet et al., 2014; Hewetson et al., 2017; Jacob et al., 2016). For instance, prolactin and growth hormone (GH) are stored in concentrated forms as protein aggregates in secretory granules. When needed, the protein aggregates are rapidly dissolved into monomers, causing a hormone burst in the bloodstream (Dannies, 2012; Jacob et al., 2016). Thirdly, reversible regulation plays a vital role in clearance of condensates as well as the degradation and clearance of disease-associated amyloid aggregates. For clearance and degradation, several pathways and machineries exist, *e.g.* autophagy, the ubiquitin-proteasome system (UPS), molecular chaperones, and protein disaggregases (Chuang et al., 2018). Accumulation of aberrant aggregates can be caused by proteostasis impairment, together with the appearance of the corresponding diseases (Hipp et al., 2014; Jackson and Hewitt, 2016). Autophagy is an essential degradation pathway in clearing aberrant aggregates, such as those formed by transactive response DNA-binding protein 43 (TDP-43), α -synuclein,

tau and the amyloid β (A β) peptide (Barmada et al., 2014; Cho et al., 2014; Falcon et al., 2018; Webb et al., 2003). Impairments in autophagy are strongly associated with neurodegeneration, such as Alzheimer's disease (AD) and Parkinson's disease (PD) (Rahman and Rhim, 2017; Zare-shahabadi et al., 2016). Compounds that stimulate autophagy have been shown to improve TDP-43 clearance and to prevent TDP-43 mediated cell death in a neuronal model with Amyotrophic Lateral Sclerosis (ALS) (Barmada et al., 2014). UPS is another pathway for protein degradation (Goldberg, 2003), and impairment in UPS is also implicated in neurodegeneration (Myeku et al., 2016). Accumulation of insoluble tau is associated with dysfunction of the proteasome and inhibition of ATPase in a mouse model. Increased cAMP concentrations in the brain can enhance the activity of the proteasome and thereby promotes degradation of tau aggregates (Myeku et al., 2016). In the cell, machineries such as molecular chaperones and proteases are required for functional protein disaggregation. Upon heat stress, Pub1 forms biological condensates that are related to a restart of the cell cycle (Kroschwald et al., 2018). Release of the cell cycle arrest coincides with condensate dissolution. *In vitro*, heat shock proteins (HSPs) such as Hsp104 are required for disassembly of heat-shock induced condensates (Kroschwald et al., 2018). Moreover, HSPs and protein disaggregases are also implicated in combating protein misfolding and aberrant protein aggregation. HSPs (*e.g.* Hsp70 and Hsp90) are important inhibitors of protein aggregation by protecting the exposed hydrophobic regions from aggregation (Lindberg et al., 2015; Mack and Shorter, 2016). Yeast Hsp104 can reverse toxic aggregates formed by α -synuclein, tau, A β , Prion protein (PrP) and amylin (Desantis and Shorter, 2012; Desantis et al., 2012), thus reducing the toxic species and restoring native function to proteins sequestered within aggregates (Mack and Shorter, 2016). Engineered Hsp104 variants have an enhanced ability to dissolve protein aggregates that are associated with neurodegenerative diseases such as PD and ALS (Jackrel et al., 2015; Torrente et al., 2016). Altogether these observations indicate that HSPs and proteases are used by cells to effectively reverse both functional and aberrant aggregates in order to maintain cellular function and homeostasis.

3 Other factors regulating functional protein aggregation

Except rapid growth rates and reversible dynamics, there are several other ways to avoid potential toxicity by regulating functional aggregation (Jackson and Hewitt, 2017). The expression and degradation of the precursors of functional amyloid fibrils are tightly controlled because high levels of an amyloidogenic precursor could initiate unwanted amyloid aggregation (Jackson and Hewitt, 2017). Moreover, in order to prevent unexpected interactions between

aggregates and other cellular components, numerous functional protein aggregation reactions occur within distinct compartments, *e.g.* melanosomes, endocrine granules and acrosomes (Guyonnet et al., 2014; Jackson and Hewitt, 2017; Maji et al., 2009; McGlinchey and Lee, 2018). Finally, diverse classes of biomolecules have been identified in regulating functional protein aggregation to ensure correct structural assembly and/or disassembly, *e.g.* lipids/membranes, glycosaminoglycans (GAGs), nucleic acids, metal ions, heat shock proteins and proteases. A full understanding of how these molecules and other biochemical factors regulate functional protein aggregation is only starting to emerge and will be briefly discussed hereafter.

3.1 Polyanions

Glycosaminoglycans (GAGs), nucleic acids, or membranes containing negatively charged lipids, can all act as polyanions, which are effective catalysts for protein aggregation. Such polyanionic platforms can attract proteins through electrostatic interactions, thus enhancing the local protein concentration. Through these interactions, monomers can adopt a conformation and orientation that promotes their assembly into fibrillar structures (Bourgault et al., 2011; Iannuzzi et al., 2015; Kinnunen, 2009; Langner and Kubica, 1999; Liu and Zhang, 2011; Solomon et al., 2011).

3.1.1 Lipids/Membranes

Membranes are involved in the amyloidogenesis of several proteins, such as A β , PrP, α -synuclein, islet amyloid polypeptide (IAPP), and Orb2A (Fantini and Yahi, 2019; Murphy, 2007; Soria et al., 2017). Upon interaction with membranes, proteins can undergo a series of conformational changes, thus inducing the formation of oligomers that are rich in cross β -sheet structures (annular pores and amyloid fibrils) (Fantini and Yahi, 2019). Membrane-binding can also be directly involved in regulating functional amyloid formation (Jiang and Lee, 2014; Soria et al., 2017). For example, Orb2 binding to anionic membranes results in a transition from a dynamic, intrinsically disordered state to a less dynamic α -helix which prevents β -sheet formation and amyloidogenic aggregation of Orb2 (Soria et al., 2017). This inhibition by anionic membranes is proposed to be a potential mechanism regulating Orb2 amyloidogenesis *in vivo*. A similar mechanism has been identified for aggregate formation of Pmel17, involved in enhancing melanin synthesis (McGlinchey and Lee, 2018). Aggregation of the repeat domain (RPT) derived from Pmel17 is modulated by lysophospholipid-containing vesicles (Jiang and Lee, 2014). The surfactant-like lysophospholipid is of particular interest due to its high content

in melanosomal membranes and it has been suggested that protein-lysophospholipid interactions within melanosomes may regulate functional aggregation of Pmel17 *in vivo* (Jiang and Lee, 2014). TasA, a major matrix protein in biofilms of *Bacillus subtilis*, interacts distinctively with bacterial model membranes. In the presence of eukaryotic model membranes as well as in the absence of membranes, TasA forms fibers of similar structure and morphology. However, upon interaction of TasA with bacterial model membranes, disordered aggregates with a different β -sheet signature are formed and bacterial membranes deformed more extensively than eukaryotic membranes, which could be crucial in providing integrity to biofilms (Malishev et al., 2018). Of note, regulation of amyloid formation by membranes must be carefully regulated as oligomers or aggregates formed on membranes can cause damage to membranes, which is considered to be a main mechanism of amyloid toxicity (Relini et al., 2014)

3.1.2 GAGs

GAGs are long, unbranched polysaccharides consisting of repeating disaccharide subunits. They exist on the surface of cells or in the extracellular matrix of multicellular organisms. GAGs, particularly heparan sulfate (HS) and its highly sulfated derivative heparin, play important roles in protein aggregation, stability and resistance to proteolysis (Iannuzzi et al., 2015). Pathological aggregates of A β 42, tau, α -synuclein and PrP induced by GAGs are implicated in neurodegenerative diseases (Dulce et al., 2011). GAGs are also able to reduce the cytotoxicity of a number of amyloid systems by different mechanisms (Dharmadana et al., 2017). GAGs-accelerated aggregation can provide protection against cytotoxicity of intermediate oligomers. For instance, heparin enhances the fibrillogenesis of IAPP aggregation that is associated with Type-II diabetes. Heparin inhibits IAPP cytotoxicity in islet cells, whereas in GAG-deficient cell lines, IAPP-induced toxicity could not be prevented (Carufel et al., 2013). Alternatively, protein interaction with GAGs can increase protein stability and decrease its propensity to aggregate, such as in the case of PrP (Vieira et al., 2014). The exact mechanism by which different GAGs influence protein structure and aggregation, as well as the intercellular spread of these aggregates, remains elusive. Subtle differences in the GAG backbone structure and charge density significantly alter the properties of the resulting amyloid fibrils, as was shown for α -synuclein (Mehra et al., 2018). Distinct fibrils displayed variable levels of cytotoxicity but also exhibited an altered ability to internalize into cells (Mehra et al., 2018). Finally, GAGs can inhibit the toxicity of protein oligomers by binding the oligomers to the cell surface and in this way preventing the interaction of the oligomers with cells, as has

been shown for *Escherichia coli* HypF (HypF-N) (Saridaki et al., 2012). GAGs can also play a role in enhancing functional protein oligomerization and aggregation. For example, low molecular weight heparin is able to induce many hormone peptides or proteins to form amyloid fibrils (Maji et al., 2009).

3.1.3 Nucleic acids

Nucleic acids (DNA and RNA) are large polymers of nucleotides with characteristics of polyanions. Nucleic acids can not only induce and accelerate protein aggregation of *e.g.* PrP, α -synuclein, amyloid- β and huntingtin (Liu and Zhang, 2011), but can also reverse protein aggregation (Chen and Cheng, 2017). For example, the Gag protein of HIV-1 undergoes nucleic acid-dependent aggregation, and excess of nucleic acids can promote disassembly of the formed aggregates (Chen and Cheng, 2017). Additionally, nucleic acid-bound proteins are common components of membraneless compartments (*e.g.* nucleoli, germ granules, Cajal bodies, stress granules (SGs) and P-bodies) that exhibit liquid-like properties (Alberti and Dormann, 2019; Banani et al., 2017; Brangwynne et al., 2011; Decker and Parker, 2012; Mao et al., 2011; Patel et al., 2015; Saha et al., 2016; Woodruff et al., 2018; Wu, 2013). These cellular compartments are associated with diverse biological processes, including RNA metabolism, ribosome biogenesis, DNA damage response and signal transduction (Banani et al., 2017). Their components are highly mobile and can exchange with the surrounding medium rapidly and specifically through protein assembly and disassembly (Dundr et al., 2004; Weidtkamp-peters et al., 2008).

3.1.4 Polyphosphate (PolyP)

PolyP contains a linear arrangement of inorganic phosphates that are connected via phosphoanhydride bonds (Brown and Kornberg, 2004). PolyP has been indicated to exhibit both anti- and pro-aggregation properties (Xie and Jakob, 2019). Specifically, under oxidative stress or heat shock condition, polyP acts as a protein-stabilizing scaffold that binds to protein unfolding intermediates and stabilizes them in a soluble β -sheet-rich conformation, which prevents protein aggregation. Once the stress is released, the polyP-bound proteins are refolded and restored into their native structures. PolyP is able to enhance both functional amyloid formation (*e.g.* bacterial CsgA (Cremers et al., 2016)) and disease-related amyloid aggregation (*e.g.* A β , α -synuclein and tau) and can also cause morphological changes in mature fibrils (Cremers et al., 2016). In general, however, amyloid aggregates formed in the presence of polyP

are not cytotoxic and therefore polyP is proposed as a physiologically relevant modifier in amyloidogenic processes (Xie and Jakob, 2019).

3.2 Metal ions

Metal ions participate in both pathological and functional protein oligomerization and aggregation via a variety of different mechanisms. Metal ions can (1) bridge two peptides or proteins; (2) change the overall charge of proteins; (3) induce a conformational change within a protein; (4) induce changes in fiber morphology (Leal et al., 2012).

Metal ions, such as Fe^{3+} , Cu^{2+} and Zn^{2+} , play essential roles in the brain and toxic exposure to metals and/or dyshomeostasis in metal metabolism is associated with protein misfolding and aggregation in neurodegenerative diseases (Cicero et al., 2017). Specifically, Zn^{2+} ions accelerate the aggregation of both $\text{A}\beta$ and tau, which are the hallmarks of AD. High concentrations of Zn^{2+} allow $\text{A}\beta$ to an immediate conformational transition into a hydrophobic state which promotes fast protein aggregation (Guo et al., 2017). Zn^{2+} also enhance tau aggregation and accelerate tau toxicity in neuronal cells via inducing the formation of intermolecular disulfide bonds (Hu et al., 2017). Metal ions are also involved in regulating functional protein oligomerization and aggregation. For example, Ca^{2+} binding to the EF-hand motifs of S100A12 and Zn^{2+} binding to the dimeric S100A12 interface cooperatively induces a conformational rearrangement within the protein that leads to protein oligomerization, which plays a role in responding to inflammation (Moroz et al., 2009; Wang et al., 2019). Zinc ions also induce growth hormone aggregation, which facilitates peptide storage (Jacob et al., 2016). Potassium channel tetramerization domain containing 1 (KCTD1) family proteins play a role in regulating different signalling pathways. Copper ions binding to KCTD1 results in increased β -sheet content, promoting amyloid aggregation that are functionally cytotoxic in initiating apoptosis (Liu et al., 2016).

3.3 Post-translational modifications

Most proteins translated from mRNA are subject to post-translational modifications (PTMs) before executing their function(s) in different cell types. PTMs play a vital role in generating protein heterogeneity and utilizing identical proteins for different cellular functions in different cell types. PTMs such as methylation (Funk et al., 2015), glycosylation (Schedin-weiss et al., 2014), acetylation (Abdolvahabi et al., 2015; Cohen et al., 2015; DiMauro et al., 2014; Gal et al., 2013), phosphorylation (Grignaschi et al., 2018; Johnson and Stoothoff, 2004; Li et al., 2011; Nonaka et al., 2016; Rhoads et al., 2018; Rodriguez-Martin et al., 2013; Saad et al., 2017;

Tenreiro et al., 2014; Zhang et al., 2015) and cysteine modification (Anoop et al., 2014; Chattopadhyay et al., 2015; Göbl et al., 2020; Gould et al., 2013; Li et al., 2013; Marinelli et al., 2018; Nakajima et al., 2007; Wineman-Fisher et al., 2016) are major factors in modulating protein self-assembly and disassembly. Phosphorylation is proposed as a protective mechanism to reduce toxic protein aggregation (Li et al., 2011; Tenreiro et al., 2014). For instance, hyperphosphorylation of the C-terminus of TDP-43 favours its dissociation from aggregation and may facilitate its degradation by UPS (Li et al., 2011). Phosphorylation and other PTMs are suggested as generic mechanisms to reversibly regulate the aggregation of proteins containing low complexity regions (LCRs) (Grignaschi et al., 2018; Saad et al., 2017). For example, phosphorylation of the hydrophobic, aggregation-prone LCR region in Cdc19 prevents protein aggregation, whereas dephosphorylation enhances protein aggregation (Grignaschi et al., 2018). Crosstalk between different PTMs provides an additional layer of regulation of protein aggregation (Carlomagno et al., 2017; Chiki et al., 2017). This is illustrated by the fact that phosphorylation of mutant huntingtin exon1(Httex1) inhibits protein aggregation, whereas acetylation reverses the inhibitory effect (Chiki et al., 2017).

Cysteine oxidation is another well-studied PTM, playing a significant role in the regulation of protein structure, stability, oligomerization and function (Bechtel and Weerapana, 2017; Gould et al., 2013; Marinelli et al., 2018). The thiol group of cysteine is sensitive to redox conversion. The free sulfhydryl group of cysteine residues can be reversibly oxidized to a disulfide bond and to sulfenic acid, or irreversibly oxidized to sulfinic acid and sulfonic acid (Cai and Yan, 2013; Poole, 2015). Sulfenic acid modification of Cys-111 triggers the formation of nascent superoxide dismutase 1 (SOD1) oligomers, which induce the fibrillization of both SOD1 and TDP-43 in cells (Xu et al., 2018). Sulfonic acid modification of a single cysteine in FF domain, a conserved domain involved in transcription, RNA splicing and signal transduction (Jiang et al., 2005; Smith et al., 2014), suffices to enhance protein aggregation through destabilization of the native conformation (Marinelli et al., 2018).

Transition between free sulfhydryl groups of two cysteines into a disulfide bond is the most commonly occurring reversible redox reaction involving cysteines and enables flexible regulation of protein folding, structure and function (Chiu and Hogg, 2019). Native disulfide bonds are crucial for protein stability (Trivedi et al., 2009) and their reduction can lead to protein destabilization and aberrant aggregation, as has been described for *e.g.* SOD1, amylin and PrP (Chattopadhyay et al., 2015; Honda, 2017; Ridgway et al., 2018; Wineman-Fisher et al., 2016). For example, the disulfide bond in the amylin monomer stabilizes the N-terminal α

-helical structure, which prevents formation of β -sheet structures (Laghaei and Mousseau, 2010; Yonemoto et al., 2009). This disulfide bond stabilizes a loop in the N-terminus that protects amylin from aggregation through binding to the amyloid-prone regions of amylin monomers (Vaiana et al., 2009). Removal of disulfide bonds in native amylin oligomers causes structural changes, decreases polymorphism and induces protein aggregation (Wineman-Fisher et al., 2016).

Disulfide bond reduction also enhances functional protein aggregation. An interesting example is presented by Premelanosome Protein (PMEL). PMEL forms a disulfide-bonded homodimer which involves a cysteine-rich Kringle-like domain (KLD). This KLD is required to resolve PMEL dimers that are formed in the endoplasmic reticulum into monomeric forms within the late Golgi or a post-Golgi compartment. The cysteine residues within this KLD initiate a disulfide bond exchange between intermolecular disulfide bonds (between PMEL monomers) to intramolecular disulfide bonds (within a PMEL monomer) in an autocatalytic manner (Ho et al., 2016). Somatostatin-14 (SST-14) is a cyclic peptide hormone and an amyloid structure is implicated in its storage. The disulfide bond in SST-14 controls the cyclization process and hence its conformational flexibility, which in turn associates strongly with its aggregation and disaggregation profiles. Native SST-14 aggregation needs prolonged incubation and the resulting amyloids readily release the monomers. In contrast, cleavage of the disulfide bond results in noncyclic SST-14, which may lead to increased accessibility to the aggregation-prone region and heparin-interaction ability. As a result, the self-association capacity of SST-14 is enhanced but with a slower monomer releasing potency (Anoop et al., 2014). These results also indicate a marked variation in the interpeptide hydrogen bonding network upon cleavage of the disulphide bridge. Formation of non-native intermolecular disulfide bonds are also associated with protein aggregation (Banci et al., 2007; Li et al., 2013; Nakajima et al., 2007; Zha et al., 2009; Zhou and Freed, 2004). For instance, upon necroptosis induction, aggregates of receptor-interacting protein kinase 1 and 3 (RIPK1/RIPK3) concentrate and phosphorylate mixed-lineage kinase domain-like protein (MLKL), inducing structural changes of MLKL and facilitating disulfide bond formation. Disulfide bonds stabilize the adopted structure and enhance downstream amyloid aggregation of MLKL which is functional in necroptosis (Liu et al., 2017). Another example is represented by p16^{INK4A}, which forms disulfide bridged homodimers under mild oxidizing conditions. This dimerization induces conformational rearrangements and leads to amyloid aggregation. The accumulation of p16^{INK4A} inhibits oncogenic transformation through regulating cell cycle arrest and senescence (Göbl et al.,

2020).

3.4 Emerging factors affecting protein aggregation

The presence of amyloid aggregates in the acrosomal matrix (AM) contributes to the stability of the AM core which plays an important role in sperm-zona pellucida (ZP) interactions. During the acrosome reaction, reversal of amyloid aggregates has been suggested to be an integral part of AM dispersion (Guyonnet et al., 2014). Active proteases are suggested to be responsible for subsequent AM disassembly (Buffone et al., 2008).

Additionally, polyphenols can also affect protein aggregation at many levels. Polyphenols in combination with β -cyclodextrin (β -CD) inhibit and also disaggregate α -synuclein aggregation (Gautam et al., 2017). The protective effect of polyphenols has also been indicated in breaking up the pathological aggregates formed by A β and tau (Velandar et al., 2017). Therefore, polyphenols provide a promising approach for targeting neurodegenerative diseases.

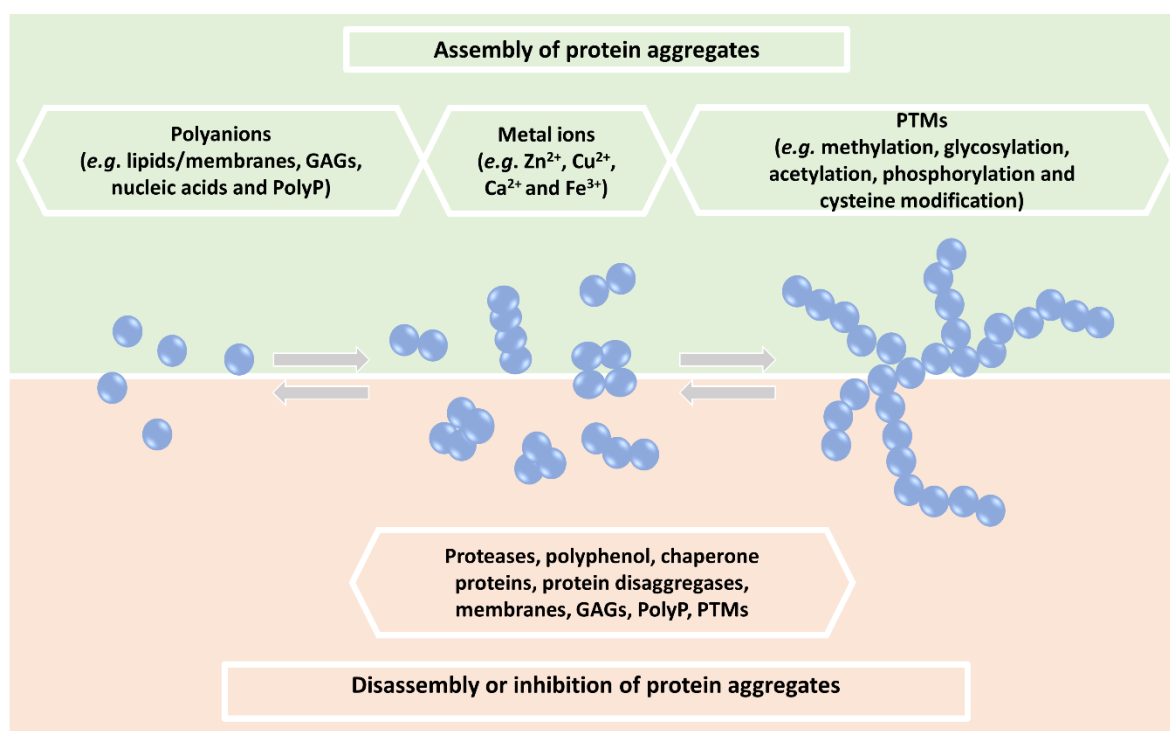


Figure 1. Factors modulating functional protein aggregation and disaggregation. Factors involved in regulating assembly of functional protein aggregates (top half) and/or disassembly to inhibit pathological aggregates (bottom half) as indicated in the figure.

4 Crosstalk between different factors affecting amyloidogenesis of GAPP-1

Protein aggregation within cells is a highly complex process that can be affected by multiple biomolecular factors, but a comprehensive view of how these factors individually and collectively contribute to this process is lacking. Difficulties to reveal clear mechanisms of the

aggregation-related diseases is one of the reasons for a lack of efficient therapeutic strategies for these devastating diseases. It has been hypothesized that functional aggregates could be a precursor of pathological events (Cereghetti et al., 2018). Therefore, understanding how functional protein oligomerization and aggregation is regulated in the cell could be vital for elucidating the molecular and cellular factors promoting pathological aggregation and for the design of new therapeutic strategies.

Our studies presented in this thesis show that amyloid-like aggregation of Golgi-associated pathogenesis-related protein 1 (GAPR-1) is mediated by a variety of biomolecular factors. The effects of zinc, copper, heparin, disulfide bond formation and membranes on the initiation of distinct aggregation pathways of GAPR-1 are summarized in Figure 2. Within each pathway, there are several characteristic elements involved in functional protein aggregation. Irrespective of the external trigger, GAPR-1 aggregation proceeds relatively fast as determined with ThT fluorescence. This indicates that upon initiation, GAPR-1 exists only for a short time in a native-like oligomeric state. In the zinc-dependent pathway, GAPR-1 aggregation can be reversed by depletion of the metal ion, whereas oxidative conditions promote fast, irreversible aggregation followed by formation of disulfide-bridged nuclei, resembling the classical nucleated growth mechanism.

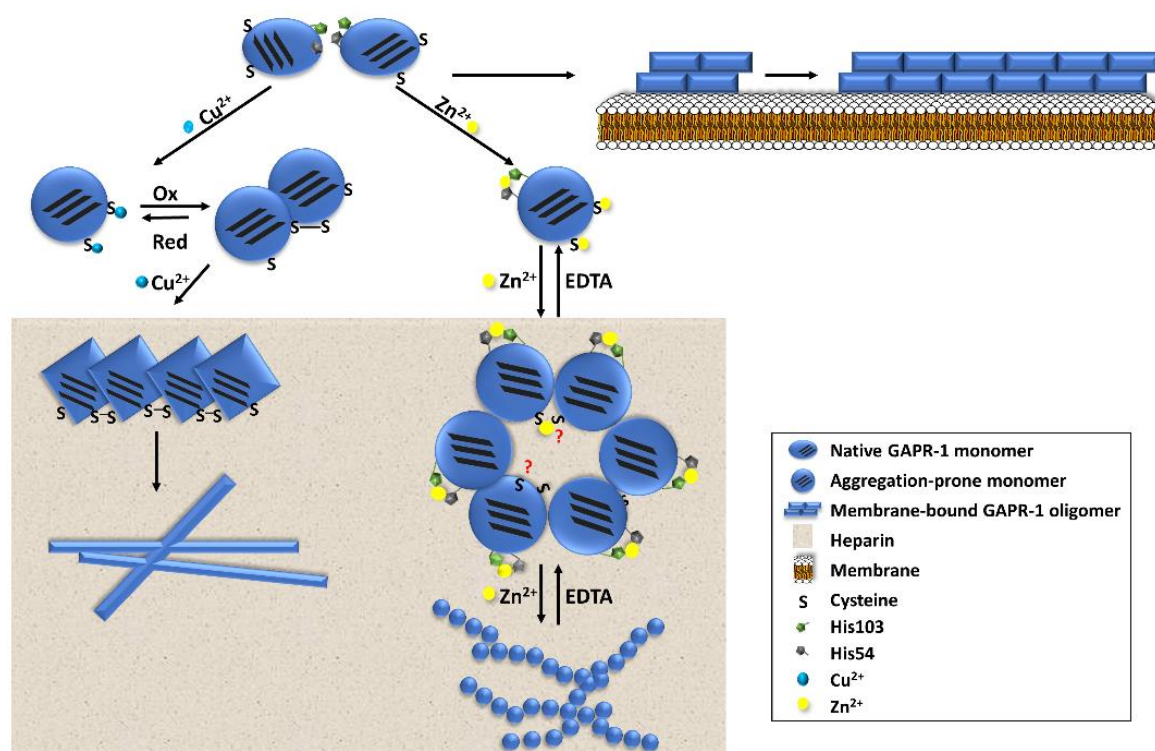


Figure 2. Hypothetical model for GAPR-1 amyloid-like aggregation. GAPR-1 binding to membranes undergoes a structural rearrangement and a concentration step, resulting in protein amyloid fibrillation (Olricks and Helms, 2016; Olricks et al., 2014). Both zinc and copper ions binding modulate

the quaternary structure of GAPR-1, shifting native multimers to monomers. Zn^{2+} induced aggregation pathway is dependent on the proposed metal binding site within GAPR-1 including His54 and His103, and independent of redox conditions. Zn^{2+} modulated GAPR-1 assembly is reversible by chelating zinc ions, which reversibly regulates the cysteine accessibility in GAPR-1. Disulfide bond formation is crucial for the initiation of Cu^{2+} induced aggregation pathway. Cu^{2+} regulated GAPR-1 self-association is irreversible and independent of the suggested metal binding site. Heparin acts as a scaffold on which GAPR-1 is concentrated and oriented to promote protein assembly.

The localization of GAPR-1 to lipid-enriched microdomains of the Golgi membrane provides beneficial conditions for the formation of oligomeric structures of GAPR-1. Additionally, GAPR-1 is able to prevent A β amyloid formation by binding to oligomeric structures (Olrachs et al., 2014). Together, these observations raise the question of how the aggregation and anti-A β aggregation properties of GAPR-1 are important in the cell. GAPR-1 acts as a negative regulator of autophagy (Shoji-Kawata et al., 2013), retaining the autophagy-inducing protein Beclin 1 in an inactive state at the Golgi apparatus (Shoji-Kawata et al., 2013). Tat-Beclin 1, a peptide derived from the evolutionary conserved domain (ECD) of Beclin 1 with high therapeutic potential, binds to GAPR-1 to release Beclin 1 and to induce autophagy (Shoji-Kawata et al., 2013). Interestingly, a similar mechanism was described in neuronal cells, where Beclin 1 was re-localized to lipid rafts of the plasma membrane by PrP to induce autophagy in response to A β (Nah et al., 2013). The interaction between GAPR-1 and Tat-Beclin 1 is proposed to be tightly associated with the quaternary structure of GAPR-1 (Li et al., 2017). Beclin 1 is known to form homo-oligomers (Adi-Harel et al., 2010) and its ECD was shown to cluster upon membrane binding, resulting in deformation of membrane surface areas (Huang et al., 2012). We hypothesize that GAPR-1 is able to interact with Beclin 1 dependent on their oligomeric/fibrillar states. In this light, the ability of GAPR-1 to interact with oligomeric A β could suggest that GAPR-1 not merely keeps Beclin 1 inactive, but is capable of interacting with multiple oligomeric structures. In this model, GAPR-1 could function as a molecular sensor for multiple amyloid oligomers in the cell, assuming this interaction is based on structural properties. Thus, potentially harmful oligomers could successfully compete with Beclin 1 for an interaction with GAPR-1, resulting in the release of Beclin 1 and subsequent activation of autophagy. We envision this mechanism of the cell to clear up potentially harmful oligomers, which could be a focus of future studies.

GAPR-1 is one of the few Cysteine-rich secretory proteins, Antigen 5 and Pathogenesis related proteins group 1 (CAP) superfamily members with an intracellular localization (Eberle et al., 2002) (Chapter 1). We have shown that cysteine oxidation of monomeric GAPR-1 enhances the exposure of C-terminal aggregation-prone regions (APRs), which in turn accelerates

GAPR-1 aggregation under oxidative conditions (Chapter 3). Whether the disulfide bond in the copper-induced aggregation pathway is formed intra- or inter-molecularly, needs to be further explored. Different from GAPR-1, the majority of CAP superfamily members are secreted and contain significantly more cysteine residues, most of which are oxidized to form disulfide bonds. These disulfide bridges are responsible for protein stability in the extracellular environment, which is highly relevant for many CAP superfamily members. Specifically, disulfide bridges contribute strongly to high thermal, pH, and proteolytic stability of PR-1-like proteins (Fernández et al., 1997). The absence of disulfide bridges in PR-1-like proteins in *Fusarium oxysporum* is proposed to render them more accessible to cleavage by host proteases, which may allow these type of fungi to evade detection by the plant immune system (Prados-Rosales et al., 2012). Moreover, *Oo*-ASP-1 from *Ostertagia ostertagi* forms inter-molecular disulfide-bond dependent dimers. The disulfide bond is important for both tertiary and quaternary structures of *Oo*-ASP-1, and is also suggested to be vital for proteolytic stability (Borloo et al., 2013). These evidences suggest that disulfide bonds and/or disulfide bridged oligomerization play crucial roles in the protein structural stability of CAP superfamily members and in the regulation of their protein function.

Our study shows that zinc (Chapter 2) and copper (Chapter 3) homeostasis can be a major factor in regulating distinct GAPR-1 aggregation pathways. Zinc and copper are the second and third most abundant transition metals in organisms, respectively (Osredkar and Sustar, 2011). The amount of zinc and copper ions in cells ($0.3\text{--}20\text{ mM Zn}^{2+}$, depending on cell type; $<10^{-18}\text{ M Cu}^{2+}$) and in blood ($12\text{--}16\text{ }\mu\text{M Zn}^{2+}$; $10\text{--}22\text{ }\mu\text{M Cu}^{2+}$) is strictly maintained at low concentrations and most of it is associated with proteins (Kaplan and Maryon, 2016; Leon-Rodriguez et al., 2012; Torkian et al., 2019). Our studies also show an altered GAPR-1 aggregation when copper ions are chelated by the addition of EDTA after a nucleation step in the presence of heparin and $20\text{--}100\text{ }\mu\text{M}$ copper. This indicates that excess copper binds to GAPR-1 non-specifically, and that specific protein structural reorientations occur at low copper concentrations.

High concentrations of zinc are present in several organs and cell types, such as in the brain (up to 150 mM) (Takeda, 2007), the mammalian testis, the epididymis and in the prostate ($1\text{--}2.5\text{ mM}$) (Kelleher et al., 2011; Larminat et al., 1981; Leon-Rodriguez et al., 2012; Mawson and Fischer, 1953; Saito et al., 1969). Zinc ions are widely associated with the reproductive process, including spermatogenesis, sperm maturation, capacitation, acrosome reaction, a response of the oocyte to the fertilization fusion (the so called Zn^{2+} spark (Que et al., 2015; Zhang et al., 2016)), conception and embryonic implantation (Fallah et al., 2018; Yamaguchi et al., 2009;

Zhang et al., 2016; Zhao et al., 2016). Cysteine-rich secretory protein 1 (CRISP1) is a member of the CAP superfamily, it is expressed in the epididymis and cumulus cells, and it plays multifunctional roles in spermatozoa maturation, capacitation, sperm-oocyte interaction and acrosome reaction (Bedford et al., 1979; Busso et al., 2007; Cohen et al., 2011; Debora J. Cohen et al., 2000; Ernesto et al., 2015; Roberts et al., 2003; Ros et al., 2015). Rat CRISP1 has been shown to oligomerize in the presence of 0.5-2 mM zinc ions *in vitro* and these oligomers play a role in rat sperm maturation (Maldera et al., 2011). Our *in vitro* study shows that human CRISP1 is able to form high molecular weight structures in the presence of physiologically relevant zinc concentrations (0.3-1 mM) and that the oligomers are dissolved upon removal of zinc ions (Chapter 4). This indicates that under physiological conditions, CRISP1 may exhibit its functions in fertilization through zinc regulated protein assembly and disassembly.

High expression levels of amyloidogenic proteins are a key factor in amyloid formation (Jackson and Hewitt, 2017). GAPR-1 is highly expressed in immune-related cells and tissues (*e.g.* monocytes, leukocytes, lung, spleen and embryonic tissue) and enriched in the lumen of the extracellular vesicles secreted from prostate cells (Aalberts et al., 2012; Eberle et al., 2002). GAPR-1 is also enriched during neonatally induced neurodegeneration in rat hippocampus (Karlsson et al., 2015). Our combined results open the possibility that GAPR-1 oligomerization and aggregation may play a functional role in immunology, fertilization and autophagy. On the other hand, the level of oligomeric precursors of functional aggregates must be tightly regulated because the presence of high concentrations of amyloidogenic precursor could result in cellular disorders (Jackson and Hewitt, 2017). The expression level of GAPR-1 is significantly enhanced in the epithelial cells of fibrotic kidney (Baxter et al., 2007). These observations indicate that changes in GAPR-1 expression level are associated with regulating its biological function, which is one of the potential mechanisms to control functional aggregation. CAP superfamily members are often found to be up-regulated under specific conditions. Many members of the PR-1 subfamily are up-regulated in the infected tissue (Breen et al., 2016, 2017). At the structural level, PR-1 proteins contain a CAP domain with only short N- and C-terminal extensions, indicating that the properties of the CAP domain (*e.g.* oligomerization) determine the function of PR-1 proteins in plants. Dimerization has been shown to enhance resistance of PR-1-5 to proteolytic attack, which may be involved in protease-mediated programmed cell death pathways in plants (Lu et al., 2013). Moreover, CRISP3 (like other CRISP family members as well as GAPR-1 belonging to the CAP superfamily) is expressed at low levels in the normal prostate and is highly up-regulated in the cancerous prostate (Ribeiro

et al., 2011). In contrast, another CRISP family member, glioma pathogenesis-related protein 1 (GLIPR1) is down-regulated in prostate cancer, while forced GLIPR1 overexpression is pro-apoptotic in prostate cancer cells and is suggested as a prostate-cancer therapy (Li et al., 2008). Altogether, these observations indicate that regulating the expression level of CAP superfamily members is a widely applied mechanism for regulating protein function. Whether these examples are related to the aggregation-related properties of CAP superfamily members remains to be investigated.

5 Summary

Functional protein aggregation is observed in several proteins, serving diverse purposes in numerous biological processes, and is regulated by complex mechanisms. To avoid potential toxicity of intermediates during protein self-association, functional protein aggregation undergoes fast growth rate to minimize the generation of detrimental oligomers. Moreover, a variety of functional protein aggregates are reversibly regulated, which indicates a highly dynamic process of efficient ways to rapidly and specifically organize protein assemblies in response to cellular changes. In this Chapter, we discussed the role of multiple biomolecular factors, such as lipids, GAGs, nuclei acids, polyP, metal ions, PTMs, HSPs, proteases and polyphenols, in regulating physiological and/or reversible protein aggregates. Diverse factors affect GAPR-1 aggregation, which is proposed to be associated with its functions in autophagy, immunology and reproduction. Moreover, by using GAPR-1 as a model protein of CAP superfamily members, we suggest that oligomerization could be a common property of the CAP superfamily. Self-association and/or disaggregation could be a general mechanism in modulating functions of CAP family members, providing new clues on a molecular understanding of these and other functional aggregates as well as potential clues for treatment and prevention of protein aggregation-related diseases.

Reference

- Aalberts, M., Dissel-Emiliani, F.M.F. van, Adrichem, N.P.H. van, Wijnen, M. van, Wauben, M.H.M., Stout, T.A.E., and Stoorvogel, W. (2012). Identification of distinct populations of prostasomes that differentially express prostate stem cell Antigen, Annexin A1, and GLIPR2 in humans. *Biol. Reprod.* 86, 82.
- Abdolvahabi, A., Shi, Y., Rhodes, N.R., Cook, N.P., Martı, A.A., and Shaw, B.F. (2015). Arresting amyloid with coulomb's Law: Acetylation of ALS-Linked SOD1 by aspirin impedes aggregation. *Biophys. J.* 108, 1199–1212.
- Adi-Harel, S., Erlich, S., Schmukler, E., Cohen-kedar, S., Segev, O., Mizrachy, L., Hirsch, J.A., and Pinkas-kramarski, R. (2010). Beclin 1 self-association is independent of autophagy induction by amino acid deprivation and rapamycin treatment. *J. Cell. Biochem.* 1271, 1262–1271.
- Aguzzi, A., and O'Conor, T. (2010). Protein aggregation diseases: pathogenicity and therapeutic perspectives. *Nat. Rev.* 9, 237–248.
- Alberti, S., and Dormann, D. (2019). Liquid–liquid phase separation in disease. *Annu. Rev. Genet.* 53.
- Alberti, S., Halfmann, R., King, O., Kapila, A., and Lindquist, S. (2009). A systematic survey identifies prions and illuminates sequence features of prionogenic proteins. *Cell.* 137, 146–158.
- Anoop, A., Ranganathan, S., Dhaked, B.D., Jha, N.N., Pratihari, S., Ghosh, S., Sahay, S., Kumar, S., Das, S., Kombrabail, M., et al. (2014). Elucidating the role of disulfide bond on amyloid formation and fibril reversibility of somatostatin-14: Relevance to its storage and secretion. *J. Biol. Chem.* 289, 16884–16903.
- Audas, T.E., Audas, D.E., Jacob, M.D., Ho, J.J.D., Khacho, M., Wang, M., Perera, J.K., Gardiner, C., Bennett, C.A., Head, T., et al. (2016). Adaptation to stressors by systemic protein amyloidogenesis. *Dev. Cell.* 39, 155–168.
- Banani, S.F., Lee, H.O., Hyman, A.A., and Rosen, M.K. (2017). Biomolecular condensates: Organizers of cellular biochemistry. *Nat. Rev. Mol. Cell Biol.* 18, 285–298.
- Banci, L., Bertini, I., Durazo, A., Girotto, S., Gralla, E.B., Martinelli, M., Valentine, J.S., Vieru, M., and Whitelegge, J.P. (2007). Metal-free superoxide dismutase forms soluble oligomers under physiological conditions: A possible general mechanism for familial ALS. *Proc Natl Acad Sci USA* 104, 11263–11267.
- Barmada, S.J., Serio, A., Arjun, A., Bilican, B., Daub, A., Ando, D.M., Tsvetkov, A., Pleiss, M., Li, X., Peisach, D., et al. (2014). Autophagy induction enhances TDP43 turnover and survival in neuronal ALS models. *Nat Chem Biol* 10, 677–685.
- Baxter, R.M., Crowell, T.P., George, J.A., Getman, M.E., and Gardner, H. (2007). The plant pathogenesis related protein GLIPR-2 is highly expressed in fibrotic kidney and promotes epithelial to mesenchymal transition in vitro. *Matrix Biol.* 26, 20–29.
- Bechtel, T.J., and Weerapana, E. (2017). From structure to redox: the diverse functional roles of disulfides and implications in disease. *Proteomics* 17, 1–34.
- Bedford, J.M., Moore, H.D.M., and Franklin, L.E. (1979). Significance of the equatorial segment of the acrosome of the spermatozoon in eutherian mammals. *Exp. Cell Res.* 119, 119–126.
- Bissig, C., Rochin, L., and Niel, G. van (2016). PMEL amyloid fibril formation: The bright steps of pigmentation. *Int. J. Mol. Sci.* 17, 1438.
- Boke, E., Ruer, M., Wühr, M., Coughlin, M., Lemaitre, R., Gygi, S.P., Alberti, S., Drechsel, D., Hyman, A.A., and Mitchison, T.J. (2016). Amyloid-like self-assembly of a cellular compartment. *Cell.* 166, 637–650.
- Borloo, J., Geldhof, P., Peelaers, I., Van Meulder, F., Ameloot, P., Callewaert, N., Vercruysse, J., Claerebout, E., Strelkov, S. V., Weeks, S.D., et al. (2013). Structure of Ostertagia ostertagi ASP-1: Insights into disulfide-mediated cyclization and dimerization. *Acta Crystallogr. Sect. D Biol. Crystallogr.* 69, 493–503.
- Bourgault, S., Solomon, J.P., Reixach, N., and Kelly, J.W. (2011). Sulfated glycosaminoglycans accelerate transthyretin amyloidogenesis by quaternary structural conversion. *Biochemistry* 50, 1001–1015.
- Brangwynne, C.P., Mitchison, T.J., and Hyman, A.A. (2011). Active liquid-like behavior of nucleoli determines their size and shape in *Xenopus laevis* oocytes. *Proc Natl Acad Sci USA* 108, 4334–4339.

- Breen, S., Williams, S.J., Winterberg, B., Kobe, B., and Solomon, P.S. (2016). Wheat PR-1 proteins are targeted by necrotrophic pathogen effector proteins. *Plant J.* *1*, 13–25.
- Breen, S., Williams, S.J., Outram, M., Kobe, B., and Solomon, P.S. (2017). Emerging insights into the functions of pathogenesis-related protein 1. *Trends Plant Sci.* *22*, 871–879.
- Brown, M.R.W., and Kornberg, A. (2004). Inorganic polyphosphate in the origin and survival of species. *Proc Natl Acad Sci USA* *101*, 16085–16087.
- Buffone, M.G., Foster, J.A., and Gerton, G.L. (2008). The role of the acrosomal matrix in fertilization. *Int. J. Dev. Biol.* *52*, 511–522.
- Busso, D., Cohen, D.J., Maldera, J.A., Dematteis, A., and Cuasnicu, P.S. (2007). A novel function for CRISP1 in rodent fertilization: Involvement in sperm-zona pellucida interaction. *Biol. Reprod.* *77*, 848–854.
- Cai, Z., and Yan, L.-J. (2013). Protein oxidative modifications: Beneficial roles in disease and health. *J. Biochem. Pharmacol. Res.* *1*, 15–26.
- Carlomagno, Y., Chung, D.C., Yue, M., Castanedes-casey, M., Madden, B.J., Dunmore, J., Tong, J., DeTure, M., Dickson, D.W., Petrucelli, L., et al. (2017). An acetylation–phosphorylation switch that regulates tau aggregation propensity and function. *J. Biol. Chem.* *292*, 15277–15286.
- Carufel, C.A. De, Nguyen, P.T., Sahnouni, S., and Bourgault, S. (2013). New insights into the roles of sulfated glycosaminoglycans in islet amyloid polypeptide amyloidogenesis and cytotoxicity. *Biopolymers* *100*, 645–655.
- Cereghetti, G., Saad, S., Dechant, R., and Peter, M. (2018). Reversible, functional amyloids: Towards an understanding of their regulation in yeast and humans. *Cell Cycle.* *17*, 1545–1558.
- Chattopadhyay, M., Nwadiibia, E., Strong, C.D., Gralla, E.B., Valentine, J.S., and Whitelegge, J.P. (2015). The disulfide bond, but not zinc or dimerization, controls initiation and seeded growth in amyotrophic lateral sclerosis-linked Cu, Zn superoxide dismutase (SOD1) fibrillation. *J. Biol. Chem.* *290*, 30624–30636.
- Chen, Z., and Cheng, W. (2017). Reversible aggregation of HIV-1 Gag proteins mediated by nucleic acids. *Biochem. Biophys. Res. Commun.* *482*, 1437–1442.
- Chiki, A., Deguire, S.M., Ruggeri, F.S., Sanfelice, D., Ansaloni, A., Wang, Z., Cendrowska, U., Burai, R., Vieweg, S., Pastore, A., et al. (2017). Mutant exon1 huntingtin aggregation is regulated by T3 phosphorylation-induced structural changes and crosstalk between T3 phosphorylation and acetylation at K6. *Angew Chem Int Ed Engl.* *56*, 5202–5207.
- Chiti, F., and Dobson, C.M. (2017). Protein misfolding, amyloid formation, and human disease: A summary of progress over the last decade. *Annu. Rev. Biochem.* *86*, 27–68.
- Chiu, J., and Hogg, P.J. (2019). Allosteric disulfides: Sophisticated molecular structures enabling flexible protein regulation. *J. Biol. Chem.* *294*, 2949–2960.
- Cho, M.-H., Cho, K., Kang, H.-J., Jeon, E.-Y., Kim, H.-S., Kwon, H.-J., Kim, H.-M., Kim, D.-H., and Yoon, S.-Y. (2014). Autophagy in microglia degrades extracellular β -amyloid fibrils and regulates the NLRP3 inflammasome. *Autophagy* *10*, 1761–1775.
- Chuang, E., Hori, A.M., Hesketh, C.D., and Shorter, J. (2018). Amyloid assembly and disassembly. *J. Cell Sci.* *131*, 1–18.
- Cicero, C.E., Mostile, G., Vasta, R., Rapisarda, V., Signorelli, S.S., Ferrante, M., Zappia, M., and Nicoletti, A. (2017). Metals and neurodegenerative diseases. A systematic review. *Environ. Res.* *159*, 82–94.
- Cohen, D.J., Maldera, J.A., Vasen, G., Ernesto, J.I., Munoz, M.W., Battistone, M.A., and Cuasnicu, P.S. (2011). Epididymal protein CRISP1 plays different roles during the fertilization process. *J. Androl.* *32*, 672–678.
- Cohen, T.J., Hwang, A.W., Restrepo, C.R., Yuan, C., John, Q., and Lee, V.M.Y. (2015). An acetylation switch controls TDP-43 function and aggregation propensity. *Nat. Commun.* *6*, 5845.
- Cremers, C.M., Knoefler, D., Gates, S., Martin, N., Dahl, J., Lempart, J., Xie, L., Chapman, M.R., Galvan, V., Southworth, D.R., et al. (2016). Polyphosphate: A conserved modifier of amyloidogenic processes. *Mol. Cell* *63*, 768–780.
- Dannies, P.S. (2012). Prolactin and growth hormone aggregates in secretory granules: The need to understand the structure of the aggregate. *Endocr. Rev.* *33*, 254–270.
- Debora J. Cohen, Rochwerger, L., Ellerman, D.A., Morgenfe, M.M., Busso, D., and Cuasnicú, P.S.

- (2000). Relationship between the association of rat epididymal protein “DE” with spermatozoa and the behavior and function of the protein. *Mol. Reprod. Dev.* 56, 180–188.
- Decker, C.J., and Parker, R. (2012). P-bodies and stress granules: possible roles in the control of translation and mRNA degradation. *Cold Spring Harb. Perspect. Biol.* 4, a012286.
- Demuro, A., Mina, E., Kayed, R., Milton, S.C., Parker, I., and Glabe, C.G. (2005). Calcium dysregulation and membrane disruption as a ubiquitous neurotoxic mechanism of soluble amyloid oligomers. *J. Biol. Chem.* 280, 17294–17300.
- Desantis, M.E., and Shorter, J. (2012). Hsp104 drives “Protein-Only” positive selection of Sup35 prion strains encoding strong [PSI⁺]. *Chem. Biol.* 19, 1400–1410.
- Desantis, M.E., Leung, E.H., Sweeny, E.A., Jackrel, M.E., Cushman-nick, M., Neuhaus-follini, A., Vashist, S., Sochor, M.A., Knight, M.N., and Shorter, J. (2012). Operational plasticity enables Hsp104 to disaggregate diverse amyloid and nonamyloid clients. *Cell* 151, 778–793.
- Dharmadana, D., Reynolds, N.P., Conn, C.E., and Valéry, C. (2017). Molecular interactions of amyloid nanofibrils with biological aggregation modifiers: Implications for cytotoxicity mechanisms and biomaterial design. *Interface Focus* 7, 20160160.
- DiMauro, M.A., Nandi, S.K., Raghavan, C.T., Kar, R.K., Wang, B., Bhunia, A., Nagaraj, R.H., and Biswas, A. (2014). Acetylation of Gly1 and Lys2 Promotes Aggregation of Human γ D-Crystallin. *Biochemistry* 53, 7269–7282.
- Dulce, P.-G., Christophe, M., Minh Bao, H., Fernando, S., Ludmilla, S., Diaz Julia Elisa, S., and Rita, R.-V. (2011). Glycosaminoglycans, protein aggregation and neurodegeneration. *Curr. Protein Pept. Sci.* 999, 1–11.
- Dundr, M., Hebert, M.D., Karpova, T.S., Stanek, D., Xu, H., Shpargel, K.B., Meier, U.T., Neugebauer, K.M., Matera, A.G., and Misteli, T. (2004). In vivo kinetics of Cajal body components. *J. Cell Biol.* 164, 831–842.
- Eberle, H.B., Serrano, R.L., Füllekrug, J., Schlosser, A., Lehmann, W.D., Lottspeich, F., Kaloyanova, D., Wieland, F.T., and Helms, J.B. (2002). Identification and characterization of a novel human plant pathogenesis-related protein that localizes to lipid-enriched microdomains in the Golgi complex. *J. Cell Sci.* 115, 827–838.
- Egge, N., Muthusubramanian, A., and Cornwall, G.A. (2015). Amyloid properties of the mouse egg zona pellucida. *PLoS ONE.* 10, e0129907.
- Ernesto, J.I., Muñoz, M.W., Battistone, M.A., Vasen, G., Martínez-López, P., Orta, G., Figueiras-Fierro, D., De la Vega-Beltran, J.L., Moreno, I.A., Guidobaldi, H.A., et al. (2015). CRISP1 as a novel CatSper regulator that modulates sperm motility and orientation during fertilization. *J. Cell Biol.* 210, 1213–1224.
- Falcon, B., Noad, J., McMahon, H., Randow, F., and Goedert, M. (2018). Galectin-8-mediated autophagy and seeded tau aggregation protects against seeded tau aggregation. *J. Biol. Chem.* 293, 2438–2451.
- Fallah, A., Mohammad-Hasani, A., and Colagar, A.H. (2018). Zinc is an essential element for male fertility: A review of Zn roles in men’s health, germination, sperm quality, and fertilization. *19*, 69–81.
- Fantini, J., and Yahi, N. (2019). Molecular insights into amyloid regulation by membrane cholesterol and sphingolipids: common mechanisms in neurodegenerative diseases. *Expert Rev. Mol. Med.* 12, 1–22.
- Fernández, C., Szyperski, T., Bruyère, T., Ramage, P., Möisinger, E., and Wüthrich, K. (1997). NMR solution structure of the pathogenesis-related protein P14a. *J. Mol. Biol.* 266, 576–593.
- Fowler, D.M., Koulov, A. V, Alory-jost, C., Marks, M.S., Balch, W.E., and Kelly, J.W. (2006). Functional amyloid formation within mammalian tissue. *Plos Biol.* 4, 0100–0107.
- Funk, K.E., Thomas, S.N., Schafer, K.N., Cooper, G.L., Clark, D.J., Yang, A.J., and Kuret, J. (2015). Lysine methylation is an endogenous post-translational modification of tau protein in human brain and a modulator of aggregation propensity. *Biochem. J.* 462, 77–88.
- Gal, J., Chen, J., Barnett, K.R., Yang, L., Brumley, E., and Zhu, H. (2013). HDAC6 regulates mutant SOD1 aggregation through two SMIR motifs and tubulin acetylation. *J. Biol. Chem.* 288, 15035–15045.
- Gautam, S., Karmakar, S., Batra, R., Sharma, P., Pradhan, P., Singh, J., Kundu, B., and Chowhury, P.K. (2017). Polyphenols in combination with β -cyclodextrin can inhibit and disaggregate α -

- synuclein amyloids under cell mimicking conditions: A promising therapeutic alternative. *Biochim. Biophys. Acta* 1865, 589–603.
- Göbl, C., Morris, V.K., Dam, L. van, Visscher, M., Polderman, P.E., Hartlmüller, C., Ruiter, H. de, Hora, M., Liesinger, L., Birner-Gruenberger, R., et al. (2020). Cysteine oxidation triggers amyloid fibril formation of the tumor suppressor p16INK4A. *BioRxiv* 28, 101316.
- Goldberg, A.L. (2003). Protein degradation and protection against misfolded or damaged proteins. *Nature* 426, 895–899.
- Gould, N., Doulias, P.T., Tenopoulou, M., Raju, K., and Ischiropoulos, H. (2013). Regulation of protein function and signaling by reversible cysteine s-nitrosylation. *J. Biol. Chem.* 288, 26473–26479.
- Grignaschi, E., Cereghetti, G., Grigolato, F., Kopp, M.R.G., Caimi, S., Faltova, L., Saad, S., Peter, M., and Arosio, P. (2018). A hydrophobic low-complexity region regulates aggregation of the yeast pyruvate kinase Cdc19 into amyloid-like aggregates in vitro. *J. Biol. Chem.* 293, 11424–11432.
- Guo, J., Yu, L., Sun, Y., and Dong, X. (2017). Kinetic insights into Zn²⁺-induced amyloid β -protein aggregation revealed by stopped-flow fluorescence spectroscopy. *J. Phys. Chem.* 121, 3909–3917.
- Guyonnet, B., Egge, N., and Cornwall, G.A. (2014). Functional amyloids in the mouse sperm acrosome. *Mol. Cell. Biol.* 34, 2624–2634.
- Hewetson, A., Do, H.Q., Myers, C., Muthusubramanian, A., Sutton, R.B., Wylie, B.J., and Cornwall, G.A. (2017). Functional amyloids in reproduction. *Biomolecules*. 7, 46.
- Hipp, M.S., Park, S., and Hartl, F.U. (2014). Proteostasis impairment in protein misfolding and aggregation diseases. *Trends Cell Biol.* 24, 506–514.
- Ho, T., Watt, B., Spruce, L.A., Seeholzer, S.H., and Marks, M.S. (2016). The Kringle-like domain facilitates post-endoplasmic reticulum changes to premelanosome protein (PMEL) oligomerization and disulfide bond configuration and promotes amyloid formation. *J. Biol. Chem.* 291, 3595–3612.
- Honda, R. (2017). Role of the disulfide bond in prion protein amyloid formation: A thermodynamic and kinetic analysis. *Biophys. J.* 114, 885–892.
- Hu, J., Zhang, D., Liu, X., Li, X., Cheng, X., Chen, J., Du, H., and Liang, Y. (2017). Pathological concentration of zinc dramatically accelerates abnormal aggregation of full-length human Tau and thereby significantly increases Tau toxicity in neuronal cells. *Biochim. Biophys. Acta* 1863, 414–427.
- Huang, W., Choi, W., Hu, W., Mi, N., Guo, Q., Ma, M., and Liu, M. (2012). Crystal structure and biochemical analyses reveal Beclin 1 as a novel membrane binding protein. *Cell Res.* 22, 473–489.
- Iadanza, M.G., Jackson, M.P., Hewitt, E.W., Ranson, N.A., and Radford, S.E. (2018). A new era for understanding amyloid structures and disease. *Nat. Rev. Mol. Cell Biol.* 19, 755–773.
- Iannuzzi, C., Irace, G., and Sirangelo, I. (2015). The effect of glycosaminoglycans (GAGs) on amyloid aggregation and toxicity. *Molecules* 20, 2510–2528.
- Jackrel, M.E., Desantis, M.E., Martinez, B.A., Castellano, L.M., Stewart, R.M., Caldwell, K.A., Caldwell, G.A., and Shorter, J. (2015). Potentiated Hsp104 variants antagonize diverse proteotoxic misfolding events. *Cell* 156, 170–182.
- Jackson, M.P., and Hewitt, E.W. (2016). Cellular proteostasis: Degradation of misfolded proteins by lysosomes. *Essays Biochem.* 60, 173–180.
- Jackson, M.P., and Hewitt, E.W. (2017). Why are functional amyloids non-toxic in humans? *Biomolecules* 7, 1–13.
- Jacob, R.S., Das, S., Ghosh, S., Anoop, A., Jha, N.N., Khan, T., Singru, P., Kumar, A., and Maji, S.K. (2016). Amyloid formation of growth hormone in presence of zinc: Relevance to its storage in secretory granules. *Sci. Rep.* 6, 23370.
- Jang, H., Arce, F.T., Mustata, M., Ramachandran, S., Capone, R., Nussinov, R., and Lal, R. (2011). Antimicrobial protegrin-1 forms amyloid-like fibrils with rapid kinetics suggesting a functional link. *Biophys. J.* 100, 1775–1783.
- Jiang, Z., and Lee, J.C. (2014). Lysophospholipid-containing membranes modulate the fibril formation of the repeat domain of a human functional amyloid, Pmel17. *J. Mol. Biol.* 426, 4074–4086.
- Jiang, W., Sordella, R., Chen, G., Hakre, S., Roy, A.L., and Settleman, J. (2005). An FF domain-

- dependent protein interaction mediates a signaling pathway for growth factor-induced gene expression. *Mol. Cell* 17, 23–35.
- Johnson, G.V.W., and Stoothoff, W.H. (2004). Tau phosphorylation in neuronal cell function and dysfunction. *J. Cell Sci.* 117, 5721–5729.
- Kaplan, J.H., and Maryon, E.B. (2016). How mammalian cells acquire copper: An essential but potentially toxic metal. *Biophys. J.* 110, 7–13.
- Karlsson, O., Berg, A.L., Hanrieder, J., Arnerup, G., Lindström, A.-K., and Brittebo, E.B. (2015). Intracellular fibril formation, calcification, and enrichment of chaperones, cytoskeletal, and intermediate filament proteins in the adult hippocampus CA1 following neonatal exposure to the nonprotein amino acid BMAA. *Arch. Toxicol.* 89, 423–436.
- Kayed, R., Sokolov, Y., Edmonds, B., McIntire, T.M., Milton, S.C., Hall, J.E., and Glabe, C.G. (2004). Permeabilization of lipid bilayers is a common conformation-dependent activity of soluble amyloid oligomers in protein misfolding diseases. *J. Biol. Chem.* 279, 46363–46366.
- Kelleher, S.L., McCormick, N.H., Velasquez, V., and Lopez, V. (2011). Zinc in specialized secretory tissues: Roles in the pancreas, prostate, and mammary gland. *Adv. Nutr.* 2, 101–111.
- Kinnunen, P.K.J. (2009). Amyloid formation on lipid membrane surfaces. *Open Biol. J.* 2, 163–175.
- Krishnan, R., Goodman, J.L., Mukhopadhyay, S., Pacheco, C.D., Lemke, E.A., Deniz, A.A., and Lindquist, S. (2012). Conserved features of intermediates in amyloid assembly determine their benign or toxic states. *Proc Natl Acad Sci USA* 109, 11172–11177.
- Kroschwald, S., Munder, M.C., Maharana, S., Franzmann, T.M., Richter, D., Ruer, M., Hyman, A.A., and Alberti, S. (2018). Different material states of Pub1 condensates define distinct modes of stress adaptation and recovery. *Cell Rep.* 23, 3327–3339.
- Laghaei, R., and Mousseau, N. (2010). Effect of the disulfide bond on the monomeric structure of human amylin studied by simulations. *J. Phys. Chem. B* 114, 7071–7077.
- Langner, M., and Kubica, K. (1999). The electrostatics of lipid surfaces. *Chem. Phys. Lipids* 101, 3–35.
- Larminat, M.A. de, Cuasnicú, P.S., and Blaquier, J.A. (1981). Changes in trophic and functional parameters of the rat epididymis during sexual maturation. *Biol Reprod* 25, 813–819.
- Leal, S.S., Botelho, H.M., and Gomes, C.M. (2012). Metal ions as modulators of protein conformation and misfolding in neurodegeneration. *Coord. Chem. Rev.* 256, 2253–2270.
- Leon-Rodriguez, L. De, Lubag, A.J.M.J., and Sherry, A.D. (2012). Imaging free zinc levels in vivo—what can be learned? *Inorganica Chim. Acta* 393, 12–23.
- Li, H., Yeh, P., Chiu, H., Tang, C., and Tu, B.P. (2011). Hyperphosphorylation as a defense mechanism to reduce TDP-43 aggregation. *PLoS One* 6, e23075.
- Li, L., Fattah, E.A., Cao, G., Ren, C., Yang, G., Goltsov, A.A., Chinault, A.C., Cai, W.-W., Timme, T.L., and Thompson, T.C. (2008). Glioma pathogenesis-related protein 1 exerts tumor suppressor activities through proapoptotic reactive oxygen species-c-Jun-NH2 kinase signaling. *Cancer Res* 68, 434–443.
- Li, Y., Yan, J., Zhang, X., and Huang, K. (2013). Disulfide bonds in amyloidogenesis diseases related proteins. *Proteins* 81, 1862–1873.
- Li, Y., Zhao, Y., Su, M., Glover, K., Chakravarthy, S., Colbert, C.L., Levine, B., and Sinha, S.C. (2017). Structural insights into the interaction of the conserved mammalian proteins GAPR-1 and Beclin 1, a key autophagy protein. *Acta Crystallogr D Struct Biol.* 73, 775–792.
- Lindberg, I., Shorter, J., Wiseman, R.L., Chiti, F., Dickey, C.A., and Mclean, X.J. (2015). Chaperones in neurodegeneration. *J. Neurosci.* 35, 13853–13859.
- Lipke, P.N., Garcia, M.C., Alsteens, D., Ramscook, C.B., Klotz, S.A., and Dufrêne, Y.F. (2012). Strengthening relationships: amyloids create adhesion nanodomains in yeasts. *Trends Microbiol.* 20, 59–65.
- Liu, C., and Zhang, Y. (2011). Nucleic acid-mediated protein aggregation and assembly. *Adv. Protein Chem. Struct. Biol.* 84, 1–40.
- Liu, S., Liu, H., Johnston, A., Hanna-Addams, S., Reynoso, E., Xiang, Y., and Wang, Z. (2017). MLKL forms disulfide bond-dependent amyloid-like polymers to induce necroptosis. *Proc Natl Acad Sci USA* 114, E7450–E7459.
- Liu, Z., Song, F., Ma, Z.L., Xiong, Q., Wang, J., Guo, D., and Sun, G. (2016). Bivalent copper ions promote fibrillar aggregation of KCTD1 and induce cytotoxicity. *Sci. Rep.* 6, 32658.
- Lu, S., Faris, J.D., Sherwood, R., and Edwards, M.C. (2013). Dimerization and protease resistance: New

- insight into the function of PR-1. *J. Plant Physiol.* **170**, 105–110.
- Mack, K.L., and Shorter, J. (2016). Engineering and evolution of molecular chaperones and protein disaggregases with enhanced activity. *Front. Mol. Biosci.* **3**, 8.
- Maji, S.K., Perrin, M.H., Sawaya, M.R., Jessberger, S., Vadodaria, K., Rissman, R.A., Singru, P.S., Nilsson, K.P.R., Simon, R., Schubert, D., et al. (2009). Functional amyloids as natural storage of peptide hormones in pituitary secretory granules. *Science*. **325**, 328–332.
- Majumdar, A., Cesario, W.C., White-Grindley, E., Jiang, H., Ren, F., Khan, M.R., Li, L., Choi, E.M.-L., Kannan, K., Guo, F., et al. (2012). Critical role of amyloid-like oligomers of *Drosophila* Orb2 in the persistence of memory. *Cell* **148**, 515–529.
- Maldera, J.A., Vasen, G., Ernesto, J.I., Weigel-Muñoz, M., Cohen, D.J., and Cuasnicu, P.S. (2011). Evidence for the involvement of zinc in the association of CRISP1 with rat sperm during epididymal maturation. *Biol. Reprod.* **85**, 503–510.
- Malishev, R., Abbasi, R., Jelinek, R., and Chai, L. (2018). Bacterial model membranes reshape fibrillation of a functional amyloid protein. *Biochemistry* **57**, 5230–5238.
- Mao, Y.S., Zhang, B., and Spector, D.L. (2011). Biogenesis and function of nuclear bodies. *Trends Genet.* **27**, 295–306.
- Marinelli, P., Navarro, S., Graña-Montes, R., Bañó-Polo, M., Fernández, M.R., Papaleo, E., and Ventura, S. (2018). A single cysteine post-translational oxidation suffices to compromise globular proteins kinetic stability and promote amyloid formation. *Redox Biol.* **14**, 566–575.
- Mawson, C.A., and Fischer, M.I. (1953). Zinc and carbonic anhydrase in human semen. *Biochem. J.* **55**, 696–700.
- Mcglinchey, R.P., and Lee, J.C. (2018). Why study functional amyloids? Lessons from the repeat domain of Pmel17. *J. Mol. Biol.* **430**, 3696–3706.
- Mehra, S., Ghosh, D., Kumar, R., Mondal, M., Gadhe, L.G., Das, S., Anoop, A., Jha, N.N., Jacob, R.S., Chatterjee, D., et al. (2018). Glycosaminoglycans have variable effects on α -synuclein aggregation and differentially affect the activities of the resulting amyloid fibrils. *J. Biol. Chem.* **293**, RA118.004267.
- Moroz, O. V., Burkitt, W., Wittkowski, H., He, W., Ianoul, A., Novitskaya, V., Xie, J., Polyakova, O., Lednev, I.K., Shekhtman, A., et al. (2009). Both Ca^{2+} and Zn^{2+} are essential for S100A12 protein oligomerization and function. *BMC Biochem.* **10**, 11.
- Munder, M.C., Midtvedt, D., Franzmann, T., Nüske, E., Otto, O., Herbig, M., Ulbricht, E., Müller, P., Taubenberger, A., Maharana, S., et al. (2016). A pH-driven transition of the cytoplasm from a fluid- to a solid-like state promotes entry into dormancy. *Elife* **5**, e09347.
- Murphy, R.M. (2007). Kinetics of amyloid formation and membrane interaction with amyloidogenic proteins. *Biochim. Biophys. Acta* **1768**, 1923–1934.
- Myeku, N., Clelland, C.L., Emrani, S., Kukushkin, N. V., Yu, W.H., Goldberg, A.L., and Duff, K.E. (2016). Tau-driven 26S proteasome impairment and cognitive dysfunction can be prevented early by activating cAMP-PKA signaling. *Nat. Med.* **22**, 46–53.
- Nah, J., Pyo, J.-O., Jung, S., Yoo, S.-M., Kam, T.-I., Chang, J., Han, J., A.An, S.S., Onodera, T., and Jung, Y.-K. (2013). BECN1/Beclin 1 is recruited into lipid rafts by prion to activate autophagy in response to amyloid β 42. *Autophagy* **9**, 2009–2021.
- Nakajima, H., Amano, W., Fujita, A., Fukuhara, A., Azuma, Y.-T., Hata, F., Inui, T., and Takeuchi, T. (2007). The active site cysteine of the proapoptotic protein glyceraldehyde-3-phosphate dehydrogenase is essential in oxidative stress-induced aggregation and cell death. *J. Biol. Chem.* **282**, 26562–26574.
- Narayanaswamy, R., Levy, M., Tsechansky, M., Stovall, G.M., O'Connell, J.D., Mirrieles, J., Ellington, A.D., and Marcotte, E.M. (2009). Widespread reorganization of metabolic enzymes into reversible assemblies upon nutrient starvation. *Proc Natl Acad Sci USA* **106**, 10147–10152.
- Nonaka, T., Suzuki, G., Tanaka, Y., Kametani, F., Hirai, S., Okado, H., Miyashita, T., Saitoe, M., Akiyama, H., Masai, H., et al. (2016). Phosphorylation of TAR DNA-binding protein of 43 kDa (TDP-43) by truncated casein kinase 1 δ triggers mislocalization and accumulation of TDP-43. *J. Biol. Chem.* **291**, 5473–5483.
- Olrichs, N.K., and Helms, J.B. (2016). Novel insights into the function of the conserved domain of the CAP superfamily of proteins. *AIMS Biophys.* **3**, 232–246.

- Olrichs, N.K., Mahalka, A.K., Kaloyanova, D., Kinnunen, P.K., and Helms, B.J. (2014). Golgi-Associated plant Pathogenesis Related protein 1 (GAPR-1) forms amyloid-like fibrils by interaction with acidic phospholipids and inhibits A β aggregation. *Amyloid* 21, 88–96.
- Osredkar, J., and Sustar, N. (2011). Copper and zinc, biological role and significance of copper/zinc imbalance. *J. Clin. Toxicol.* 3, 3.
- Patel, A., Lee, H.O., Jawerth, L., Maharana, S., Jahnel, M., Hein, M.Y., Stoyanov, S., Mahamid, J., Saha, S., Franzmann, T.M., et al. (2015). A liquid-to-solid phase transition of the ALS protein FUS accelerated by disease mutation. *Cell* 162, 1066–1077.
- Pepling, M.E., Wilhelm, J.E., Hara, A.L.O., Gephardt, G.W., and Spradling, A.C. (2007). Mouse oocytes within germ cell cysts and primordial follicles contain a Balbiani body. *Proc Natl Acad Sci USA* 104, 187–192.
- Poole, L.B. (2015). The basics of thiols and cysteines in redox biology and chemistry. *Free Radic. Biol. Med.* 80, 148–157.
- Prados-Rosales, R.C., Roldán-Rodríguez, R., Serena, C., López-Berges, M.S., Guarro, J., Martínez-del-Pozo, Á., and Di Pietro, A. (2012). A PR-1-like protein of *Fusarium oxysporum* functions in virulence on mammalian hosts. *J. Biol. Chem.* 287, 21970–21979.
- Que, E.L., Bleher, R., Duncan, F.E., Kong, B.Y., Gleber, S.C., Vogt, S., Chen, S., Garwin, S.A., Bayer, A.R., Dravid, V., et al. (2015). Quantitative mapping of zinc fluxes in the mammalian egg reveals the origin of fertilization-induced zinc sparks. *Nat Chem* 7, 130–139.
- Rahman, M.A., and Rhim, H. (2017). Therapeutic implication of autophagy in neurodegenerative diseases. *BMB Rep.* 50, 345–354.
- Relini, A., Marano, N., and Gliozzi, A. (2014). Probing the interplay between amyloidogenic proteins and membranes using lipid monolayers and bilayers. *Adv. Colloid Interface Sci.* 207, 81–92.
- Rhoads, S.N., Monahan, Z.T., Yee, D.S., and Shewmaker, F.P. (2018). The role of post-translational modifications on prion-like aggregation and liquid-phase separation of FUS. *Int. J. Mol. Sci.* 19, 886.
- Ribeiro, F.R., Paulo, P., Costa, V.L., Barros-Silva, J.D., Ramalho-Carvalho, J., Jerónimo, C., Henrique, R., Lind, G.E., Skotheim, R.I., Lothe, R.A., et al. (2011). Cysteine-Rich Secretory Protein-3 (CRISP3) is strongly up-regulated in prostate carcinomas with the TMPRSS2-ERG fusion gene. *PLoS One* 6, e22317.
- Ridgway, Z., Zhang, X., Wong, A.G., Abedini, A., Schmidt, A.M., and Raleigh, D.P. (2018). Analysis of the role of the conserved disulfide in amyloid formation by human islet amyloid polypeptide in homogeneous and heterogeneous environments. *Biochemistry* 57, 3065–3074.
- Roan, N.R., Sandi-Monroy, N., Kohgadai, N., Usmani, S.M., Hamil, K.G., Neidلمان, J., Montano, M., Ständker, L., Röcker, A., Cavois, M., et al. (2017). Semen amyloids participate in spermatozoa selection and clearance. *ELife.* 6, e24888.
- Roberts, R.G. (2016). Good amyloids, bad amyloids-what’s the difference? *Plos Biol.* 14, e1002362.
- Roberts, K.P., Wamstad, J.A., Ensrud, K.M., and Hamilton, D.W. (2003). Inhibition of capacitation-associated tyrosine phosphorylation signaling in rat sperm by epididymal protein Crisp-1. *Biol. Reprod.* 69, 572–581.
- Rodriguez-Martin, T., Cuchillo-ibáñez, I., Noble, W., Nyenya, F., Anderton, B.H., and Hanger, D.P. (2013). Tau phosphorylation affects its axonal transport and degradation. *Neurobiol. Aging.* 34, 2146–2157.
- Ros, V.G. Da, Muñoz, M.W., Battistone, M.A., Brukman, N., Carvajal, G., Curci, L., Gomez-Elias, M.D., Cohen, D.J., and Cuasnicú, P.S. (2015). From the epididymis to the egg: Participation of CRISP proteins in mammalian fertilization. *Asian J. Androl.* 17, 711–715.
- Rubén Hervás, Li, L., Majumdar, A., Fernández-Ramírez, M.D.C., Unruh, J.R., Slaughter, B.D., Galera-Prat, A., Santana, E., Suzuki, M., Nagai, Y., et al. (2016). Molecular basis of Orb2 amyloidogenesis and blockade of memory consolidation. *Plos Biol.* 14, e1002361.
- Saad, S., Cereghetti, G., Feng, Y., Picotti, P., Peter, M., and Dechant, R. (2017). Reversible protein aggregation is a protective mechanism to ensure cell cycle restart after stress. *Nat. Cell Biol.* 19, 1202–1213.
- Saha, S., Weber, C.A., Nusch, M., Adame-Arana, O., Hoege, C., Hein, M.Y., Osborne-Nishimura, E., Mahamid, J., Jahnel, M., Jawerth, L., et al. (2016). Polar positioning of phase-separated liquid compartments in cells regulated by an mRNA competition mechanism. *Cell* 166, 1572–1584.

- Saito, S., Zeitz, L., Bush, I.M., Lee, R., and Jr, W.F.W. (1969). Zinc uptake in canine or rat spermatozoa. *Am. J. Physiol.* *217*, 1039–1043.
- Saridaki, T., Zampagni, M., Mannini, B., Evangelisti, E., Taddei, N., Cecchi, C., and Chiti, F. (2012). Glycosaminoglycans (GAGs) suppress the toxicity of HypF-N prefibrillar aggregates. *J. Mol. Biol.* *421*, 616–630.
- Sawaya, M.R., Sambashivan, S., Nelson, R., Ivanova, M.I., Sievers, S.A., Apostol, M.I., Thompson, M.J., Balbirnie, M., Wiltzius, J.J.W., McFarlane, H.T., et al. (2007). Atomic structures of amyloid cross-beta spines reveal varied steric zippers. *Nature*. *447*, 453–457.
- Schedin-weiss, S., Winblad, B., and Tjernberg, L.O. (2014). The role of protein glycosylation in Alzheimer disease. *FEBS J.* *281*, 46–62.
- Sengupta, U., Nilson, A.N., and Kaye, R. (2016). The role of amyloid- β oligomers in toxicity, propagation, and immunotherapy. *EBioMedicine* *6*, 42–49.
- Shoji-Kawata, S., Sumpter, R., Leveno, M., Campbell, G.R., Zou, Z., Kinch, L., Wilkins, A.D., Sun, Q., Pallauf, K., MacDuff, D., et al. (2013). Identification of a candidate therapeutic autophagy-inducing peptide. *Nature* *494*, 201–206.
- Sleutel, M., Broeck, I. Van Den, Gerven, N. Van, Feuille, C., Jonckheere, W., Valotteau, C., Dufrêne, Y.F., and Remaut, H. (2017). Nucleation and growth of a bacterial functional amyloid at single-fiber resolution. *Nat. Chem. Biol.* *13*, 902–910.
- Smith, M.J., Kulkarni, S., and Pawson, T. (2014). FF domains of CA150 bind transcription and splicing factors through multiple weak interactions. *Mol. Cell. Biol.* *24*, 9274–9285.
- Solomon, J.P., Bourgault, S., Powers, E.T., and Kelly, J.W. (2011). Heparin binds 8 kDa gelsolin cross- β -sheet oligomers and accelerates amyloidogenesis by hastening fibril extension. *Biochemistry* *50*, 2486–2498.
- Soria, M.A., Cervantes, S.A., Bajakian, T.H., and Siemer, A.B. (2017). The functional amyloid Orb2A binds to lipid membranes. *Biophys. J.* *113*, 37–47.
- Stefani, M. (2010). Biochemical and biophysical features of both oligomer/fibril and cell membrane in amyloid cytotoxicity. *FEBS J.* *277*, 4602–4613.
- Stefani, M., and Dobson, C.M. (2003). Protein aggregation and aggregate toxicity: new insights into protein folding, misfolding diseases and biological evolution. *J. Mol. Med.* *81*, 678–699.
- Takeda, A. (2007). Involvement of zinc in neuronal death in the hippocampus. *Biomed Res Trace Elem.* *18*, 204–210.
- Tenreiro, S., Reimão-Pinto, M.M., Antas, P., Rino, J., Wawrzycka, D., Macedo, D., Rosado-Ramos, R., Amen, T., Waiss, M., Magalhães, F., et al. (2014). Phosphorylation modulates clearance of alpha-synuclein inclusions in a yeast model of Parkinson's disease. *PLoS Genet.* *10*, e1004302.
- Torkian, S., Khanjani, N., Mahmoodi, M.R., and Khosravi, V. (2019). A review of copper concentrations in Iranian populations. *Environ. Monit. Assess.* *191*, 537.
- Torrente, M.P., Chuang, E., Noll, M.M., Jackrel, M.E., Go, M.S., and Shorter, J. (2016). Mechanistic insights into Hsp104 potentiation. *J. Biol. Chem.* *291*, 5101–5115.
- Trivedi, M., Laurence, J., and Siahaan, T. (2009). The role of thiols and disulfides on protein stability. *Curr. Protein Pept. Sci.* *10*, 614–625.
- Vaiana, S.M., Best, R.B., Yau, W., Eaton, W.A., and Hofrichter, J. (2009). Evidence for a partially structured state of the amylin monomer. *Biophys. J.* *97*, 2948–2957.
- Velander, P., Wu, L., Henderson, F., Zhang, S., Bevan, D.R., and Xu, B. (2017). Natural product-based amyloid inhibitors. *Biochem Pharmacol.* *139*, 40–55.
- Vieira, T.C.R.G., Cordeiro, Y., Caghey, B., and Silva, J.L. (2014). Heparin binding confers prion stability and impairs its aggregation. *FASEB J.* *28*, 2667–2676.
- Wallace, E.W.J., Kear-scott, J.L., Pilipenko, E. V, Schwartz, M.H., Laskowski, P.R., Rojek, A.E., Katanski, C.D., Riback, J.A., Dion, M.F., Franks, A.M., et al. (2015). Reversible, specific, active aggregates of endogenous proteins assemble upon heat stress. *Cell* *162*, 1286–1298.
- Wang, Q., Aleshintsev, A., Zhuang, J., Brenowitz, M., and Gupta, R. (2019). Ca(II) and Zn(II) cooperate to modulate the structure and self-assembly of S100A12. *Biochemistry* *58*, 2269–2281.
- Watt, B., Niel, G. Van, Fowler, D.M., Hurbain, I., Luk, K.C., Stayrook, S.E., Lemmon, M.A., Raposo, G., Shorter, J., Kelly, J.W., et al. (2009). N-terminal domains elicit formation of functional Pmel17 amyloid fibrils. *J. Biol. Chem.* *284*, 35543–35555.

- Watt, B., Tenza, D., Lemmon, M.A., Kerje, S., Raposo, G., Andersson, L., and Marks, M.S. (2011). Mutations in or near the transmembrane domain alter PMEL amyloid formation from functional to pathogenic. *PLoS Genet.* 7, e1002286.
- Webb, J.L., Ravikumar, B., Atkins, J., Skepper, J.N., and Rubinsztein, D.C. (2003). Alpha-synuclein is degraded by both autophagy and the proteasome. *J. Biol. Chem.* 278, 25009–25013.
- Weidtkamp-peters, S., Lenser, T., Negorev, D., Gerstner, N., Hofmann, T.G., Schwanitz, G., Hoischen, C., Maul, G., Dittrich, P., and Hemmerich, P. (2008). Dynamics of component exchange at PML nuclear bodies. *J. Cell Sci.* 121, 2731–2743.
- Wineman-Fisher, V., Tudorachi, L., Nissim, E., and Miller, Y. (2016). The removal of disulfide bonds in amylin oligomers leads to the conformational change of the “native” amylin oligomers. *Phys. Chem. Chem. Phys.* 18, 12438–12442.
- Woodruff, J.B., Hyman, A.A., and Boke, E. (2018). Organization and function of non-dynamic biomolecular condensates. *Trends Biochem. Sci.* 43, 81–94.
- Wu, H. (2013). Higher-order assemblies in a new paradigm of signal transduction. *Cell* 153, 287–292.
- Xie, L., and Jakob, U. (2019). Inorganic polyphosphate, a multifunctional polyanionic protein scaffold. *J. Biol. Chem.* 294, 2180–2190.
- Xu, W., Liang, J., Li, C., He, Z., Yuan, H., Huang, B., Liu, X., Tang, B., Pang, D., Du, H., et al. (2018). Pathological hydrogen peroxide triggers the fibrillization of wild-type SOD1 via sulfenic acid modification of Cys-111. *Cell Death Dis.* 9, 67.
- Yamaguchi, S., Miura, C., Kikuchi, K., Celino, F.T., Agusa, T., Tanabe, S., and Miura, T. (2009). Zinc is an essential trace element for spermatogenesis. *Proc Natl Acad Sci USA* 106, 10859–10864.
- Yonemoto, L.T., Kroon, G.J.A., Dyson, H.J., Balch, W.E., and Kelly, J.W. (2009). Amylin proprotein processing generates progressively more amyloidogenic peptides that initially sample the helical state. *Biochemistry* 47, 9900–9910.
- Zare-shahabadi, A., Masliah, E., Johnson, G.V.W., and Rezaei, N. (2016). Autophagy in Alzheimer’s disease. *Rev Neurosci* 26, 385–395.
- Zha, X., Wang, R., Collier, D.M., Snyder, P.M., Wemmie, J.A., and Welsh, M.J. (2009). Oxidant regulated inter-subunit disulfide bond formation between ASIC1a subunits. *Proc Natl Acad Sci USA* 106, 3573–3578.
- Zhang, N., Duncan, F.E., Que, E.L., O’Halloran, T. V., and Woodruff, T.K. (2016). The fertilization-induced zinc spark is a novel biomarker of mouse embryo quality and early development. *Sci. Rep.* 6, 22772.
- Zhang, S., Xie, J., Xia, Y., Yu, S., Gu, Z., Feng, R., Luo, G., Wang, D., Wang, K., Jiang, M., et al. (2015). LK6/Mnk2a is a new kinase of alpha synuclein phosphorylation mediating neurodegeneration. *Sci. Rep.* 5, 12564.
- Zhao, J., Dong, X., Hu, X., Long, Z., Wang, L., Liu, Q., Sun, B., Wang, Q., Wu, Q., and Li, L. (2016). Zinc levels in seminal plasma and their correlation with male infertility: A systematic review and meta-analysis. *Sci. Rep.* 6, 22386.
- Zhou, W., and Freed, C.R. (2004). Tyrosine-to-cysteine modification of human α -synuclein enhances protein aggregation and cellular toxicity. *J. Biol. Chem.* 279, 10128–10135.

Nederlandse Samenvatting

1. Eiwitaggregatie: een tweeledig zwaard

Eiwitaggregatie is een biochemisch proces waarin eiwitten in of buiten de cel samenklonteren tot verschillende typen aggregaten zonder een omringende membraan. Lange tijd werd eiwitaggregatie beschouwd als een pathologisch proces vanwege de sterke correlatie met een aantal ziekten. Een voorbeeld zijn amyloïden, een specifieke vorm van eiwitaggregatie, waarbij de eiwitten zeer geordende en biochemisch stabiele fibrillen vormen met een karakteristieke 'cross- β ' structuur. Er zijn ongeveer 50 amyloïde-vormende peptiden en eiwitten geïdentificeerd die kenmerkend zijn voor menselijke ziektes. Het feit dat eiwitaggregatie alleen nadelig is voor cellen moest echter worden bijgesteld door de identificatie van eiwitaggregaten die betrokken zijn bij fysiologische processen. De vergelijkbare structurele eigenschappen tussen zowel pathologische als fysiologische assemblages maakt het op dit moment moeilijk om een duidelijk onderscheid te maken tussen 'goede' en 'slechte' amyloïde aggregaten. Hiervoor is een betere karakterisering van de eiwitaggregaten noodzakelijk, waar meerdere eigenschappen bij betrokken moeten worden zoals de functie, reversibiliteit, besmettelijkheid, lokalisatie, samenstelling en structuur.

2. Regulatie van functionele aggregatie

Tijdens het aggregatieproces van pathologische amyloïden vormen zich tijdelijke oligomere intermediaire structuren die toxisch zijn voor cellen. Alhoewel functionele amyloïden zelf niet toxisch zijn, ontstaan er tijdens de vorming van deze amyloïden ook toxische intermediaire structuren. Om deze reden moet het proces van functionele eiwitaggregatie nauwkeurig gereguleerd worden. Ten eerste verloopt het aggregatie proces van functionele amyloïden vaak relatief snel, waardoor de levensduur van oligomere intermediaire structuren tot een minimum beperkt wordt. Ten tweede is het proces van de vorming van functionele amyloïden vaak reversibel. De vorming van reversibele aggregaten is geassocieerd met processen als stress, eiwitopslag, afbraak en verwijdering van pathologische aggregaten. Ten derde wordt de expressie en afbraak van eiwitten die betrokken zijn bij de vorming van functionele aggregaten vaak nauwkeurig gereguleerd omdat hoge expressie niveaus ongewenste amyloïde vorming teweeg kan brengen. Om ongewenste interacties tussen aggregaten en andere cellulaire componenten te vermijden, vinden verschillende aggregatieprocessen plaats in organellen die omsloten zijn met een membraan. Ten slotte zijn er diverse biomoleculen geïdentificeerd die het aggregatieproces van functionele amyloïden kunnen reguleren.

3. Cross-talk van verschillende factoren bij de vorming van GPR-1 amyloïden

Het is niet bekend hoe verschillende biomoleculen individueel en/of samen de eiwitaggregatie in cellen kunnen beïnvloeden en bijdragen aan dit proces. Er is gespeculeerd dat functionele eiwitaggregatie voorafgaat aan pathologische eiwitaggregatie. Het is daarom van essentieel belang de regulatie van functionele oligomerisatie en aggregatie bij de betrokken eiwitten te bestuderen. Met deze kennis kunnen de moleculaire en cellulaire factoren die een rol spelen bij pathologische aggregatie opgehelderd worden en kunnen tevens nieuwe therapeutische strategieën ontwikkeld worden.

Onze studies laten zien dat er verschillende biomoleculen betrokken zijn bij de amyloïde-achtige aggregatie van het Golgi-geassocieerde pathogenese-gerelateerde eiwit 1 (*Golgi-associated pathogenesis-related protein 1*; GPR-1). Een samenvatting van de effecten van zink- en koper-ionen, heparine, eiwitzwavelbruggen en membranen op het induceren van verschillende GPR-1 aggregatie processen wordt beschreven in **Hoofdstuk 5**. Ieder aggregatie proces wordt gekenmerkt door karakteristieke eigenschappen van functionele eiwitaggregatie. Onafhankelijk van de manier van aggregaat inductie, gaat de vorming van GPR-1 aggregaten relatief snel. In het zink-afhankelijke proces is de aggregatie reversibel, terwijl onder oxidatieve condities een snelle en irreversibele aggregatie wordt waargenomen.

De lokalisatie van GPR-1 aan Golgi-membranen kan de vorming van oligomere structuren bevorderen. Tevens kan GPR-1 de vorming van A β -amyloïden voorkomen door binding aan oligomere structuren. De vraag is hoe deze aggregatie en anti-aggregatie eigenschappen een rol spelen in de cel. GPR-1 is een negatieve regelaar van autofagie. GPR-1 induceert de binding van Beclin-1 aan het Golgi-apparaat waardoor het niet meer vrij beschikbaar is en autofagie geremd wordt. We speculeren dat de eigenschap van GPR-1 om aan oligomere A β -structuren te binden, erop kan duiden dat vergelijkbare processen betrokken zijn bij de binding aan Beclin-1 en andere niet-verwante oligomere structuren.

GPR-1 is één van de weinige eiwitten uit de superfamilie van Cysteïne-rijke secretoire eiwitten, Antigeen 5 en Pathogenese gerelateerde eiwitgroep 1 (*Cysteine-rich secretory proteins, Antigen 5 and Pathogenesis related proteins group 1*; CAP) eiwitten die een intracellulaire lokalisatie hebben (**Hoofdstuk 1**). We laten zien dat eiwitzwavelbruggen belangrijk zijn voor de aggregatie van GPR-1 onder oxidatieve omstandigheden (**Hoofdstuk 3**). In tegenstelling tot GPR-1 worden veel andere CAP eiwitten gesecreteerd en bevatten ze meer cysteïne residuen. Dit suggereert dat zwavelbruggen en/of zwavelbrug-verbonden

oligomeren een belangrijke rol spelen in de structurele stabiliteit van eiwitten van de CAP-familie en/of in de regulatie van hun functie.

Zink- (**Hoofdstuk 2**) en koper- (**Hoofdstuk 3**) homeostase zijn belangrijke factoren bij de regulatie van verschillende GAPR-1 aggregatieprocessen. Onder fysiologische omstandigheden zijn zink- en koper-ionen in lage concentraties aanwezig in zowel cellen als in extracellulaire vloeistoffen zoals bloed. Specifieke structurele veranderingen van eiwitstructuren vinden plaats bij lage metaalionconcentraties, terwijl aspecifieke effecten optreden door additionele binding van koper-ionen bij hoge concentraties.

Zink-ionen zijn betrokken bij het voortplantingsproces. In **Hoofdstuk 4** laten we zien dat het menselijke cysteïne-rijke secretoire eiwit (*cysteine-rich secretory protein 1*; CRISP1) hoog moleculaire aggregaten kan vormen in aanwezigheid van fysiologisch relevante zink-ion concentraties en dat deze aggregaten weer dissociëren na verwijdering van de zink-ionen. Deze resultaten doen vermoeden dat de regulatie van de functie van CRISP1 (mede) wordt bewerkstelligd door zink-gereguleerde eiwit- oligomerisatie en -dissociatie.

Hoge expressie-niveaus van eiwitten met intrinsieke amyloïde eigenschappen zijn van belang bij de vorming van amyloïden. GAPR-1 heeft hoge expressie-niveaus in immuun-gerelateerde cellen en is verrijkt in het lumen van extracellulaire blaasjes die uitgescheiden worden door prostaat cellen. GAPR-1 expressie is ook verhoogd tijdens de neonataal-geïnduceerde neurodegeneratie in de hippocampus van ratten. De gecombineerde resultaten duiden op een functionele rol van GAPR-1 oligomerisatie en aggregatie bij immunologische processen, bevruchting en bij autofagie. Tevens kunnen veranderingen in expressie-niveaus van verschillende CAP-eiwitten betrokken zijn bij de regulatie van hun biologische functie. Of deze eigenschappen gelden voor alle leden van de CAP-eiwitfamilie moet nog blijken.

4 Samenvatting

Verscheidende eiwitten vertonen eigenschappen van functionele eiwitaggregatie die een rol spelen in meerdere biologische processen en die gereguleerd worden door complexe mechanismen. Om potentiële toxische effecten van intermediairen tijdens het aggregatieproces te voorkomen, vindt functionele eiwitaggregatie plaats met een snelle kinetiek en veel van deze processen zijn tevens reversibel. In dit proefschrift wordt de rol van meerdere biomoleculaire factoren bestudeerd bij de regulatie van fysiologische en/of reversibele eiwit aggregaten van het eiwit GAPR-1. Op basis van GAPR-1 als een model eiwit voor de superfamilie van CAP-

Summarizing discussion

eiwitten, postuleren we dat eiwit-oligomerisatie een gemeenschappelijke eigenschap is van alle familieleden. Zelf-associatie en dissociatie kan een algemeen mechanisme zijn in de regulatie van de functie van CAP-eiwitten. Opheldering van deze regulatiemechanismen op moleculair niveau kan tevens nieuwe inzichten geven in de behandeling en het voorkomen van eiwitaggregatie-gerelateerde ziekten.

About the author

Jie was born in Xi'an, Shaanxi Province, China on Jan 10th, 1989. She attended primary, middle and high school in Xi'an. In 2007, she started her undergraduate study at the College of Life Science, Northwest A&F University. During those years, she developed a strong interest in animal science. After she obtained her Bachelor degree in 2011, she started her master research at the College of Veterinary Medicine under the supervision of Prof. Dr. S. Qing in the same university. Her project is to study the location of oocyte-specific linker histone in pig ovaries. She obtained her Master degree in 2014. In the same year, she got an opportunity to start her PhD at Utrecht University (Department of Biochemistry & Cell Biology, Faculty of Veterinary Medicine) in the Netherlands under supervision of Prof. Dr. J. B. Helms.

List of publications

Sheng, J., Olich, N. K., Geerts, W. J., Li, X., Rehman, A. U., Gadella, B. M., Kaloyanova, D. V. and Helms, J. B. (2019). Zinc binding regulates amyloid-like aggregation of GAPR-1. Biosci. Rep. **39**, BSR20182345.

Sheng, J., Olich, N. K., Geerts, W. J., Kaloyanova, D. V. and Helms, J. B. (2019). Metal ions and redox balance regulate distinct amyloid-like aggregation pathways of GAPR-1. Sci. Rep. **9**, 15048.

Sheng, J., Olich, N. K., Gadella, B. M., Kaloyanova, D. V. and Helms, J. B. The less conserved metal-binding site in human CRISP1 remains sensitive to zinc ions and permits Zn^{2+} -dependent protein oligomerization. *Submitted for publication.*

Sheng, J., Olich, N. K., Gadella, B. M., Kaloyanova, D. V. and Helms, J. B. Regulation of functional protein aggregation by multiple factors: Implications for the amyloidogenic behavior of the CAP superfamily. *Submitted for publication.*